# Generation of monohormonal INSULIN$^{+}$ cells from human embryonic stem cells

**Jacqueline Victoria Schiesser**
**BBiomedSc. (Hons)**

Monash Immunology and Stem Cell Laboratories
Faculty of Medicine
Monash University, Australia

Submitted in total fulfilment
of the requirements of the degree of
Doctor of Philosophy

2012

And you will find that, after all, it isn't as horrible as it looks

*-Richard Feynmann*

# TABLE OF CONTENTS

## CHAPTER 3

## INSULIN-GFP$^+$ cells generated from human embryonic stem cells resemble human pancreatic endocrine cells



## CHAPTER 4

## *In vitro* and *in vivo* potential of human embryonic stem cell derived INSULIN-GFP$^+$ cells

## CHAPTER 5

## General Discussion

## BIBLIOGRAPHY



## APPENDICIES

## Abstract

Human Embryonic Stem Cells (hESCs) are immortal, pluripotent cells derived from the inner cell mass of the pre implantation embryo. These cells have the potential to differentiate into all cell types including insulin producing beta cells, which could provide an alternative to cadaver-derived islets for the treatment of type 1 diabetes.

We have explored the formation of pancreatic progenitor cells and mature β-cells using hESC reporter lines which express GFP under the control of regulatory sequences from the PDX1 and INSULIN genes respectively. Using serum-free media, we have found that specific combinations of factors applied in a sequential fashion result in the formation of a pancreatic precursor population, which can be further differentiated to hormone expressing cells. These endocrine cells have been shown to be a heterogeneous population that contains a substantial population of INSULIN expressing cells that do not express either glucagon or somatostatin, of which a subpopulation expresses NKX6.1.

An INSULIN$^{GFP/w}$ hESC reporter line was further modified by the addition of a luciferase transgene under the control of an EF1α promoter, which allowed for *in vivo* imaging of transplanted INSULIN expressing cells. Differentiated Tg-EF1α$^{Luc}$.INSULIN$^{GFP/w}$ cells were sorted based on INSULIN-GFP expression, and transplanted under the kidney capsule of immunocompromised mice and assessed for the retention of INSULIN-GFP$^{+}$ cells. It was found that the transplanted INSULIN$^{+}$ cells had the ability to form monohormonal endocrine cells of three different lineages. Additionally it was seen that persisting INSULIN$^{+}$ cells co-expressed transcription factors associated with beta-cell maturity, such as NKX6.1 and MAFA.

# List of Publications

Yu QC, Hirst CE, Costa M, Ng ES, **Schiesser JV**, Gertow K, Stanley EG, Elefanty AG (2012). APELIN promotes hematopoiesis from human embryonic stem cells. Blood **119**(26): 6243-54

Micallef SJ, Li X, **Schiesser JV**, Hirst C, Yu QC, Lim SM, Nostro MC, Elliot DA, Sarangi F, Harrison LG, Keller G, Elefanty AG, Stanley EG (2012). Isolation and characterisation of human insulin expressing cells using differentiated $INS^{GFP/w}$ hESCs. Diabetologia **55**(3): 694-706

Lim SM, Li X, **Schiesser J**, Holland AM, Elefanty AG, Stanley EG, Micallef SJ (2012). Temporal restriction of pancreatic branching competence during embryogenesis is mirrored in differentiating embryonic stem cells. Stem Cells and Development **21**(10): 1662-74

Jackson SA, **Schiesser J**, Stanley EG, Elefanty AG (2010). Differentiating embryonic stem cells pass through 'temporal windows' that mark responsiveness to exogenous and paracrine mesendoderm inducing signals. PLoS One **5**(5):e10706

**Monash University**

# General Declaration

In accordance with Monash University Doctorate Regulation 17 / Doctor of Philosophy (PhD) and Master of Philosophy (MPhil) regulations the following declarations are made:

I hereby declare that this thesis contains no material which has been accepted for the award of any other degree or diploma at any university or equivalent institution and that, to the best of my knowledge and belief, this thesis contains no material previously published or written by another person, except where due reference is made in the text of the thesis.

This thesis includes one original paper published in a peer-review journal and two unpublished manuscripts. The core theme of the thesis is the differentiation of human embryonic stem cells to form INSULIN expressing cells, and the characterisation of these cells and their *in vivo* and *in vitro* potential. The ideas, development, provision of data and/or writing up of all the papers in the thesis were partly the responsibility of myself, the candidate, working within the Monash Immunology and Stem Cell Laboratories (MISCL), Monash University under the supervision of Dr. Suzanne Micallef, Professor Andrew Elefanty and Professor Edouard Stanley.

The inclusion of co-authors reflects the fact that the work came from active collaboration between researchers and acknowledges input into team-based research.

The first chapter was written by myself. The differentiation method described in chapter 2 was developed by myself. The cell lines described in this chapter were developed by Dr. Suzanne Micallef, Dr. Xueling Li ($INS^{GFP/w}$ hESC line), Dr Andrew Holland and Prof. Edouard Stanley (Tg-$PDX^{GFP}$ hESC line). The $INS^{GFP/w}$ hESC line described in chapter 3 was developed by Dr. Suzanne Micallef and Dr. Xueling Li. Work relating to the development of the Spin EB differentiation protocol was performed by myself. Chapter 4 was predominantly my own work. Dr. Suzanne Micallef and Ms. Tania Hatzistavrou provided assistance with cell transplantation experiments that contributed to data in figure 3, 5 and

6. Staff at the Animal Research Laboratories provided assistance with testis teratoma injections, which contributed data to figure 3.

Overall, my contribution to the work included in this thesis was 80%

| Thesis Chapter | Publication title | Publication status | Nature and extent of candidate's contribution |
|---|---|---|---|
| 1 | Differentiation of Embryonic Stem Cells towards Pancreatic Beta Cells | In preparation | Writing of manuscript |
| 2 | A novel protocol for the generation of pancreatic cells from human embryonic stem cells | In preparation | Development and optimisation of the techniques described; Writing of manuscript |
| 3 | INSGFP/w human embryonic stem cells facilitate isolation of *in vitro* derived insulin-producing cells | Published | Provision of data; development and optimisation of some techniques described |

Jacqueline Schiesser

March 2013

## Acknowledgments

Throughout the course of my PhD a multitude of people have supported and encouraged me in a number of different ways.

Firstly, I need to thank my supervisors Ed Stanley, Andrew Elefanty and Sue Micallef for all their assistance, support and suggestions as I have undertaken my PhD. In particular, Ed has had the patience to help me redesign the luciferase targeting vector, for what felt like a thousand times, managed to put up with my 'single' questions for the 4 years of my candidature, as well provided editorial assistance with the writing and corrections of this thesis. Andrew has been a fantastic source of knowledge when it comes to any and all FACS work, as well as providing much needed assistance during the first year of my PhD. Sue has been a wonderful supervisor who has always provided support and suggestions when experiments just won't work, and has assisted me greatly in learning how to undertake anything related to immuno.

Secondly I must thank the members of the diabetes group both past and present: Sue Micallef, Xueling Li, Andrew Holland, Sue-Mei Lim, Sonia Holland, Susan Hawes and Roy Lee. This group of people has provided a source for both general discussion regarding diabetes and pancreas related things, as well as discussion of the results, which were generated during my time as a PhD student.

My fellow Elefanty/Stanley PhD students (or should that read inmates): Cissy, Chew-Li and Jen, as well as former inmates Rob, Michael, Richard and Steve – have been a wonderful source of commiserations, congratulations and gossip sessions – this surely has helped to keep me at least somewhat sane throughout my PhD, especially throughout the writing process.

The members of the Elefanty/Stanley lab (whom are too numerous to list) have made this a wonderful place to undertake my PhD –along the way everyone has helped me out in some form or another, whether it be related to troubleshooting an experiment, providing a protocol or much-needed encouragement, or just making the lab a fun place to work in.

I need to thank both Chris Siatskas and John Price for initially guiding me through the ins and outs of bioluminescence imaging. Without your assistance, much of my luciferase data would not exist. A special thanks must also be made to the staff members from FlowCore for sorting expertise, at the Histology Platform for sectioning and staining troubleshooting, and at the Animal Research Laboratories for assistance with the teratoma formation experiments.

My friends, especially Hugh and Lauren, deserve tremendous thank-you for the amount of support they have provided me throughout my PhD. Lauren has managed to always make me feel better about writing my thesis – both by telling me about her 720 page thesis (I knew that science was the better choice!), and by taking me out and commiserating or celebrating with me – whichever the occasion may have required. Hugh, despite not physically being here, always is up for a late-night phone call, and complaint session, as well as manages to have a somewhat psychic sense, about when I need to hear about total inane gossip/news, in order to distract me from result related troubles.

My family has been a source of support and encouragement. I am especially grateful, that as the years have gone on, they have managed to both refrain from asking, and deflected other peoples enquires, as to when I will be getting a 'real job'.

And finally: Kamel, thank-you for everything. Your love and support has helped make this thesis, and the work contained within it possible.

## List of Abbreviations

| | |
|---|---|
| AmpR | ampicillin resistance |
| bFGF | basic fibroblast growth factor |
| BMP | bone morphogenic protein |
| bp | base pair(s) |
| CDH1 | cadherin-1; E-Cadherin |
| CMF | calcium- and magnesium-free |
| CXCR4 | chemokine (C-X-C motif) receptor 4 |
| d | day |
| DAPI | 4'-6' diamidino-2-phenylindole |
| DE | definitive endoderm |
| EB | embryoid body |
| EC | endocrine cell |
| E-CAD | e-cadherin |
| EDTA | ethylenediamine-tetra-acetic acid |
| EGFP | enhanced green fluorescent protein |
| EMT | epithelial-mesenchymal transition |
| EphB3 | ephrin B3 |
| ESC | embryonic stem cell |
| FACS | fluorescence activated cell sorting |
| FCS | foetal calf serum |
| FGF | fibroblast growth factor |
| FOX | forkhead box |
| g | gram |
| GFP | green fluorescent protein |
| GCG | glucagon |
| GHRL | ghrelin |
| GSIS | glucose stimulated insulin secretion |
| G418 | geneticin |
| hESC | human embryonic stem cell |
| INS | insulin |
| iPSC | induced pluripotent stem cell |
| IRES | internal ribsosome entry site |

| | |
|---|---|
| kb | kilobase pair(s) |
| KOSR | knock-out serum replacement |
| MEF | mouse embryonic fibroblast |
| MIXL1 | mix1 homeobox-like 1 |
| ml | millilitre |
| μF | microfarard |
| μg | microgram |
| μl | microlitre |
| NEAA | non-essential amino acids |
| Neo | neomycin phosphotransferase |
| NGN3 | neurogenin 3 |
| PAX | paired box gene |
| PBS | phosphate buffered saline |
| pc | prohormone convertase |
| PE | pancreatic endoderm |
| PI | propidium iodide |
| PI3K | phosphoinositol 3-kinase |
| PMEF | primary mouse embryonic fibroblast |
| PP | pancreatic polypeptide |
| PS | primitive streak |
| PSC | pluripotent stem cell |
| PVA | polyvinyl alcohol |
| RA | retinoic acid |
| ROCK | Rho-associated kinase (inhibitor) |
| rpm | revolutions per minute |
| SOX | SRY-box containing gene |
| SST | somatostatin |
| TE | tris-EDTA |
| TGFβ | transforming growth factor β |
| WNT | wingless-related MMTV integration site |

# CHAPTER 1

## LITERATURE REVIEW

## 1.1 Introduction

Embryonic stem cells (ESCs) are immortal cells derived from the inner cell mass of the pre-implantation embryo and have the capacity to differentiate into extraembryonic tissue as well as somatic cells representative of all three germ layers (pluripotency) ((Evans and Kaufman, 1981), (Martin, 1981)). The isolation of human ESCs in 1998 (Thomson et al., 1998) and their subsequent demonstrated differentiation capacity (Reubinoff et al., 2000) provided an opportunity to develop *in vitro* models of post implantation stages of early human development. Furthermore, the ability of hESCs to be differentiated towards specific cell types raised the possibility that hESC-derived cell types could form a platform for cell based therapies in the future. This possibility has heightened interest in directing hESC differentiation *in vitro* to therapeutically relevant cell types, such as insulin producing beta cells that could potentially replace cadaveric derived islets for the treatment of type 1 diabetes. This review examines protocols designed to differentiate pluripotent stem cells (PSCs) towards pancreatic endocrine cells and discusses how these methodologies relate to the developmental principles upon which they are based.

## 1.2 Embryonic Stem Cell Differentiation to Beta Cells

A number of studies have reported protocols for the derivation of pancreatic endoderm from differentiating human PSCs (hPSCs). One such protocol, published by D'Amour *et.al,* incorporated combinations of growth factors that had been implicated in normal pancreatic development. In this method, hESCs were guided from their undifferentiated state to insulin-expressing cells via a series of obligate intermediate cell types identified through developmental studies (D'Amour et al., 2006). Following this, many other groups have published methods for the generation of pancreatic cells from hPSCs. In general, these protocols follow the same ontogeny based approach articulated by D'Amour and colleagues. Figure 1.1 summarises features common to many of these protocols and provides an overview of the important developmental milestones passed as cells leave the pluripotent cell state and differentiate towards pancreatic endoderm.

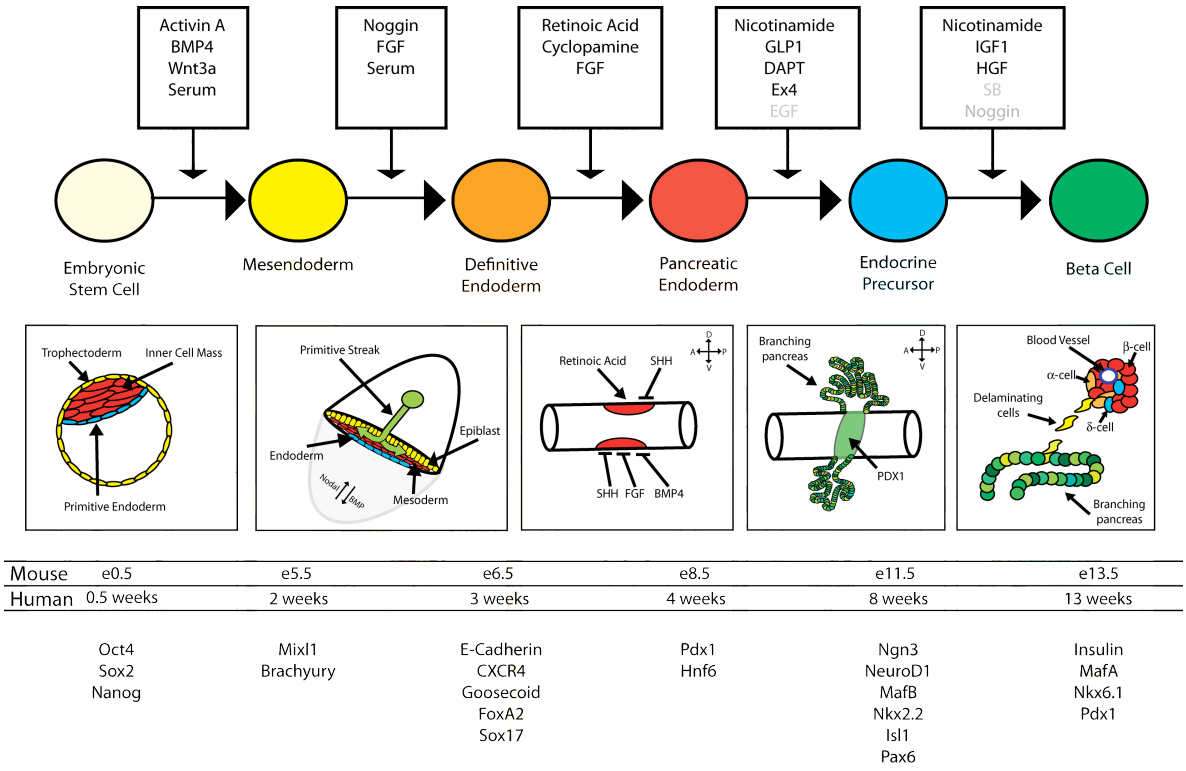


**Figure 1.1** Specific growth factors can be used to guide pluripotent stem cell differentiation to beta cells via intermediate cell types observed during embryogenesis. The upper row shows growth factor combinations frequently used to promote each step. Molecules shown in grey text are examples of specific supplements sometimes added in addition to, or in place of, more commonly used factors. The central rows show the developmental stages and corresponding key morphogenetic processes occurring within the embryo. The lower rows show the relative mouse and human development stages as well as some of the specific genes used to identify these stages.

### 1.2.1 Step 1: Formation of Definitive Endoderm from Pluripotent Stem Cells

The first steps in the process of making pancreatic cells from hPSCs involve the generation of mesendoderm and its subsequent differentiation towards definitive endoderm. Both *in vitro* and *in vivo*, mouse mesendoderm cells are marked by the expression of the transcription factors *Mixl1* and *Brachyury* ((Wilkinson et al., 1990), (Pearce and Evans, 1999), (Robb et al., 2000)). The commitment of this population into definitive endoderm is accompanied by the up-regulation of three other transcription factors, *Gsc*, *Sox17*, and *FoxA2* ((Blum et al., 1992), (Ang et al., 1993), (Sasaki and Hogan, 1993), (Hudson et al., 1997)). In addition, mouse ESC differentiation experiments indicate that definitive endoderm can also be identified by the co-expression of two cell surface receptors: E-cadherin (Cdh1) and CXCR4 (Yasunaga et al., 2005). However, an important caveat with endoderm-associated markers is that their ability to identify definitive, as opposed to primitive endoderm, is predicated on the earlier transit of cells through a stage where they

express primitive streak (mesendoderm) genes, such as *Mixl1* and *Brachyury*. This same progression is thought to occur in both human development and during human PSC differentiation.

In the majority of differentiation protocols, induction of definitive endoderm almost always involves treating cells with relatively high concentrations of Activin A, a transforming growth factor beta (TGFβ) family member used in place of Nodal, the molecule required to drive mesendoderm formation within the developing embryo (Conlon et al., 1994). The use of high levels of Activin A to induce robust nodal signalling during hPSC differentiation is based upon a number of observations from *in vivo* and *in vitro* studies. Mouse knock out experiments demonstrated that nodal null embryos failed to form a primitive streak, the morphological structure that marks gastrulation – the process during which definitive endoderm, mesoderm and ectoderm are generated (reviewed in: (Tam and Loebel, 2007)). A series of experiments performed by Lu and Robertson showed that Nodal played an imperative role in the formation of the global anterior-posterior axis, and that the level of Nodal expression affected the anteriorisation of mesendoderm (Lu and Robertson, 2004).

Early work with mouse ESCs examined the induction of mesoderm and definitive endoderm via the mesendoderm by members of the TGFβ family. Kubo *et.al* tested the ability of Activin A to induce mesoderm and endoderm in embryoid bodies using a serum-free differentiation system. They concluded that different concentrations of Activin A induced different developmental outcomes: low concentrations of Activin A (used in place of Nodal) seemed to favour a mesodermal fate, whereas high concentrations seemed to favour an endodermal fate (Kubo et al., 2004).

Subsequent studies demonstrated that in order for hESCs to efficiently respond to Activin/Nodal signalling, PI3K signalling must be suppressed (McLean et al., 2007). Compounds such as wortmannin, which acts to suppress Pi3K signalling, were shown to promote definitive endoderm formation (McLean et al., 2007), and have been used in conjunction with Activin A to form definitive endoderm from hESCs (Zhang et al., 2009). Because of the expense and batch-to-batch variability associated with preparations of Activin A, researchers have also sought to discover small molecules that promote hESC differentiation towards definitive endoderm. Borowiak and colleagues identified two such molecules, IDE1 and IDE2, which induced differentiation (in the presence of serum) with

similar efficiencies to Activin A. The exact biological target on which these molecules act was not identified, although experiments indicated that activation of TGFβ signalling might be involved (Borowiak et al., 2009).

In addition to Activin A, or molecules thought to stimulate or augment this pathway, many protocols incorporate other factors which have also been implicated in fate decisions of the early embryo. For example, Wnt3a is sometimes included during the earliest stages, presumably to enhance mesendoderm formation (for example: (D'Amour et al., 2006), (Rezania et al., 2012)). In these circumstances, Wnt3a is used as a surrogate for Wnt3, a molecule expressed in the in the proximal epiblast prior to gastrulation, and then later in the primitive streak. Mice lacking Wnt3 fail to undergo gastrulation and blocking Wnt signalling during ESC differentiation blocks mesendoderm formation ((Liu et al., 1999), (Gadue et al., 2006), (Jackson et al., 2010)). In this context, Bone and colleagues found that 1m, a small molecule inhibitor of the Wnt signalling regulator, GSK-3, induced differentiation of hESCs towards definitive endoderm (Bone et al., 2011).

Another member of the TGFβ superfamily that is critical for mesendoderm formation is BMP4, which is expressed in the amnion, extraembryonic mesoderm and posterior primitive streak during mouse development (Winnier et al., 1995). Mouse embryos lacking BMP4 fail to express mesendoderm associated genes such as *Brachyury* and die during gastrulation, at ~embryonic day (E)6.5 (Winnier et al., 1995). A number of groups have used BMP4 to augment the affects of Activin A when differentiating hESCs to definitive endoderm (for example: (Nostro et al., 2011), (Micallef et al., 2012), (Teo et al., 2012)).

A common feature of many differentiation protocols is the inclusion of low levels of serum (typically, fetal calf serum) as part of the mesendoderm induction regime. The role played by serum is unclear, but may relate to either its positive affect on cell survival (Ling et al., 1994), or the presence of unidentified growth factor activities, such as, but not limited to, Activin A (Sakai et al., 1992).

### 1.2.2 Step 2: Definitive Endoderm to Foregut/Pancreatic Endoderm

Following the induction of definitive endoderm by high levels of Activin A, most hPSC differentiation protocols incorporate factors to direct this endoderm towards a pancreatic fate; a differentiation step marked by the expression of the pancreatic transcription factor

PDX1. This is most commonly achieved by treating cultures for a number of days with retinoic acid (RA) (See figure 1.1).

It has been demonstrated that RA plays an essential role in the morphogenesis and organogenesis of a number of organs; including the pancreas (reviewed in: (Rhinn and Dolle, 2012)). Within the embryo, RA is synthesised from circulating retinol in a two-step reaction involving three specific alcohol dehydrogenases and aldehyde dehydrogenases – known as retinaldehyde dehydrogenases (RALDHs) (Martin et al., 2005). During gastrulation, Raldh2 is expressed in the mesendoderm before becoming localised to the lateral plate and paraxial mesoderm during segmentation (Stafford et al., 2006). Gain- and loss- of function studies indicate that retinoid signalling is required for pancreatic specification in the zebrafish, Xenopus, quail and mouse ((Stafford and Prince, 2002), (Martin et al., 2005), (Molotkov et al., 2005)). In zebrafish, for example, it has been shown that retinoid signalling is required for pancreas and liver specification, and that treatment with exogenous RA induces ectopic expression of pancreatic and liver markers (Stafford and Prince, 2002). In Xenopus, inhibition of retinoid signalling at the gastrula stage resulted in the loss of dorsal pancreas but had little effect on ventral pancreas development (Chen et al., 2004). Further studies demonstrated that whilst RA was sufficient to induce pancreatic-specific genes in the dorsal pancreas, it failed to do so in the ventral pancreas (Pan et al., 2007). Similarly, in the quail, it was shown that RA deficient embryos lacked a dorsal pancreas. Additionally, in mice, it was demonstrated that RA signalling was sufficient to induce Pdx1 expression in anterior endoderm (Martin et al., 2005).

Based on earlier developmental studies, a number of groups showed that addition of exogenous RA could promote the differentiation of mouse ESCs to *Pdx1*$^{+}$ endoderm (for example: (Micallef et al., 2005), (Shi et al., 2005), (Schroeder et al., 2006)). This finding was subsequently confirmed in human ESCs, where it was demonstrated that RA was required to convert posterior foregut endoderm to pancreatic endoderm (D'Amour et al., 2006). The addition of exogenous RA to differentiating hESCs was also shown to affect the later expression of pancreatic-associated genes such as *NEUROGENIN3* (*NGN3*), and hormones including *INSULIN* and *GLUCAGON* (D'Amour et al., 2006).

At ~E9.5 in the mouse, the splanchnic mesenchyme pushes against the dorsal evagination to form the dorsal pancreatic bud. This same process is then repeated with the ventral

evaginations to form the ventral pancreatic bud ((Kim and Hebrok, 2001), (Slack, 1995)). At ~E16.5, fusion of the dorsal and ventral anlage occurs as the result of gut rotation, bringing the ventral pancreas anlagen into juxtaposition with its dorsal counterpart ((Seymour et al., 2004), (Slack, 1995)).

A similar process is through to occur in the human embryo, where following gastrulation, the endoderm forms a flat sheet, which then rotates to form the gut tube. Following specification of the pancreatic endoderm within the regionalised gut tube, the dorsal bud appears at 26 days and begins to grow into the dorsal mesenchyme, opposite the hepatic diverticulum. The ventral bud appears several days later, and begins to grow into the ventral mesenchyme, just caudal to the gallbladder (Moore et al., 1995). The epithelial cells forming both buds then continue to proliferate and branch into the surrounding mesenchyme. By week 5, the ventral bud has commenced migrating posteriorly around the duodenum and by early in 6$^{th}$ week, lies adjacent to the dorsal pancreatic bud. The two pancreatic buds then fuse late in 6wpc (Moore et al., 1995).

It is the developmental equivalent of this stage that many groups undertaking hESC to pancreas differentiation experiments choose to transplant cells into mice, in order to produce functional beta cells. This strategy was first employed by Kroon and colleagues, who differentiated hESCs for 12 days to form PDX1$^{+}$ pancreatic endoderm prior to transplantation into immunodeficient non-diabetic mice. Grafts were allowed to develop for between 90 and 140 days post-transplant prior to treating animals with streptozotocin (STZ), a chemical that can be used to selectively ablate mouse beta cells. It was subsequently demonstrated that the implanted pancreatic endoderm cells had the ability to maintain normoglycaemia for up to 88 days post-STZ treatment (Kroon et al., 2008). A number of other groups have also followed this approach, as summarised below in table 1.1.

Recently, Rezania and colleagues demonstrated that hESC derived pancreatic progenitors could ameliorate diabetes in both diabetic mice and immunodeficient rats (Rezania et al., 2012). This is the first time that PSC-derived pancreatic cells have been shown to function in non-mouse animal models, an important proof of principle for future efforts to translate this platform into a clinical setting.

### 1.2.3. Step 3: Pancreatic Endoderm to Endocrine Precursor Cells

Although the commitment of pancreatic endoderm to endocrine precursor cells is an obligate intermediate step during beta cell formation, most differentiation protocols have not yet incorporated factors specifically designed to either promote or enhance this process. This is possibly because the key marker of this step, the transcription factor Neurogenin 3 (Ngn3), is only expressed transiently, making identification of cells undergoing this process difficult to identify. Nevertheless, there are hints from developmental studies concerning which signalling pathways may need to be modulated to enhance endocrine precursor formation. In mouse experiments, impaired Notch receptor activation or signalling resulted in profound up-regulation of Ngn3 gene expression, leading to premature endocrine cell differentiation at the expense of pancreatic progenitor expansion and exocrine cell differentiation ((Apelqvist et al., 1999); (Jensen et al., 2000)). In contrast, cells with active Notch-signalling most likely remain as undifferentiated progenitors that can contribute to subsequent proliferation, morphogenesis, and later differentiation events. The function of Notch signalling during this process is analogous to its function during early mammalian neurogenesis ((Lewis, 1996), (Beatus and Lendahl, 1998)).

As noted above, Ngn3 is a key maker of endocrine commitment. In the mouse, Ngn3 has a bimodal expression pattern with the first wave observed between 8.5dpc and 11dpc. A second wave of expression is initiated at 12dpc and reaches its peak at 15.5dpc before being rapidly downregulated by 17.5dpc ((Gu et al., 2002), (Villasenor et al., 2008)). Studies in the chick and mouse have shown that Ngn3 plays an essential role in endocrine precursor cell delamination (by the process of epithelial-mesenchymal transition (EMT)) (Gouzi et al., 2011), during which delaminating cells are marked by the expression of EphB3 ((Villasenor et al., 2012)). Endocrine specification begins around 16.5dpc in the mouse, with the induction of Ngn3 in response to the repression of Notch signalling (Apelqvist et al., 1999). Expression of Ngn3 is essential for endocrine cell specification – in Ngn3 deficient mice, the pancreas fails to develop endocrine cells (Gradwohl et al., 2000).

The mesenchyme associated with the developing mouse pancreas has also been shown to play a role in controlling both Ngn3 induction (Duvillie et al., 2006) and pancreatic epithelial cell proliferation (Bhushan et al., 2001). A key factor in this process is mesenchymally derived FGF10. FGF10 null mice exhibit severe pancreatic hypoplasia, due to a striking reduction in the proliferation of the pancreatic epithelial progenitor cells

(Bhushan et al., 2001). In contrast, transgenic mice over-expressing FGF10 display pancreatic hyperplasia resulting from attenuation of differentiation and expansion of pancreatic progenitor cell numbers due to increased proliferation ((Hart et al., 2003), (Norgaard et al., 2003)). The effect of FGF10 on pancreatic progenitor cell proliferation has been also been demonstrated *in vitro* using both isolated rat (Miralles et al., 1999) and mouse (Miralles et al., 2006) pancreatic epithelia. It was found that addition of FGF10 to isolated E10.5 mouse pancreatic epithelium led to an expansion of pancreatic progenitor numbers due to increased proliferation. Furthermore, this study also showed that in contrast to control samples, FGF10 treatment maintained expression of Hes1, a downstream target of Notch1 signalling. Confirming this link between the FGF10 and Notch pathways, Miralles *et.al*, showed that the inhibition of Notch signalling by addition of a γ-secretase inhibitor, downregulated both Hes1 expression and decreased pancreatic progenitor cell proliferation in FGF10 treated epithelium. These results strongly suggest that Notch is required as a downstream mediator of FGF10 signalling in pancreatic progenitors (Miralles et al., 2006).

In addition to effects on pancreatic progenitor cell proliferation, it has also been demonstrated that FGF10 addition can enhance expression of Ngn3 and increase the number of $Ngn3^+$ cells in the absence of mesenchyme ((Duvillie et al., 2006), (Attali et al., 2007)), though neither FGF10 or the presence of mesenchyme are essential for the induction of Ngn3 expression. This regulatory circuit is hypothesised to be a layer of control that allows for the maturation of the epithelial cells prior to Ngn3 expression, making these cells competent to respond to downstream signals (Duvillie et al., 2006). This hypothesis was supported by a study that used a conditional FGF10 gain-of-function model to demonstrate that the timing of FGF10 expression affects the competence of pancreatic progenitor cells to differentiate to different pancreatic lineages (Kobberup et al., 2010).

As previously noted, in the mouse, Ngn3 is expressed in a biphasic pattern – with the first wave of expression between 8.5dpc and 11dpc, and a second wave beginning at 12dpc (Villasenor et al., 2008). These two waves of expression correspond with the so-called primary and secondary transitions events, which represent two separate waves of endocrine cell differentiation. It has been postulated that only endocrine cells specified during the secondary transition form the definitive single-hormone positive cells in the adult pancreas (Pictet et al., 1972). In contrast, endocrine cells specified during the primary

transition are not thought to contribute to the adult pancreas, instead playing a role in embryonic pancreatic function (Herrera, 2000). However, this paradigm is not supported by all studies of pancreatic cell development, some of which have demonstrated that endocrine cells (or their progenitors) formed during the primary transition can contribute to the adult pancreas (Gu et al., 2002).

During human pancreatic organogenesis, NGN3 expression is observed as early as 8wpc, where it is co-expressed with other transcription factors such as PDX1, as well as the hormones INSULIN and GLUCAGON. As development proceeds, NGN3 expression was seen to gradually decrease, although it was still observable at 21wpc (Lyttle et al., 2008). In contrast to the mouse, a biphasic expression pattern of NGN3 has not been reported. This may indicate that distinct primary and secondary transition events do not occur during human pancreatic organogenesis, or may simply reflect difficulties in obtaining appropriately staged human fetal tissues.

### 1.2.4 Step 4: Commitment of Endocrine Precursors to Beta Cells

The factors controlling the last step of differentiation, in which endocrine precursor cells are converted to insulin-expressing cells, are still somewhat controversial. Although some protocols incorporate factors that have been implicated from developmental studies, most rely on the presence of nicotinamide, a small molecule shown to promote endocrine differentiation of fetal pancreatic precursors (Otonkoski et al., 1993), and increase expression of both insulin and the beta-cell associated transcription factor, MafA (Ye et al., 2006).

In the human embryo, the first endocrine cells appear as scattered insulin-expressing cells at 8wpc – one study suggests that at this point in development, expression of other hormones, such as glucagon or somatostatin, has not initiated (Polak et al., 2000). At 8.5wpc, the first glucagon- and somatostatin-expressing cells are observed, followed by pancreatic polypeptide (PP)-expressing cells, which are first seen at 10wpc (Jeon et al., 2009). A proportion of these early hormone-expressing cells are polyhormonal in nature: at 8wpc, insulin-expressing cells have been reported to co-express glucagon at frequencies ranging from 10% to 92% ((Polak et al., 2000), (Piper et al., 2004), (Jeon et al., 2009)), and to co-express somatostatin at frequencies ranging from less than 10% to 97% ((Polak et al., 2000), (Piper et al., 2004)). Tri-hormone expressing cells have also been observed at

varying frequencies at 8wpc. Cells expressing more than one hormone have frequently been observed during hPSC differentiation *in vitro*, with the proportion of cells expressing insulin alone or in conjunction with glucagon or somatostatin varying between studies (Figure 1.2).

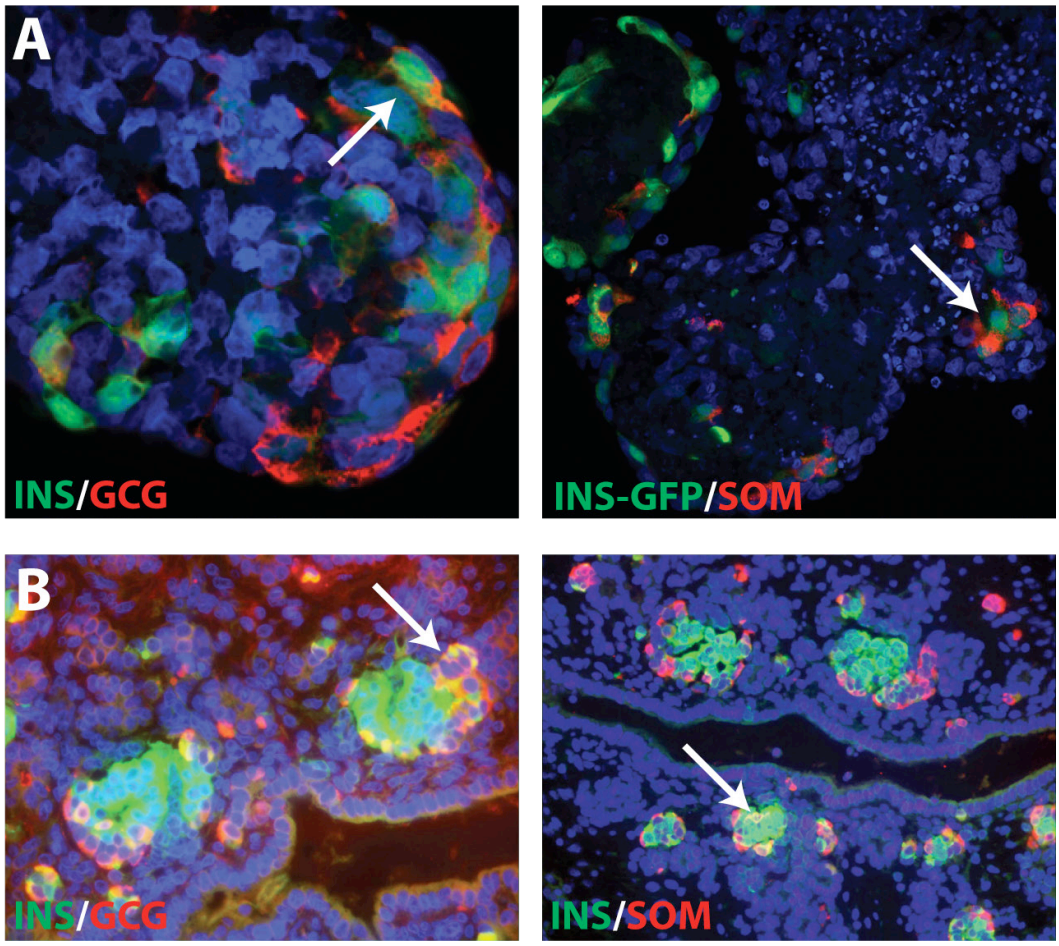


**Figure 1.2** Polyhormonal cells are observed during both human ESC differentiation and embryogenesis. **(A)** INSULIN and GLUCAGON, as well as INSULIN and SOMATOSTATIN co-expression is observed following 25 days of human ESC differentiation; **(B)** Similarly, INSULIN and GLUCAGON, as well as INSULIN and SOMATOSTATIN are seen to be co-expressed at ~10wpc. Immunofluorescence studies by Dr. S. Micallef (Panel A) and Dr. S Hawes (Panel B).

In contrast, PP-cells have only ever observed as single-hormone expressing cells (Polak et al., 2000). Endocrine cells that co-expressed hormones decreased in frequency from 9wpc (Polak et al., 2000), and were not detected in preterm infant pancreata at 22wpc (De Krijger et al., 1992). The varying amounts of hormone co-expression observed in developing human foetal endocrine cells may relate to difficulties in accurately staging foetal material, or reflect sampling 'errors' resulting from different regions of the pancreas being analysed.

It is at this stage, where hormone expression (specifically insulin expression) is observed, some researchers have chosen to transplant *in vitro* derived cells to test for functionality. This is summarized in table 1.2

Whilst the expression of insulin in the absence of other hormones is a defining characteristic beta cells, this property is not sufficient to ensure functionality: that is, the ability to regulate insulin release in response to glucose challenge. A number of transcription factors have been proposed to play a role in the maturation and maintenance of beta-cell function – these include Nkx6.1, MafB and MafA.

Nkx6.1 is a transcription factor (Rudnick et al., 1994) that is first observed in the mouse pancreas at 10.5dpc, where it is expressed in most pancreatic epithelial cells. This broad expression is maintained until 13dpc (at the start of the secondary transition), after which it's expression begins to become restricted, and by 15.5dpc, is only found in insulin-expressing cells as well as scattered ductal cells. In the adult, Nkx6.1 is exclusively found in insulin expressing cells (Sander et al., 2000). Nkx6.1 plays an important role in beta-cell specification and *Nkx6.1*$^{-/-}$ mice show a deficit in beta-cell numbers that can be observed as early as 14dpc (Sander et al., 2000). *In vitro,* overexpression of Nkx6.1 in isolated rat islets resulted in an improvement in their glucose stimulated insulin secretion (GSIS) response and an increase in beta-cell replication (Schisler et al., 2008). Studies such as those described above have implicated Nkx6.1 as a marker of definitive beta cells; however, *in vivo* it has been demonstrated that Nkx6.1 overexpression cannot enhance either beta cell GSIS response or proliferation under either diabetic or nondiabetic conditions (Schaffer et al., 2011). A similar expression pattern of NKX6.1 is observed during human pancreatic development as compared to the mouse. NKX6.1 is initially broadly expressed throughout the pancreatic epithelium (from 9wpc), before a decrease in expression in non-insulin expressing cells is observed by 13wpc. Like the mouse, NKX6.1 expression is restricted to beta cells of the adult pancreas (Riedel et al., 2012).

Few groups who have differentiated human PSCs towards a beta cell fate have analysed for the expression of NKX6.1. Early reports of NKX6.1 expression were made both at the RNA (Jiang et al., 2007a) and protein level (D'Amour et al., 2006), with both groups observing NKX6.1 expression from ~d15 of differentiation. Neither of these reports however, demonstrated the co-expression of NKX6.1 with other markers of beta-cell differentiation.

More recently, a number of groups have demonstrated the co-expression of NKX6.1 with either C-PEPTIDE (Zhang et al., 2009), PDX1 ((Zhang et al., 2009, {Kelly, 2011 #716)}, (Van Hoof et al., 2011), (Xu et al., 2011)) or INSULIN (Micallef et al., 2012). However, despite co-expression with these other pancreatic genes, the differentiated cells either showed limited functionality (Zhang et al., 2009), or functionality was not examined ((Van Hoof et al., 2011), (Xu et al., 2011), (Micallef et al., 2012)), suggesting that, NKX6.1 co-expression with either PDX1 or C-PEPTIDE may not be sufficient to generate fully functional beta cells

MafB and MafA are members of the Maf transcription factor family and are both expressed in the pancreas in a temporospatially regulated fashion, in both mouse and human. In the mouse, MafB expression is first observed, at ~10.5dpc in the epithelium of the pancreas (Artner et al., 2006). MafB expression is found in both insulin$^+$ and glucagon$^+$ cells during the primary transition, as well as in Ngn3$^+$ pancreatic progenitor cells, before becoming restricted to the adult glucagon$^+$ (alpha) cells ((Artner et al., 2006), (Artner et al., 2010)). In contrast, MafA expression is observed later during development, at ~13.5dpc. The spatial distribution of MafA expression also differs from MafB, as expression of MafA is only observed in the insulin$^+$ cells specified during the secondary transition (Matsuoka et al., 2004). Additionally, MafB and MafA play different functional roles during beta-cell differentiation. Only MafB is required for beta-cell development in the mouse – in mice in which *MafA* has been specifically deleted from the pancreatic lineage, there is no observable defect in beta-cell numbers. However, it is possible that MafB is able to compensate for loss of MafA in this context (Artner et al., 2010). By comparison, MafA has been shown to control the glucose-responsive transcription of insulin and other associated genes in definitive beta cells ((Matsuoka et al., 2003), (Wang et al., 2007)). Additionally, *Mafa*$^{-/-}$ mice have impaired glucose tolerance and defects in insulin secretion ((Zhang et al., 2005)), emphasising the importance of MafA in maintaining an appropriate glucose stimulated insulin secretion (GSIS) response.

In contrast to the similarities between the expression patterns of transcription factors such as NKX6.1 in mice and humans, the patterns of MAFA and MAFB expression in the human differ to those of the mouse, both spatially and temporally. MAFA expression is observed throughout the developing pancreatic epithelium, including in the developing endocrine cells, from 9wpc (Riedel et al., 2012). In INSULIN$^+$ cells, strong nuclear expression of MAFA is observed, whereas, weaker expression is seen throughout the remaining epithelium. By

13wpc, MAFA has begun to be downregulated, with weak MAFA expression restricted to the INSULIN$^+$ cells, and by 21wpc, no expression of MAFA is observed. However, nuclear localized beta-cell specific of MAFA expression is observed in the adult human pancreas, similar to that observed for the mouse (Riedel et al., 2012). In contrast to the findings of Riedel *et.al,* others have found that transcripts encoding *MAFA* are first detected at 9wpc and increase thereafter, with expression being maintained until at least 23wpc (albeit at levels lower than found in the adult) (Sarkar et al., 2008). Taking these two studies together raises the possibility that expression of MAFA might be modulated at both the transcriptional and post-transcriptional level during human pancreatic development.

In a study by Riedel and colleagues, MAFB expression was also first observed in a similar spatial pattern to MAFA expression at 9wpc in both the INSULIN$^+$ cells and developing pancreatic epithelium. However, by 14wpc, expression of MAFB had become restricted to INSULIN$^+$ and GLUCAGON$^+$ cells. This expression was then maintained throughout development, and was observed in the both the alpha- and beta-cells of the adult (Riedel et al., 2012). In contrast, MafB expression has not been observed in insulin$^+$ cells of the adult mouse islet (Artner et al., 2006).

**Table 1.1. Studies reporting the differentiation of human ES cells to pancreatic endoderm and their subsequent transplantation**

| Reference | Differentiation conditions | Endocrine hormones | Human C-peptide | GSIS | Transplantation site | Amelioration of hyperglycaemia |
|---|---|---|---|---|---|---|
| (Kroon et al., 2008) | Adherent monolayer on MEFs | INS, GCG, SST, PP, GHRL | Yes | *In vivo* | Epididymal fat pad | Yes |
| (Jiang et al., 2007b) | Adherent monolayer on matrigel | INS, GCG, SST | Yes | Marginal *in vitro*; *in vivo* | Kidney capsule | Yes |
| (Shim et al., 2007) | Suspension | INS, GCG, SST | Yes | *In vivo* | Kidney capsule | Yes |
| (Rezania et al., 2012) | Adherent monolayer on Matrigel | INS, GCG, SST, PP | Yes | *In vivo* | Kidney capsule | Yes |

GCG – Glucagon; GHRL – Ghrelin; GSIS – Glucose stimulated insulin secretion; INS – Insulin; MEF – Mouse embryonic fibroblast; SST – Somatostatin; PP – Pancreatic polypeptide

**Table 1.2. Studies reporting the differentiation of human ES cells to insulin-expressing cells and their subsequent transplantation**

| Reference | Differentiation conditions | Endocrine hormones | Human C-peptide | GSIS | Transplantation site | Amelioration of hyperglycaemia |
|---|---|---|---|---|---|---|
| ADDIN EN.CITE ( | Suspension | INS, GCG, SST | Yes | Marginal *in vitro* | Intraperitoneal injection | No |
| (Eshpeter et al., 2008) | Adherent monolayer on matrigel | INS, GCG, SST | Yes | Moderate *in vitro* | Kidney capsule | No |
| (Mao et al., 2009) | Adherent on gelatin | INS, GCG, SST | Yes | Not detected | Kidney capsule; Subcutaneous | Only when fasting |
| (Basford et al., 2012) | Suspension, then adherent on gelatin | INS, GCG, SST | Yes | Not detected *in vitro* | Mammary fat pad | No, as only $GCG^+$ cells observed |

GCG – Glucagon; GSIS – Glucose stimulated insulin secretion; INS – Insulin; MEF – Mouse embryonic fibroblast; SST – Somatostatin;

## 1.3 Summary

Over the past 6 years, numerous thematically related methods for the generation of pancreatic progenitor cells have been reported. Many of these protocols derive pancreatic progenitors *in vitro* and then subsequently transplant these progenitors to allow the further development of functional beta cells that display glucose-stimulated insulin release. The use of pancreatic progenitors as a platform for the treatment of type 1 diabetes has a number of advantages over the use of more differentiated INSULIN$^+$ cells. First and foremost of these is that cues required for the final steps of differentiation may not need to be identified, nor understood, in order to achieve a therapeutic endpoint.

In contrast to the situation with pancreatic progenitors, whilst methods for the production of INSULIN$^+$ cells have been developed, these insulin-expressing cells do not generally display an ability to release insulin in response to glucose *in vivo*. In fact, several groups have reported the loss of insulin$^+$ cells following transplantation and their replacement with alternative cell types (see table 1.2). The fact that adult islets do not show the same paucity of function or longevity suggests that INSULIN$^+$ cells generated *in vitro* from differentiating hESCs still require further instructions before they reach a stage of functionality akin to that of mature beta cells.

Ultimately, whether progenitors or fully differentiated and functional beta cells prove to be the best hope of a transplantation based cell therapy for the treatment of type 1 may not be resolved until *in vitro* derived cell populations are trialed in humans. In the interim, efforts to further refine the generation of both progenitor populations and fully functional beta cells will still remain an area of intense interest for ongoing research.

## 1.4 Aims of the study

This study had three specific aims: First, to derive INSULIN$^+$ cells from hESCs, using an animal product-free, serum-free medium in combination with specific growth factors. Second, modify to an existing INSULIN$^{GFP/w}$ hESC reporter line by the insertion of a luciferase transgene in order to facilitate the analysis of transplantation of cells in mice. The final aim of this study was to analyse the maturity and functionality of INSULIN$^+$ cells and to compare their stage of development to both previously published hESC-derived INSULIN$^+$ cells and to human beta cells.

# CHAPTER 2

## A NOVEL PROTOCOL FOR THE GENERATION OF PANCREATIC CELLS FROM HUMAN ES CELLS

## 2.1 Introduction

Embryonic stem cells (ESCs) are pluripotent cells derived from blastocyst stage pre-implantation embryos ((Evans and Kaufman, 1981), (Martin, 1981), (Thomson et al., 1998)) and have the capacity to generate cells representative of both extra-embryonic tissues and all three somatic germ layers *in vitro* ((Vallier et al., 2009), (Macfarlan et al., 2012)). The *in vitro* differentiation capacity of human ESCs (Reubinoff et al., 2000) has raised the possibility for ESC-derived cell based therapies in the future, such as for the treatment of type 1 diabetes. In this context, many groups have reported methods for generation of either pancreatic endoderm or endocrine cells from hESCs *in vitro* (reviewed in: (Van Hoof et al., 2009), also (Shi, 2010), (Nostro et al., 2011), (Rezania et al., 2012)). We recently described one such protocol that generated INSULIN$^+$ cells following approximately 20 days of differentiation. Unlike many protocols reported previously, our method produced an endocrine population that included mono-hormonal INSULIN$^+$ cells, a substantial fraction of which co-expressed the late stage differentiation marker NKX6.1. In this report, we describe a step-by-step description of how to perform this method along with a detailed list of reagents required for its execution.

### 2.1.1 Overview of the protocol

This protocol employs a modified version of a fully recombinant protein based medium (APEL) in conjunction with 96 well tray spin embryoid body (Spin EB) format ((Ng et al., 2008a), (Ng et al., 2008b)), and growth factors identified from the literature as contributing towards both pancreatic embryogenesis as well as in the formation of obligate intermediate cell types. The generation of INSULIN-producing cells (and other endocrine cell types) takes approximately 1 month, although the emergence of INSULIN$^+$ cells can be observed as early as d20 of differentiation. This protocol for the generation of INSULIN$^+$ cells has 5 main steps: 3 days of exposure to BMP4 and Activin A (stage 1); 3 days exposure to Dorsomorphin, a small molecule inhibitor of BMP signalling that is included to promote and pattern the hESC-derived definitive endoderm (stage 2); 3 days of exposure to all-trans retinoic acid (RA) to generate foregut endoderm (stage 3); 7 days of exposure to nicotinamide, glucagon-like peptide-1 (GLP-1), B27 supplement and RA to form pancreatic endoderm (stage 4); and a minimum of 5 days of exposure to nicotinamide and IGF-1 in order to induce INSULIN (and other endocrine hormone) expression (stage 5) (shown below in figure 2.1). During this differentiation period, cells are seen to transit through obligate intermediate cell types including definitive and pancreatic endoderm. A subset of

the INSULIN+ cells produced by this method lack expression of other hormones, such as glucagon or somatostatin and express the transcription factor NKX6.1, which is thought to mark mature beta cells.

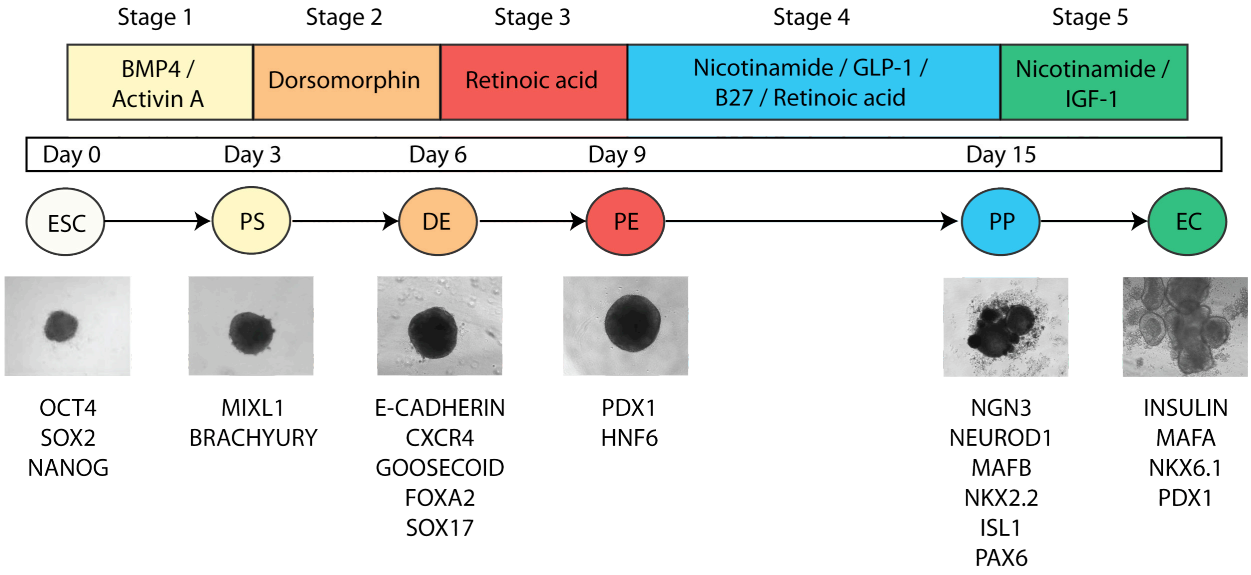


**Figure 2.1.** Overview of a 5-stage protocol, which results in the generation on INSULIN+ cells from human embryonic stem cells. The upper row shows the specific growth factors used to promote each step. The central rows show the developmental stages and appearance of EBs at each step of the differentiation process. The lower row shows genes commonly used to identify cells at each step. *DE – Definitive Endoderm; EC – Endocrine cell; ESC- Embryonic stem cell; PE – Pancreatic endoderm; PP – Pancreatic Progenitor; PS – Primitive streak.*

This protocol utilises two genetically modified human ESC reporter lines – a transgenic PDX$^{GFP}$ hESC line (A. Holland and E. Stanley, unpublished) and a targeted INSULIN$^{GFP/w}$ hESC line (Micallef et al., 2012) in order to objectively monitor the formation of PDX1+ pancreatic endoderm and INSULIN+ cells respectively.

### 2.1.2 Applications of the method

Apart from their utility in monitoring the progress of differentiation, the use of hESC reporter lines allows for the facile purification of either INSULIN+ or PDX1+ cells by FACS. These purified populations can then be employed for further experiments including *in vitro* assays to assess beta-cell maturation and replication or *in vivo* studies to assess cell function.

### 2.1.3 Comparison with other methods

It has been demonstrated by a number of groups that hESCs (and induced pluripotent stem cells, (iPSCs)) have the capacity to generate insulin-producing cells. However, many of these methods utilise serum (including, but not limited to: (Kroon et al., 2008), (Chen et al., 2009), (Rezania et al., 2012)), which may limit the ease with which such methods can be transferred to other laboratories and may undermine the efforts to control of the direction of differentiation. For example, it is possible that undefined factors present in serum may be in part responsible for the predominance of polyhormonal INSULIN$^+$ cells generated by many protocols. These polyhormonal cells are thought to represent an immature endocrine cell phenotype whose developmental relationship to fully functional mature β-cells remains unclear.

In addition to those studies mentioned above, numerous other groups have reported methods for the differentiation of hESCs to INSULIN$^+$ cells (reviewed in: (Van Hoof et al., 2009), also (Nostro et al., 2011), (Cheng et al., 2012)). Our differentiation method differs from previous protocols for a number of reasons: firstly, this protocol generates INSULIN$^+$ cells, of which a substantial subpopulation lack expression of other endocrine hormones (i.e. are monohormonal) and co-express the transcription factor NKX6.1. These monohormonal INSULIN$^+$ cells potentially represent a more mature cell type than has been previously reported in the literature. Secondly, as this protocol utilises an animal-product free, completely defined media (APEL) (Ng et al., 2008a), this allows for the effects of growth factor addition to be more accurately verified. In particular, this medium base lacks components such as serum or serum-derivatives, which may influence the differentiation of human ESCs towards a pancreatic endocrine cell fate. The use of the APEL medium also permits inconsistencies arising from batch to batch variation to be minimised. Finally, the 96-well plate format used during the differentiation process, facilitates the testing of large numbers of parameters, and is compatible with the potential use of high-throughput screening methodologies.

## 2.2 Materials

### 2.2.1 Reagents

**Cells**

- INSULIN$^{GFP/w}$ or Tg.PDX1$^{GFP}$ human ESCs ((Micallef et al., 2012), (A. Holland and E. Stanley, unpublished))
- Mitotically inactivated mouse embryonic fibroblasts (MEFs)

**Growth media and supplements**

- DMEM, high glucose (Invitrogen, cat. no. 11960-044)
- IMDM, no phenol-red (Invitrogen, cat. no. 21056-025)
- Hams F-12 nutrient mix with GlutaMaxI (Invitrogen, cat. no. 31765-035)
- DMEM/F12 (Invitrogen, cat. no. 11320-033)
- 2-mercaptoethanol (Invitrogen, cat. no. 21985-023)
- α-Monothioglycerol (Sigma, cat. no. M6145)
- Albucult (rh Albumin) (Novozymes Delta, cat. no. 230-005)
- Ascorbic acid 2-phosphate (Sigma-Aldrich, cat. no. A8960)
- B27 supplement (50x; Invitrogen cat. no. 17504044)
- DeltaFerrin (rh holotransferrin) (Novozymes Delta, cat. no. 122-001)
- Ethanolamine ≥98% (16.6M; Sigma-Aldrich, cat. no. EO135)
- GlutaMaxI (200mM; Invitrogen cat. no. 35050-061)
- Knockout serum replacement (Invitrogen, cat. no. 10828-028)
- L-glutamine (100x; Invitrogen cat. no. 25030-81)
- Linoleic acid (Sigma-Aldrich, cat. no. L2376)
- Linolenic acid (Sigma-Aldrich, cat. no. L1012)
- MEM Non Essential Amino Acids (100x; Invitrogen, cat. no. 11140-050)
- Penicillin-streptomycin (100x; Invitrogen cat. no. 15140-122)
- Polyvinyl alcohol (Sigma-Aldrich, cat. no. P8136)
- rh Insulin (Sigma-Aldrich, cat. no. I2643)
- Sodium Selenite (Sigma, cat. no. S5261)
- SyntheChol (Sigma-Aldrich, cat. no. C1231)

**Enzymes and growth factors**

- TryPLE select (Invitrogen, cat. no. 12563-029)
- Activin A (StemRD, cat. no. ACT-100)
- BMP4 (R&D Systems, cat. no. 314-BP)
- Dorsomorphin (Stemgent, cat. no. 04-0024)
- All-trans Retinoic Acid (Sigma-Aldrich, cat. no. R2625)
- Nicotinamide (Sigma-Aldrich, cat. no. 72340)
- GLP-1 (Sigma-Aldrich, cat. no. G3265)
- IGF-1 (R&D Systems, cat. no. 291-G1-01M)
- bFGF (Peprotech, cat. no. 100-18B)
- Y-27632 (Calbiochem, cat. no. 688000)

**Other reagents and chemicals**

- CMF-PBS (Invitrogen, cat. no. 10010-023)
- Gelatin Powder (Sigma-Aldrich, cat. no. G9136)
- Trypan Blue (Sigma-Aldrich, cat. no. T8154)

### 2.2.2 Equipment

- 150cm$^2$ tissue culture flask with vented cap (BD Falcon, cat. no. 355001)
- 75cm$^2$ tissue culture flask with vented cap (BD Falcon, cat. no. 353136)
- 15ml centrifuge tube (BD Falcon, cat. no 352096)
- 50ml centrifuge tube (BD Falcon, cat. no. 352070)
- 0.22mm SteriCup filtration unit, 250ml (Millipore, cat. no. SCGPUO2RE)
- 0.22mm SteriCup filtration unit, 500ml (Millipore, cat. no. SCGPUO5RE)
- Corning 96 well plates, round-bottom (Costar, cat. no. 3788)
- Serological pipettes (Falcon 5ml; cat. no. 357543, 10ml; cat. no. 357551)
- Sterilized filter pipette tips (2, 20, 200, 1000ml)
- Pipetman single-channel pipettes (Gilson 2ml; cat. no. F144801, 20ml; cat. no. F123615, 200ml; F123601, 1000ml; F123602)
- Pipet-aid AP cordless motorized serological pipettor (BD Falcon, cat. no. 357590)
- Refrigerated centrifuge (Sigma 4K15, Sigma) and 96-well plate spinner attachment
- Tissue culture incubator at 5% $CO_2$

### 2.2.3 Reagent Setup

**Note:** This protocol is specifically designed for hESCs passaged enzymatically using TryPLE select or trypsin. A detailed description of methods for passaging cells in this manner is provided elsewhere ((Costa et al., 2008)).

**Human ES cell medium**

Combine DMEM/F12 with 20% (vol/vol) knockout serum replacer, 10mM MEM Non-essential amino acids, 2mM GlutaMaxI, 1x penicillin/streptomycin, 50mM 2-mercaptoethanol and 10ng/ml bFGF. Filter sterilize prior to use. Can be stored at 4°C for up to 2 weeks ((Amit et al., 2000))

**MEF medium**

Combine DMEM with 10% (vol/vol) heat-inactivated FCS, 2mM L-Glutamine and1x penicillin/streptomycin. Filter sterilize prior to use. Can be stored at 4°C for up to 2 weeks.

**Sodium Selenite**

Dissolve 70mg sodium selenite in 100ml of CMF-PBS. Filter sterilize prior to be use. Can be stored at 4°C for up to 12 months.

**Linoleic and Linolenic acids**

Prepare 10,000x stock solutions by dissolving 10ml of pure oil in 10ml of ethanol. Mix thoroughly, and aliquot into smaller volumes. Can be stored at -20°C for up to 12 months.

**rh Insulin**

Prepare a 5mg/ml suspension in CMF-PBS. Can be stored at 4°C for up to 3 months

**rh Insulin-transferrin-selenium-ethanolamine solution (rhITS-X)**

To make 10ml of 100x rhITS-X solution, combine 10ml sodium selenite solution, 2ml rh insulin suspension, 270ml rh holotransferrin and 20ml ethanolamine, with 7.7ml of CMF-PBS. Can be stored at 4°C for at least 3 months.

**Differentiation medium (APEL medium)**

Prepare a 5% (wt/vol) stock solution of polyvinyl alcohol (PVA), by adding 5g of PVA to 100ml of $dH_2O$ and leave to dissolve at 4°C for 48 hours. Make a PVA lipids mixture by adding ~20ml of IMDM/F12 mixture to a 50ml tube, followed by the required volumes of PVA stock, SyntheChol, linoleic and linolenic acids for 200ml APEL medium as shown in table 1. Mix the contents of the tube thoroughly. Add the remaining media components directly to the upper chamber of a 0.22mm SteriCup filtration unit, followed by the PVA-lipids mixture, then filter the medium. APEL medium can be prepared the day prior to differentiation setup, and can be stored at 4°C for at least 2 weeks.

**Table 1. Formulation for 200ml APEL medium**

| Medium Component | Stock solution | Volume per 200ml APEL | Final concentration |
|---|---|---|---|
| IMDM | 1x | 90.2ml | 1x |
| Hams F12 nutrient mixture | 1x | 90.2ml | 1x |
| Albucult (rh Albumin) | 100mg/ml (10%) | 10ml | 5mg/ml |
| PVA | 5% | 2ml | |
| Linoleic acid | 10,000x | 20ml | 100ng/ml |
| Linolenic acid | 10,000x | 20ml | 100ng/ml |
| SyntheChol | 7,200x | 28ml | 2.2mg/ml |
| a-MTG | 13ml in 1ml IMDM | 600ml | 39nl/ml |
| rhITS-X | 100x | 2ml | 1x |
| Ascorbic acid 2 phosphate | 5mg/ml | 2ml | 5mg/ml |
| GlutaMaxI | 200mM | 2ml | 2mM |
| Penicillin/streptomycin | 200x | 1ml | 1x |

**Growth Factor reconstitution**

Reconstitute growth factors as follows:

- In 1x CMF-PBS to the following concentrations: Activin A - 100mg/ml, IGF1 – 100mg/ml
- In DMSO to the following concentrations: Dorsomorphin – 10mM, all trans retinoic acid -10mM
- In 4mM HCl with 0.1% BSA to the following concentrations: BMP4 – 100mg/ml
- In 50mM acetic acid to the following concentrations: GLP1 – 100mM
- In 5mM Tris buffer, pH: 7.6 to the following concentrations: bFGF – 1mg/ml

**Stage 1 differentiation medium**

Combine APEL medium with BMP4 (final concentration - 10ng/ml) and Activin A (final concentration - 200ng/ml). Stage 1 differentiation medium is best if made fresh, but can be stored at 4°C for 1-2 days.

**Stage 2 differentiation medium**

Combine APEL medium with Dorsomorphin (final concentration – 1.75mM). Stage 2 differentiation medium is best if made fresh, but can be stored at 4°C for 1-2 days.

**Stage 3 differentiation medium**

Combine APEL medium with all trans retinoic acid (final concentration – $10^{-5}$M). Stage 3 differentiation medium is best if made fresh, but can be stored at 4°C for 1-2 days.

**Stage 4 differentiation medium**

Combine APEL medium with nicotinamide (final concentration – 10mM), GLP1 (final concentration – 100nM), all trans retinoic acid ($10^{-5}$M) and B27 supplement (final concentration – 1x). Stage 4 differentiation medium is best if made fresh, but can be stored at 4°C for 1-2 days.

**Stage 5 differentiation medium**

Combine APEL medium with nicotinamide (final concentration – 10mM) and IGF1 (final concentration – 50ng/ml). Stage 5 differentiation medium is best if made fresh, but can be stored at 4°C for 1-2 days.

## 2.3 Procedure

**Passaging human ESCs TIMING 2 hours**

**1)** At least 1 hour prior to passaging hESCs, prepare a 150cm$^2$ gelatinised tissue culture flask seeded with MEFs at a density of 1.0 x $10^4$/cm$^2$ (low density) in MEF medium.

**2)** Start with a 150cm$^2$ flask of human ESCs that are 80-90% confluent and are free of differentiated cell types. Aspirate human ES cell medium from the flask.

**3)** Rinse the flask with 10ml CMF-PBS, then aspirate CMF-PBS from the flask.

**4)** Cover the flask with 5ml TryPLE select, ensuring that the solution coats the entire flask surface, and incubate at 37°C for 4 minutes. Tap the flask gently to ensure that cells have dislodged from the plastic.

**5)** Add 10ml of CMF-PBS to the flask and using a pipette triturate cell clumps by withdrawing solution then forcefully expelling back into the flask.

**6)** Transfer the cell suspension to a 15ml conical tube, and centrifuge for 3 minutes at 480g, at 4°C

**7)** Aspirate the supernatant and resuspend the cell pellet in hESC medium. Distribute the resuspended cells onto the 150cm$^2$ flask pre-seeded with MEFs (step 1 above) at a 1:2 – 1:3 ratio (dependant on hESC line used).

**8)** Incubate the newly passaged human ESCs overnight at 37°C, 5% $CO_2$

**Harvesting hESCs for spin EB generation and differentiation to definitive endoderm**

**TIMING 6 days**

**9)** Approximately 2-3 hours prior to the setup of differentiation, aspirate the medium from the human ESCs that were passaged the day before, and replace with 20mls of fresh hESC medium.

**10)** To initiate the differentiation process, harvest the hESCs by first aspirating the hESC medium and then rinsing the flasks with 10ml CMF-PBS. Aspirate the CMF-PBS from the flask(s).

**11)** Add 5ml of TryPLE select to the flask and incubate at 37°C for 4 minutes. Gently tap the flasks in order to dislodge the hESCs from the flask surface.

**12)** Add 10ml of CMF-PBS to the flask, and using a pipette, triturate cell clumps by withdrawing solution then forcefully expelling back into the flask.

**13)** Transfer the cell suspension into a 15ml conical tube, and centrifuge for 3 minutes at 480g, at 4°C.

**14)** Aspirate the supernatant and resuspend the hESC pellet in 10ml of differentiation medium. Remove a 10μl volume for a cell count.

**15)** Perform a cell count ((Phelan, 2006)), and subtract the total number of MEFs (1.5 x 10$^6$ MEFs per 150cm$^2$ flask) from the count. The total number of hESCs required will depend both on the cell line and the number of 96-well plates required for the differentiation.

**16)** Determine the total number of cells required and the total volume of stage 1 differentiation medium needed for the experiment. Generally, between 2,500 and 3,500 hESCs in 100ml of stage 1 differentiation medium per well are used, dependent on cell line. Add cells to the stage 1 differentiation medium

**17)** Using a multichannel pipette, pipette the cell suspension into the 96-well plates.

**18)** Centrifuge for 5 minutes at 480g, at 4°C in order to aggregate cells within the wells of the plate.

**19)** Place 96-well plates in an incubator at 37°C, 5% $CO_2$.

**20)** After 3 days, remove 96-well plates from incubator and aspirate the media from the wells, being careful not to aspirate the spin EBs that have formed. No wash step is required.

**21)** Add 100ml per well of stage 2 differentiation medium, using a multichannel pipette. Place 96-well plates in an incubator at 37°C, 5%$CO_2$ for a further 3 days.

**Differentiating human DE into foregut endoderm TIMING 3 days**

**22)** Remove 96-well plates from incubator, and aspirate media from wells, being careful not to aspirate spin EBs. No wash step is required.

**23)** Using a multichannel pipette, add 100ml per well of stage 3 differentiation medium

**24)** Place 96-well plates in an incubator at 37°C, 5% $CO_2$ for a further 3 days

**Differentiating human foregut endoderm to pancreatic endoderm TIMING 7 days**

**25)** Remove 96-well plates from incubator, and aspirate medium from wells, being careful not to aspirate spin EBs. No wash step is required.

**26)** Using a multichannel pipette, add 100ml per well of stage 4 differentiation medium.

**27)** Place 96-well plates in an incubator at 37°C, 5% $CO_2$ for 7 days.

**28)** At this stage of differentiation, if the Tg.PDX1$^{GFP}$ human ESC line has been used, GFP expression should be visible by either fluorescence microscopy or flow cytometric analysis.

**Differentiating human pancreatic endoderm to INSULIN- expressing endocrine cells TIMING 5 days**

**29)** Remove 96-well plates from incubator, and aspirate media from wells, being careful not to aspirate spin EBs. No wash step is required.

**30)** Using a multichannel pipette, add 100ml per well of stage 5 differentiation medium.

**31)** Place 96-well plates in an incubator at 37°C, 5% CO2, for at least 5 days.

**32)** At this stage of differentiation, if the INSULIN$^{GFP/w}$ hESC line has been used, GFP expression should begin to become evident by either fluorescence microscopy or flow cytometric analysis.

**Isolation of INSULIN-GFP$^+$ or PDX-GFP$^+$ cells following differentiation, by fluorescence-activated cell sorting (FACS) TIMING 3-5 hours**

**33)** Remove 96-well plates from the incubator and harvest medium and spin EBs using a pipette. Transfer the spin EBs to 50ml conical tubes and place the filled tubes on ice, until ready to centrifuge all tubes.

**34)** Centrifuge for 3 minutes at 480g, at 4°C.

**35)** Aspirate supernatant, and resuspend spin EBs in 1ml of TryPLE select. Place tubes containing the EBs in a 37°C waterbath for 20mins.

**36)** Add 1ml of CMF-PBS per tube, and using a pipette, pipette cell suspension vigorously, to ensure a single-cell suspension is formed. Transfer cell suspension into a cell-strainer cap on top of a 5ml polystyrene tube.

**37)** Centrifuge tubes for 5 minutes at 480g, at 4°C, in order to filter cell clumps from the cell suspension, and to pellet single-cells in the 5ml tubes.

**38) Optional –** if required, staining of cell surface antigens, or intracellular antigens can be performed at this point in the protocol.

**39)** Add 2ml of stage 5 differentiation media to a 5ml polystyrene tube for each sample to be collected following cell sorting.

**40)** Resuspend cell pellets in 1x propidium iodide solution, and keep on ice until cell sorting is performed.

**41)** If the cells are to be cultured following sorting, a sterilised flow cytometer should be used. During sorting, viable cells can be identified by propidium iodide exclusion. Both GFP$^+$ and GFP$^-$ cells can be collected for further culture or preparation of RNA samples. Collect sorted cells in previously prepared collection tubes.

**42)** If cells are to be re-cultured they should be kept on ice until they are reaggregated (see below).

**Re-aggregation of isolated INSULIN-GFP$^+$ or PDX1-GFP$^+$ cells for further culture**

**TIMING Variable**

**Note:** In our experience, isolated hESC-derived pancreatic cells survive very poorly as either single cell suspensions or if transferred to an adherent promoting substrate. This problem can be circumvented by re-aggregating the cells within (2 hours) following isolation by FACS.

**43)** Best results are obtained when cells are formed into aggregates of between 2,000 and 3,000 cells. Estimate the number of cells recovered from FACS by either using the data from flow cytometer or performing a cell count using traditional methods (i.e. use of a haemocytometer).

**44)** Add the determined number of cells to a sufficient volume of stage 5 differentiation medium to yield a final concentration of 2000-3000 cells per / 100 µl. Then add the Rho Kinase (ROCK) inhibitor Y27632 to a final concentration of 10µM. This agent is added to assist the re-aggregation process ((Watanabe et al., 2007)). Using a pipette, distribute 100µl of cell suspension into each well of a 96-well plate.

**45)** Aggregate the cells by centrifugation at 480g, at 4°C for 5 minutes, then place 96-well plates in an incubator at 37°C, 5% $CO_2$.

**46)** After 24-48 hours, remove the 96-well plates from the incubator, and aspirate the media from each well, being careful not to aspirate the re-aggregated cells.

**47)** Add 100µl per well of stage 5 differentiation media. The purpose of this step is to remove the ROCK inhibitor. At this stage, other factors that investigators may wish to examine can be added. Replace 96-well plates into an incubator at 37°C, 5% $CO_2$.

**48)** Media should continue to be replaced every 5-7 days. We have cultured reaggregated cells in this format for up to 120 days post FACS.

## 2.4 Troubleshooting

Troubleshooting advice can be found in table 2.

**Table 2. Commonly encountered problems when differentiating hESC cells towards a pancreatic fate**

| Step | Problem | Possible reason(s) | Solution |
|---|---|---|---|
| 9-19 | Low viability following setup | Feeder Batches | Setup using different feeder batch; Screen feeder batches prior to use |
| 20-21 | EBs generate heart | BMP4 concentration may be too high producing mesoderm rather than endoderm | Examine EpCAM/PDGFRα levels at day 6 and re-titrate BMP4 level |
| 25-28 | Little PDX1+ endoderm | Retinoic acid concentration is too high or too low | Re-titrate retinoic acid concentration |
| 29-32 | Uneven distribution of INSULIN+ EBs across plate | Oxygenation levels | Check frequency of incubator access |

## 2.5 Timing

Steps 1-8, Passaging human ESCs: 2 hours

Steps 9-21, Harvesting human ESCs for differentiation setup and differentiation to DE: 6 days

Steps 22-24, Differentiating DE to foregut endoderm: 3 days

Steps 25-28, Differentiating foregut endoderm to pancreatic endoderm: 7 days

Steps 29-32, Differentiating pancreatic endoderm to endocrine cells: 5 days

Steps 33-42, Isolating $GFP^+$ cells using FACS: 3-5 hours

Steps 43-48, Re-aggregating isolated cells for further culture: variable, up to 120 days (in our hands, cells are still viable at 120 days, but we have not extended culture past this time point)

## 2.6 Anticipated Results

This protocol describes a directed differentiation method that results in the generation of pancreatic endocrine cells, including insulin-expressing cells, from human ESCs. Each step of the differentiation procedure aims to recapitulate aspects of processes occurring during human endocrine cell development. As such, the method generates cell populations representing obligate intermediates observed during embryogenesis as cells transit from the pluripotent state towards committed endocrine cells. Similar to methods reported by others, the formation of definitive endoderm can be observed following 6 days of differentiation. This cell type is marked by the co-expression of CXCR4 and E-Cadherin, and comprises ~80% of the population. Following the formation of the definitive endoderm, a number of patterning steps are used to guide the cells towards an endocrine cell fate. By day 15 of culture, the pancreatic endoderm has begun to form, as marked by the appearance of $PDX1^{+}$ cells. If using the $Tg.PDX1^{GFP}$ human ESCs, GFP can be quantified using flow cytometric analysis – in a typical experiment, it is expected that up to 30% of cells will express PDX1-GFP by day 20 of differentiation. Following the addition of nicotinamide and IGF-1, endocrine cells, and specifically, $INSULIN^{+}$ cells have begun to form. If using the $INSULIN^{GFP/w}$ human ESCs, GFP can be quantified using flow cytometric analysis. In a typical experiment, it is expected that up to 5-15% of cells will express INSULIN-GFP by day 30 of differentiation (figure 2.2).

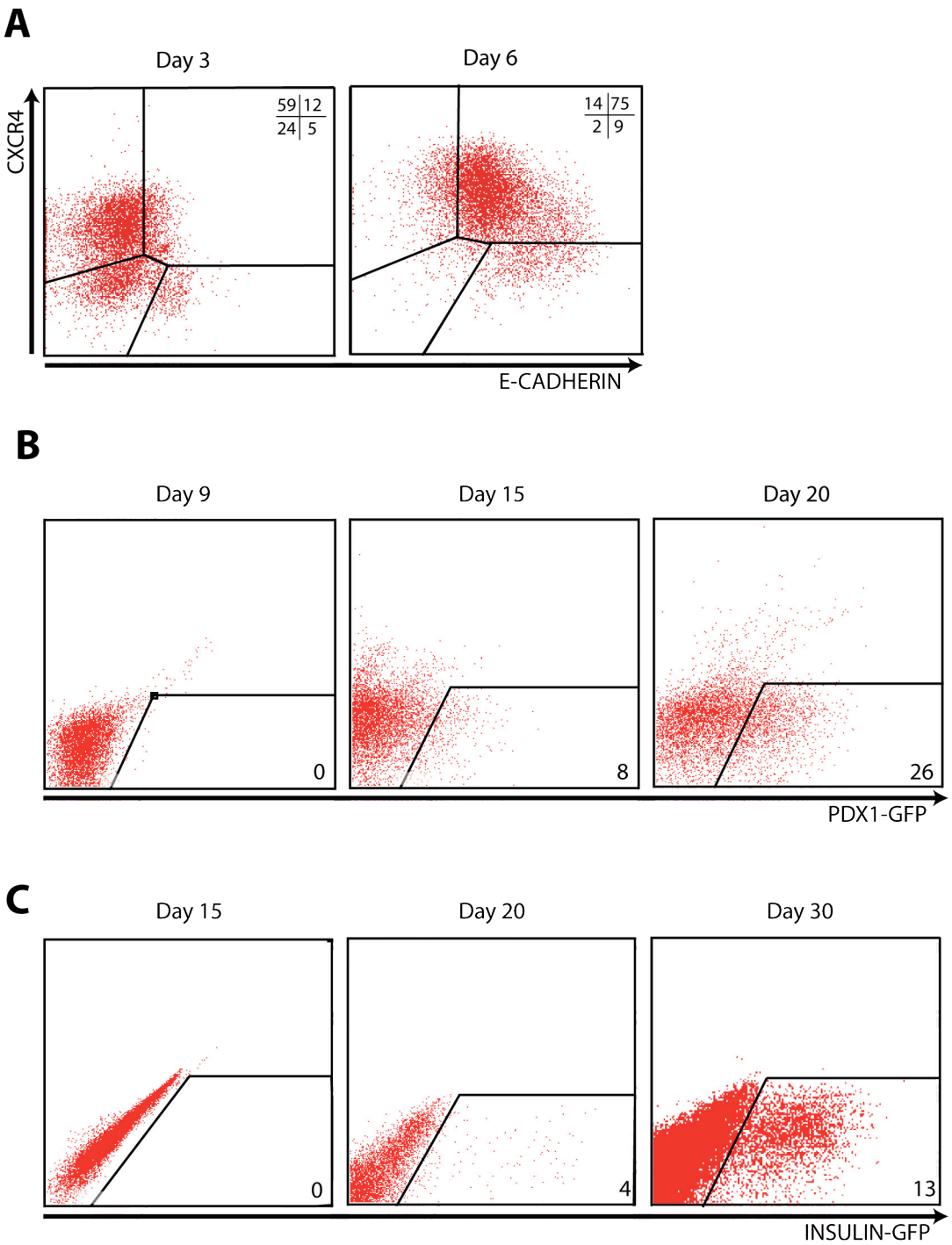


**Figure 2.2:** Flow cytometric analysis of differentiating hESCs. **(A)** Developing definitive endoderm can be identified by co-expression of CXCR4 and E-CAD, **(B)** The emergence of PDX1-GFP$^+$ cells can first be observed at day 15 of differentiation, **(C)** INSULIN-GFP$^+$ cells can first be observed at day 20 of differentiation. The numbers present in the bottom right-hand corner represent the percentage of positive cells. The gene being analysed by flow cytometry is labelled on either the x- or y-axis as relevant.

Following the specification of INSULIN$^+$ cells, if using an INSULIN$^{GFP/w}$ hESC reporter line, these can be isolated on the basis of GFP expression using FACS. FACS purified INSULIN$^+$ cells may be re-aggregated in the presence of Y27632, Nicotinamide and IGF-1 (figure 2.3).

These may then be kept in culture in order to allow for further maturation for at least 4 months (with regular media changes). It is likely that the re-aggregates may be cultured for longer periods of time; however, this has not yet been tested. FACS purified INSULIN-GFP$^-$ cells are also able to be aggregated in the presence of Y27632 (figure 2.3D), though whilst many of the INSULIN-GFP$^-$ cells fail to survive within the aggregates, >95% of the raggregates have formed by day 5, which is comparable to what is seen with INSULIN-GFP$^+$ cells.

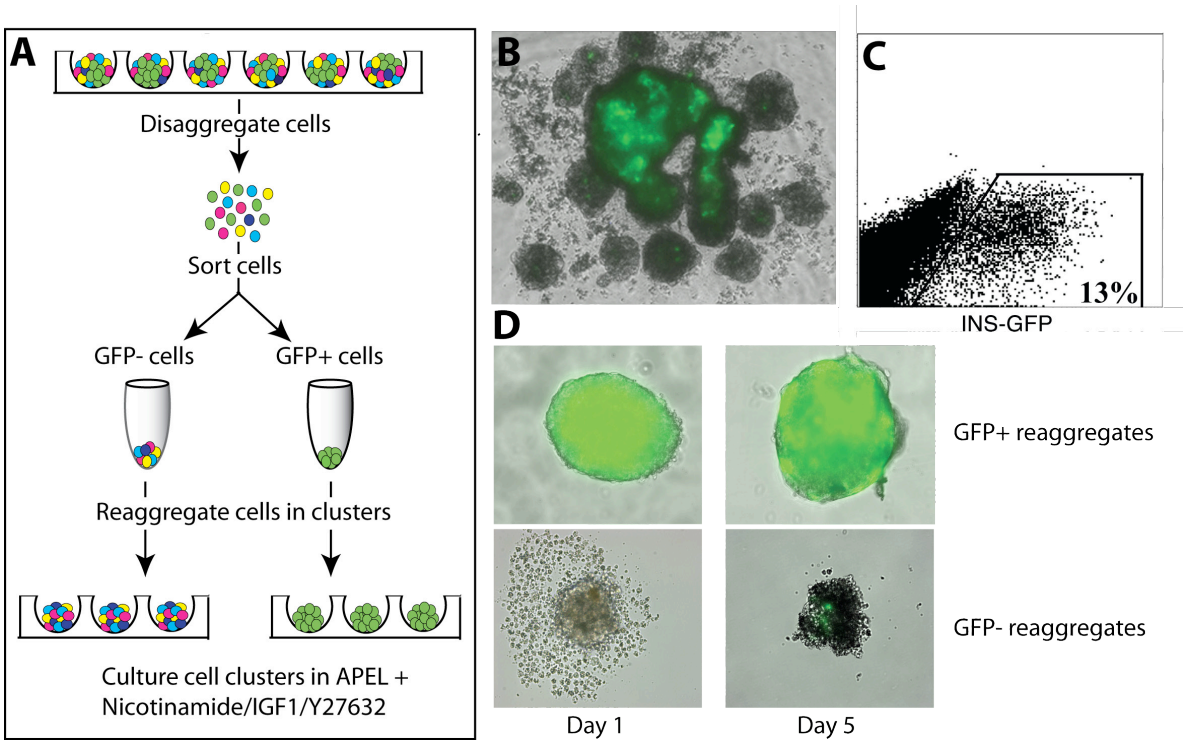


**Figure 2.3.** Isolation and re-culture of INSULIN-GFP$^+$ and INSULIN-GFP$^-$ cells **(a)** Schematic demonstrating the process of isolating both INSULIN-GFP$^+$ and INSULIN-GFP$^-$ cells and their subsequent reaggregation; **(b)** Appearance of a spin EB composed of INSULIN$^{GFP/w}$ hESCs following 30 days of differentiation; **(c)** Following 30 days of differentiation, INSULIN-GFP$^+$ cells can be isolated using flow cytometry – in this example, 13% of differentiated cells expressed GFP; **(d)** Following isolation by flow cytometry, INSULIN-GFP$^+$ and INSULIN-GFP$^-$ cells can be aggregated to form cell clusters. In wells containing aggregates of GFP$^+$, most cells contribute to the cell clusters. Conversely, in wells containing GFP$^-$ cells, many cells fail to contribute the main cell cluster. These orphan cells have a dull morphology and eventually fragment, consistent with a loss of viability.

In summary, this chapter has described a novel protocol for the generation of pancreatic cells from hESCs. These pancreatic cells formed express both PDX1 and INSULIN, and are examined further in chapters 3 and 4. A subpopulation of INSULIN$^+$ cells generated using this novel protocol, are monohormonal – i.e. lack the expression of other endocrine hormones (such as GCG and/or SST). This is in contrast to many previously published protocols, as earlier discussed. Whilst there are many potential contributors that could

account for this result, such as specific growth factors; we hypothesise that the 3D environment present in the spin EBs more closely mimics normal embryogenesis, both in regards to cell arrangement in space, and through the presence of other cell types – such as mesoderm-derived mesenchyme and endothelial cells (data not shown).

# Chapter 3

# INSULIN-GFP$^{+}$ CELLS GENERATED FROM HUMAN EMBRYONIC STEM CELLS RESEMBLE HUMAN PANCREATIC ENDOCRINE CELLS

**Monash University**

**Declaration for Thesis Chapter 3**

**Declaration by candidate**

In the case of Chapter 3, the nature and extent of my contribution to the work was the following:

| Nature of contribution | Extent of contribution (%) |
|---|---|
| Collection and assembly of data; data analysis and interpretation; critical revision and final approval of manuscript | 10 |
| Remainder of chapter | 100 |

The following co-authors contributed to the work described in the paper by Micallef *et. al* 2012:

| Name | Nature of contribution | Extent of contribution (%) for student co-authors only |
|---|---|---|
| **Dr Suzanne Micallef** | Conception of design; collection and assembly of data; data analysis and interpretation; manuscript writing; final approval of manuscript | |
| **Dr Xueling Li** | Collection and assembly of data; data analysis and interpretation; critical revision and final approval of manuscript | |
| **Dr Claire Hirst** | Collection and assembly of data; data analysis and interpretation; critical revision and final approval of manuscript | |
| **Ms Qing Yu** | Collection and assembly of data; data analysis and interpretation; critical revision and final approval of manuscript | 5 |
| **Dr Sue Mei Lim** | Collection and assembly of data; data analysis and interpretation; critical revision and final approval of manuscript | |
| **Dr M. Cristina Nostro** | Collection and assembly of data; data analysis and interpretation; critical revision and final approval of manuscript | |
| **Dr. David Elliot** | Collection and assembly of data; data analysis and interpretation; critical revision and final approval of manuscript | |

| | | |
|---|---|---|
| **Ms Farida Sarangi** | Collection and assembly of data; data analysis and interpretation; critical revision and final approval of manuscript | |
| **Prof. Leonard Harrison** | Provision of study materials; data analysis and interpretation ; critical revision and final approval of manuscript | |
| **Prof. Gordon Keller** | Provision of study materials; data analysis and interpretation ; critical revision and final approval of manuscript | |
| **Prof. Andrew Elefanty** | Conception and design; data analysis and interpretation; manuscript writing; financial support; final approval of manuscript | |
| **Prof. Ed Stanley** | Conception and design; data analysis and interpretation; manuscript writing; financial support; final approval of manuscript | |

| | | |
|---|---|---|
| **Candidate's Signature** | [redacted] | **Date:** 03/10/2012 |

**Declaration by co-authors**

The undersigned hereby certify that:

(1) the above declaration correctly reflects the nature and extent of the candidate's contribution to this work, and the nature of the contribution of each of the co-authors;
(2) They meet the criteria for authorship in that they have participated in the conception, execution, or interpretation, of at least part of the publication in their field of expertise;
(3) They take public responsibility for their part of the publication, except the responsible author who accepts overall responsibility for the publication;
(4) There are no other authors of the publication according to these criteria;
(5) Potential conflicts of interest have been disclosed to (a) granting bodies, (b) the editor or publisher of journals or other publications, and (c) the head of the responsible academic unit; and
(6) The original data are stored at the following location(s) and will be held for at least five years from the date indicated below:

| | |
|---|---|
| **Locations** | Monash Immunology and Stem Cell Laboratories, Monash University |
| | McEwan Centre for Regenerative Medicine, Toronto, Canada |

| | | |
|---|---|---|
| **Signature 1** | Dr. Suzanne Micallef | 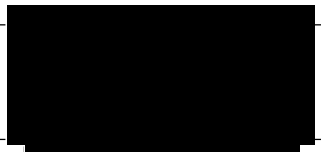 |
| **Signature 2** | Dr. Xueling Li |  |
| **Signature 3** | Dr. Claire Hirst |  |
| **Signature 4** | Ms. Qing Yu |  |
| **Signature 5** | Dr. Sue Mei Lim |  |
| **Signature 6** | Dr. M. Cristina Nostro |  |
| **Signature 7** | Dr. David Elliot |  |
| **Signature 8** | Ms. Farida Sarangi | 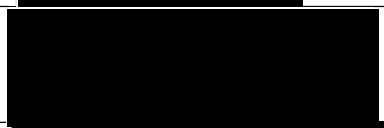 |
| **Signature 9** | Prof. Leonard Harrison | 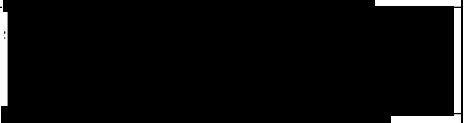 |
| **Signature 10** | Prof. Gordon Keller | 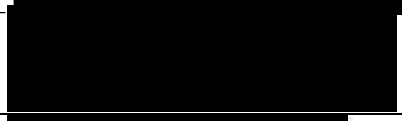 |
| **Signature 11** | Prof. Andrew Elefanty | 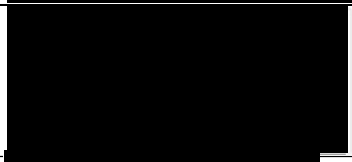 |
| **Signature 12** | Prof. Ed Stanley |  |

## 3.1 Introduction

The derivation of INSULIN+ cells from human embryonic stem cells has been reported previously by a number of groups (reviewed in: (Van Hoof et al., 2009), also more recently: (Nostro et al., 2011), (Xu et al., 2011), (Rezania et al., 2012)). However, many of these protocols utilise serum, or serum-derivatives, such as BSA, containing undefined constituents that are likely to influence both the efficiency of differentiation and method reproducibility. In particular, use of these agents can lead to batch dependent variation in differentiation outcomes as well as creating difficulties for the transfer of protocols between laboratories. Indeed, because components such as BSA may include signalling molecules known to play roles in pancreatic embryogenesis, such as retinoids ((Belatik et al., 2012)), and activin A ((Sakai et al., 1992)), inclusion of these agents is likely to confound attempts to achieve high levels of reproducibility.

In addition to the confounding affects caused by medium constituents, many differentiation protocols generate polyhormonal endocrine cells. Such cells, when investigated, appear to lack the expression of key beta cell associated transcription factors, such as NKX6.1 and MAFA. In the mouse, expression of transcription factors such as Nkx6.1 is an important characteristic that separates primary transition Insulin+ cells from secondary transition Insulin+ cells. Primary transition (or immature) Insulin+ cells lack expression of Nkx6.1 and are polyhormonal, whereas secondary transition (or mature) Insulin+ cells co-express Nkx6.1 and are monohormonal ((Teitelman et al., 1993), (Sander et al., 2000)). Hence, when characterising INSULIN+ cells derived from human ES cells, it is important to examine the transcriptome of the differentiated cells.

Genetic modification of human embryonic stem cells to create reporter lines can facilitate the identification of specific differentiated derivatives. In some instances, a reporter gene such as GFP, under the control of the promoter of the gene of interest, is inserted randomly into the hESC genome to create a transgenic reporter line. Alternatively, a 'knock-in' cell line can be generated by inserting the reporter gene is directly into the locus of interest via homologous recombination, thus bringing the reporter under the control of endogenous control elements (reviewed in: (Giudice and Trounson, 2008)). In both cases, the aim of these genetic modifications is to generate a line in which a fluorescent reporter protein (typically GFP or mCherry) is expressed when the hESCs differentiate to produce a cell type of interest. This allows for ease of both identification and isolation of specific differentiated

derivatives, and in turn, facilitates optimisation of differentiation protocols. Our laboratory has generated a number of these reporter lines which have aided in the generation cell types representing a variety of different cell types, including, blood, heart, neuronal lineages as well as cell representing the primitive streak ((Davis et al., 2008) (Elliott et al., 2011), (Goulburn et al., 2011)).

The paper contained in this chapter describes the generation of a genetically tagged cell line, in which sequences encoding a GFP tag were inserted into one allele of the INSULIN locus. The value of the line is demonstrated by utilising it to develop the spin EB protocol described in detail in chapter 2. As noted in the previous chapter, this protocol, which utilises a defined differentiation medium, results in the generation of a INSULIN+ population that contains a substantial fraction of cells that are monohormonal for insulin expression cells (~40%). In addition, our analysis showed that a proportion of these INSULIN+ cells co-express NKX6.1 (~35%). The novel character of the cells generated using this protocol was highlighted by microarray analysis of INSULIN+ cells isolated by FACS. These analyses showed that, relative to cells generated by 2 previously published protocols ((D'Amour et al., 2006), (Nostro et al., 2011)), spin EB derived cells were more similar to both fetal pancreatic tissue, adult pancreatic tissue and isolated islets.

Diabetologia (2012) 55:694–706
DOI 10.1007/s00125-011-2379-y

ARTICLE

# *INS*$^{GFP/w}$ human embryonic stem cells facilitate isolation of in vitro derived insulin-producing cells

**S. J. Micallef · X. Li · J. V. Schiesser · C. E. Hirst · Q. C. Yu · S. M. Lim · M. C. Nostro · D. A. Elliott · F. Sarangi · L. C. Harrison · G. Keller · A. G. Elefanty · E. G. Stanley**

Received: 27 July 2011 / Accepted: 20 October 2011 / Published online: 26 November 2011


**Abstract**
*Aims/hypothesis* We aimed to generate human embryonic stem cell (hESC) reporter lines that would facilitate the characterisation of insulin-producing (INS$^+$) cells derived in vitro.
*Methods* Homologous recombination was used to insert sequences encoding green fluorescent protein (GFP) into the *INS* locus, to create reporter cell lines enabling the prospective isolation of viable INS$^+$ cells.
*Results* Differentiation of *INS*$^{GFP/w}$ hESCs using published protocols demonstrated that all GFP$^+$ cells co-produced insulin, confirming the fidelity of the reporter gene. INS-GFP$^+$ cells often co-produced glucagon and somatostatin, confirming conclusions from previous studies that early hESC-derived insulin-producing cells were polyhormonal. *INS*$^{GFP/w}$ hESCs were used to develop a 96-well format spin embryoid body (EB) differentiation protocol that used the recombinant protein-based, fully defined medium, APEL. Like INS-GFP$^+$ cells generated with other methods, those derived using the spin EB protocol expressed a suite of pancreatic-related transcription factor genes including *ISL1*, *PAX6* and *NKX2.2*. However, in contrast with previous methods, the spin EB protocol yielded INS-GFP$^+$ cells that also co-expressed the beta cell transcription factor gene, *NKX6.1*, and comprised a substantial proportion of monohormonal INS$^+$ cells.
*Conclusions/interpretation INS*$^{GFP/w}$ hESCs are a valuable tool for investigating the nature of early INS$^+$ progenitors in beta cell ontogeny and will facilitate the development of novel protocols for generating INS$^+$ cells from differentiating hESCs.

**Keywords** Diabetes · Gene targeting · GFP · Human embryonic stem cells · Insulin

**Abbreviations**

| | |
|---|---|
| BMP4 | Bone morphogenetic protein 4 |
| BrdU | Bromodeoxyuridine |
| EB | Embryoid body |
| GFP | Green fluorescent protein |
| FGF2 | Fibroblast growth factor 2 |
| hESC | Human embryonic stem cell |
| HGF | Hepatocyte growth factor |
| INS | Insulin |
| IPA | Insulin-positive aggregates |
| ISL | ISL LIM homeobox |
| KGF | Fibroblast growth factor 7 |
| NKX2-2 | NK2 homeobox 2 |
| NKX6.1 | NK6 homeobox 1 |
| PAX6 | Paired box 6 |

S. J. Micallef and X. Li contributed equally to this study.

**Electronic supplementary material** The online version of this article (doi:10.1007/s00125-011-2379-y) contains peer-reviewed but unedited supplementary material, which is available to authorised users.

S. J. Micallef · X. Li · J. V. Schiesser · C. E. Hirst · Q. C. Yu · S. M. Lim · D. A. Elliott · A. G. Elefanty · E. G. Stanley (✉)
Monash Immunology and Stem Cell Laboratories (MISCL), Level 3, Building 75, STRIP1, West Ring Road, Monash University, Clayton, Victoria 3800, Australia
e-mail: ed.stanley@monash.edu

M. C. Nostro · F. Sarangi · G. Keller
McEwen Centre for Regenerative Medicine, University Health Network, Toronto, ON, Canada

L. C. Harrison
The Walter and Eliza Hall Institute of Medical Research, Parkville, VIC, Australia

Diabetologia (2012) 55:694–706 

PDX1 Pancreatic and duodenal homeobox 1
RA Retinoic acid
ROCK Rho associated kinase

## Introduction

Type 1 diabetes is an autoimmune disease characterised by destruction of beta cells in the pancreas, deficient insulin production, and persistent high levels of blood glucose. Treatment with exogenous insulin, although life-saving, does not restore physiological control of blood glucose, leaving people with type 1 diabetes at risk of long-term complications. Control can be improved by islet transplantation (reviewed by Speight et al. [1]), but this treatment option will always be limited by the scarcity of cadaveric donor tissue.

Beta cells derived from the differentiation of human embryonic stem cells (hESCs) in vitro potentially represent an inexhaustible source of insulin-producing cells for the treatment of type 1 diabetes. Several laboratories have demonstrated that hESC-derived endocrine cells can regulate blood glucose in a diabetic mouse model, providing proof of principle for future clinical application (for example, see studies by Kroon et al. [2] and Jiang et al. [3] and a review by van Hoof et al. [4]). However, while attempts to generate $INS^+$ cells from pluripotent stem cells have been encouraging, the biology of this process remains poorly understood. In this light, better tools and reagents to facilitate the understanding of beta cell development are required.

We describe the generation and characterisation of two independently derived hESC lines in which sequences encoding green fluorescent protein (GFP) have been targeted to the insulin locus ($INS^{GFP/w}$ hESCs). We demonstrate the utility of these lines by characterising the transcriptional signature of hESC-derived insulin-producing ($INS^+$) cells generated using established differentiation protocols. Analysis of these data in conjunction with immunofluorescence studies confirms that such cells display an immature phenotype, with the majority of $INS^+$ cells also producing glucagon. We used $INS^{GFP/w}$ hESCs to develop a novel 96-well format spin embryoid body (EB) differentiation protocol for the differentiation of hESCs to $INS^+$ pancreatic endoderm. This method is based on a protocol originally developed for the differentiation of hESCs to mesodermal populations [5] and uses a defined wholly recombinant protein-based medium (APEL) [6]. Characterisation of $INS^+$ cells generated with this platform reveals that, unlike $INS^+$ cells derived with previous methods, a substantial proportion also produce the beta cell-associated marker, NK6 homeobox 1 (NKX6.1), suggesting that the EB environment is conducive to ongoing differentiation. $INS^{GFP/w}$ hESCs are therefore a valuable tool for investigating and refining the generation of $INS^+$ cells from pluripotent stem cells in vitro.

## Methods

*Generation and identification of targeted $INS^{GFP/W}$ hESCs* The INS-targeting vector comprised a 10.7 kb 5′ homology arm, GFP coding sequences, a loxP flanked phosphoglycerol kinase (PGK)-promoter-neomycin resistance cassette and 2.9 kb 3′ homology arm. The 5′ homology arm was derived from a bacterial artificial chromosome (RP11 889I17) encompassing the human insulin locus using ET cloning as described previously [7]. The 3′ homology arm was derived by PCR using the same bacterial artificial chromosome clone as a template. The vector was digested with the restriction enzyme PacI before electroporation into the hESC lines HES3 (http://www.escellinternational.co/) and MEL1 (Millipore, Billerica, MA, USA) as described previously [8]. Targeted hESC clones were identified by a PCR-based screening strategy using primer P1, a forward primer in the neomycin resistance gene, in conjunction with P2, a reverse primer located immediately 3′ of genomic sequences encompassed by the targeting vector. The fidelity of homologous recombination within the 5′ arm was confirmed by PCR using P3, a forward primer located immediately 5′ of genomic sequences included in the targeting vector, in conjunction with P4, a reverse primer in the GFP gene. By these criteria, a number of clones were identified in which the vector was correctly integrated into the *INS* locus in both HES3 and MEL1 lines. One HES3-derived and one MEL1-derived $INS^{GFPNeo/w}$ clone was expanded, and the neomycin resistance cassette removed as described previously [9]. Single-cell cloning was performed by single-cell deposition using a FACSaria FACS station as described previously [9]. Several colonies representing each primary clone were picked and screened for the loss of the neomycin resistance cassette by PCR. Southern blot analysis using a probe encompassing the coding sequences of enhanced green fluorescent protein (EGFP) (Invitrogen, Carlsbad, CA, USA) was performed on EcoRV-digested genomic DNA from each cell line (Fig. 1b). As this enzyme cuts only once within the vector, the presence of a single band indicated that each cell line contained a single integration of the targeting vector. The DNA fragments generated by PCR using the primers P1 and P2, P3 and P4 were cloned and sequenced to establish that the targeting vector had been correctly integrated into the *INS* locus.

*hESC culture and differentiation* hESCs were cultured and passaged as reported elsewhere [10]. The differentiation of

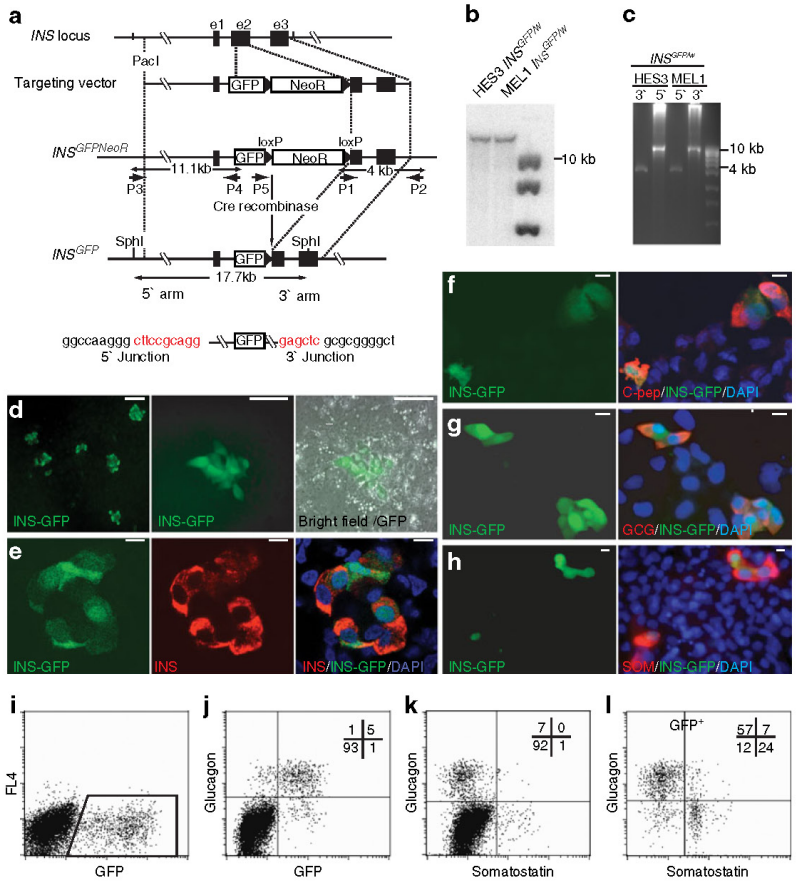


**Fig. 1** Generation and characterisation of $INS^{GFP/w}$ hESCs. **a** Vector used to target the *INS* locus in hESCs. The G418 antibiotic resistance (NeoR) cassette, flanked by loxP sites (black triangles), was removed with Cre recombinase. PCR primers (P1, P2) and (P3, P4) were used to identify targeted clones. The sequences of PCR fragments shown below represent the junctions between the extremities of the targeting vector (red text) and the *INS* locus (black text). **b** Southern blot analysis of SphI-digested genomic DNA isolated from single-cell cloned MEL1 and HES3 $INS^{GFP/w}$ hESCs showed a single *GFP* insert present in both lines. **c** PCR analysis with primer pairs (P3, P4) and (P5, P2) generated DNA fragments of ~10 and 4 kb, respectively, the size predicted for correct integration of the targeting vector into the *INS* locus. **d** Images showing clusters of $GFP^+$ cells in differentiated cultures of $INS^{GFP/w}$ hESCs. Scale bar, 100 μm. **e**–**h** Immunofluorescence analysis of flat cultures showing that INS-$GFP^+$ cells produce insulin, C-peptide (C-pep), glucagon (GCG) and somatostatin (SOM). Scale bar, 10 μm. **i** Flow cytometry analysis showing that INS-$GFP^+$ cells can be clearly distinguished from the $GFP^-$ population. **j**–**l** Intracellular flow cytometry (ICF) analysis confirming that the majority of INS-$GFP^+$ cells co-produce glucagon and/or somatostatin. FACS plot shows the production of glucagon and somatostatin in cells gated on INS-$GFP^+$ expression. Note: GFP intensity is decreased by ~1 log in processing samples for ICF

hESCs into $INS^+$ cells was performed using several different protocols. Adherent, flat culture differentiations based on the work of D'Amour et al. [11] and Kroon et al. [2] (referred to as 'flat cultures'). Spin EB differentiations (referred to as 'spin EBs') [5], were set up in APEL medium [6]. Differentiation of spin EBs under pancreatic-specific conditions was as follows. EBs were formed by the forced aggregation of 2,000 (HES3) or 3,500 (MEL1) hESCs in APEL (the protein-free hybridoma medium component was omitted from this formulation) containing 10 ng/ml bone morphogenetic protein 4 (BMP4) and 150–200 ng/ml activin A (batch dependent) in low-attachment

96-well plates. After 3 days, medium was replaced with APEL containing 200–400 ng/ml noggin (batch dependent). At day 6, medium was replaced with APEL containing $1\times10^{-5}$ mol/l retinoic acid (RA). At day 9, the medium was changed to APEL without polyvinyl alcohol (AEL) containing $1\times10^{-5}$ mol/l RA, 100 μmol/l glucagon-like peptide 1 (GLP1), 1×B27 and 10 mmol/l nicotinamide. At day 15 of differentiation, EBs were transferred to gelatinised, adherent 96-well plates, and insulin production was induced in AEL containing 10 mmol/l nicotinamide and 50 ng/ml IGF-I. With this system, most EBs contained INS-GFP$^+$ cells by day 30 of differentiation. In addition, INS-GFP$^+$ cells were also differentiated according to a protocol developed by Nostro and colleagues [12], referred to as the 'Nostro protocol'. Recombinant human activin A, fibroblast growth factor 10 (FGF10), fibroblast growth factor 7 (KGF), IGF-I and hepatocyte growth factor (HGF) were purchased from R&D Systems (Minneapolis, MN, USA). Basic FGF (FGF2) was purchased from Peprotech (Rocky Hill, NJ, USA). Wingless-type MMTV integration site family, member 3A (WNT3A) and noggin were purchased from R&D Systems or provided by the Australia Stem Cell Centre (Melbourne, VIC, Australia). KAAD-cyclopamine was purchased from Toronto Research Chemicals (North York, ON, Canada); all-*trans* RA, nicotinamide, SB431542 and GLP1 were purchased from Sigma-Aldrich (St Louis, MO, USA).

*Live cell imaging and immunofluorescence* Live cell imaging of spin EBs in a 96-well plate format was performed with a Leica TCS NT inverted microscope, and images were processed with ImageJ software. For immunofluorescence analysis of flat cultures, differentiated cells were fixed for 15 min in 4% (wt/vol.) paraformaldehyde in PBS, permeablised in 0.2% (vol./vol.) Triton X-100 at room temperature for 10 min, and blocked for 60 min in 10% (vol./vol.) goat serum. Primary antibodies were incubated overnight at 4°C, and secondary antibodies were incubated for 1 h at 24°C. The following antibodies were used: rabbit anti-pancreatic and duodenal homeobox 1 (PDX1) (kindly provided by C. Wright, Vanderbilt University, Nashville, TN, USA); mouse anti-NK2 homeobox 2 (NKX2-2) (Developmental Studies Hybridoma Bank (DSHB; Iowa City, IA, USA; clone 74.5A5); mouse anti-NKX6.1 (DSHB); mouse anti-ISL LIM homeobox (ISL)1/2 (DSHB clone 39.4D5); mouse anti-paired box 6 (PAX6) (DSHB); guinea pig anti-insulin (Dako, Glostrup, Denmark; clone A0564); rabbit anti-C-peptide (Millipore; clone 4020; note that this antibody detects both C-peptide and proinsulin); rabbit anti-glucagon (Dako; clone A0565); anti-glucagon (Sigma; clone K79bB10); rat anti-somatostatin (Millipore; clone MAB354). Secondary antibodies used were Alexa-488- and Alexa-568-conjugated goat antibodies against mouse, rat, rabbit and goat (Invitrogen) and a tetramethyl rhodamine iso-thiocyanate (TRITC)-conjugated antibody against guinea pig (Sigma).

For wholemount immunofluorescence of spin EBs [13], differentiated EBs were removed from 96-well plates and fixed for 90 min on ice in 4% (wt/vol.) paraformaldehyde in PBS and permeablised in 1% (vol./vol.) Triton X-100 at room temperature for 90 min. EBs were blocked for 90 min in 10% (vol./vol.) goat serum. Incubation of primary and secondary antibodies was as described above. All washes were for 15 min in PBS/10% FCS.

*Flow cytometric analysis* For flow cytometric analysis and sorting of live cells, hESCs differentiated in flat cultures or as spin EBs were dissociated with TrypLE-select (Invitrogen) to give a single-cell suspension and purified as described previously [7]. High-throughput flow cytometric analysis of cells in 96-well plates was performed with an LSR II multi-laser benchtop flow cytometer (BD Biosciences, Franklin Lakes, NJ, USA), and FACS plots processed using Gatelogic software (www.inivai.com/GatelogicHome.html).

*Reculture experiments* By using flow cytometry we purified day 20 INS-GFP$^+$ cells generated with the flat culture protocol and then added between $2\times10^3$ and $5\times10^3$ INS-GFP$^+$ cells to each well of a low-attachment 96-well tray in APEL medium containing 10 μmol/l rho-associated, coiled-coil containing protein kinase 1 (ROCK) inhibitor Y27632 [7, 14]. FGF10, HGF, FGF2, BMP4, KGF and noggin (10–100 ng/ml) were added singly or in combination at the time of aggregation or after 24 h. Medium containing the ROCK inhibitor was replaced with APEL containing combinations of the above growth factors after aggregates had formed (usually 24–72 h). Half of the medium was changed every 3–4 days over a 3-week period. When used, 20 μl Matrigel (diluted 2:1 in APEL medium) was added directly to reaggregated INS-GFP$^+$ cells. After Matrigel polymerisation, 100 μl APEL medium containing combinations of the above growth factors was added to each well. Medium was refreshed periodically as described above. Intracellular flow cytometric analysis was performed as described by Nostro et al. [12]. Bromodeoxyuridine (BrdU) incorporation measured by flow cytometry was performed according to the manufacturer's (BD Biosciences) instructions.

*Gene expression analysis* RNA preparation, Illumina microarray analysis and real-time quantitative PCR was performed essentially as described previously [7]. Briefly, total RNA for each sample was amplified, labelled and hybridised to human WG-6v2, human HT12v3 or HT12v4 BeadChips according to Illumina standard protocols (Illumina, San Diego, CA, USA) at the Australian Genome Research Facility. Initial data analysis was performed using GenomeStudio version 2010.3 (Illumina),

using average normalisation across all the samples. Alternatively, data were analysed using R/BioConductor using algorithms within the lumi package [15] (function: bgAdjust.affy and quantile normalisation [16]). Subsequent data analysis was performed using MultiExperiment Viewer [17, 18]. Hierarchical clustering was performed using Pearson correlation with average linkage clustering. Differentially expressed genes were subjected to functional clustering analysis using the DAVID public database (Database for Annotation, Visualization and Integrated Discovery) [19, 20].

## Results

We targeted a GFP reporter gene to the *INS* locus of HES3 and MEL1 hESCs, creating a reagent to enable detailed study of the potential and characteristics of $INS^+$ cells (Fig. 1a). Undifferentiated $INS^{GFP/w}$ hESCs had a normal karyotype (46XX for the HES3-derived line and 46XY for the MEL1-derived line), produced stem cell markers and generated teratomas containing derivatives of the three primary germ layers upon transplantation into immunodeficient mice (electronic supplementary material [ESM] Fig. 1). Southern blotting analysis indicated that both lines contained a single GFP insertion, while PCR and DNA sequencing confirmed that the targeting vector had been integrated by homologous recombination (Fig. 1a–c). Differentiation of $INS^{GFP/w}$ hESCs in flat culture (ESM Fig. 2) revealed that INS-$GFP^+$ cells appeared as small clusters, which co-stained with insulin and C-peptide (Fig. 1d–f), confirming the fidelity of the reporter gene. Immunofluorescence experiments also demonstrated that INS-$GFP^+$ cells co-produced somatostatin and glucagon (Fig. 1g, h), confirming previous reports [11] that early hESC-derived $INS^+$ cells are polyhormonal. This conclusion was supported by flow cytometry analysis, which showed that ~80% of INS-$GFP^+$ cells co-produced glucagon, and ~20% produced somatostatin (Fig. 1i–l). INS-$GFP^+$ cells producing neither hormone constituted a minor proportion of the population; however, it is possible that these cells produced other hormones that were not assayed (e.g. pancreatic polypeptide [PPY], ghrelin [GHRL]).

Two distinct but not necessarily mutually exclusive scenarios may explain the prevalence of polyhormonal $INS^+$ cells generated by many current in vitro differentiation protocols. First, it has been postulated that the first wave of $INS^+$ cells emerging during human embryonic development represent a primary wave of endocrine cells, the contribution of which to the mature endocrine organ is still undetermined [21]. Alternatively, the cells produced in current differentiation systems may have the potential for further maturation and proliferation, but this requires appropriate culture conditions. We attempted to address these possibilities by asking if INS-$GFP^+$ cells derived from flat culture differentiation could mature further in vitro. To perform these experiments, purified INS-$GFP^+$ cells were reaggregated in APEL medium containing 10 μmol/l ROCK inhibitor Y27632 [7] (Fig. 2a). This reaggregation step substantially improved the viability of cells after sorting. After 24 h, INS-$GFP^+$ cells formed tight E-cadherin$^+$ clusters (insulin-positive aggregates [IPAs]) that displayed the same spectrum of GFP intensities as present in the original sorted population and continued to co-produce glucagon (Fig. 2b, c).

The growth and differentiation potential of IPAs was subsequently examined in vitro. We first tested the ability of previously reported pancreatic growth factors to either sustain INS-GFP production over a 3-week period or promote expansion of the $GFP^+$ population. Extended cultures of IPAs in APEL medium alone revealed that INS-GFP production waned rapidly after IPA formation (data not shown). We also observed that factors previously reported to have a role in expansion of the pancreatic primordium, such as HGF and FGF10 [22–24], promoted the slow growth of the population overall, particularly in the presence of Matrigel (Fig. 2d and data not shown). However, none of the factor combinations tested (see Methods) sustained GFP production for more than 3 weeks nor promoted expansion of the INS-$GFP^+$ pool. Instead, $GFP^-$ cells (either derived from $INS^+$ cells or representing contaminants in the original sorted population) eventually became the predominant cell type within the IPAs (Fig. 2d), raising the possibility that INS-$GFP^+$ cells generated in flat cultures were postmitotic. To address this, we performed BrdU incorporation analysis of cells differentiated using the flat culture protocol. This analysis indeed showed that, at later differentiation stages, few INS-$GFP^+$ cells and/or their immediate precursors incorporated BrdU (Fig. 2e), consistent with the notion that these cells were essentially non-proliferative.

In order to further characterise INS-$GFP^+$ cells generated using the flat culture and Nostro protocols, cells were isolated by flow cytometry and processed for gene expression microarray analysis (Fig. 3a). Data were compared with those of the INS-$GFP^-$ fraction from the same cultures, as well as from fetal pancreas, adult pancreas and adult islets. Differentially expressed genes were identified by performing sequential pair-wise comparisons between the $GFP^+$ and $GFP^-$ fractions from four independent sorting experiments using two different cell lines, performed in two different laboratories. A total of 202 probes (186 genes) were identified that were upregulated more than twofold across all four comparisons (see ESM Fig. 3 for scatter plots for individual pair-wise comparisons). For display purposes, a selected subset of these 186 genes was grouped into functional categories based on their

Diabetologia (2012) 55:694–706 

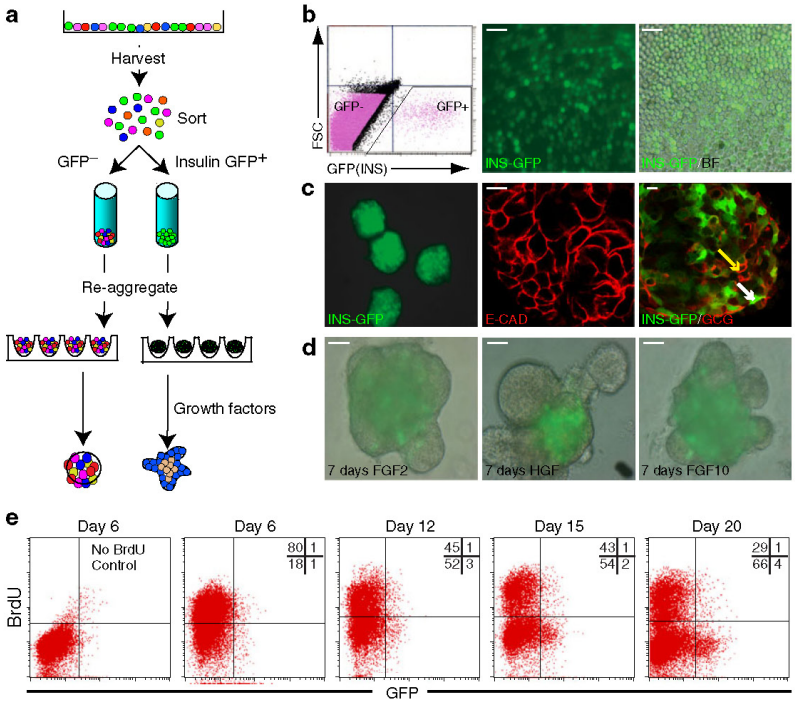


**Fig. 2** INS-GFP$^+$ cells can be viably isolated and recultured. **a** Schematic depicting the experimental outline of sorting and reculture experiments. **b**, **c** Cells sorted on the basis of INS-GFP expression display a wide spectrum of GFP fluorescence intensities (**c**; scale bar, 50 μm). After reaggregation, INS-GFP$^+$ cells form tight E-cadherin$^+$ (E-CAD) insulin producing aggregates (IPAs) that continue to express glucagon (GCG). Scale bar, 10 μm. **d** Bright field (BF)–GFP overlay images of IPAs cultured in APEL medium supplemented with 100 ng/ml of the indicated growth factors for 7 days. Note the significant growth of the GFP$^-$ population and diminishing proportion of INS-GFP$^+$ cells present within these aggregates. Scale bar, 50 μm. **e** Flow cytometric analysis of differentiating cultures of *INS*$^{GFP/w}$ hESCs labelled with BrdU for 24 h at the indicated time points. Note that GFP expression is not observed before day 15. At day 20, the majority of INS-GFP$^+$ cells had not incorporated BrdU. The percentage of cells within each quadrant is indicated. FSC, forward scatter

gene ontology (secretory, transcription factors, diabetes associated) (Fig. 3a).

Comparison of GFP$^+$ and GFP$^-$ fractions indicated that GFP$^+$ cells had upregulated a suite of genes that confirmed the commitment of this population to endocrine differentiation (Fig. 3b). Genes that were substantially upregulated in the GFP$^+$ fraction included those for hormones traditionally associated with pancreatic endocrine cells (*GCG*, *INS*, *SST*, *PPY*), a suite of known pancreatic transcription factor genes (*NKX2.2* [also known as *NKX2-2*], *ARX*, *NEUROD1*, *MAFB*) as well as a number of genes associated with type 1 diabetes (*HLA*, *GAD*, *PTPRN*). This analysis also revealed that, within this restricted set, INS-GFP$^+$ samples were most similar to islets, consistent with their endocrine nature.

Gene profiling data were compared with the results of immunofluorescence experiments, confirming that INS-GFP$^+$ cells produced transcription factors such as PAX6, NKX2.2 and ISL1 (Fig. 4). We also investigated the expression of *PDX1* and *NKX6.1*, two genes that were absent from the composite list derived from comparison of all four sorting experiments as well as being absent from pair-wise comparison of individual experiments. In the case of *PDX1*, quantitative PCR studies (ESM Fig. 4) suggested that its absence from the GFP$^+$ fraction appeared to partly reflect low sensitivity of the Illumina probe set to detect this particular gene. However, although GFP$^+$ cells appeared to produce elevated levels of PDX1 (Fig. 4), it is also possible that the relatively high frequency of *PDX1*$^+$ cells present in the INS$^-$ fraction overall may have contributed to the poor enrichment of *PDX1* transcripts observed in the former population (see ESM Fig. 5). In contrast with PDX1, co-production of NKX6.1 with INS-GFP was not observed in

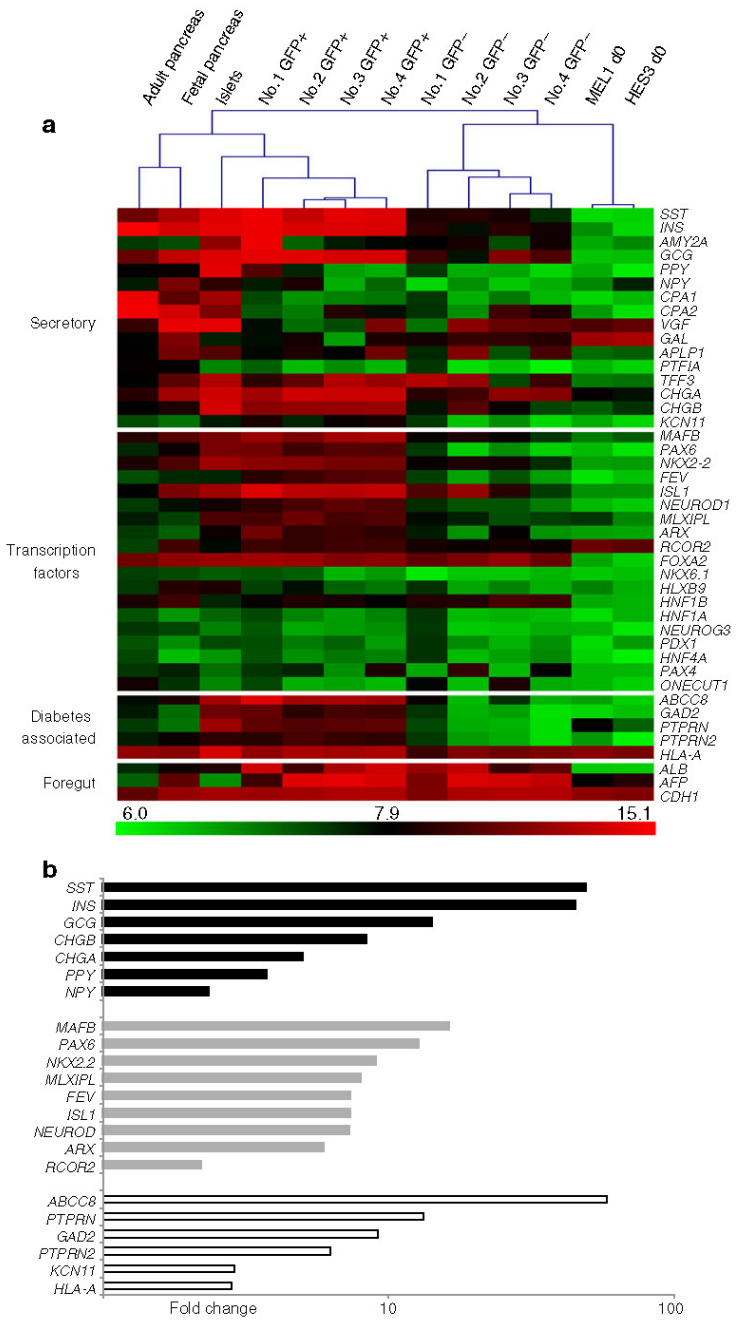


**Fig. 3** Gene expression profiling of INS-GFP+ cells using Illumina microarrays. **a** Two-colour heat map representation of selected data derived from Illumina gene chip analysis of GFP+ and GFP− cell fractions from four independent differentiation experiments on two independent $INS^{GFP/w}$ hESC lines. Genes included were upregulated more than twofold in all pair-wise comparisons of each of the independently derived samples. Heat map represents $\log_2$ transformed data that have been average normalised. Hierarchical clustering of the samples was performed by Pearson correlation with average linkage. **b** Bar graph showing selected genes, the expression of which was upregulated more than twofold in the INS-GFP+ cells versus the GFP− cells, calculated as an average of all four differentiation experiments. Secretory, black bars; transcription factor, grey bars; diabetes associated, white bars

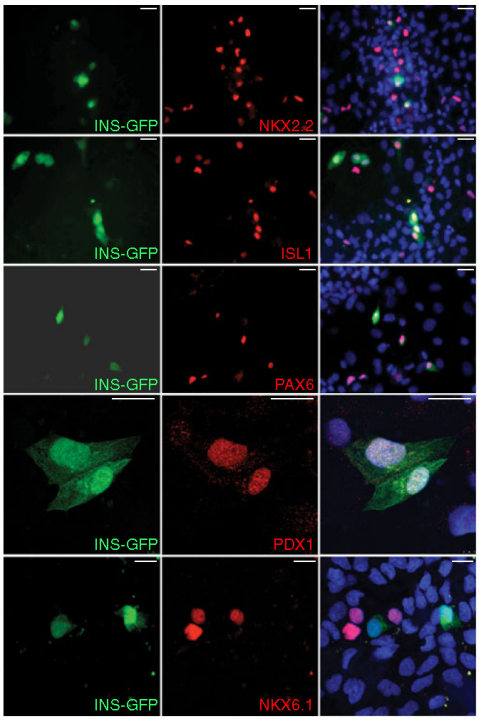


**Fig. 4** Gene expression analysis reveals that INS-GFP$^+$ cells express a suite of pancreas-associated transcription factors. Immunofluorescence studies show that INS-GFP$^+$ cells generated with the flat culture protocol express *PAX6, NKX2.2, ISL1* (scale bar, 20 μm) and *PDX1* (scale bar, 10 μm) but not *NKX6.1* (scale bar, 20 μm). Note that all transcription factors are also produced by GFP$^-$ cells present in these cultures

flat cultures, and transcripts were not detected in samples generated in either the flat culture or the Nostro protocols. This last observation is consistent with other reports and the notion that these hESC-derived INS$^+$ cells represent an immature precursor population that is not yet fully committed to beta cell differentiation [11].

Analysis of INS-GFP$^+$ cells confirmed that both protocols generated cells at a stage of pancreas development that precedes the onset of overt beta cell differentiation. Therefore, we reasoned that the further testing of variables affecting the course of in vitro pancreatic differentiation would be required before more mature phenotypes could be generated. We used *INS*$^{GFP/w}$ hESCs to develop a novel 96-well format spin EB protocol [5] for generating INS-GFP$^+$ cells (Fig. 5a). With this method, we observed that INS-GFP$^+$ cells emerged with slower kinetics compared with the flat culture or the Nostro protocols, with the onset of GFP expression at differentiation day 20 (compared with day 15 for flat cultures). Late-stage spin EBs displayed a spectrum of morphologies with respect to the localisation of INS-GFP$^+$ cells (Fig. 5b). In general, these cells appeared in clusters either within the main body of the EB or as isolated spheres surrounding the GFP$^-$ EB core. Visual inspection suggested that some EBs contained a substantial fraction of GFP$^+$ cells, an observation confirmed by FACS analysis that showed that single EBs contained up to 37% INS-GFP$^+$ cells (Fig. 5c). However, without specific preselection of GFP$^+$ EBs, the overall frequency of GFP$^+$ cells generated with this protocol was ~2–5%.

Immunofluorescence and flow cytometry analysis of spin EB-derived cells indicated that, unlike cells generated using the flat culture protocol, a substantial fraction (40%) of INS-GFP$^+$ cells produced neither glucagon nor somatostatin (Fig. 6a–e). Immunofluorescence analysis showed that, like cells generated in flat cultures, spin EB-derived INS-GFP$^+$ cells produced PAX6, ISL1, NKX2.2 and PDX1. In addition, similar to that observed with flat cultures, PDX1$^+$ nuclei were also observed in a substantial proportion of GFP$^-$ cells within spin EBs that contained INS-GFP$^+$ cells (Fig. 6f). However, unlike cells derived with either the flat culture or the Nostro protocols, many INS-GFP$^+$ cells within spin EBs co-produced NKX6.1 (Fig. 6c) (see ESM Fig. 6 for single-colour images). In a survey of EBs immunostained for NKX6.1, we observed that 34% (122/363) of cells were GFP$^+$ and 16% (58/363) of cells were NKX6.1$^+$. In these EBs, INS-GFP$^+$/NKX6.1$^+$ cells comprised 11% (39/363) of the total cell population or 32% (39/122) of the INS-GFP$^+$ cell population (data not shown). The presence of an INS-GFP$^+$/NKX6.1$^+$ population using the spin EB method suggests that the differentiation conditions are conducive to ongoing differentiation of pancreatic endoderm.

Microarray analysis confirmed that INS-GFP$^+$ cells generated by the spin EB method had upregulated a similar cohort of pancreatic genes to those derived using the flat culture differentiation protocol (Fig. 7a). However, given the presence of INS-GFP$^+$/NKX6.1$^+$ cells in spin EBs, we used microarray analysis to explicitly compare the gene expression profiles of INS-GFP$^+$ cells generated using all three protocols. Specifically, we were interested in genes that might provide information relating to differentiation status and/or cellular identity. This comparison showed that INS-GFP$^+$ cells derived from flat cultures expressed elevated levels of a number of genes that are associated with non-pancreatic derivatives of foregut endoderm (Fig. 7b). In particular, transcripts encoding apolipoproteins (liver), claudin 18 (CLDN18) (lung) and pepsinogen (stomach) were more abundant in INS-GFP$^+$ cells generated using previously described methods. Conversely, INS-GFP$^+$

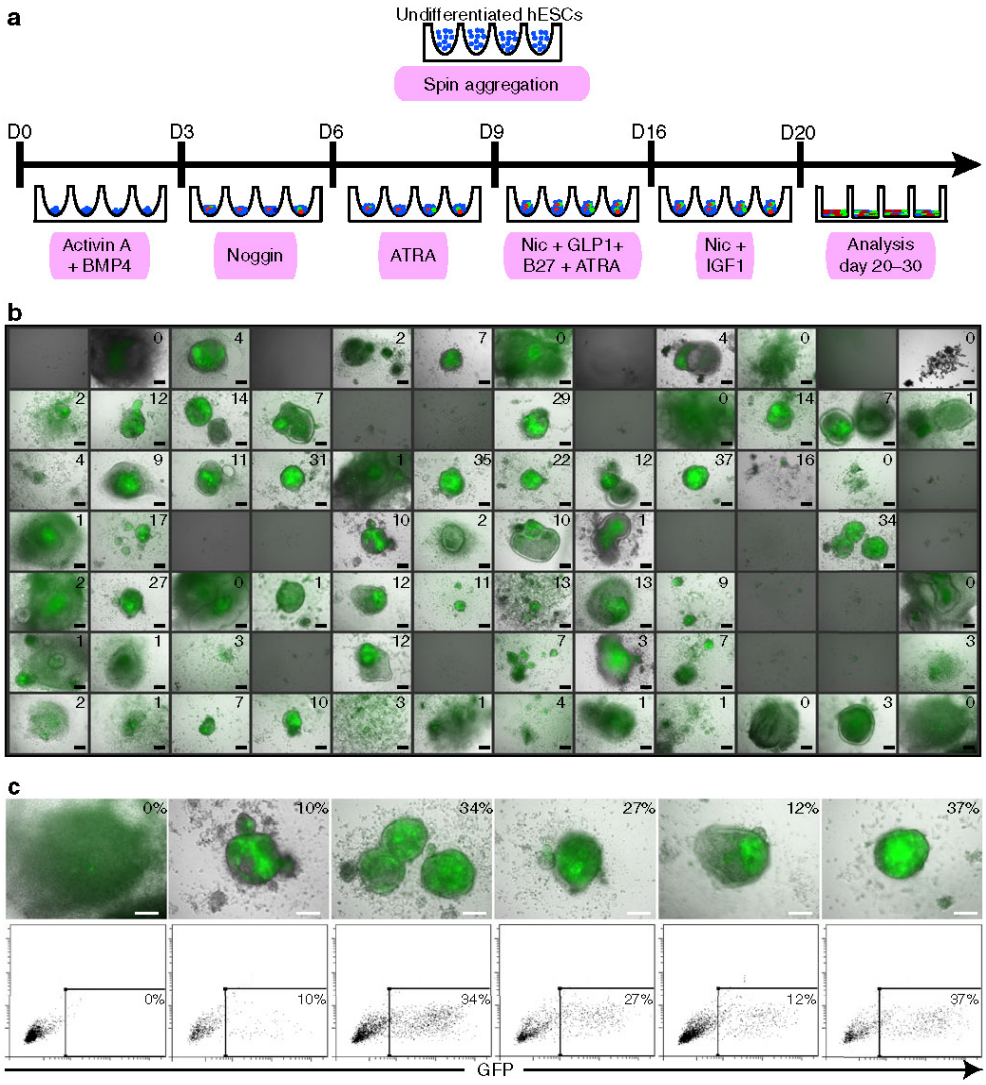


**Fig. 5** Generation and analysis of INS-GFP$^+$ cells using the spin EB differentiation platform. **a** Schematic representation of the spin EB protocol, which uses the wholly recombinant protein-based medium, APEL. Concentration ranges given for specific growth factors reflect variation in the specific activity of individual batches. ATRA, all-*trans* retinoic acid; Nic, nicotinamide. **b** Composite image showing the variation in the size and INS-GFP$^+$ cell content of individual EBs. Greyed boxes indicate wells that contained EBs lost during processing (medium changes). The numbers in the upper right hand corners indicate the percentage of GFP$^+$ cells in each EB determined by flow cytometric analysis. **c** Selected images from **a** showing the morphology of INS-GFP$^+$ EBs and the primary flow cytometry data associated with each sample. Scale bar, 100 μm

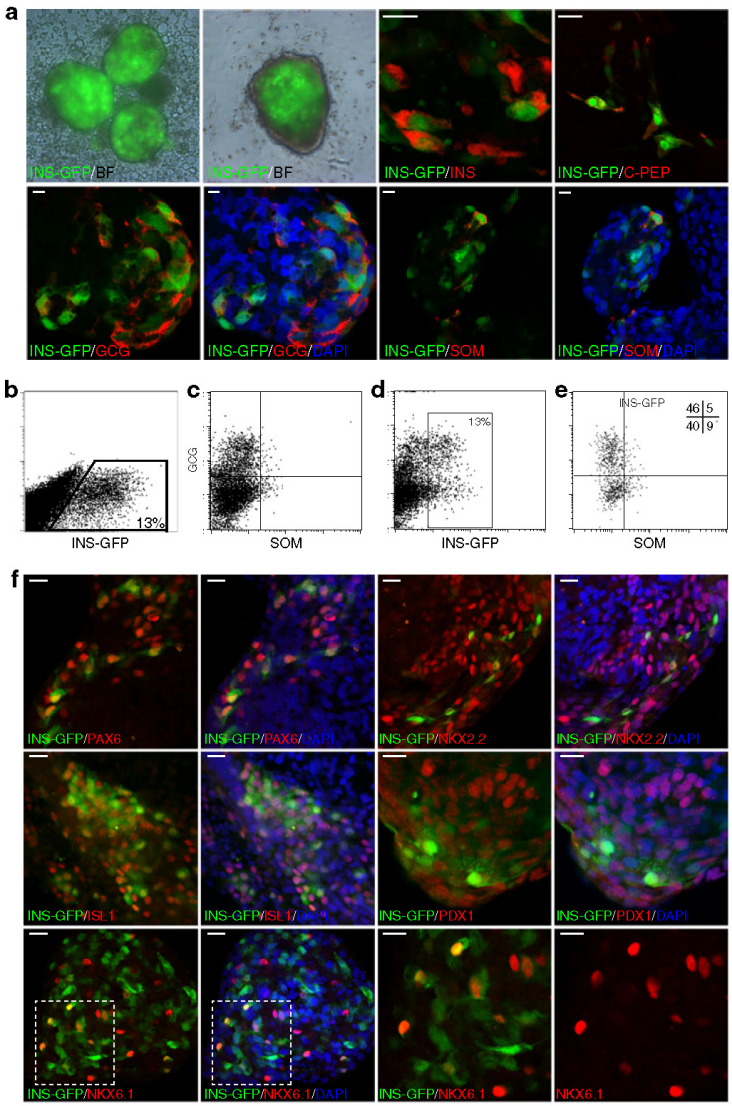


**Fig. 6** Hormone and transcription factor production by cells within INS-GFP$^+$ spin EBs. **a** Individual spin EBs containing INS-GFP$^+$ cells were collected, immunolabelled with antibodies directed against endocrine hormones as indicated and imaged by confocal microscopy. Scale bar, 10 μm. **b**–**e** Flow cytometric analysis of HES3 INS-GFP$^+$ cells representing selected EBs for co-production of glucagon (GCG) and somatostatin (SOM). Note that GFP intensity is lost during fixation and permeabilisation (compare **b** with **d**). The percentage of cells within specific regions or quadrants is indicated. **e** The expression of glucagon and somatostatin in the INS-GFP$^+$ population. **f** Whole-mount immunofluorescence of INS-GFP$^+$ EBs generated with the spin EB platform showing production of PAX6, NKX2.2, ISL1, PDX1 and NKX6.1. Scale bar, 20 μm. Note that all transcription factors are also produced by GFP$^-$ cells present in these cultures

cells derived from spin EB cultures were enriched for transcripts encoding a number of *HOX* genes, some of which have been previously associated with axial patterning of the developing gut tube [25]. Whether these differences are indicative of differences in relative developmental maturity or reflect some underlying difference in the specification process remains to be determined.

## Discussion

*INS*$^{GFP/w}$ hESCs reported on here represent a novel reagent for the study of beta cell differentiation in vitro. By directly tagging the *INS* locus, cells can be viably isolated for further studies or followed in real time, allowing their growth and response to culture manipulations to be directly

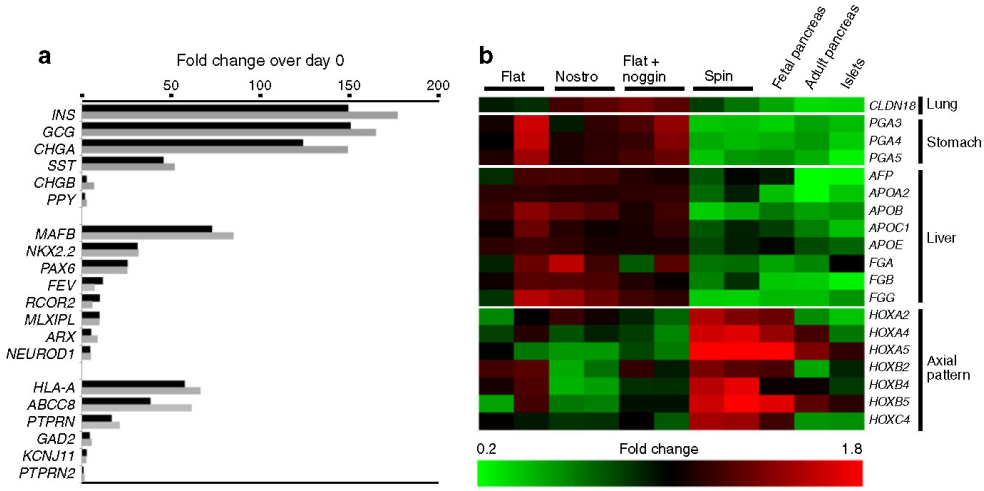


**Fig. 7** Gene expression profiling of spin EB-derived INS-GFP$^+$ cells using Illumina microarrays. **a** Bar graph showing selected pancreas-associated genes, the expression of which was upregulated in INS-GFP$^+$ cells derived from MEL1- and HES3-based *INS*$^{GFP/w}$ hESCs differentiated using the spin EB (grey) and flat culture + noggin (black) protocols. Fold change was calculated from the average signal obtained from two independent spin EB- and flat culture-derived samples divided by the average signal obtained for those genes in the undifferentiated MEL1 and HES3 *INS*$^{GFP/w}$ hESCs. **b** Two-colour heat map representation of selected data derived from Illumina gene chip analysis of INS-GFP$^+$ cell fractions generated using the protocols indicated. Only genes that were upregulated more than twofold in pair-wise comparisons from two independently derived samples from the spin EB and flat culture differentiation protocols are shown. Expression levels were background adjusted, quantile normalised and $\log_2$ transformed using R/Bioconductor. The heat map represents expression of each gene relative to its average expression level across all eight INS-GFP$^+$ samples

monitored. We have used these cells to generate a set of gene profiling data that will serve as a baseline for future studies on hESC-derived endocrine cells. These data, in conjunction with immunofluorescence studies, reveal that INS-GFP$^+$ cells generated with two distinct but related protocols [11, 12] have hallmarks of immature endocrine cells. This conclusion was drawn from the observation that most INS-GFP$^+$ cells in late-stage (day 20–25) cultures produced other endocrine hormones, most commonly glucagon. Although cells producing multiple hormones are present in the developing human pancreas, their relative abundance as a fraction of the hormone-positive population is minor [26]. Several theories have been proposed to account for polyhormonal cells in cultures of differentiating hESCs. The preponderance of INS$^+$ cells that express other hormones may indicate a bona fide differentiation-intermediate population, further development of which is arrested because culture conditions are not appropriate. Alternatively, the appearance of this cell type may signify that current culture conditions drive the generation of an in vitro artefact that lacks the capacity for further differentiation along the beta cell lineage. BrdU labelling experiments suggest that the polyhormonal cells generated under these conditions are postmitotic, a conclusion consistent with other studies suggesting that the major source of new islets during development is not pre-existing hormone-producing cells [27–30].

Taken together, the above observations emphasise that further work will be required before mature beta cells can be readily generated from hESCs. Therefore, methodologies that lend themselves to testing large numbers of variables will assist efforts to refine or reconstruct hESC to beta cell differentiation protocols. In this context, we used *INS*$^{GFP/w}$ hESCs to develop a 96-well format spin EB differentiation protocol that used the recombinant protein-based medium, APEL [6]. This platform has a number of advantages that will facilitate further exploration of pathways governing pancreatic differentiation of hESCs. First, the 96-well format is compatible with high-throughput methodologies that enable the simultaneous assessment of large numbers of variables. Second, because APEL contains only recombinant proteins (albumin, transferrin and insulin), inconsistencies arising from batch to batch variation intrinsic to media components such as BSA are minimised. Using the spin EB platform, we observed that INS-GFP$^+$ cells appeared in the context of a variety of morphologically distinct structures, some of which appeared to derive and/or separate from the main mass of the EB and resembled

islet-like clusters described by others [3, 31]. Interestingly, islet-like clusters in both reports contained a substantial fraction of $INS^+$ cells that did not co-produce either glucagon or somatostatin, mirroring our findings with spin EB-derived INS-$GFP^+$ cells. This phenotype would be consistent with the idea that spin EB-derived INS-$GFP^+$ cells represented a more mature stage of development, a conclusion supported by the substantial number of INS-$GFP^+$ cells in spin EBs producing the later-stage beta cell differentiation marker, NKX6.1 [32].

Nevertheless, with the notable exception of *INS*, *GCG* and *SST*, our microarray data indicated that INS-$GFP^+$ cells generated using all of the protocols (flat, Nostro or spin EB) expressed relatively low levels of genes recently reported by Dorrell and colleagues [33] to be associated with mature alpha or beta cells (ESM Fig. 7). This observation reinforces the notion that establishing culture conditions that promote appropriate maturation represents a significant hurdle for the generation of functional beta cells in vitro.

Our microarray data also suggested that spin EB-derived INS-$GFP^+$ cells expressed lower levels of transcripts associated with non-pancreatic endodermal cell types and higher levels of *HOX* genes—genes with a known role in setting axial position within the developing embryo. In this light, it is tempting to speculate that the spin EB environment may provide differentiative cues that more precisely specify positional identity and/or more closely resemble those in the embryo. While further studies are necessary to determine if INS-$GFP^+$ cells can be further differentiated, the $INS^{GFP/w}$ hESCs and 96-well spin EB format protocol described here represent new tools for optimising generation of beta cells in vitro for the treatment of type 1 diabetes.

**Acknowledgements** We thank R. Mayberry, K. Koutsis and A. Bruce for the provision of hESCs, S. Hawes for the provision of human fetal pancreas RNA, FlowCore for flow cytometric sorting, and Monash Micro Imaging for confocal microscopy and time-lapse video services. All work involving experimentation with human ES cell lines was performed under approval of the Monash University Human Ethics Committee (2002-225MC). This work was supported by the Australian Stem Cell Centre (ASCC), The National Health and Medical Research Council (NHMRC) of Australia and the Juvenile Diabetes Research Foundation. M. C. Nostro was supported by a postdoctoral fellowship from the McEwen Centre for Regenerative Medicine. L. C. Harrison is a Senior Principal Research Fellow, and A. G. Elefanty and E. G. Stanley are Senior Research Fellows of the NHMRC.

**Contribution statement** SJM contributed to the conception and design, collection and assembly of data, data analysis and interpretation, manuscript writing and final approval of the manuscript. XL, JVS, CEH, QCY, SML, MCN, DAE and SF contributed to the collection and assembly of data, data analysis and interpretation and critical revision, and gave final approval of the manuscript. LCH and GK contributed to provision of study materials, data analysis and interpretation and critical revision, and gave final approval of manuscript. AGE and EGS contributed to conception and design, data analysis and interpretation, manuscript writing and financial support, and gave final approval of manuscript.

**Duality of interest** The authors declare that there is no duality of interest associated with this manuscript.



## References

1. Speight J, Reaney MD, Woodcock AJ, Smith RM, Shaw JA (2010) Patient-reported outcomes following islet cell or pancreas transplantation (alone or after kidney) in type 1 diabetes: a systematic review. Diabet Med 27:812–822
2. Kroon E, Martinson LA, Kadoya K et al (2008) Pancreatic endoderm derived from human embryonic stem cells generates glucose-responsive insulin-secreting cells in vivo. Nat Biotechnol 26:443–452
3. Jiang W, Shi Y, Zhao D et al (2007) In vitro derivation of functional insulin-producing cells from human embryonic stem cells. Cell Res 17:333–344
4. Van Hoof D, D'Amour KA, German MS (2009) Derivation of insulin-producing cells from human embryonic stem cells. Stem Cell Res 3:73–87
5. Ng ES, Davis RP, Azzola L, Stanley EG, Elefanty AG (2005) Forced aggregation of defined numbers of human embryonic stem cells into embryoid bodies fosters robust, reproducible hematopoietic differentiation. Blood 106:1601–1603
6. Ng ES, Davis R, Stanley EG, Elefanty AG (2008) A protocol describing the use of a recombinant protein-based, animal product-free medium (APEL) for human embryonic stem cell differentiation as spin embryoid bodies. Nat Protoc 3:768–776
7. Goulburn AL, Alden D, Davis RP et al (2011) A targeted NKX2.1 human embryonic stem cell reporter line enables identification of human basal forebrain derivatives. Stem Cells 29:462–473
8. Costa M, Dottori M, Sourris K et al (2007) A method for genetic modification of human embryonic stem cells using electroporation. Nat Protoc 2:792–796
9. Davis RP, Costa M, Grandela C et al (2008) A protocol for removal of antibiotic resistance cassettes from human embryonic stem cells genetically modified by homologous recombination or transgenesis. Nat Protoc 3:1550–1558
10. Costa M, Dottori M, Ng E et al (2005) The hESC line Envy expresses high levels of GFP in all differentiated progeny. Nat Methods 2:259–260
11. D'Amour KA, Bang AG, Eliazer S et al (2006) Production of pancreatic hormone-expressing endocrine cells from human embryonic stem cells. Nat Biotechnol 24:1392–1401
12. Nostro MC, Sarangi F, Ogawa S et al (2011) Stage-specific signaling through TGFbeta family members and WNT regulates patterning and pancreatic specification of human pluripotent stem cells. Development 138:861–871
13. Micallef SJ, Li X, Janes ME et al (2007) Endocrine cells develop within pancreatic bud-like structures derived from mouse ES cells differentiated in response to BMP4 and retinoic acid. Stem Cell Res 1:25–36. doi:10.1634/stemcells.2006-0713

14. Watanabe K, Ueno M, Kamiya D et al (2007) A ROCK inhibitor permits survival of dissociated human embryonic stem cells. Nat Biotechnol 25:681–686
15. Du P, Kibbe WA, Lin SM (2008) lumi: a pipeline for processing Illumina microarray. Bioinformatics 24:1547–1548
16. Bolstad BM, Irizarry RA, Astrand M, Speed TP (2003) A comparison of normalization methods for high density oligonucleotide array data based on variance and bias. Bioinformatics 19:185–193
17. Saeed AI, Bhagabati NK, Braisted JC et al (2006) TM4 microarray software suite. Methods Enzymol 411:134–193
18. Saeed AI, Sharov V, White J et al (2003) TM4: a free, open-source system for microarray data management and analysis. Biotechniques 34:374–378
19. Dennis G Jr, Sherman BT, Hosack DA et al (2003) DAVID: database for annotation, visualization, and integrated discovery. Genome Biol 4:P3
20. da Huang W, Sherman BT, Lempicki RA (2009) Systematic and integrative analysis of large gene lists using DAVID bioinformatics resources. Nat Protoc 4:44–57
21. Pang K, Mukonoweshuro C, Wong GG (1994) Beta cells arise from glucose transporter type 2 (Glut2)-expressing epithelial cells of the developing rat pancreas. Proc Natl Acad Sci USA 91:9559–9563
22. Miralles F, Czernichow P, Ozaki K, Itoh N, Scharfmann R (1999) Signaling through fibroblast growth factor receptor 2b plays a key role in the development of the exocrine pancreas. Proc Natl Acad Sci USA 96:6267–6272
23. Otonkoski T, Cirulli V, Beattie M et al (1996) A role for hepatocyte growth factor/scatter factor in fetal mesenchyme-induced pancreatic beta-cell growth. Endocrinology 137:3131–3139
24. Bhushan A, Itoh N, Kato S et al (2001) Fgf10 is essential for maintaining the proliferative capacity of epithelial progenitor cells during early pancreatic organogenesis. Development 128:5109–5117
25. Kawazoe Y, Sekimoto T, Araki M, Takagi K, Araki K, Yamamura K (2002) Region-specific gastrointestinal Hox code during murine embryonal gut development. Dev Growth Differ 44:77–84
26. Jeon J, Correa-Medina M, Ricordi C, Edlund H, Diez JA (2009) Endocrine cell clustering during human pancreas development. J Histochem Cytochem 57:811–824
27. Castaing M, Peault B, Basmaciogullari A, Casal I, Czernichow P, Scharfmann R (2001) Blood glucose normalization upon transplantation of human embryonic pancreas into beta-cell-deficient SCID mice. Diabetologia 44:2066–2076
28. Bouwens L, Lu WG, de Krijger R (1997) Proliferation and differentiation in the human fetal endocrine pancreas. Diabetologia 40:398–404
29. Piper K, Brickwood S, Turnpenny LW et al (2004) Beta cell differentiation during early human pancreas development. J Endocrinol 181:11–23
30. Castaing M, Duvillie B, Quemeneur E, Basmaciogullari A, Scharfmann R (2005) Ex vivo analysis of acinar and endocrine cell development in the human embryonic pancreas. Dev Dyn 234:339–345
31. Jiang J, Au M, Lu K et al (2007) Generation of insulin-producing islet-like clusters from human embryonic stem cells. Stem Cells 25:1940–1953
32. Lyttle BM, Li J, Krishnamurthy M et al (2008) Transcription factor expression in the developing human fetal endocrine pancreas. Diabetologia 51:1169–1180
33. Dorrell C, Schug J, Lin CF et al (2011) Transcriptomes of the major human pancreatic cell types. Diabetologia 54:2832–2844

## 3.2 Discussion

Most protocols described for the generation of pancreatic cells from hESCs utilise an ontogenetic approach in which the cells are guided stepwise through the same differentiation intermediates as those observed during pancreatic embryogenesis. Generally, most groups have observed the formation of polyhormonal endocrine cells, with limited evidence of formation of monohormonal INSULIN+ cells. As there is no evidence for the retention of polyhormonal cells in the adult, this observation suggests that the INSULIN+ cells generated *in vitro* represent embryonic or fetal-like precursors. These polyhormonal endocrine cells, which can co-express two or more of the pancreatic hormones, have been well described during human fetal development ((Bocian-Sobkowska et al., 1999), (Piper et al., 2004) (Jeon et al., 2009), (Riedel et al., 2012)). Nevertheless, the true lineage relationship between the polyhormonal cells observed during embryogenesis and monohormonal endocrine cells of the adult is yet to be established. Two models (shown below in figure 3.1) have been proposed. The first theory, based on evidence accrued from the study of mouse pancreatic development, suggests that polyhormonal cells are formed during a primary transition and play a role restricted to the control of glucose homeostasis during development. As such, polyhormonal cells have been postulated to represent a so-called developmental dead-end. This theory therefore requires that the monohormonal cells seen in the islets of the adult are generated from a separate progenitor pool to the one that generates polyhormonal cells.

A second theory proposes that the monohormonal cells are descendants of the polyhormonal cells, and are the result of the further maturation and lineage restriction of the polyhormonal cells observed during human development (contrary to what is though to occur during mouse development). This second theory is supported by studies of pre-term neonatal infants, where evidence for the persistence of polyhormonal cells is observed, along with identifiable defects in the synthesis of insulin from its precursor, proinsulin (Mitanchez-Mokhtari et al., 2004).

The third possibility is that both pathways contribute to the final make up of insulin+ cells within the islets of the adult. The work contained in this thesis does not aim address the question of the relationship between monohormonal and polyhormonal cells during pancreatic endocrine development, and is insufficient to adequately support either theory of endocrine cell formation. Although all of the above theories would be difficult to test with human fetal pancreatic material, hESC derived INSULIN+ cells derived *in vitro* represent a tractable model for addressing this interesting biological question. Specifically, single INSULIN-GFP+ cells isolated by FACS could be observed for down stream differentiation potential. In such experiments it would be of particular interest to determine if a single cell could give rise to more than one endocrine cell type.

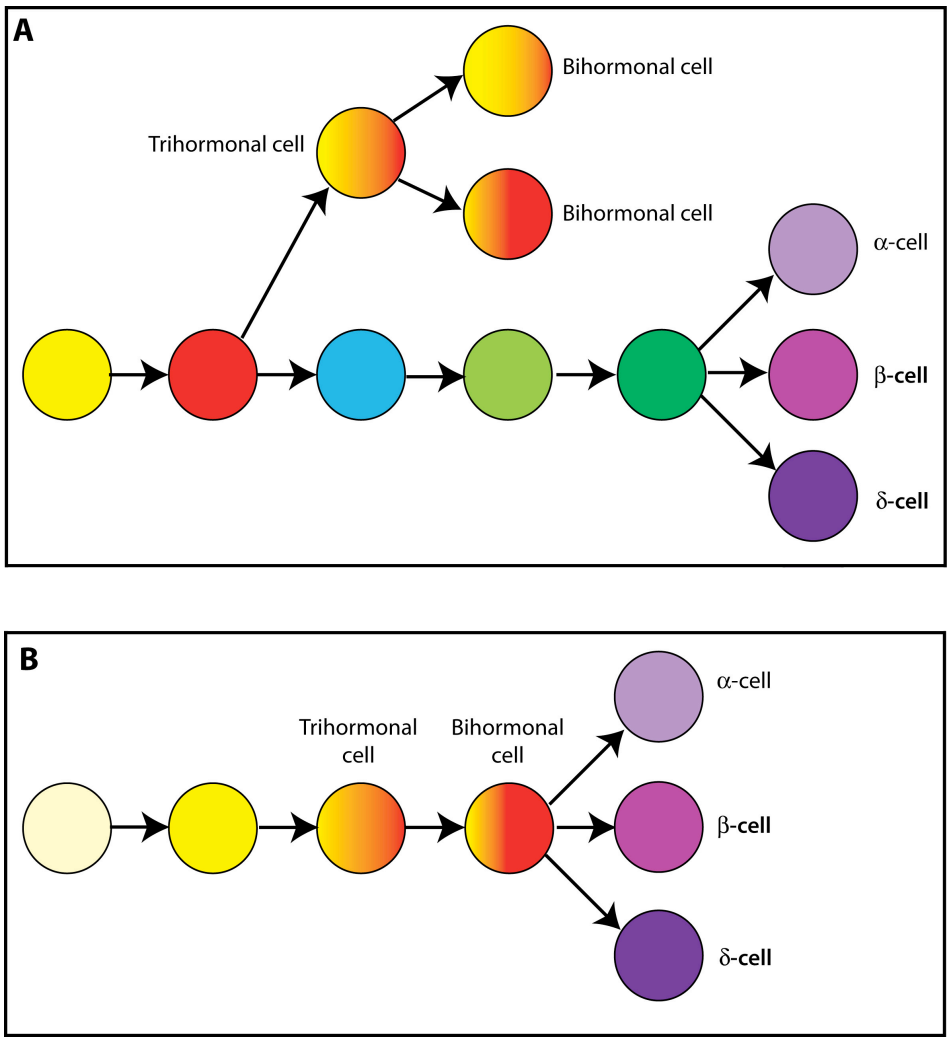


**Figure 3.1 –** Schematic of two alternate theories concerning the role of polyhormonal cells during pancreatic endocrine development. **(A)**. Polyhormonal cells, such as trihormonal cells, are unable to give rise to monohormonal endocrine cells, but instead represent a developmental dead-end. **(B)** Polyhormonal cells are able to mature further and form monohormonal endocrine cells representing the three predominant endocrine cells of the adult islet.

The 'spin EB' protocol described in this paper results in the generation of both monohormonal INSULIN+ cells, as well as INSULIN+ cells that co-express NKX6.1. Whether or not these two populations overlap was not directly investigated in this paper, although this question is specifically addressed in the following chapter.

A clear finding from gene profiling studies was that INSULIN+ cells produced via the 'spin EB' protocol had lower expression levels of non-pancreatic endodermal genes associated with organs such as the stomach and lung, and increased levels of HOX genes – which are associated with axial patterning. We hypothesised that the greater 'pancreatic' character of cells generated by this method may be due to the presence of other non-endodermal cell types; cells which might provide additional instructive information to the developing INSULIN+ cells. Although the identity of these auxiliary cells was not specifically investigated, subsequent studies by our laboratory (Dr. Suzanne Micallef) suggest that spin EBs contain mesodermal derivatives including mesenchymal cells and endothelial cells. Given that these lineages are also known to play a key role in pancreatic development ((Attali et al., 2007; Sand et al., 2011)), it is tempting to speculate that these non-endodermal cell types may positively contribute to the overall differentiation process.

The growth factors used to guide differentiation in our protocol are not so different to other methods published previously (reviewed in (Van Hoof et al., 2009) and more recently (Shi, 2010), (Nostro et al., 2011) (Xu et al., 2011), (Rezania et al., 2012)). However, most of these protocols report that a high proportion of definitive endoderm is formed during the early phases of differentiation (generally 90-100%). We hypothesise that in spin EB protocol, a lower proportion of definitive endoderm is formed (described in chapter 2), allowing for the formation of other cell types, such as mesoderm-derived mesenchymal cells that may play a patterning role in INSULIN+ cell generation.

In summary, this chapter has described both the generation of an INSULIN$^{GFP/w}$ human ES cell line, and it's utility in the establishment of a 'spin EB' protocol. This protocol appeared to generate INSULIN+ cells that were more closely related to human pancreatic tissues than endocrine cells derived from other methods.. Additionally, the INSULIN+ cells had decreased expression of genes associated with 'off-target' endodermal organs. Immunofluorescence analysis and intracellular flow cytometry revealed that, in contrast to previously published protocols, INSULIN+ cells generated using this spin EB method

contained a subset of monohormonal cells and a subset of INSULIN+ cells that co-express NKX6.1.

# Chapter 4

## *In vitro* and *in vivo* potential of human ES cell derived insulin-GFP$^+$ cells

## 4.1 Introduction

Most studies in which hESC derived cells have been shown to ameliorate diabetes in animal models have utilised cells representing the pancreatic progenitor stage ((Jiang et al., 2007b), (Shim et al., 2007), (Kroon et al., 2008), (Rezania et al., 2012)). Although some studies have been performed with cultures containing INSULIN$^+$ cells, the lack of cell surface markers enabling isolation of this cell type means it is difficult to attribute functional outcomes to specific cell populations within the transplanted material. Nevertheless, when late stage differentiation cultures containing INSULIN$^+$ cells have been transplanted into animal models, they have been either unable to ameliorate diabetes ((Phillips et al., 2007), (Eshpeter et al., 2008)), or have been unable to ameliorate hyperglycaemia under non-fasting conditions (Mao et al., 2009). Collectively, these studies illustrate that there is still scant evidence in the literature to suggest that INSULIN$^+$ cells generated *in vitro* can function as mature beta cells following transplantation.

The availability of an INSULIN$^{GFP/w}$ human ES cell line provided an opportunity to directly address questions relating to the functionality of late stage differentiated INSULIN$^+$ cells produced in vitro. Using this line, Basford *et.al* found that polyhormonal INSULIN$^+$ cells transplanted into the mammary fat pad of immunocompromised mice formed a homogenous GLUCAGON$^+$ cell population after 4 weeks ((Basford et al., 2012)). This result resembled that reported in a previous study in which human ES cell derived CD318$^+$ polyhormonal endocrine cells were found to give rise to mostly GLUCAGON$^+$ cells, with a few scattered SOMATOSTATIN$^+$ cells following transplantation. In contrast pancreatic progenitor cells (CD318$^-$ cells) present at the same stage of differentiation went on to form clear INSULIN$^+$ cell clusters (Kelly et al., 2011).

As we have developed a protocol that resulted in the generation of a population containing monohormonal INSULIN$^+$ cells, we sought to investigate the *in vitro* and *in vivo* potential of these cells. However, as it was difficult to generate large numbers of these cells, we first set about constructing a cell line that would allow us to follow small numbers of cells following transplantation. In the longer term, we envisaged that such tools might also be useful for experiments in which the effect of transplantation site on graft proliferation, differentiation and function was addressed. Such studies would be particularly interesting given recent evidence suggesting that the choice of transplantation site can have a significant effect on both cell survival and differentiation outcome (Sui et al., 2012).

In order to monitor the survival and growth of small numbers of transplanted cells, we took advantage of recent advances in *in vivo* bioluminescent imaging technology. This technology allows for the real-time evaluation and monitoring of transplanted cells, as compared to having to identify transplanted cells *ex vivo* using histological methods. Additionally, bioluminescent reporters do not require extrinsic light for excitation and the light that they generate has an increased tissue penetrance, as compared to fluorochromes, such as eGFP, thereby making them a good choice for *in vivo* studies.

Bioluminescence imaging (BLI) is based on the detection of light emitted by cells that express light generating enzymes – typically luciferase. Luciferase generates visible light as a result of the oxidation of enzyme specific substrates, for example D-luciferin (for firefly luciferase) or coelenterazine (for *Renilla* luciferase). The generation of light by luciferase does not require excitation by an external light source, and imaging can be conducted 10-15 minutes after the administration of the substrate, for example, by either intraperitoneal (IP) or intravascular (IV) injection. Luciferase expressing cells can be visualised by placing the animal in a light-tight box fitted with a cooled charged-coupled device (CCD) camera. The CCD camera has the ability to detect very low levels of light emitted by the internal organs (Contag et al., 2000) and this image can be superimposed onto a photograph of the animal, to give a composite image of both the intensity and location of the bioluminescence source (Wu et al., 2001).

We envisaged that a hESC line that constitutively expressed luciferase would have a number of uses. First, it would enable the optimal cell number of cells required to ensure graft survival to be easily and quickly assessed. Second, it would enable expansion of the transplanted population to followed over time. Third, it would facilitate experiments aimed at determining whether co-transplantation of supportive cells aided either survival or proliferation of the initial INSULIN$^+$ population. In order to achieve this aim, the INSULIN$^{GFP/w}$ human ES cell line described in chapter 3 was further genetically modified to constitutively express firefly luciferase. This chapter will describe both the generation of this cell line, denoted TgEF1$\alpha^{Luc}$.INS$^{GFP/w}$, and preliminary experiments performed to demonstrate it's utility in cell transplantation studies.

## 4.2 Methods

### 4.2.1 Generation and extraction of plasmids from bacteria

Molecular biology and recombinant DNA techniques used were essentially as described in Sambrook and Russell ((Sambrook et al., 2001)). Typically, plasmid DNA was extracted from 5-10ml of bacterial cultures following overnight growth, by an alkaline lysis method, and purified using the QIAGEN Plasmid Mini kit (Qiagen) according to the manufacturer's instructions. The resulting DNA was dissolved in TE (pH 8.0) and the concentration determined spectrophotometrically.

### 4.2.2 Construction of the luciferase expression vector

The luciferase expression vector was constructed in 5 discrete steps. First, a 298bp T2A-luciferase fragment was amplified by PCR using Phusion high-fidelity DNA polymerase (New England Biolabs), using a pEFBOSLuciferaseIRESPuro plasmid (A. Conscience and E.Stanley, unpublished) as a template. The PCR primers used were LucT2afwd and LucRev (see appendix 5). The PCR fragment was purified using a QIAquick PCR purification kit (Qiagen) as per the manufacturers instructions and cloned into the endogenous cloning site of a TOPO-XL plasmid (Invitrogen corporation) as per the manufacturers instructions. The TOPO-XL-T2ALuciferase plasmid was then digested with SalI and BstBI to generate a 254bp DNA fragment encompassing the T2A and a partial luciferase cDNA coding sequences. This fragment was then cloned between the SalI and BstBI sites present in the pEFBOSLuciferaseIRESPuro plasmid. The puromycin resistance gene was then removed by digestion with AscI and ClaI and replaced with a resistance gene that has been codon optimised for expression in mammalian cells (synthesised by Genescript). All plasmid and primer sequences can be found in appendix 5. A schematic outlining the key steps in the construction process is provided in figure 4.1A.

### 4.2.3 Maintenance of undifferentiated human ES cells

Two genetically modified human ES cell lines were used in this study – a HES3 ((Richards et al., 2002)) derived INSULIN$^{GFP/w}$ human ES cell line and a MEL1 (Obtained from the Australian Stem Cell Centre) derived INSULIN$^{GFP/w}$ human ES cell line ((Micallef et al., 2012)). The materials and methods for culturing human ES cells are detailed in Chapter 2. Briefly, cells were cultured in tissue culture flasks (T25 – T150cm$^2$, IWAKI) pre-seeded with primary mouse embryonic fibroblasts (PMEFs) in human ES cell media supplemented with 10ng/ml bFGF (R&D systems) ((Amit et al., 2000)). Cells were passaged either

mechanically or enzymatically as described in Costa *et.al,* 2008 ((Costa et al., 2008)). Karyotype analysis was performed by Southern Cross Pathology, Monash Medical Centre, Melbourne ((Costa et al., 2008)).

### 4.2.4 Electroporation and selection of stably transfected INSULIN$^{GFP/w}$ human ES cells

Electroporation of INSULIN$^{GFP/w}$ human ES cells with the luciferase expression vector were carried out as previously described ((Costa et al., 2007)). Briefly, INSULIN$^{GFP/w}$ human ES cells were expanded using enzymatic passaging to generate ~ 1 x $10^7$ undifferentiated cells. The cells were harvested and dissociated with TryPLE select (Gibco, Invitrogen Corporation) to form a single cell suspension. Approximately 1 x $10^7$ cells were resuspended in 500μl of PBS, transferred into a 1ml cuvette and electroporated (250V, 500μF) (Gene Pulser II System, BioRad) in the presence of 25-50μg of luciferase expression vector. The expression vector had been linearised with the restriction enzyme ZraI prior to electroporation.

Electroporated cells were seeded into 10 x 6cm$^2$ dishes (BD Biosciences) and cultured for 2 weeks before G418 (Gibco, Invitrogen Corporation) selection was applied. Stably transfected G418-resistant colonies were enzymatically harvested and dissociated to form a single cell suspension. Using the single cell deposition function of a FACS-DIVA flow cytometer (BD Biosciences), single cells representing each clone were deposited into individual wells of 96-well plates (Falcon) that had been pre-seeded with 1.0 x $10^4$/cm$^2$ of mitotically inactivated MEFs. Colonies arising from this procedure were maintained under G418 selection and expanded via manual passaging as previously described ((Costa et al., 2007)). Following a further 4 weeks of expansion, individual clones were split between corresponding wells of two 48-well plates (Falcon). Two thirds of each colony was transferred to the first 48-well plate and used for *in vitro* luciferase screening whilst one third of the colony was transferred to the second 48-well plate, which was used for maintenance of the individual clones until screening had been completed.

### 4.2.5 *In vitro* luciferase screening for identification of transgenic luciferase-INSULIN$^{GFP/w}$ human ES cells

In order to identify clones that robustly expressed the luciferase transgene, cells were lysed and the cell lysate mixed with luciferin, using a ONE-Glo luciferase assay (Promega), as per the manufacturers instructions. Luciferase expression from each clone was then

analysed using a BMG fluostar optima (BMG Labtech). Clones with luciferase expression, measured in relative light units, that was more than ~300-fold higher than the negative control (the relevant parental INSULIN$^{GFP/w}$ human ES cell line) were selected for further analysis (see section 4.2.3)

### 4.2.6 Teratoma formation by transgenic luciferase-INSULIN$^{GFP/w}$ human ES cells

Testis teratoma formation assays were performed by staff at the Animal Research Laboratories (ARL), Monash University. Approximately 2 x $10^5$ undifferentiated TgEF1$\alpha^{Luc}$.INS$^{GFP/w}$ hESCs were injected into the testis capsule of 6 week old NOD-SCID-IL2rγ deficient mice. Alternatively, defined numbers of undifferentiated TgEF1$\alpha^{Luc}$.INS$^{GFP/w}$ hESCs were transplanted in 10μl of growth factor reduced matrigel (BD Biosciences) under the kidney capsule of 6 week old NOD-SCID-IL2rγ deficient mice by Dr. Suzanne Micallef and Ms. Tanya Hatzistavrou.

### 4.2.7 Transplantation of differentiated TgEF1$\alpha^{Luc}$.INS$^{GFP/w}$ hESCs

TgEF1$\alpha^{Luc}$.INS$^{GFP/w}$ hESCs were differentiated according to protocols describe in chapters 2 and 3. Following this, cells were sorted using a BD Influx flow cytometer (BD Biosciences) based on GFP expression. Sorted cells were reaggregated in 10mM rho kinase inhibitor, Y27632, as described in chapter 2. Following 48 hours of incubation at 37°C, 5% $CO_2$, reaggregates were harvested and coalesced by low speed centrifugation. The reaggregates were then resuspended in 10μl of growth factor reduced matrigel and transplanted under the kidney capsule of 6 week old NOD-SCID-IL2rγ deficient mice by Dr. Suzanne Micallef and Ms. Tanya Hatzistavrou.

### 4.2.8 *In vivo* bioluminescence imaging

In order to visualise TgEF1$\alpha^{Luc}$.INS$^{GFP/w}$ hESCs, or their derivatives, mice were administered with 150mg/kg of VivoGlo luciferin (Promega) by intraperitoneal (IP) injection. 5 minutes post-administration of luciferin, mice were anesthetised by inhalation of isofluorane (2% in oxygen) for 5 minutes, and then imaged using a Xenogen IVIS-200 imaging system (Caliper). Images obtained were processed using Living Image software (Caliper) to normalise luciferase expression data collected across multiple timepoints.

### 4.2.9 Immunostaining of grafts

Animals harbouring grafts were killed by cervical dislocation and the kidney and associated transplanted material removed. The region of kidney containing the graft was then identified under a dissecting microscope. Often the graft appeared as a small area of opaque tissue on the surface of the kidney. The regions surrounding the graft were then resected and placed in 4% wt/vol paraformeldehyde in PBS at 4°C overnight. The fixed tissue was transferred to a histology processing cassette and paraffin embedded and sectioned by Monash Histology Services. Sections were placed on histological slides and approximately every 10$^{th}$ slide was stained with haematoxylin and eosin (Monash Histology Platform). Stained slides were then examined under a standard transmission light microscope to determine which sections warranted further investigation using immunofluorescence analysis.

Immunofluorescence imaging was performed using a Nikon C1 upright microscope and images processed with Fiji and Image J software. For immunofluorescence analysis of sectioned material, non-specific antibody binding was blocked with PBS supplemented with 10% vol/vol FCS for 1 hour at room temperature. Samples were incubated with primary antibodies overnight at 4°C. Following washing in PBS for 15 minutes, secondary antibodies were applied for 1 hour at room temperature. The samples were washed in PBS and cover-slips mounted using fluorescent mounting medium (Dako) prior to analysis. The antibodies used in immunofluorescence analysis are shown below table 4.1.

**Table 4.1 List of antibodies used immunofluorescence analysis**

| Antibody | Supplier | Catalogue Number | Concentration |
|---|---|---|---|
| Mouse anti-NKX6.1 | Developmental Studies Hybridoma Bank | F55A12 | 1:20 |
| Guinea-pig anti-insulin | Dako | A056401-2 | 1:100 |
| Mouse anti-glucagon | Sigma | G2654 | 1:50 |
| Rat anti-somatostatin | Millipore | MAB354 | 1:50 |
| Rabbit anti-MafA | Bethyl Laboratories | IHC-00352 | 1:500 |
| Goat anti-guinea pig Alexa-488 | Invitrogen | A11073 | 1:1000 |
| Goat anti-mouse Alexa-568 | Invitrogen | A11061 | 1:1000 |
| Goat anti-rat Alexa-555 | Invitrogen | A21434 | 1:1000 |
| Goat anti-rabbit Alexa-568 | Invitrogen | A11011 | 1:1000 |
| Goat anti-mouse Alexa-647 | Invitrogen | A21236 | 1:1000 |

For wholemount immunofluorescence of reaggregated cells, reaggregates were fixed for 90 minutes on ice in 4% wt/vol paraformeldehyde in PBS and permeabilised using 1% Triton X-100 (in PBS) at room temperature for 90 minutes. Reaggregates were blocked in PBS containing 10% vol/vol FCS. Detection of primary and secondary antibodies was as described above.

### 4.2.10 Analysis of proinsulin processing

Reaggregates were washed for 1 hour in Krebs-Ringer buffer (129mM NaCl, 4.8mM KCl, 2.5mM $CaCl_2$, 1.2mM $KH_2PO_4$, 1.2mM $MgSO_4$, 5mM $NaHCO_3$, 10mM HEPES, 0.1% wt/vol rhAlbumin), then incubated for 1 hour in Krebs-Ringer buffer with 2mM D-glucose and 18mM L-glucose. Following this, reaggregates were incubated in Krebs-Ringer buffer with 20mM D-glucose for 1 hour, then in Krebs-Ringer buffer with 20mM D-glucose and 30mM KCl, and finally in Krebs-Ringer buffer with 2mM D-glucose and 18mM L-glucose for 1 hour, before being moved back into APEL medium with 10mM Nicotinamide and 50ng/ml IGF-1. Buffer was collected at each medium change and analysed for the presence of proinsulin and C-peptide using a proinsulin ELISA and ultrasensitive c-peptide ELISA (Alpco). The ratio of proinsulin to C-peptide was then calculated.

## 4.3 Results

### 4.3.1 Generation of a TgEF1α$^{Luc}$.INS$^{GFP/w}$ human ES cell line

A luciferase expression vector of 8656bp was generated using standard cloning procedures (figure 4.1A). The final vector consisted of a 1505bp EF1α promoter, a 1743bp firefly luciferase cDNA, a 576bp internal ribosome entry site (IRES), and a 826bp neomycin resistance gene optimised for expression in mammalian cells. The correct vector configuration was confirmed by restriction enzyme analysis and sequencing of junctions between the individual components of the vector (data not shown). A ZraI restriction site present in the plasmid backbone was used to linearize the vector prior to electroporation.

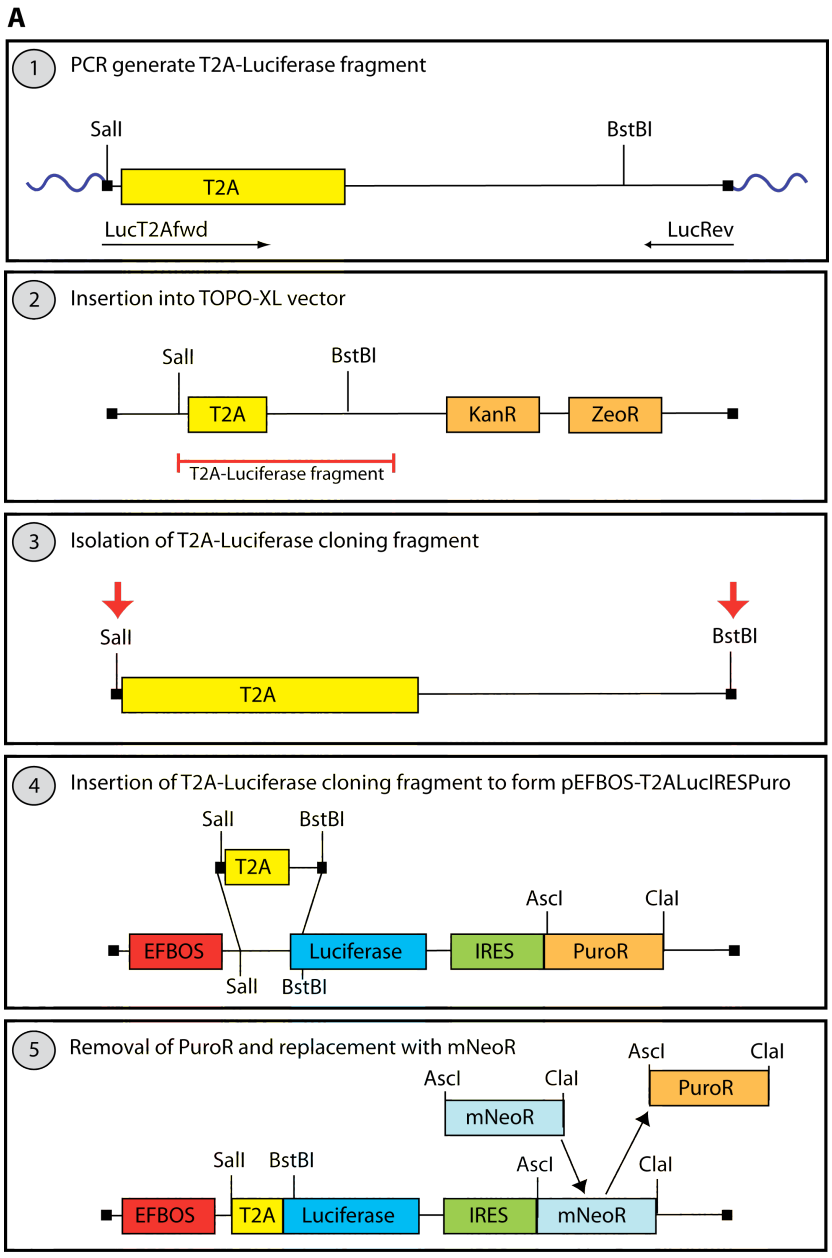


**Figure 4.1 – (A)** Schematic representing stepwise construction of the luciferase expression vector. Step 1: A T2A flanked by a partial luciferase cDNA was generated by PCR using the pEFBOSLuciferaseIRESPuro plasmid as a template in conjunction with LucT2Afwd and LucRev primers (sequences shown in appendix 5). Step 2: The T2A-Luciferase PCR fragment was inserted into a TOPO-XL plasmid using the TOPO endogenous cloning site. Step 3: The T2A-Luciferase cloning fragment was isolated by digestion with SalI and BstBI. Step 4: The T2A-Luciferase fragment was inserted into pEFBOSLuciferaseIRESPuro that had been previously digested with SalI and BstBI, to form pEFBOS-T2ALucIRESPuro. Step 5: Standard molecular cloning was used to excise the PuroR cDNA and ligate a mNeoR cDNA. Luc*, Luciferase*; mNeo, *mammalian Neomycin;* Puro, *Puromycin*

**B**

| Clone# | HES3 TgEF1α$^{Luc}$.INS-GFP clones | | | | | | | |
|---|---|---|---|---|---|---|---|---|
| #1 | 242 | 1111 | 501424 | 1655 | 163 | 184 | 366 | 129 |
| #9 | 134 | 270 | 1223 | 329 | 141 | 313 | 333 | 219 |
| #17 | 435 | 351 | | | | | | |
| | **MEL1 TgEF1α$^{Luc}$.INS-GFP clones** | | | | | | | |
| #1 | 149329 | 59007 | 4339 | 1027 | 508308 | 2125 | 1913 | 706446 |
| #9 | 443 | 50168 | 308 | 306 | 2281 | 318234 | 8120 | 1270 |
| | **Negative control** | | | | | | | |
| #1 | 161 | | | | | | | |

**Figure 4.1 - (B)** Table showing the results of *in vitro* luciferase screening of a stably integrated copy of the luciferase expression vector. Each box in this table shows the raw data representing the relative light units of luciferase expression derived from independent single clones of hESC lines transfected with the luciferase expression vector shown in A. Clones corresponding to wells circled in red were selected for further analysis based on their high level of luciferase expression, as compared to the negative control. Clones represented by wells highlighted in green text were later found to have an abnormal karyotype by G-band analysis.

Following electroporation with the luciferase expression vector, cells carrying a stably integrated copy of the vector were identified by their ability to form colonies following 10 days selection in 100ug/ml G418. After selection, colonies were pooled and then sub-cloned by sorting single cells into each well of a 96-well plate using the single cell deposition function of a FACS-DIVA flow cytometer (BD Biosciences). Clones that eventuated from this process were then screened using an *in vitro* luciferase assay, the results of which are shown below in figure 4.1B. Clones that showed luciferase expression of greater than ~300 fold above the negative control (absolute value of light emitted of greater than 50,000 relative light units), were expanded and further analysed for retention of stem cell properties.

### 4.3.2 TgEF1$\alpha^{Luc}$.INS$^{GFP/w}$ human ES cells retain stem cell properties

Clones identified following G418 selection and *in vitro* luciferase screening were karyotyped using G-band analysis, performed by Southern Cross Pathology Services at Monash Medical Centre, Melbourne. This analysis showed that of 7 initial clones (figure 4.1B), 2 had karyotypic abnormalities – specifically a chromosome 12 duplication (tri-12). Though this type of abnormality has not been shown to render the cells with a growth advantage ((Gertow et al., 2007)), these aneuploid clones were not used in any further analyses. A representative karyotype of both a normal (figure 4.2A) and an abnormal clone (figure 4.2B) is shown below.

Four of the remaining clones were analysed for retention of stem cell properties. Transplantation experiments were conducted to assess the ability of the clones to form teratomas containing tissues representative of all three germ layers – endoderm, mesoderm and ectoderm. Each clone was injected into the testis capsule of 2 mice. Following injection of undifferentiated TgEF1$\alpha^{Luc}$.INS$^{GFP/w}$ hESCs, teratomas were allowed to form for 12 weeks. Subsequent analysis showed that all clones produced teratomas containing cell types representing derivatives of all three germ layers. An example of this for one clone is shown below in figure 4.2C.

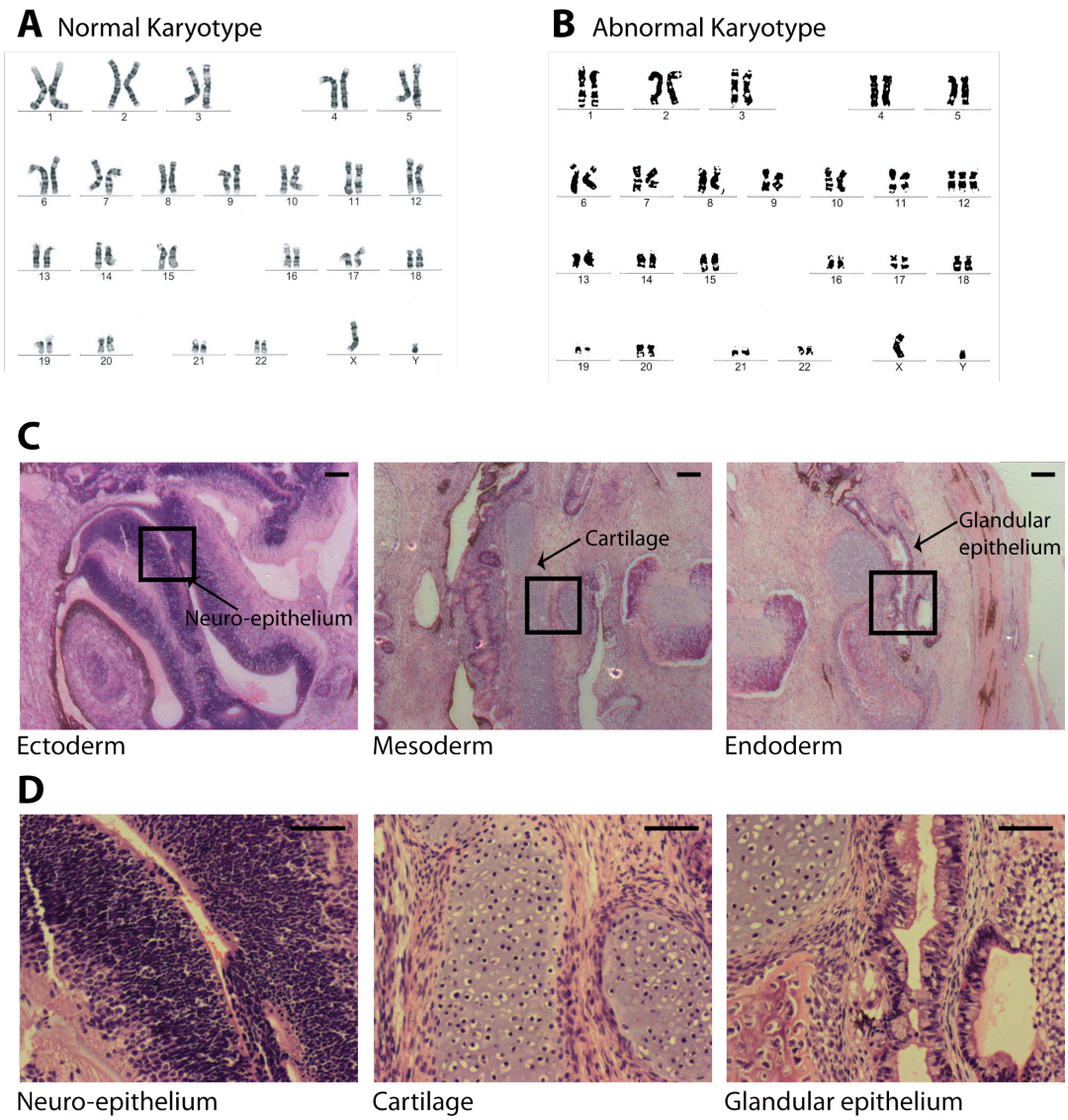


**Figure 4.2 – (A)** A representative example of a normal karyotype from a TgEF1α$^{Luc}$.INS$^{GFP/w}$ hESC clone, **(B)** A representative example of an abnormal karyotype (trisomy-12) from a TgEF1α$^{Luc}$.INS$^{GFP/w}$ hESC clone, **(C)** Derivatives of all three germ layers can be seen following haematoxylin and eosin staining of 12 week old teratomas. Scale bar 100μm

### 4.3.3 Luciferase expression is maintained *in vivo* following teratoma formation

In order to monitor teratoma formation *in vivo*, mice were imaged 6- and 12-weeks post injection of cells into the testis capsule or following transplantation of cells under the kidney capsule, using bioluminescence imaging. These experiments indicated that not all clones produced detectable luciferase expression over this time course. For example, in clone#10, teratoma 2, luciferase expression was observed 6 weeks post transplant, however, by 12 weeks post transplant, luciferase expression was no longer detectable (data not shown). In contrast, other clones maintained luciferase expression throughout the analysis period whether injected into the testis capsule (figure 4.3A), or transplanted

under the kidney capsule (figure 4.3B). This variability in expression was anticipated as it has been previously observed that transgenes driven by an EF1α promoter sometimes undergo silencing during ES cell differentiation (Lim et al., 2009).

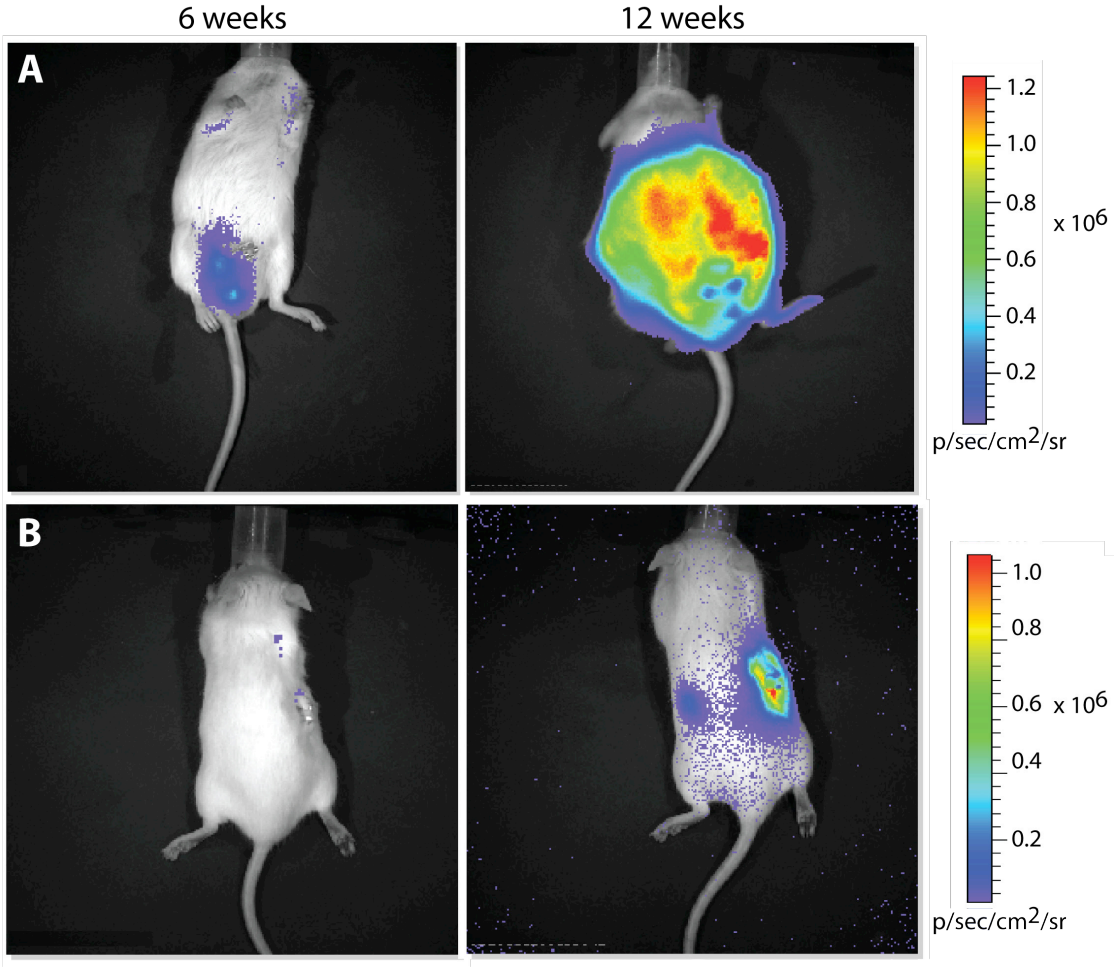


**Figure 4.3** – *In vivo* bioluminescence imaging of teratoma formation in mice
**(A)** Luciferase expression as seen by *in vivo* bioluminescence imaging following injection of undifferentiated TgEF1α$^{Luc}$.INS$^{GFP/w}$ hESC into the testis capsule, **(B)** Luciferase expression as seen by *in vivo* bioluminescence imaging following transplantation of undifferentiated TgEF1α$^{Luc}$.INS$^{GFP/w}$ hESC under the kidney capsule

### 4.3.4 Luciferase expression in TgEF1α$^{Luc}$.INS$^{GFP/w}$ human ES cells is maintained *in vitro* following differentiation

TgEF1α$^{Luc}$.INS$^{GFP/w}$ hESCs were differentiated towards an endocrine fate using protocols previously described in chapters 2 and 3. Following the onset of INSULIN-GFP expression, cells were sorted on the basis of GFP expression in order to verify that luciferase expression was maintained in the INSULIN⁺ population (a schematic of this process is shown in figure 4.4A). The aim of this experiment was to ensure that bioluminescence could be used to locate and track INSULIN⁺ cells following transplantation.

1 x $10^4$ INSULIN-GFP$^+$, INSULIN-GFP$^-$ and undifferentiated TgEF1$\alpha^{Luc}$.INS$^{GFP/w}$ hESCs were reaggregated in separate wells of a 96-well plate and were then subsequently incubated with VivoGlo luciferin for 10 minutes prior to bioluminescent imaging. This experiment demonstrated that in addition to the undifferentiated parental cells, luciferase expression was maintained in both the GFP$^+$ and GFP$^-$ differentiated cell fractions. Wells that did not contain cells failed to produce detectable luminescence (figure 4.4B).

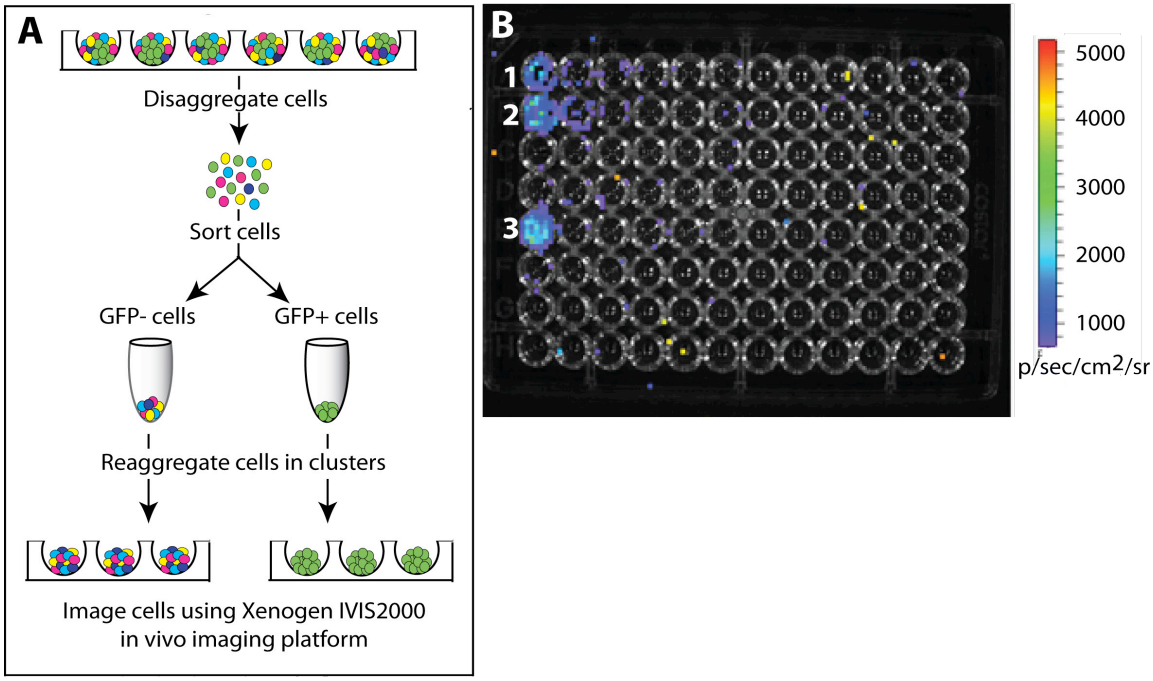


**Figure 4.4 – (B)** Schematic demonstrating the process used to analyse luciferase expression in INSULIN-GFP$^+$ and INSULIN-GFP$^-$ cells derived from TgEF1$\alpha^{Luc}$.INS$^{GFP/w}$ hESC**, (B)** *In vivo* bioluminescence imaging of 1 x $10^4$ INSULIN-GFP$^+$ (1), INSULIN-GFP$^-$ (2), and undifferentiated TgEF1$\alpha^{Luc}$.INS$^{GFP/w}$ hESC (3). Only the wells in the first left-hand column marked 1-3 contain cells – all other wells are devoid of cells.

### 4.3.5 Luciferase expression is maintained *in vivo* following isolation and transplantation of INSULIN-GFP$^+$ cells from differentiated TgEF1α$^{Luc}$.INS$^{GFP/w}$ human ES cells

As it appeared that cells retained luciferase expression throughout the differentiation process, cell transplantation experiments were undertaken. TgEF1α$^{Luc}$.INS$^{GFP/w}$ hESCs were differentiated towards an endocrine fate, and INSULIN-GFP$^+$ cells were isolated by flow cytometry. In addition, INSULIN-GFP$^-$ cells were also isolated by flow cytometry. Both groups of cells were reaggregated into clusters of 2.0 x $10^3$ cells in APEL media supplemented with 10μm Rho kinase inhibitor, 10mM Nicotinamide and 50ng/ml IGF-1 and incubated for 48 hours at 37°C, 5% $CO_2$, prior to transplantation. For the GFP$^+$ aggregates, between eight and twenty aggregates were resuspended in 10μl of growth factor reduced matrigel and transplanted under the kidney capsule of NOD-SCID-IL2rγ deficient mice. For the GFP$^-$ aggregates, between three and twenty reaggregates were transplanted. Mice were imaged immediately after transplantation and then again at approximately 1-, 2- and 3-months.

Bioluminescence derived from the grafts could not be detected on the day of transplantation or on the day following cell transplantation (data not shown). This may have been due to the low number of cells transplanted or substantial cell death associated with the transplantation procedure. At one (figure 4.5A) and two months following transplantation, grafts were still unable to be detected (figure 4.5B). However, grafts in mice that has been transplanted with twenty reaggregates of either INSULIN-GFP$^+$ cells or INSULIN-GFP$^-$ cells could be detected by bioluminescence imaging approximately 3 months post-cell transplantation (figure 4.5C). Grafts in mice that had been transplanted with less than 20 reaggregates of either INSULIN-GFP$^+$ or INSULIN-GFP$^-$ cells, were still undetectable using bioluminescence imaging at 3 months post-transplantation.

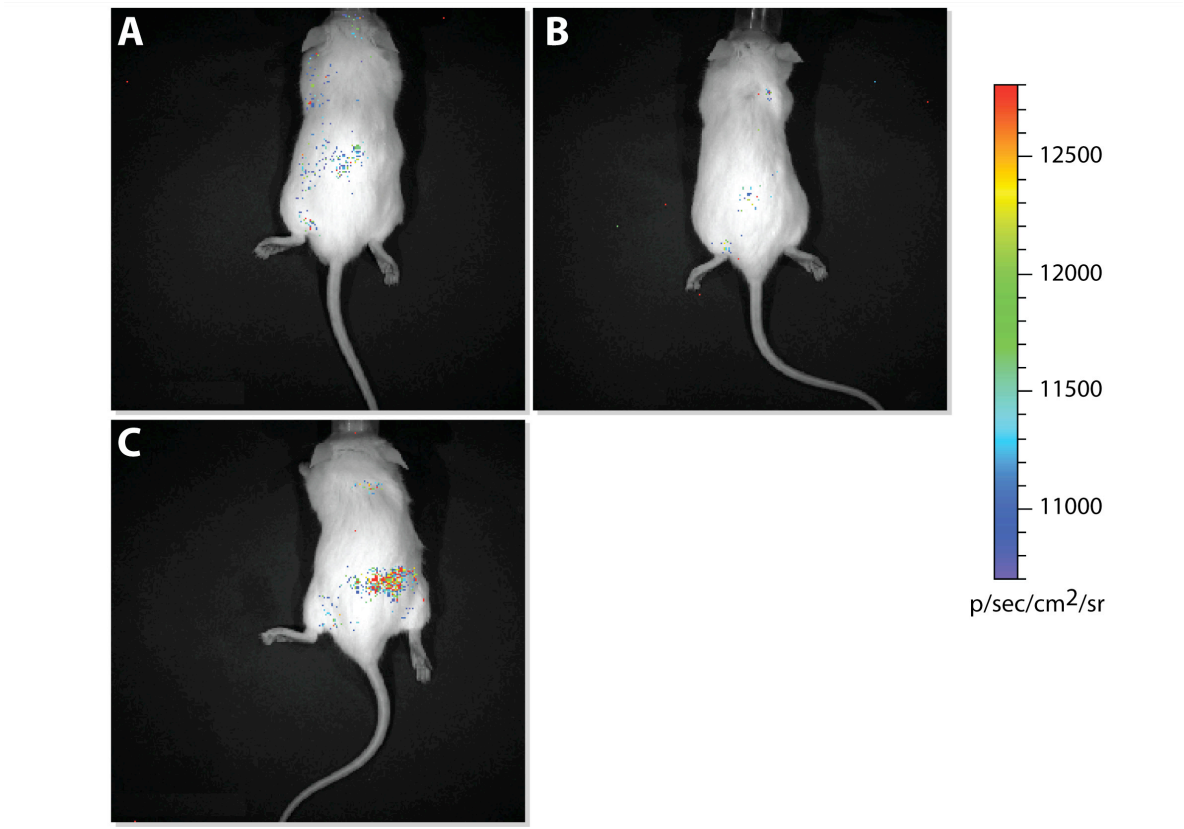


**Figure 4.5** *In vivo* bioluminescence imaging of a mouse transplanted with 20 reaggregates of 2 x $10^3$ isolated INSULIN-GFP$^+$ cells derived from TgEF1$\alpha^{Luc}$INS$^{GFP/w}$ cells at **(A)** one month post-transplant, **(B)** two months post-transplant, **(C)** three months post-transplant

### 4.3.6 Transplanted INSULIN-GFP$^+$ cells have the potential to form monohormonal endocrine cells *in vivo*

On the basis of luciferase expression, grafts were harvested 3 months following cell transplantation. Examination of grafts under a dissecting fluorescent microscope revealed that, in some instances, transplanted reaggregates retained punctate regions of clearly visible GFP expression (as shown in figure 4.6A). Grafts were then paraffin embedded, sectioned, and stained with haematoxylin and eosin. Histological analysis revealed a well vascularised graft that was clearly distinguishable from the surrounding mouse kidney. Cells within the graft had an overall appearance that resembled pancreatic endocrine tissue (figure 4.6B).

The cells contained within the graft were further analysed for the expression of endocrine hormones and beta cell associated transcription factors. Cells within the graft expressed GLUCAGON, SOMATOSTATIN and INSULIN and, generally, this expression was mutually exclusive (figure 4.6C-E). Examination of the grafts for the co-expression of INSULIN and either NKX6.1 (figure 4.6F) or MAFA (figure 4.6G), revealed that almost all INSULIN$^+$ cells

co-expressed NKX6.1, and a substantial fraction (60-70%) of INSULIN$^+$ cells co-expressed MAFA. Additionally, INSULIN$^+$ cells lacked expression of cytokeratin-19 (CK19) (figure 4.6H) – a gene that is expressed in immature endocrine cells but is lost as development proceeds (Piper et al., 2004). The fact that monohormonal INSULIN$^+$ cells expressed transcription factors commonly used as markers of beta cell maturity, such as NKX6.1 and MAFA and that CK19 expression had been down-regulated, suggested that d30 INSULIN-GFP$^+$ population included progenitors of relatively mature INSULIN$^+$ cells, as well as those representative of other endocrine lineages.

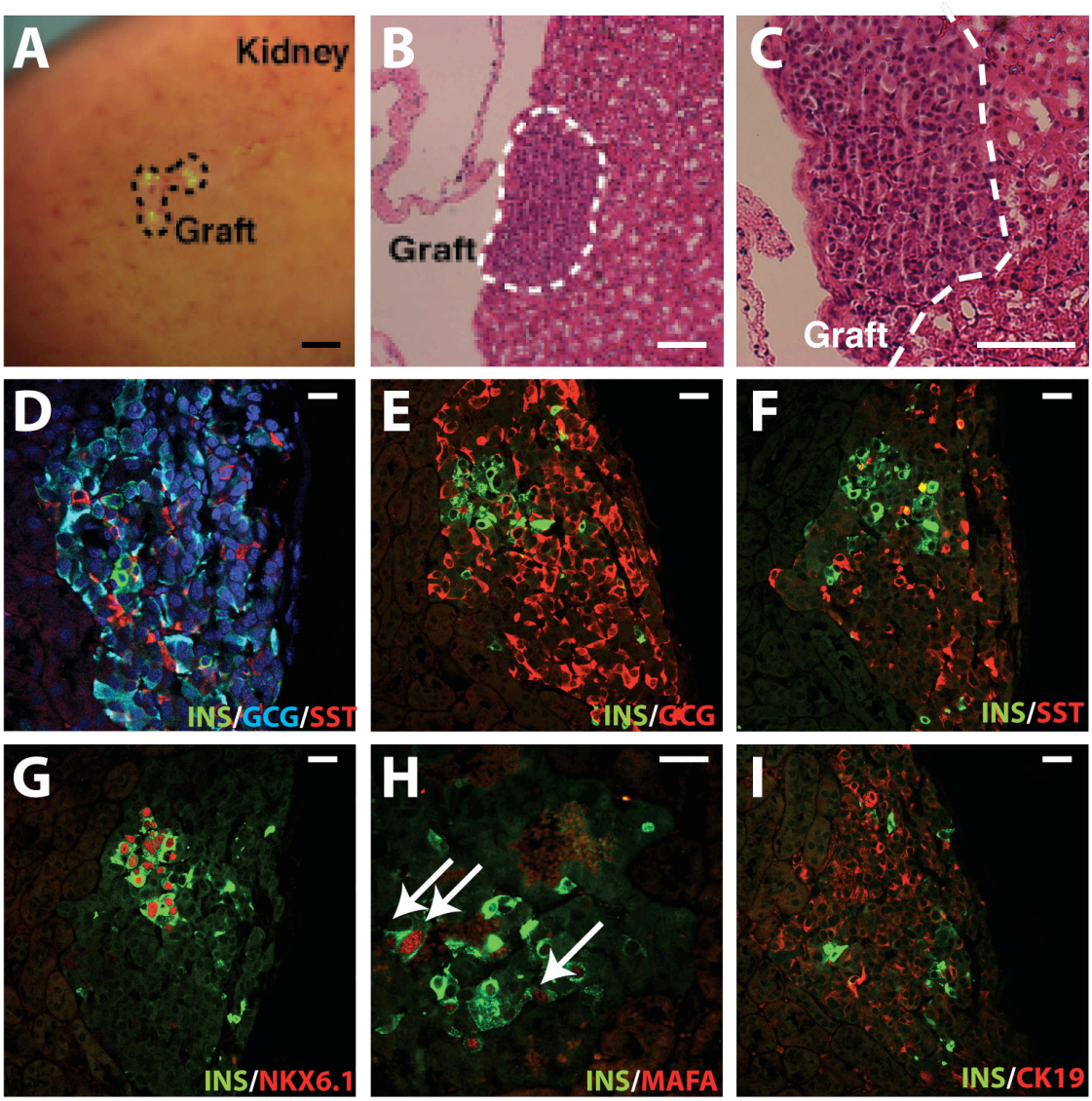


**Figure 4.6** – Analysis of three-month old grafts derived from a mouse transplanted with TgEF1α$^{Luc}$INS$^{GFP/w}$ cells. **(A)** GFP$^{+}$ cells contained within the graft could be identified *in situ* using fluorescence microscopy, **(B-C)** Haematoxylin and eosin staining of the sectioned graft demonstrated that grafted tissue has a morphology similar to pancreatic endocrine tissue, **(D)** INSULIN, GLUCAGON and SOMATOSTATIN staining of the sectioned graft, shows single hormone positive cells **(E)** INSULIN and GLUCAGON staining of the sectioned graft shows a lack of co-expression, **(F)** INSULIN and SOMATOSTATIN staining also shows that these hormones are not co-expressed. **(G)** INSULIN and NKX6.1 staining of the sectioned graft demonstrated that most INSULIN$^{+}$ cells are NKX6.1$^{+}$. **(H)** INSULIN and MAFA staining of the sectioned graft shows a subset of cells co-expressed these markers. White arrows mark cells that show co-expression of INSULIN and MAFA, **(I)** INSULIN and CK19 staining showed that the expression of these two markers did not overlap. Scale bars (A-C): 100μm; (D-I): 20μm.

### 4.3.7 INSULIN-GFP$^+$ cells have the potential to form monohormonal endocrine cells *in vitro*

Following flow cytometric isolation of INSULIN-GFP$^+$ cells at d30 of differentiation, cells were reaggregated in APEL medium with 10μm Rho kinase inhibitor, 10mM Nicotinamide and 50ng/ml IGF-1 with 2.5 x $10^3$ cells per aggregate. Reaggregates were incubated at 37°C, 5% $CO_2$, for 48 hours before the medium was then changed in order to remove the Rho kinase inhibitor. Reaggregates were incubated for up to 3 months, with the medium being changed weekly. Due to low or absent cell proliferation, reaggregates did not require passaging during the culture period.

In the first month following reaggregation, some cells within the reaggregates downregulated INSULIN-GFP, whilst approximately 10-20% of cells retained INSULIN-GFP expression (figure 4.7A). Reaggregates were kept in culture for up to 3 months before immunofluorescence staining was used to examine patterns of hormone and beta cell associated transcription factor expression.

As was observed with INSULIN$^+$ cells matured *in vivo*, cells within aggregates expressed either GLUCAGON, SOMATOSTATIN or INSULIN and this expression was mutually exclusive (figure 4.7B and 4.7C). Immunofluorescence analysis also indicated that the INSULIN$^+$ cells expressed the beta cell associated transcription factor NKX6.1 (figure 4.7D), indicating that these persisting INSULIN$^+$ cells shared some characteristics with mature beta cells. In summary, these data suggest that d30 INSULIN$^+$ population has the capacity to form monohormonal cells *in vitro* that represent the three different predominant endocrine lineages found within the adult islet.

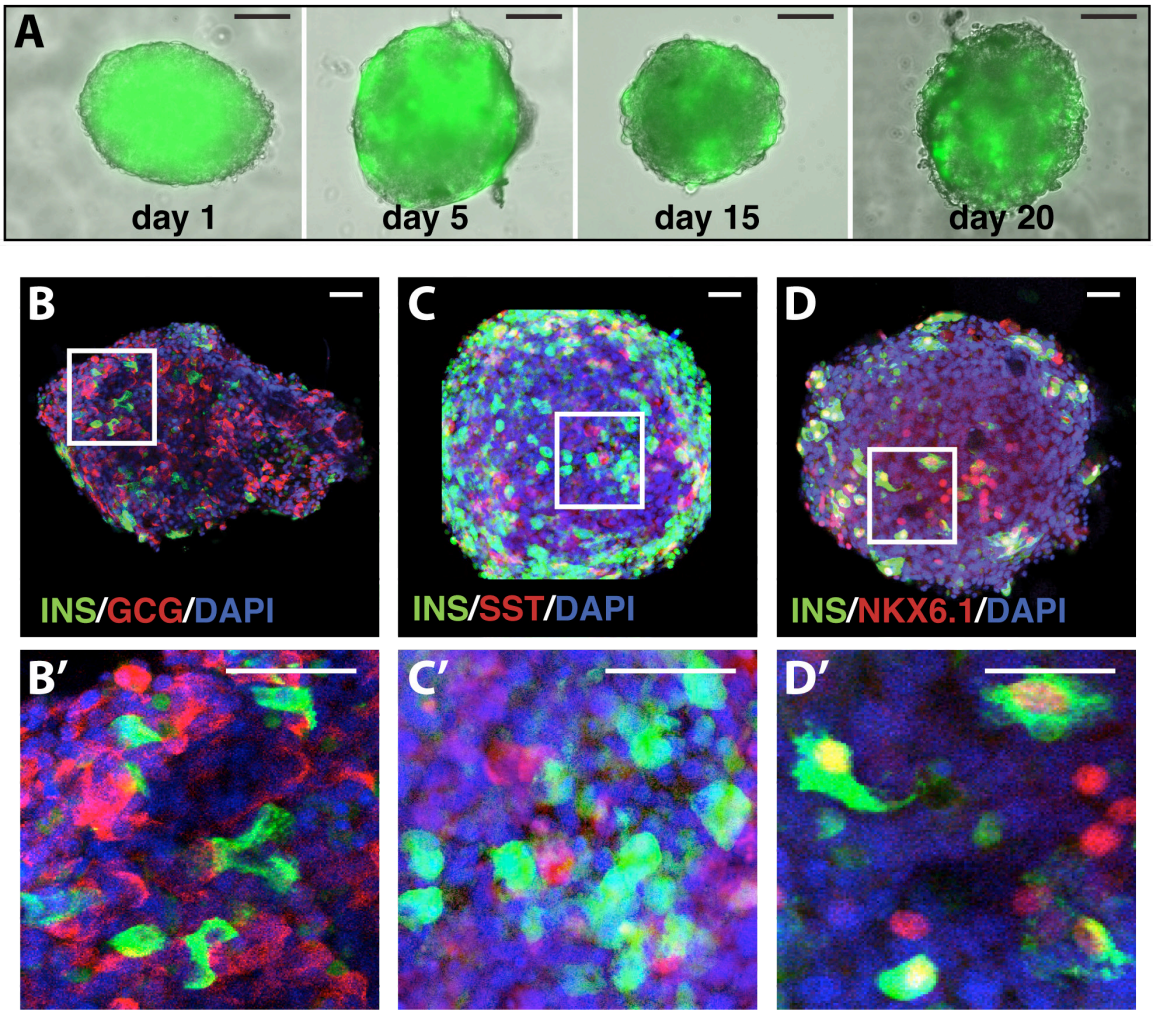


**Figure 4.7** – Analysis of reaggregated INSULIN-GFP⁺ cells cultured *in vitro*
**(A)** Following isolation and reaggregation of INSULIN-GFP⁺ cells, over 20 days, INSULIN-GFP expression was downregulated in most cells, Scale bars 100μm **(B-D)** Similar to *in vivo* matured cells, reaggregates show that INSULIN and GLUCAGON, or SOMATOSTATIN are not co-expressed, whilst, INSULIN⁺ cells that are retained co-express NKX6.1. Scale bars 20μm, **(B'-D')** Boxed areas of (B-D) are shown at higher magnification. Scale bars 20μm

### 4.3.8 INSULIN⁺ cells matured *in vitro* have the capacity to efficiently process proinsulin to form insulin and C-peptide

Further analysis was performed on INSULIN⁺ cells to examine their capacity to process proinsulin to form insulin and C-peptide. The ability to process proinsulin is a characteristic of beta cells which occurs quite late during development. For example, preterm neonates (<30 weeks) have a defect in proinsulin processing that contributes to transient hyperglycaemia associated with premature birth (Mitanchez-Mokhtari et al., 2004). Similarly, D'Amour et al observed that immature hESC derived polyhormonal INSULIN⁺ cells were not able to efficiently process proinsulin to form insulin and C-peptide (D'Amour et al., 2006).

Proinsulin is processed to form insulin and C-peptide by three enzymes – proprotein convertase 1 (PCSK1), proprotein convertase 2 (PCSK2) and carboxypeptidase E (CPE). Although there are multiple pathways that can be utilised to process proinsulin to form insulin and C-peptide, the preferred pathway is for proinsulin to be first cleaved by PCSK1 to form the intermediate des-31,32 proinsulin, which is then cleaved by PCSK2. Finally, lysine and arginine residues, which have been exposed by the previous cleavage steps, are removed by CPE (Steiner et al., 2010). This process results in the generation of the mature insulin and C-peptide molecules, and is shown below in figure 4.8A

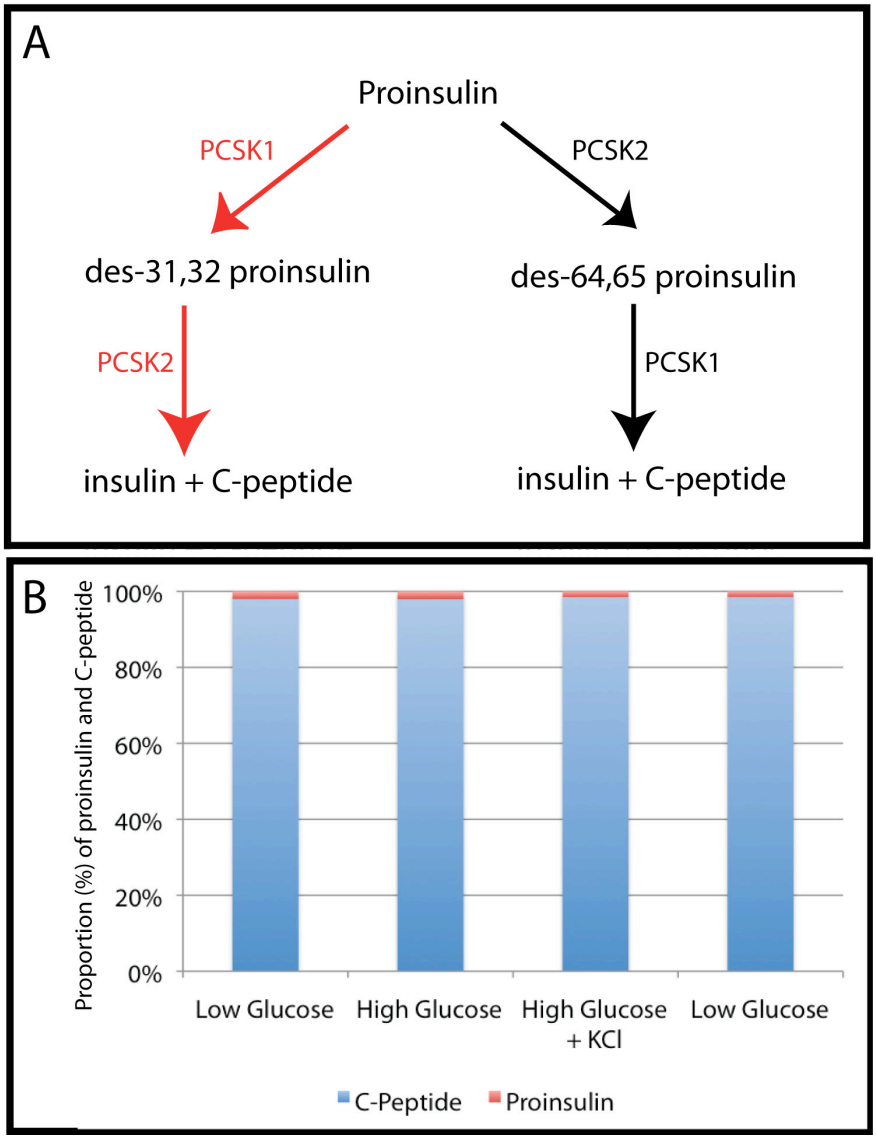


**Figure 4.8** – Analysis of cell processing of proinsulin. **(A)** Schematic demonstrating the processing of proinsulin to form insulin and C-peptide (the preferred pathway is shown in red), **(B)** Reaggregated INSULIN-GFP⁺ cells are able to efficiently process proinsulin under a number of different stimulatory conditions, n=5.

INSULIN$^+$ cell reaggregates that had been cultured for 3 months were analysed for their ability to process proinsulin to insulin and C-peptide. Proinsulin processing was examined in the context of a variety of conditions including low glucose, high glucose and high glucose with the addition of KCl, a molecule known to potentiate insulin secretion (Gomez and Curry, 1973). This analysis showed that, irrespective of culture conditions, reaggregates efficiently processed proinsulin to form C-peptide (and thus by proxy insulin) (figure 4.8B) with little (unprocessed) proinsulin secreted. This data suggested that the INSULIN$^+$ cells that were retained following *in vitro* maturation were more mature than INSULIN$^+$ cells previously reported in the literature and had a similar capacity to process proinsulin to form C-peptide and insulin as do mature islet derived INSULIN$^+$ cells.

### 4.3.9 INSULIN$^+$ cells matured *in vitro* secrete C-peptide in response to insulin secretion potentiators but lack a glucose-stimulated insulin secretion response

Following from the analysis of C-peptide and proinsulin secretion, reaggregregates were analysed for their ability to secrete C-peptide in response to glucose load. This was performed in the same manner as for analysis of C-peptide and proinsulin secretion in section 4.3.8. In addition, reaggregates were also examined for their ability to secrete C-peptide in response to IBMX , a non-specific cAMP inhibitor, known to potentiate the secretion of insulin ((Siegel et al., 1980)). These analyses showed that whilst the vast majority of reaggregates secreted C-peptide in response to both KCl and IBMX, few reaggregates responded to glucose load alone (as shown by an increase in C-peptide secretion between low glucose and high glucose) (figure 4.9). This suggests that there was still a degree of functional immaturity in the INSULIN$^+$ cells present within the reaggregates.

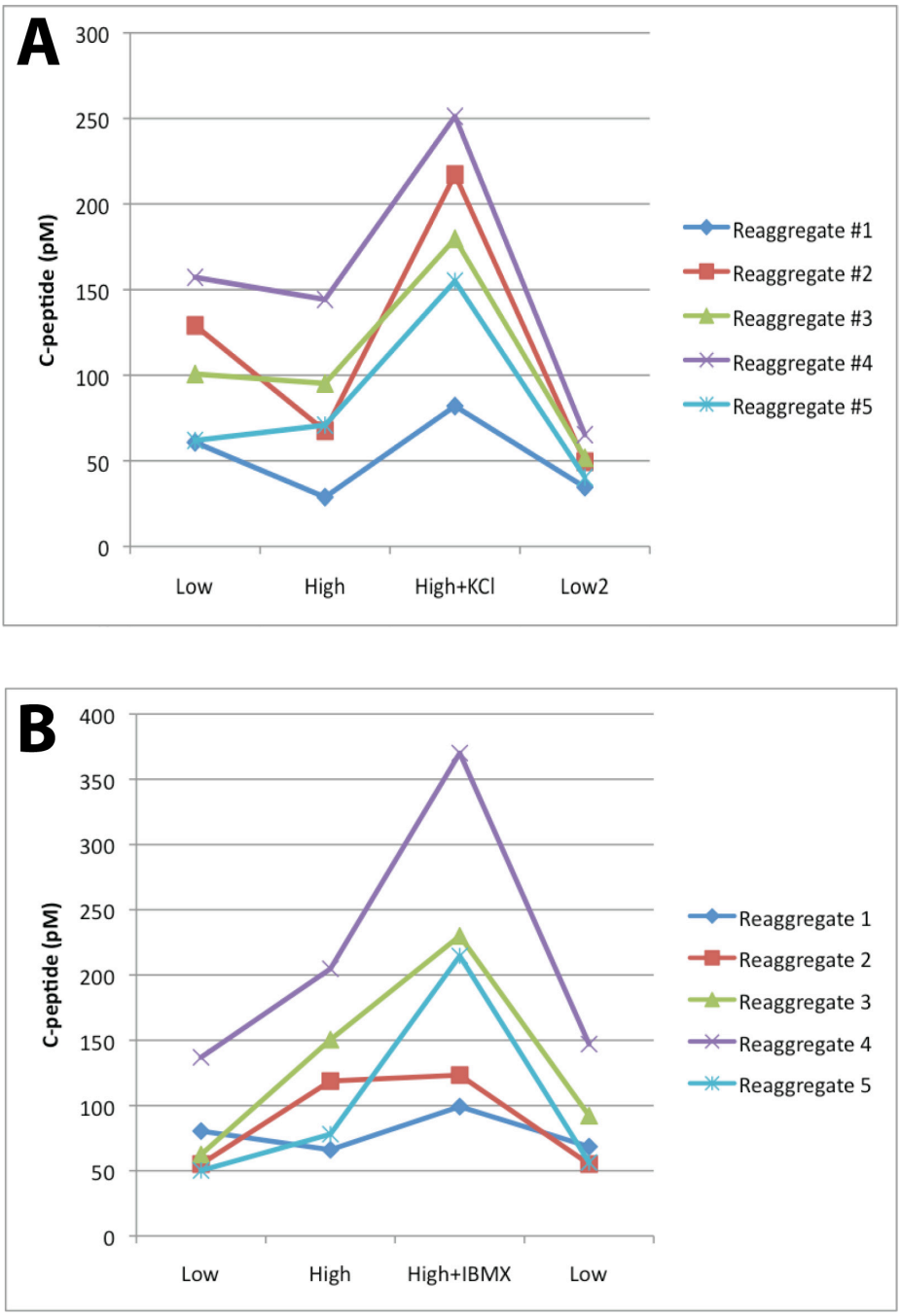


**Figure 4.9 Analysis of c-peptide secretion by INSULIN+ reaggregates. (A)** C-peptide secretion from INSULIN+ cell reaggregates in response to sequential stimulation with low glucose (2mM D-glucose), high glucose (20mM D-glucose) and high glucose with 30mM KCl, n=5, **(B)** C-peptide secretion from INSULIN+ cell reaggregates in response to sequential stimulation with low glucose (2mM D-glucose), high glucose (20mM D-glucose) and high glucose with 0.5mM IBMX, n=5

## 4.4 Discussion

A number of previous studies have investigated the potential of a purified INSULIN$^+$ cell population or endocrine cell populations following transplantation. By and large, these studies have been performed on the back of differentiation protocols that had a propensity to generate polyhormonal endocrine or INSULIN$^+$ cell populations. For example, Basford *et al*, using INSULIN-GFP$^+$ cells generated according to the method of Nostro and colleagues found that the mostly polyhormonal population differentiated in to GLUCAGON$^+$ cells following transplantation (Basford et al., 2012). Similarly, Kelly and co-workers found that endocrine cells expressing the surface marker chromogranin A gave rise to cell population composed of predominately GLUCAGON$^+$ cells with scattered SOMATOSTATIN$^+$ cells (Kelly et al., 2011). Finally, Rezania *et.al* found that late stage differentiation cultures containing polyhormonal INSULIN$^+$ cells formed fully functional alpha cells (GLUCAGON$^+$) following transplantation into immunodeficient hosts (Rezania et al., 2011),

In our study, we examined the potential of isolated INSULIN$^+$ cells, of which a significant component were monohormonal (~40%) (Micallef et al., 2012). When these INSULIN$^+$ cells were cultured further *in vitro* or allowed to develop *in vivo* following transplantation, we found that around 10-20% of cells retained INSULIN expression over the longer term (up to 3 months). These persisting INSULIN$^+$ cells co-expressed transcription factors that are associated with beta cell maturity and lacked expression of either GLUCAGON$^+$ or SOMATOSTATIN$^+$. In addition, to INSULIN$^+$ cells, we also observed that monohormonal cells expressing either GLUCAGON or SOMATOSTATIN were present following extended culture. Thus, our studies suggest that mono-hormonal cells expressing all three of the major islet endocrine hormones can be derived from the initial INSULIN$^+$ cell pool.

The *in vitro* maturation of INSULIN$^+$ cells has previously not been studied, with prior reports focusing on the characteristics of INSULIN$^+$ cells immediately following their generation. These reports have found that INSULIN$^+$ cells are generally polyhormonal and express genes such as CK19, a marker of immature endocrine cells (Basford et al., 2012). Additionally, immature polyhormonal endocrine cells have a proinsulin-processing defect, where only approximately 55% of proinsulin is processed to form C-peptide (and insulin) (D'Amour et al., 2006). In contrast, we found that INSULIN$^+$ cells matured *in vitro* for 3 months, processed approximately 98% of proinsulin to form C-peptide. This finding, in combination with monohormonal INSULIN expression and the co-expression of beta cell

associated transcription factors (such as NKX6.1) suggested that the persisting INSULIN$^+$ cells represent a relatively mature phenotype.

The ability of INSULIN$^+$ cells that have been matured either *in vitro* or *in vivo* to secrete insulin in response to either glucose stimulation (or other secretogogues such as KCl or IBMX) was not examined in detail. However, we performed a small scale analysis on a limited number of *in vitro* matured cells that showed that, while reaggregates had the capacity to secrete C-peptide in response to known insulin secretion potentiators, such as KCl and IBMX, they did not exhibit any consistent C-peptide secretory response to a high glucose load. This suggests that in *in vitro* matured cells, there is still a degree of functional immaturity. Whilst several reports describe the ability of transplanted pancreatic progenitors to give rise to cells that respond to glucose challenge *in vivo* ((Jiang et al., 2007b), (Shim et al., 2007), (Kroon et al., 2008), (Kelly et al., 2011), (Rezania et al., 2012)), these cells have either not been tested or are unable to secrete insulin in response to glucose stimulation *in vitro*. As such, the generation of glucose-responsive INSULIN$^+$ cells wholly *in vitro* has not been reported. Hence, an important next step for studies such as the one described in this chapter will be tests aimed at determining whether *in vitro* generated INSULIN$^+$ cells have the capacity to respond to glucose *in vitro*. Having said this, it will also be important to determine whether human islets cultured under similar conditions for extended periods retain their capacity for glucose stimulated insulin secretion (GSIS).

In addition to the persisting INSULIN$^+$ cells found in our *in vitro* cultures, further experiments examining properties of monohormonal cells that express either GLUCAGON or SOMATOSTATIN are warranted. In particular, it would be of interest to determine whether such cells represent mature and functional alpha (GLUCAGON) or delta (SOMATOSTAIN) cells. These studies might include immunofluorescence analysis to look for expression of transcription factors associated with alpha cells, such as ARX and BRN4, as well as transcription factors associated with delta cells, such as PAX4. As with the case of INSULIN$^+$ cells, these additional studies would ideally be accompanied by parallel experiments using alpha and delta cells derived from adult islets cultured under similar conditions.

Perhaps the most interesting question relating to our current observations concerns the relationship between 3 endocrine cell types – INSULIN, GLUCAGON and SOMATOSTATIN

that derive from the initial heterogeneous INSULIN$^+$ population. This population contains both a polyhormonal population, and a monohormonal population. The simplest hypothesis is that monohormonal INSULIN$^+$ cells present in the starting population give rise to the persisting INSULIN$^+$ cells and that the polyhormonal INSULIN$^+$ cells give rise to the GLUCAGON$^+$ and SOMATOSTATIN$^+$ cells observed following *in vitro* or *in vivo* maturation. Although this idea would fit with the data already reported in the literature, we currently lack tools (either by targeted or transgenic cell lines, or by cell surface markers) that would allow us to separate the monohormonal INSULIN$^+$ cells from the polyhormonal counterparts. Such experiments may require the generation of additional reporter lines that co-express different fluorescent proteins under the control of genes representing INSULIN, GLUCAGON and SOMATOSTATIN.

In summary, this chapter has described the genetic modification of an INSULIN$^{GFP/w}$ hESC line to constitutively express firefly luciferase. This allowed for the *in vivo* imaging of cells that are able to be isolated based on INSULIN-GFP expression and transplanted into animal models. Examination of grafts arising from these transplantation experiments showed they contained cells that were monohormonal in their expression of INSULIN, GLUCAGON and SOMATOSTATIN. Additionally, when a similar INSULIN$^+$ population was cultured for a further 3 months *in vitro*, the same result was seen – that the initial heterogeneous INSULIN$^+$ population had the ability to form monohormonal INSULIN$^+$, GLUCAGON$^+$ and SOMATOSTATIN$^+$ cells. Immunofluorescence analysis of the monohormonal INSULIN$^+$ cells revealed that they co-expressed the beta cell associated transcription factor NKX6.1. This implies that the cells have some degree of maturity. This was further confirmed when the cells were examined for their ability to process proinsulin. It was found that the cells, similar to mature INSULIN$^+$ cells, were able to efficiently process proinsulin to form insulin and C-peptide. Future studies will be focused on determining whether or not such cells display GSIS and, if sufficient numbers can be generated, whether such cells can ameliorate diabetes in animal models.

# Chapter 5

## General Discussion

## 5.1 Introduction

This thesis describes a differentiation protocol that results in the generation of an INSULIN$^+$ cell population, which after further maturation, forms single-hormone insulin expressing cells. Chapter 2 contained a detailed outline of the protocol, which utilised a spin EB, 96-well plate format in conjunction with a serum-free defined medium. Chapter 3 was based around a paper describing the generation of a genetically modified human ES cell in which GFP was inserted into the INSULIN locus, allowing the identification of cells that express INSULIN. This INSULIN$^{GFP/w}$ cell line was then used to differentiate cells using the spin EB protocol described in chapter 2. Analysis of cells generated by this method suggested that, compared to INSULIN$^+$ cells derived using other published protocols, spin EB INSULIN$^+$ cells were more similar to human fetal and adult pancreatic tissues. Chapter 4 described a further genetic modification of the INSULIN$^{GFP/w}$ hESC cell line, in which a constitutively expressed luciferase tag was added. Experiments using this line demonstrated that luciferase expression was maintained following cell differentiation both *in vitro* and *in vivo*. INSULIN$^+$ cells generated using this TgEF1$\alpha^{Luc}$.INSULIN$^{GFP/w}$ hESC line were then isolated and matured both *in vitro* and *in vivo*. These studies showed that INSULIN$^+$ cells had the capacity to form single-hormone positive cells of a variety of endocrine lineages (alpha, beta and delta). Most importantly, INSULIN$^+$ cells which were retained following this maturation process co-expressed transcription factors associated with mature beta cells, such as NKX6.1 and MAFA, and additionally had the capacity to efficiently process proinsulin to form insulin and C-peptide, as is seen in adult beta cells.

## 5.2 Further work.

The results presented in this thesis represent a promising starting point in the aim of generating fully functional beta cells from the *in vitro* differentiation of hESCs. Apart from further work required to identify factors that can drive the INSULIN$^+$ cells to a point where they are glucose responsive, there are several other issues that will need to be addressed. The most pressing of these relate to efficiency and scale. Like many of the methods present in the literature, our differentiation protocol generates only a small fraction of INSULIN$^+$ cells. Although this situation is workable for experimental purposes, such inefficiency would render this methodology unviable for the generation of large numbers of beta cells. Thus, further efforts will be required to increase the efficiency of differentiation. This could be tackled from a number of different angles. One possibility would be to identify an expandable intermediate population that could be uniformly induced to differentiate

towards beta cells. In this regard, Gadue and colleagues (Cheng et al., 2012) have recently isolated an endodermal progenitor that can be grown indefinitely and yet retains its potential to differentiate towards pancreatic lineages. A second possibility would be to continue protocol optimization studies in an effort to increase the frequency of INSULIN$^+$ cells formed by the end of the differentiation period. Ultimately, a combination of both approaches might be required to generate the kinds of efficiencies that would facilitate future large-scale production.

Given that between 500,000 and 1,000,000 islets are required to affectively treat people with type 1 diabetes, scale is a critical issue that needs to be overcome. Although the spin EB format is very useful for optimization studies, it is not appropriate for large-scale generation of differentiated cell types. In this context, bulk culture technology that takes advantage of some aspects of the spin EB system (most notably, EB uniformity) is commercially available (Stem cell Technologies, AggreWell™). Nevertheless, it is still likely that large scale bioreactor technology will need to be explored by groups that have specific expertise in this area.

Overall, the studies in this thesis provide a platform for ongoing efforts to generate fully functional beta cells *in vitro* for the treatment of type 1 diabetes. Given the speed at which the hESC differentiation field is moving, it is timely to consider other hurdles that may be encountered if and when hESC derived beta cells are ready for clinical use.

## 5.3 Prospects for developing a cell-based therapy for type 1 diabetes

Type 1 diabetes is an autoimmune disorder resulting in the destruction of endogenous beta cells (Gillespie, 2006), which is relatively common in Australia with nearly 87,000 diagnosed type 1 diabetics (AIHW, 2011). Currently, treatment options are either insulin replacement therapy, or in limited cases, islet transplantation, in which cadaver islets are transplanted into the patient's portal vein and the patient subjected to lifelong immunosuppresion (Shapiro et al., 2000). Islet transplantation has a number of limitations – primarily that only limited amounts of cadaver derived islets are available (and hence, many patients cannot be treated using this method), and that over time, insulin independence is lost, and patients require a new transplant (Shapiro et al., 2006). It has been suggested that stem cells could provide a source of beta cells to be used in islet

transplantation, as they could be used to produce large numbers of cells for transplant, thus overcoming one of the limitations of cadaver-derived islet transplants.

### 5.3.1 Use of progenitor cells versus mature cells for cell transplantation

Multiple studies have now been published which have reported the amelioration of type 1 diabetes in animal models. Most of these studies have transplanted human ES cell-derived pancreatic progenitor cells, which have then been allowed to mature to form INSULIN$^+$ cells *in vivo*. In contrast, studies, which have transplanted later stage isolated INSULIN$^+$ cells, or isolated endocrine cells, have reported a loss of INSULIN expression *in vivo*, and formation of GLUCAGON$^+$ and SOMATOSTATIN$^+$ cells. These studies are summarised in table 5.1 below:

**Table 5.1 Summary of published protocols that have examined the transplantation of human ES cell derived pancreatic progenitor cells or INSULIN+ cells**

| | **Transplanted Cell Type** | **Length of time transplanted** | **Amelioration of diabetes (*in vivo* GSIS)** | **Observed cell types following transplant** | **Transplant site** |
|---|---|---|---|---|---|
| (Jiang et al., 2007b) | Non-enriched Pancreatic progenitors | 42 days | Yes, in 30% of mice | INS, other hormones not investigated | Kidney capsule |
| (Phillips et al., 2007) | Non-enriched population containing INS+ cells | 15 days | No | INS, other hormones not investigated | Intraperitoneal injection |
| (Shim et al., 2007) | Non-enriched Pancreatic progenitors | 4 weeks | Yes | INS, GCG | Kidney capsule |
| (Eshpeter et al., 2008) | Non-enriched population containing INS+ cells | Up to 64 days | No | INS, GCG, SST | Kidney capsule |
| (Kroon et al., 2008) | Pancreatic progenitors | Up to 210 days | Yes | INS, GCG, SST, GHRL, PP | Epididymal fat pad |
| (Mao et al., 2009) | Non-enriched population containing INS+ cells | 7 weeks | Only under fasting conditions | INS, other hormones not investigated | Subcutaneous, Kidney capsule |
| (Kelly et al., 2011) | Enriched endocrine cells | Up to 9 weeks | Not assessed | GCG, SST; lack INS | Epididymal fat pad |
| (Kelly et al., 2011) | Enriched pancreatic progenitors | Up to 9 weeks | Yes | INS, GCG, SST | Epididymal fat pad |
| (Rezania et al., 2011) | Non-enriched population containing INS+ cells | Up to 5 months | No | GCG; lack INS | Kidney capsule |
| (Basford et al., 2012) | Isolated polyhormonal INSULIN+ cells | 4 weeks | No | GCG; lack INS | Kidney capsule |
| (Rezania et al., 2012) | Non-enriched Pancreatic progenitors | Up to 8 months | Yes | INS, GCG, SST, PP | Kidney capsule |

By far, the best results have been obtained from transplanting cells at a progenitor stage. This is due to the fact that the later maturation of the progenitor stage to a mature beta cell occurs due to factors provided in the *in vivo* environment. Currently, the signals and growth factors involved in this process are not well understood. Perhaps, as we gain a better understanding of signals required for later beta cell maturation, we will be able to translate this to cell differentiation protocols, and produce functional beta cells *in vitro*, despite this currently remaining elusive. Nevertheless, if fully functional differentiated beta cells are to be used, some of the issues discussed immediately below will need to be overcome.

### 5.3.2 Rejection of transplanted cells

As with any sort of cell or organ transplantation, rejection of transplanted tissue is of concern within the allotransplantation setting. As type 1 diabetes is an autoimmune disorder that results in destruction of the endogenous beta cells, both destruction of transplanted tissue and immune rejection must be considered when contemplating transplantation into immunocompetent animal models, or later, into human patients.

Current approaches to this issue have utilised physical separation methods or immunosuppression. In the former, transplanted cells are isolated in a device or capsule that cells of the immune system are unable permeate. In the latter, traditional drug-based methods are used to suppress the host immune system. The physical separation approaches can be classified as either microencapsulation, where small microbeads (with diameters in the vicinity of hundreds of microns), most commonly made from alginate are used to coat the cells; or macroencapsulation, where larger devices (commonly up to 1.5mm in diameter and a few centimetres in length) are used to isolate a larger number of cells. A schematic of how these two approaches are used in immunoisolation is shown below in figure 5.1

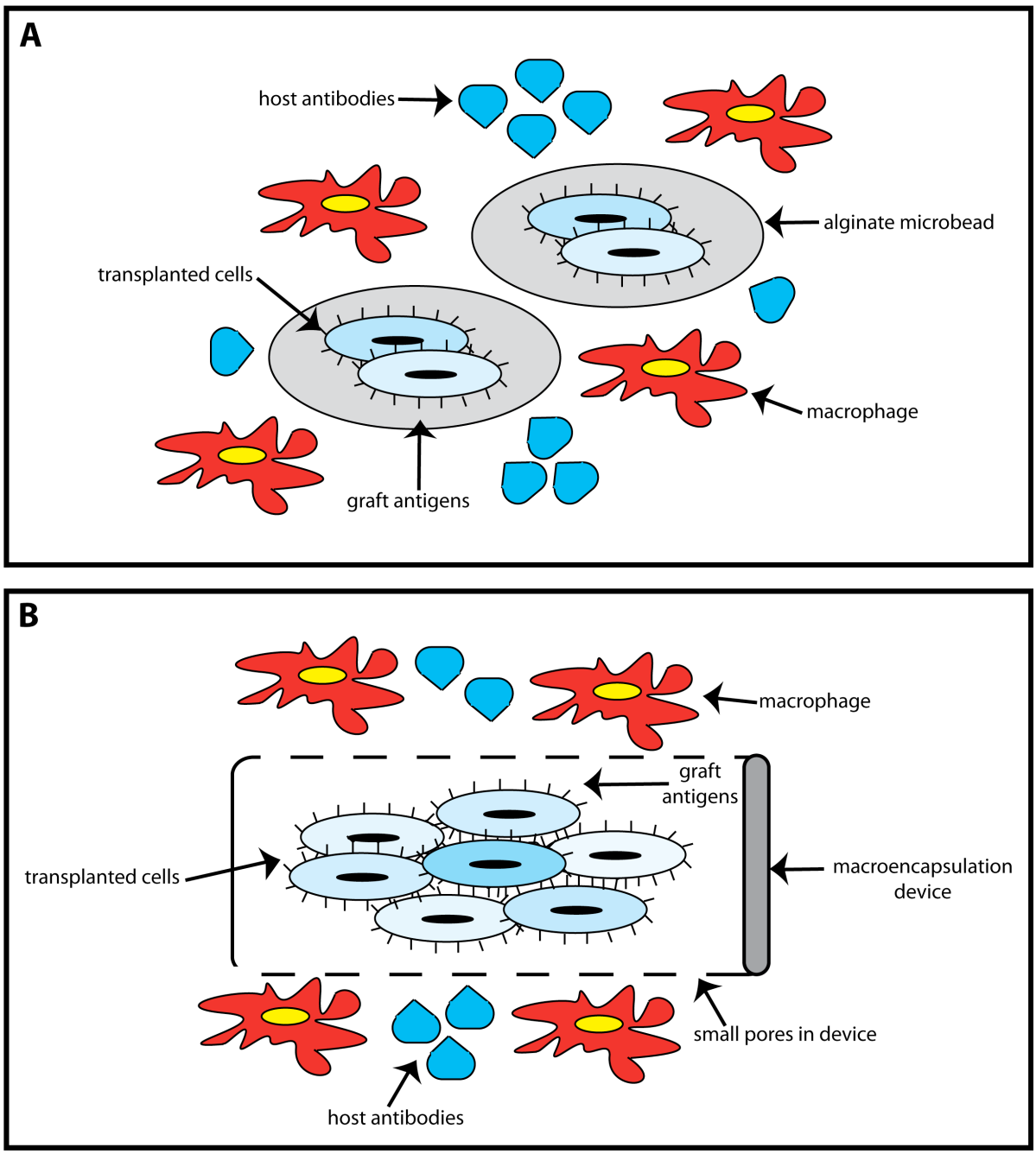


**Figure 5.1** Schematic of potential immunoisolation approaches used in conjunction with human ES cell-derived pancreatic cells. **(A)** Alginate microbeads can be used to isolate transplanted cells in a microencapsulation approach; **(B)** Porous encapsulation devices can be used to isolate transplanted cells in a macroencapsulation approach (Adapted from (Krishnamurthy and Gimi, 2011)).

The most common substance used in microencapsulation is alginate – a polysaccharide derived from marine algae and bacterium (Govan et al., 1981), though other substances such as agarose (Iwata et al., 1989), chitosan (Zielinski and Aebischer, 1994), poly (hydroxyethyl metacrylate-methyl methacrylate (HEMA-MMA) (Dawson et al., 1987), polyethylene glycol (PEG) (Cruise et al., 1999) and acrylonitrile (Kessler et al., 1991) have

also been used in the formation of microcapsules. No matter what substance is used, the same basic principles apply – the cells to be transplanted are encased in the substance.

Initial studies of alginate microencapsulated cells utilised isolated islets. Microencapsulated islets cultured *in vitro* for up to 4 months retained viability and functionality, although they displayed a delay in glucose stimulated insulin secretion as compared to non-encapsulated islets. This delay was attributed to be due to the time required for insulin to cross the microcapsule membrane. These encapsulated islets also possessed a normal degree of granulation and sub-cellular localisation of pancreatic hormones was comparable to non-encapsulated islets. When transplanted into diabetic rats, it was found that microencapsulated islets had the ability to restore normoglycaemia for approximately 3 weeks, as compared to the 6-8 days observed with non-encapsulated islets (Lim and Sun, 1980). These results are consistent with the hypothesis that encapsulation can confer some degree of protection from immune mediated beta cell destruction.

Despite this initial success, (alginate) microencapsulation is not without disadvantages. Alginate still contains residual proteins that are immunogenic and induce inflammation (Zimmermann et al., 2007). Human studies suggest that both short-term and long-term function of either cells or islets transplanted in microcapsules may be problematic. A recent study found that transplanted barium alginate encapsulated human islets examined after 16 months contained necrotic islets and were surrounded by fibrous tissue – suggesting graft loss due to immunorejection. In addition, despite some graft function being observed 1 day post-transplant, graft functionality was quickly lost, with no transplanted patient ever achieving insulin independence (Tuch et al., 2009). In contrast, a phase 1 clinical trial investigating the safety of transplantation of human islets encapsulated in sodium alginate found that whilst the microcapsules were not rejected, graft function was not sufficient to result in insulin independence in the trial participants (Calafiore et al., 2006). These results would suggest, that whilst microencapsulation approaches may help to delay graft rejection, the encapsulation material used will need to ensure that transplanted material can function sufficiently well to provide therapeutic benefit.

Macroencapsulation devices are named due to their larger size, as compared to microencapsulation, and similar to microcapsules, can be constructed from a wide variety of materials, including polyurethane-polyvinyl pyrrolidone (Muthyala et al., 2011), polytetrafluoroethylene (Sorenby et al., 2008), polyvinyl alcohol hydrogels (Qi et al., 2004), polyamide or nylon (Prochorov et al., 2005). Due to their larger size, macrocapsules have the ability to contain larger numbers of cells. However this larger size comes with a greater propensity to induce inflammatory tissue responses, and thus, the material used to construct the macrocapsule must be chosen with care (Gentile et al., 1995).

Macrocapsules are constructed to contain cells within a pouch, or membrane, that has small pores that are large enough to allow the diffusion of small molecules (such as insulin), but are small enough to disallow entry of host immune cells, thereby preventing destruction of the graft. Of interest, is the development of macrocapsules, which allow for the vascularisation of grafts (for example: (Prochorov et al., 2005), (Geller et al., 1997)), as a lack of vascularisation has been demonstrated to be a contributing factor to graft failure. Therefore, the development of such devices, which both promote vascularisation, and prevent host immune cell access to the graft, are of great interest to the scientific community.

### 5.3.3 Vascularisation of transplanted cells

One challenge in islet or cell transplantation therapies for the treatment of diabetes is the early loss of grafted tissue. This can be caused by both inflammatory responses from the host, or importantly, from inadequate vascularisation of the grafted tissue.

Normally, the pancreatic islets are a highly vascularised tissue (shown below in figure 5.2), and despite only consisting of 1-2% of pancreatic mass, receive 5-10% of pancreatic blood flow (Brissova and Powers, 2008). It has been demonstrated by multiple groups that in the period immediately following transplantation, grafted islets are avascular, and even following the revascularisation process, are less vascularised than endogenous islets in the pancreas (Carlsson et al., 2001), (Carlsson et al., 2002), (Mattsson et al., 2002). This lack of vascular supply to the transplanted tissue is likely a contributing factor to ischemia and low blood flow, which in turn may lead to necrosis of transplanted islets that additionally can trigger a host immune response. Hence, strategies to improve vascularisation of transplanted islets are not only of relevance to islet transplantation studies, but also to

studies focussing on the transplantation of human ES cell derived pancreatic cells, such as pancreatic progenitor cells or INSULIN$^+$ cells.

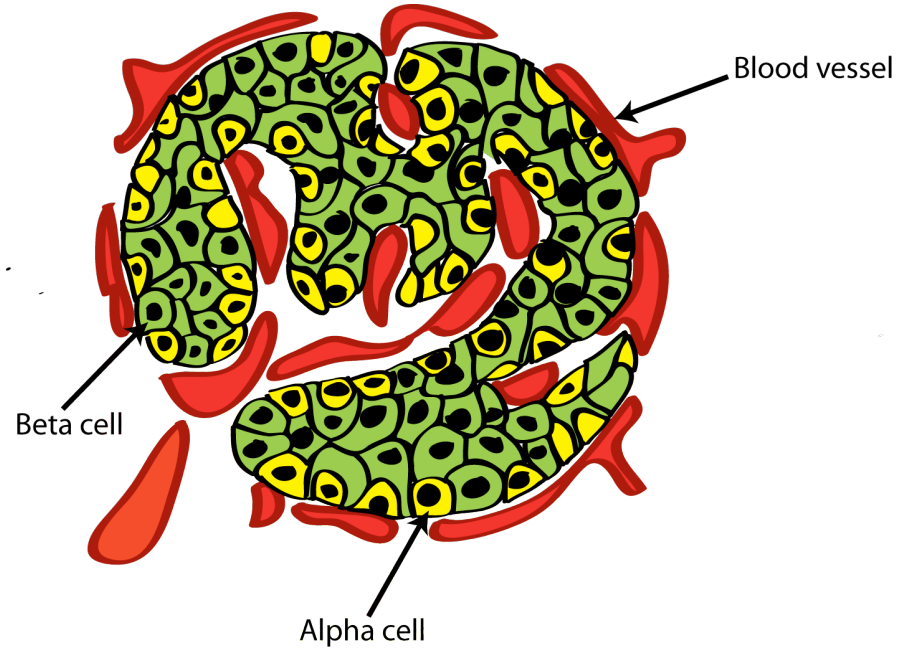


**Figure 5.2** Schematic demonstrating the vascularisation of a non-diseased human islet. It can be seen that a high level of vascularisation is present (Adapted from: (Bosco et al., 2010))

There have been several suggested approaches for increasing revascularisation of transplanted islets – firstly, one could stimulate the proliferation, migration and maturation of both endogenous pancreatic and donor-derived endothelial cells or their progenitors. This could be achieved by either increasing the action of proangiogenic factors and/or inhibiting the action of antiangiogenic factors. These possibilities have been investigated for two different proangiogenic factors: vascular endothelial factor (VEGF) and angiopoeitin-1 (Ang-1).

The role of VEGF has been investigated in transgenic mouse models (Lai et al., 2005) or using transducible vectors (Zhang et al., 2004). Both studies found that the increased VEGF expression resulted in increased microvasculature of islet grafts as compared to control islet grafts; and also observed relatively higher insulin content, and improved blood glucose profiles as compared to controls ((Zhang et al., 2004), (Lai et al., 2005)). Similarly, a study by Su and colleagues, found that when islets were transduced with Ang-1 prior to transplantation, 1 month post-transplantation, increased amounts of microvasculature

could be observed and enhanced glucose-induced insulin secretion was seen (Su et al., 2007).

A complementary approach examined the affect of inhibiting thrombospondin-1 (TSP-1), a factor that is thought to restrict intra-vascular expansion. This study employed knockout mouse models and siRNA knockdown technology to suppress TSP-1 in transplanted islets. The authors found that islets lacking expression of TSP-1 had increased vasculature and improved glucose-stimulated insulin secretion, as compared to control islets (Olerud et al., 2008).

Although these studies provide mechanistic insights into what factors might assist graft retention, for regulatory reasons, they are unlikely to be directly applicable to either islet transplantation or future clinical application of hESC derived beta cells.

Another possibility to improve the vascularisation of islets involves the co- transplantation of supportive cell types, such as mesenchymal stem cells (MSCs), or endothelial progenitor cells. This approach is attractive, as it does not require any genetic modification of transplanted tissue and does not involve any additional modalities, as cells are being transplanted already. In particular, MSCs and bone marrow derived cells (including endothelial progenitor cells) have already been approved for clinical use in a variety of different contexts.

Early studies examining this approach appear promising. A study in which MSCs were co-transplanted with islets into diabetic mice found that islets had increased endothelial cell numbers within the endocrine tissue. This observation was correlated with an improved outcome with 92% of the co-transplanted mice achieving normoglycaemia as compared to 42% of mice transplanted with islets alone. It was also observed that the islet architecture more closely resembled that of endogenous islets in co-transplanted islets (Rackham et al., 2011). A second study, by Johansson *et.al*, examined the transplantation of islets that were previously recombined with endothelial cells (Johansson et al., 2005) both in the presence and absence of MSCs. The authors found that the inclusion of MSCs enhanced endothelial cell sprouting from the recombined islets, which promoted islet engraftment following transplantation. Although the functionality of the recombined islets, either with or without

MSCs following transplantation, was not examined, it was shown that following *in vitro* culture, that MSCs did not affect islet functionality or survival (Johansson et al., 2008).

A more recent study by Kang and collegues, examined the effect of co-transplanting islets with cord-blood derived endothelial progenitor cells (Kang et al., 2012). The authors found that mice transplanted with islets in conjunction with endothelial progenitor cells had improved glycaemic control, and achieved euglycaemia more rapidly, compared to mice transplated with islets alone. Additionally in the group co-transplanted with islets and endothelial progenitor cells, an enhanced revascularisation rate was observed as compared to the islet only controls, which lead to better graft perfusion and recovery from hypoxia and ultimately, improved islet engraftment.

In terms of hESC differentiation work presented in this thesis, the considerations outline above are issues that will no doubt need to be explored in the context of *in vitro* derived beta cells. In view of this, it is noteworthy that many laboratories have devised methods for the generation of both MSCs and endothelial cells from hESCs, raising the possibility that a composite cellular product may be an avenue worthy of further investigation. In the meantime, there are still many issues relating to hESC differentiation, safety, graft survival and transplantation protocols that will need to be resolved before are readily accessible form of beta cell replacement therapy becomes a reality.

## 5.4 Summary

Whilst the results of this study are promising in the generation of a monohormonal INSULIN$^{+}$ cell population, there are many factors that are yet to be considered when designing transplantation strategies to assess their ability to ameliorate diabetes. These factors will include the design of experiments that involve immunocompetent models, thereby more accurately recapitulating the human diabetic setting, and the consideration of cell survival post-transplantation. In this context, the TgEF1$\alpha^{Luc}$.INSULIN$^{GFP/w}$ cell line, used in conjunction with the protocols developed as a part of this study, will hopefully provide insight into regimes that improve cell survival post-transplantation and provide unique tools to continue investigations into commitment of stem cells to an INSULIN$^{+}$ cell fate.

# BIBLIOGRAPHY

AIHW 2011. Diabetes prevalence in Australia: detailed estimates for 2007-08. Diabetes series no. 17. Cat. no. CVD 56. Canberra: AIHW. Viewed 6 March 2013 <http://www.aihw.gov.au/publication-detail/?id=10737419311>.

Amit, M., Carpenter, M.K., Inokuma, M.S., Chiu, C.P., Harris, C.P., Waknitz, M.A., Itskovitz-Eldor, J., and Thomson, J.A. (2000). Clonally derived human embryonic stem cell lines maintain pluripotency and proliferative potential for prolonged periods of culture. Developmental biology *227*(2), 271-278.

Ang, S.L., Wierda, A., Wong, D., Stevens, K.A., Cascio, S., Rossant, J., and Zaret, K.S. (1993). The formation and maintenance of the definitive endoderm lineage in the mouse: involvement of HNF3/forkhead proteins. Development *119*(4), 1301-1315.

Apelqvist, A., Li, H., Sommer, L., Beatus, P., Anderson, D.J., Honjo, T., Hrabe de Angelis, M., Lendahl, U., and Edlund, H. (1999). Notch signalling controls pancreatic cell differentiation. Nature *400*(6747), 877-881.

Artner, I., Hang, Y., Mazur, M., Yamamoto, T., Guo, M., Lindner, J., Magnuson, M.A., and Stein, R. (2010). MafA and MafB regulate genes critical to beta-cells in a unique temporal manner. Diabetes *59*(10), 2530-2539.

Artner, I., Le Lay, J., Hang, Y., Elghazi, L., Schisler, J.C., Henderson, E., Sosa-Pineda, B., and Stein, R. (2006). MafB: an activator of the glucagon gene expressed in developing islet alpha- and beta-cells. Diabetes *55*(2), 297-304.

Attali, M., Stetsyuk, V., Basmaciogullari, A., Aiello, V., Zanta-Boussif, M.A., Duvillie, B., and Scharfmann, R. (2007). Control of beta-cell differentiation by the pancreatic mesenchyme. Diabetes *56*(5), 1248-1258.

Basford, C.L., Prentice, K.J., Hardy, A.B., Sarangi, F., Micallef, S.J., Li, X., Guo, Q., Elefanty, A.G., Stanley, E.G., Keller, G.*, et al.* (2012). The functional and molecular characterisation of human embryonic stem cell-derived insulin-positive cells compared with adult pancreatic beta cells. Diabetologia *55*(2), 358-371.

Beatus, P., and Lendahl, U. (1998). Notch and neurogenesis. Journal of neuroscience research *54*(2) 125-136.

Belatik, A., Hotchandani, S., Bariyanga, J., and Tajmir-Riahi, H.A. (2012). Binding sites of retinol and retinoic acid with serum albumins. European journal of medicinal chemistry *48*, 114-123.

Bhushan, A., Itoh, N., Kato, S., Thiery, J.P., Czernichow, P., Bellusci, S., and Scharfmann, R. (2001). Fgf10 is essential for maintaining the proliferative capacity of epithelial progenitor cells during early pancreatic organogenesis. Development *128*(24), 5109-5117.

Blum, M., Gaunt, S.J., Cho, K.W., Steinbeisser, H., Blumberg, B., Bittner, D., and De Robertis, E.M. (1992). Gastrulation in the mouse: the role of the homeobox gene goosecoid. Cell *69*(7), 1097-1106.

Bocian-Sobkowska, J., Zabel, M., Wozniak, W., and Surdyk-Zasada, J. (1999). Polyhormonal aspect of the endocrine cells of the human fetal pancreas. Histochemistry and cell biology *112*(2), 147-153.

Bone, H.K., Nelson, A.S., Goldring, C.E., Tosh, D., and Welham, M.J. (2011). A novel chemically directed route for the generation of definitive endoderm from human embryonic stem cells based on inhibition of GSK-3. Journal of cell science *124*(Pt 12), 1992-2000.

Borowiak, M., Maehr, R., Chen, S., Chen, A.E., Tang, W., Fox, J.L., Schreiber, S.L., and Melton, D.A. (2009). Small molecules efficiently direct endodermal differentiation of mouse and human embryonic stem cells. Cell stem cell *4*(4), 348-358.

Bosco, D., Armanet, M., Morel, P., Niclauss, N., Sgroi, A., Muller, Y.D., Giovannoni, L., Parnaud, G., and Berney, T. (2010). Unique arrangement of alpha- and beta-cells in human islets of Langerhans. Diabetes *59*(5), 1202-1210.

Brissova, M., and Powers, A.C. (2008). Revascularization of transplanted islets: can it be improved? Diabetes *57*(9), 2269-2271.

Calafiore, R., Basta, G., Luca, G., Lemmi, A., Montanucci, M.P., Calabrese, G., Racanicchi, L., Mancuso, F., and Brunetti, P. (2006). Microencapsulated pancreatic islet allografts into nonimmunosuppressed patients with type 1 diabetes: first two cases. Diabetes care *29*(1), 137-138.

Carlsson, P.O., Palm, F., Andersson, A., and Liss, P. (2001). Markedly decreased oxygen tension in transplanted rat pancreatic islets irrespective of the implantation site. Diabetes *50*(3), 489-495.

Carlsson, P.O., Palm, F., and Mattsson, G. (2002). Low revascularization of experimentally transplanted human pancreatic islets. The Journal of clinical endocrinology and metabolism *87*(12), 5418-5423.

Chen, S., Borowiak, M., Fox, J.L., Maehr, R., Osafune, K., Davidow, L., Lam, K., Peng, L.F., Schreiber, S.L., Rubin, L.L.*, et al.* (2009). A small molecule that directs differentiation of human ESCs into the pancreatic lineage. Nature chemical biology *5*(4), 258-265.

Chen, Y., Pan, F.C., Brandes, N., Afelik, S., Solter, M., and Pieler, T. (2004). Retinoic acid signaling is essential for pancreas development and promotes endocrine at the expense of exocrine cell differentiation in Xenopus. Developmental biology *271*(1), 144-160.

Cheng, X., Ying, L., Lu, L., Galvao, A.M., Mills, J.A., Lin, H.C., Kotton, D.N., Shen, S.S., Nostro, M.C., Choi, J.K.*, et al.* (2012). Self-renewing endodermal progenitor lines generated from human pluripotent stem cells. Cell stem cell *10*(4), 371-384.

Conlon, F.L., Lyons, K.M., Takaesu, N., Barth, K.S., Kispert, A., Herrmann, B., and Robertson, E.J. (1994). A primary requirement for nodal in the formation and maintenance of the primitive streak in the mouse. Development *120*(7), 1919-1928.

Contag, C.H., Jenkins, D., Contag, P.R., and Negrin, R.S. (2000). Use of reporter genes for optical measurements of neoplastic disease in vivo. Neoplasia *2*(1-2), 41-52.

Costa, M., Dottori, M., Sourris, K., Jamshidi, P., Hatzistavrou, T., Davis, R., Azzola, L., Jackson, S., Lim, S.M., Pera, M.*, et al.* (2007). A method for genetic modification of human embryonic stem cells using electroporation. Nature protocols *2*(4), 792-796.

Costa, M., Sourris, K., Hatzistavrou, T., Elefanty, A.G., and Stanley, E.G. (2008). Expansion of human embryonic stem cells in vitro. Current protocols in stem cell biology *Chapter 1*, Unit 1C 1 1-1C 1 7.

Cruise, G.M., Hegre, O.D., Lamberti, F.V., Hager, S.R., Hill, R., Scharp, D.S., and Hubbell, J.A. (1999). In vitro and in vivo performance of porcine islets encapsulated in interfacially photopolymerized poly(ethylene glycol) diacrylate membranes. Cell transplantation *8*(3), 293-306.

D'Amour, K.A., Bang, A.G., Eliazer, S., Kelly, O.G., Agulnick, A.D., Smart, N.G., Moorman, M.A., Kroon, E., Carpenter, M.K., and Baetge, E.E. (2006). Production of pancreatic hormone-

expressing endocrine cells from human embryonic stem cells. Nature biotechnology *24*(11), 1392-1401.

Dawson, R.M., Broughton, R.L., Stevenson, W.T., and Sefton, M.V. (1987). Microencapsulation of CHO cells in a hydroxyethyl methacrylate-methyl methacrylate copolymer. Biomaterials *8*(5), 360-366.

De Krijger, R.R., Aanstoot, H.J., Kranenburg, G., Reinhard, M., Visser, W.J., and Bruining, G.J. (1992). The midgestational human fetal pancreas contains cells coexpressing islet hormones. Developmental biology *153*(2), 368-375.

Duvillie, B., Attali, M., Bounacer, A., Ravassard, P., Basmaciogullari, A., and Scharfmann, R. (2006). The mesenchyme controls the timing of pancreatic beta-cell differentiation. Diabetes *55*(3), 582-589.

Elliott, D.A., Braam, S.R., Koutsis, K., Ng, E.S., Jenny, R., Lagerqvist, E.L., Biben, C., Hatzistavrou, T., Hirst, C.E., Yu, Q.C., *et al.* (2011). NKX2-5(eGFP/w) hESCs for isolation of human cardiac progenitors and cardiomyocytes. Nature methods *8*(12), 1037-1040.

Eshpeter, A., Jiang, J., Au, M., Rajotte, R.V., Lu, K., Lebkowski, J.S., Majumdar, A.S., and Korbutt, G.S. (2008). In vivo characterization of transplanted human embryonic stem cell-derived pancreatic endocrine islet cells. Cell proliferation *41*(6), 843-858.

Evans, M.J., and Kaufman, M.H. (1981). Establishment in culture of pluripotential cells from mouse embryos. Nature *292*(5819), 154-156.

Gadue, P., Huber, T.L., Paddison, P.J., and Keller, G.M. (2006). Wnt and TGF-beta signaling are required for the induction of an in vitro model of primitive streak formation using embryonic stem cells. Proceedings of the National Academy of Sciences of the United States of America *103*(45), 16806-16811.

Geller, R.L., Loudovaris, T., Neuenfeldt, S., Johnson, R.C., and Brauker, J.H. (1997). Use of an immunoisolation device for cell transplantation and tumor immunotherapy. Annals of the New York Academy of Sciences *831*, 438-451.

Gentile, F.T., Doherty, E.J., Rein, D.H., Schoichet, M.S., and Winn, S.R. (1995). Polymer science for macroencapsulation of cells for central nervous system transplantation. Reactive Polymers *25*(2-3), 207-227.

Gertow, K., Cedervall, J., Unger, C., Szoke, K., Blennow, E., Imreh, M.P., and Ahrlund-Richter, L. (2007). Trisomy 12 in HESC leads to no selective in vivo growth advantage in teratomas, but induces an increased abundance of renal development. Journal of cellular biochemistry *100*(6), 1518-1525.

Gillespie K.M. (2006) Type 1 Diabetes: Pathogenesis and Prevention. Canadian Medical Association Journal *152*(2), 165-170

Giudice, A., and Trounson, A. (2008). Genetic modification of human embryonic stem cells for derivation of target cells. Cell stem cell *2*(5), 422-433.

Gomez, M., and Curry, D.L. (1973). Potassium stimulation of insulin release by the perfused rat pancreas. Endocrinology *92*(4), 1126-1134.

Goulburn, A.L., Alden, D., Davis, R.P., Micallef, S.J., Ng, E.S., Yu, Q.C., Lim, S.M., Soh, C.L., Elliott, D.A., Hatzistavrou, T., *et al.* (2011). A targeted NKX2.1 human embryonic stem cell reporter line enables identification of human basal forebrain derivatives. Stem cells *29*(3), 462-473.

Gouzi, M., Kim, Y.H., Katsumoto, K., Johansson, K., and Grapin-Botton, A. (2011). Neurogenin3 initiates stepwise delamination of differentiating endocrine cells during

pancreas development. Developmental dynamics : an official publication of the American Association of Anatomists *240*(3), 589-604.

Govan, J.R., Fyfe, J.A., and Jarman, T.R. (1981). Isolation of alginate-producing mutants of Pseudomonas fluorescens, Pseudomonas putida and Pseudomonas mendocina. Journal of general microbiology *125*(1), 217-220.

Gradwohl, G., Dierich, A., LeMeur, M., and Guillemot, F. (2000). neurogenin3 is required for the development of the four endocrine cell lineages of the pancreas. Proceedings of the National Academy of Sciences of the United States of America *97*(4), 1607-1611.

Gu, G., Dubauskaite, J., and Melton, D.A. (2002). Direct evidence for the pancreatic lineage: NGN3+ cells are islet progenitors and are distinct from duct progenitors. Development *129*(10), 2447-2457.

Hart, A., Papadopoulou, S., and Edlund, H. (2003). Fgf10 maintains notch activation, stimulates proliferation, and blocks differentiation of pancreatic epithelial cells. Developmental dynamics : an official publication of the American Association of Anatomists *228*(2), 185-193.

Herrera, P.L. (2000). Adult insulin- and glucagon-producing cells differentiate from two independent cell lineages. Development *127*(11), 2317-2322.

Hudson, C., Clements, D., Friday, R.V., Stott, D., and Woodland, H.R. (1997). Xsox17alpha and -beta mediate endoderm formation in Xenopus. Cell *91*(3), 397-405.

Iwata, H., Amemiya, H., Matsuda, T., Takano, H., Hayashi, R., and Akutsu, T. (1989). Evaluation of microencapsulated islets in agarose gel as bioartificial pancreas by studies of hormone secretion in culture and by xenotransplantation. Diabetes *38 Suppl 1*, 224-225.

Jackson, S.A., Schiesser, J., Stanley, E.G., and Elefanty, A.G. (2010). Differentiating embryonic stem cells pass through 'temporal windows' that mark responsiveness to exogenous and paracrine mesendoderm inducing signals. PloS one *5*(5), e10706.

Jensen, J., Pedersen, E.E., Galante, P., Hald, J., Heller, R.S., Ishibashi, M., Kageyama, R., Guillemot, F., Serup, P., and Madsen, O.D. (2000). Control of endodermal endocrine development by Hes-1. Nature genetics *24*(1), 36-44.

Jeon, J., Correa-Medina, M., Ricordi, C., Edlund, H., and Diez, J.A. (2009). Endocrine cell clustering during human pancreas development. The journal of histochemistry and cytochemistry : official journal of the Histochemistry Society *57*(9), 811-824.

Jiang, J., Au, M., Lu, K., Eshpeter, A., Korbutt, G., Fisk, G., and Majumdar, A.S. (2007a). Generation of insulin-producing islet-like clusters from human embryonic stem cells. Stem cells *25*(8), 1940-1953.

Jiang, W., Shi, Y., Zhao, D., Chen, S., Yong, J., Zhang, J., Qing, T., Sun, X., Zhang, P., Ding, M., *et al.* (2007b). In vitro derivation of functional insulin-producing cells from human embryonic stem cells. Cell research *17*(4), 333-344.

Johansson, U., Elgue, G., Nilsson, B., and Korsgren, O. (2005). Composite islet-endothelial cell grafts: a novel approach to counteract innate immunity in islet transplantation. American journal of transplantation : official journal of the American Society of Transplantation and the American Society of Transplant Surgeons *5*(11), 2632-2639.

Johansson, U., Rasmusson, I., Niclou, S.P., Forslund, N., Gustavsson, L., Nilsson, B., Korsgren, O., and Magnusson, P.U. (2008). Formation of composite endothelial cell-mesenchymal stem cell islets: a novel approach to promote islet revascularization. Diabetes *57*(9), 2393-2401.

Kelly, O.G., Chan, M.Y., Martinson, L.A., Kadoya, K., Ostertag, T.M., Ross, K.G., Richardson, M., Carpenter, M.K., D'Amour, K.A., Kroon, E.*, et al.* (2011). Cell-surface markers for the isolation of pancreatic cell types derived from human embryonic stem cells. Nature biotechnology *29*(8), 750-756.

Kessler, L., Pinget, M., Aprahamian, M., Dejardin, P., and Damge, C. (1991). In vitro and in vivo studies of the properties of an artificial membrane for pancreatic islet encapsulation. Hormone and metabolic research = Hormon- und Stoffwechselforschung = Hormones et metabolisme *23*(7), 312-317.

Kim, S.K., and Hebrok, M. (2001). Intercellular signals regulating pancreas development and function. Genes & development *15*(2), 111-127.

Kobberup, S., Schmerr, M., Dang, M.L., Nyeng, P., Jensen, J.N., MacDonald, R.J., and Jensen, J. (2010). Conditional control of the differentiation competence of pancreatic endocrine and ductal cells by Fgf10. Mechanisms of development *127*(3-4), 220-234.

Krishnamurthy, N.V., and Gimi, B. (2011). Encapsulated cell grafts to treat cellular deficiencies and dysfunction. Critical reviews in biomedical engineering *39*(6), 473-491.

Kroon, E., Martinson, L.A., Kadoya, K., Bang, A.G., Kelly, O.G., Eliazer, S., Young, H., Richardson, M., Smart, N.G., Cunningham, J.*, et al.* (2008). Pancreatic endoderm derived from human embryonic stem cells generates glucose-responsive insulin-secreting cells in vivo. Nature biotechnology *26*(4), 443-452.

Kubo, A., Shinozaki, K., Shannon, J.M., Kouskoff, V., Kennedy, M., Woo, S., Fehling, H.J., and Keller, G. (2004). Development of definitive endoderm from embryonic stem cells in culture. Development *131*(7), 1651-1662.

Lai, Y., Schneider, D., Kidszun, A., Hauck-Schmalenberger, I., Breier, G., Brandhorst, D., Brandhorst, H., Iken, M., Brendel, M.D., Bretzel, R.G.*, et al.* (2005). Vascular endothelial growth factor increases functional beta-cell mass by improvement of angiogenesis of isolated human and murine pancreatic islets. Transplantation *79*(11), 1530-1536.

Lewis, J. (1996). Neurogenic genes and vertebrate neurogenesis. Current opinion in neurobiology *6*(1), 3-10.

Lim, F., and Sun, A.M. (1980). Microencapsulated islets as bioartificial endocrine pancreas. Science *210*(4472), 908-910.

Lim, S.M., Pereira, L., Wong, M.S., Hirst, C.E., Van Vranken, B.E., Pick, M., Trounson, A., Elefanty, A.G., and Stanley, E.G. (2009). Enforced expression of Mixl1 during mouse ES cell differentiation suppresses hematopoietic mesoderm and promotes endoderm formation. Stem cells *27*(2), 363-374.

Ling, Z., Hannaert, J.C., and Pipeleers, D. (1994). Effect of nutrients, hormones and serum on survival of rat islet beta cells in culture. Diabetologia *37*(1), 15-21.

Liu, P., Wakamiya, M., Shea, M.J., Albrecht, U., Behringer, R.R., and Bradley, A. (1999). Requirement for Wnt3 in vertebrate axis formation. Nature genetics *22*(4), 361-365.

Lu, C.C., and Robertson, E.J. (2004). Multiple roles for Nodal in the epiblast of the mouse embryo in the establishment of anterior-posterior patterning. Developmental biology *273*(1), 149-159.

Lyttle, B.M., Li, J., Krishnamurthy, M., Fellows, F., Wheeler, M.B., Goodyer, C.G., and Wang, R. (2008). Transcription factor expression in the developing human fetal endocrine pancreas. Diabetologia *51*(7), 1169-1180.

Macfarlan, T.S., Gifford, W.D., Driscoll, S., Lettieri, K., Rowe, H.M., Bonanomi, D., Firth, A., Singer, O., Trono, D., and Pfaff, S.L. (2012). Embryonic stem cell potency fluctuates with endogenous retrovirus activity. Nature *487*(7405), 57-63.

Mao, G.H., Chen, G.A., Bai, H.Y., Song, T.R., and Wang, Y.X. (2009). The reversal of hyperglycaemia in diabetic mice using PLGA scaffolds seeded with islet-like cells derived from human embryonic stem cells. Biomaterials *30*(9), 1706-1714.

Martin, G.R. (1981). Isolation of a pluripotent cell line from early mouse embryos cultured in medium conditioned by teratocarcinoma stem cells. Proceedings of the National Academy of Sciences of the United States of America *78*(12), 7634-7638.

Martin, M., Gallego-Llamas, J., Ribes, V., Kedinger, M., Niederreither, K., Chambon, P., Dolle, P., and Gradwohl, G. (2005). Dorsal pancreas agenesis in retinoic acid-deficient Raldh2 mutant mice. Developmental biology *284*(2), 399-411.

Matsuoka, T.A., Artner, I., Henderson, E., Means, A., Sander, M., and Stein, R. (2004). The MafA transcription factor appears to be responsible for tissue-specific expression of insulin. Proceedings of the National Academy of Sciences of the United States of America *101*(9), 2930-2933.

Matsuoka, T.A., Zhao, L., Artner, I., Jarrett, H.W., Friedman, D., Means, A., and Stein, R. (2003). Members of the large Maf transcription family regulate insulin gene transcription in islet beta cells. Molecular and cellular biology *23*(17), 6049-6062.

Mattsson, G., Jansson, L., and Carlsson, P.O. (2002). Decreased vascular density in mouse pancreatic islets after transplantation. Diabetes *51*(5), 1362-1366.

McLean, A.B., D'Amour, K.A., Jones, K.L., Krishnamoorthy, M., Kulik, M.J., Reynolds, D.M., Sheppard, A.M., Liu, H., Xu, Y., Baetge, E.E.*, et al.* (2007). Activin a efficiently specifies definitive endoderm from human embryonic stem cells only when phosphatidylinositol 3-kinase signaling is suppressed. Stem cells *25*(1), 29-38.

Micallef, S.J., Janes, M.E., Knezevic, K., Davis, R.P., Elefanty, A.G., and Stanley, E.G. (2005). Retinoic acid induces Pdx1-positive endoderm in differentiating mouse embryonic stem cells. Diabetes *54*(2)*,* 301-305.

Micallef, S.J., Li, X., Schiesser, J.V., Hirst, C.E., Yu, Q.C., Lim, S.M., Nostro, M.C., Elliott, D.A., Sarangi, F., Harrison, L.C.*, et al.* (2012). INS ( GFP/w derived insulin-producing cells. Diabetologia *55*(3), 694-706.

Miralles, F., Czernichow, P., Ozaki, K., Itoh, N., and Scharfmann, R. (1999). Signaling through fibroblast growth factor receptor 2b plays a key role in the development of the exocrine pancreas. Proceedings of the National Academy of Sciences of the United States of America *96*(11), 6267-6272.

Miralles, F., Lamotte, L., Couton, D., and Joshi, R.L. (2006). Interplay between FGF10 and Notch signalling is required for the self-renewal of pancreatic progenitors. The International journal of developmental biology *50*(1), 17-26.

Mitanchez-Mokhtari, D., Lahlou, N., Kieffer, F., Magny, J.F., Roger, M., and Voyer, M. (2004). Both relative insulin resistance and defective islet beta-cell processing of proinsulin are responsible for transient hyperglycemia in extremely preterm infants. Pediatrics *113*(3 Pt1), 537-541.

Molotkov, A., Molotkova, N., and Duester, G. (2005). Retinoic acid generated by Raldh2 in mesoderm is required for mouse dorsal endodermal pancreas development.

Developmental dynamics : an official publication of the American Association of Anatomists *232*(4), 950-957.

Moore, K.L., Persaud, T.V.N., and Shiota, K. (1995). Colour Atlas of Clinical Embryology (Philadelphia, W.B. Saunders).

Muthyala, S., Raj, V.R., Mohanty, M., Mohanan, P.V., and Nair, P.D. (2011). The reversal of diabetes in rat model using mouse insulin producing cells - a combination approach of tissue engineering and macroencapsulation. Acta biomaterialia *7*(5), 2153-2162.

Ng, E.S., Davis, R., Stanley, E.G., and Elefanty, A.G. (2008a). A protocol describing the use of a recombinant protein-based, animal product-free medium (APEL) for human embryonic stem cell differentiation as spin embryoid bodies. Nature protocols *3*(5), 768-776.

Ng, E.S., Davis, R.P., Hatzistavrou, T., Stanley, E.G., and Elefanty, A.G. (2008b). Directed differentiation of human embryonic stem cells as spin embryoid bodies and a description of the hematopoietic blast colony forming assay. Current protocols in stem cell biology *Chapter 1*, Unit 1D 3.

Norgaard, G.A., Jensen, J.N., and Jensen, J. (2003). FGF10 signaling maintains the pancreatic progenitor cell state revealing a novel role of Notch in organ development. Developmental biology *264*(2), 323-338.

Nostro, M.C., Sarangi, F., Ogawa, S., Holtzinger, A., Corneo, B., Li, X., Micallef, S.J., Park, I.H., Basford, C., Wheeler, M.B.*, et al.* (2011). Stage-specific signaling through TGFbeta family members and WNT regulates patterning and pancreatic specification of human pluripotent stem cells. Development *138*(5), 861-871.

Olerud, J., Johansson, M., Lawler, J., Welsh, N., and Carlsson, P.O. (2008). Improved vascular engraftment and graft function after inhibition of the angiostatic factor thrombospondin-1 in mouse pancreatic islets. Diabetes *57*(7), 1870-1877.

Otonkoski, T., Beattie, G.M., Mally, M.I., Ricordi, C., and Hayek, A. (1993). Nicotinamide is a potent inducer of endocrine differentiation in cultured human fetal pancreatic cells. J Clin Invest *92*(3), 1459-1466.

Pan, F.C., Chen, Y., Bayha, E., and Pieler, T. (2007). Retinoic acid-mediated patterning of the pre-pancreatic endoderm in Xenopus operates via direct and indirect mechanisms. Mechanisms of development *124*(7-8), 518-531.

Pearce, J.J., and Evans, M.J. (1999). Mml, a mouse Mix-like gene expressed in the primitive streak. Mechanisms of development *87*(1-2), 189-192.

Phelan, M.C. (2006). Techniques for mammalian cell tissue culture. Current protocols in molecular biology / edited by Frederick M Ausubel [et al] *Appendix 3*, Appendix 3F.

Phillips, B.W., Hentze, H., Rust, W.L., Chen, Q.P., Chipperfield, H., Tan, E.K., Abraham, S., Sadasivam, A., Soong, P.L., Wang, S.T.*, et al.* (2007). Directed differentiation of human embryonic stem cells into the pancreatic endocrine lineage. Stem cells and development *16*(4), 561-578.

Pictet, R.L., Clark, W.R., Williams, R.H., and Rutter, W.J. (1972). An ultrastructural analysis of the developing embryonic pancreas. Developmental biology *29*(4), 436-467.

Piper, K., Brickwood, S., Turnpenny, L.W., Cameron, I.T., Ball, S.G., Wilson, D.I., and Hanley, N.A. (2004). Beta cell differentiation during early human pancreas development. The Journal of endocrinology *181*(1), 11-23.

Polak, M., Bouchareb-Banaei, L., Scharfmann, R., and Czernichow, P. (2000). Early pattern of differentiation in the human pancreas. Diabetes *49*(2), 225-232.

Prochorov, A.V., Roudenok, V.V., and Goranov, V.A. (2005). Histological study of macroencapsulation of pancreatic islet cells after transplantation into the bloodstream. Transplantation proceedings *37*(10), 4446-4448.

Qi, M., Gu, Y., Sakata, N., Kim, D., Shirouzu, Y., Yamamoto, C., Hiura, A., Sumi, S., and Inoue, K. (2004). PVA hydrogel sheet macroencapsulation for the bioartificial pancreas. Biomaterials *25*(27), 5885-5892.

Rackham, C.L., Chagastelles, P.C., Nardi, N.B., Hauge-Evans, A.C., Jones, P.M., and King, A.J. (2011). Co-transplantation of mesenchymal stem cells maintains islet organisation and morphology in mice. Diabetologia *54*(5), 1127-1135.

Reubinoff, B.E., Pera, M.F., Fong, C.Y., Trounson, A., and Bongso, A. (2000). Embryonic stem cell lines from human blastocysts: somatic differentiation in vitro. Nature biotechnology *18*(4), 399-404.

Rezania, A., Bruin, J.E., Riedel, M.J., Mojibian, M., Asadi, A., Xu, J., Gauvin, R., Narayan, K., Karanu, F., O'Neil, J.J.*, et al.* (2012). Maturation of Human Embryonic Stem Cell-Derived Pancreatic Progenitors Into Functional Islets Capable of Treating Pre-existing Diabetes in Mice. Diabetes *61*(8), 2016-2029.

Rezania, A., Riedel, M.J., Wideman, R.D., Karanu, F., Ao, Z., Warnock, G.L., and Kieffer, T.J. (2011). Production of functional glucagon-secreting alpha-cells from human embryonic stem cells. Diabetes *60*(1), 239-247.

Rhinn, M., and Dolle, P. (2012). Retinoic acid signalling during development. Development *139*(5), 843-858.

Richards, M., Fong, C.Y., Chan, W.K., Wong, P.C., and Bongso, A. (2002). Human feeders support prolonged undifferentiated growth of human inner cell masses and embryonic stem cells. Nature biotechnology *20*(9), 933-936.

Riedel, M.J., Asadi, A., Wang, R., Ao, Z., Warnock, G.L., and Kieffer, T.J. (2012). Immunohistochemical characterisation of cells co-producing insulin and glucagon in the developing human pancreas. Diabetologia *55*(2), 372-381.

Robb, L., Hartley, L., Begley, C.G., Brodnicki, T.C., Copeland, N.G., Gilbert, D.J., Jenkins, N.A., and Elefanty, A.G. (2000). Cloning, expression analysis, and chromosomal localization of murine and human homologues of a Xenopus mix gene. Developmental dynamics : an official publication of the American Association of Anatomists *219*(4), 497-504.

Rudnick, A., Ling, T.Y., Odagiri, H., Rutter, W.J., and German, M.S. (1994). Pancreatic beta cells express a diverse set of homeobox genes. Proceedings of the National Academy of Sciences of the United States of America *91*(25), 12203-12207.

Sakai, R., Shiozaki, M., Tabuchi, M., and Eto, Y. (1992). The measurement of activin/EDF in mouse serum: evidence for extragonadal production. Biochemical and biophysical research communications *188*(2), 921-926.

Sambrook, J., Russell, D.W., and Laboratory, C.S.H. (2001). Molecular cloning: a laboratory manual, 3rd edn (Cold Spring Harbour, N.Y., Cold Spring Harbour Laboratory).

Sand, F.W., Hornblad, A., Johansson, J.K., Loren, C., Edsbagge, J., Stahlberg, A., Magenheim, J., Ilovich, O., Mishani, E., Dor, Y.*, et al.* (2011). Growth-limiting role of endothelial cells in endoderm development. Developmental biology *352*(2), 267-277.

Sander, M., Sussel, L., Conners, J., Scheel, D., Kalamaras, J., Dela Cruz, F., Schwitzgebel, V., Hayes-Jordan, A., and German, M. (2000). Homeobox gene Nkx6.1 lies downstream of Nkx2.2 in the major pathway of beta-cell formation in the pancreas. Development *127*(24), 5533-5540.

Sarkar, S.A., Kobberup, S., Wong, R., Lopez, A.D., Quayum, N., Still, T., Kutchma, A., Jensen, J.N., Gianani, R., Beattie, G.M.*, et al.* (2008). Global gene expression profiling and histochemical analysis of the developing human fetal pancreas. Diabetologia *51*(2), 285-297.

Sasaki, H., and Hogan, B.L. (1993). Differential expression of multiple fork head related genes during gastrulation and axial pattern formation in the mouse embryo. Development *118*(1), 47-59.

Schaffer, A.E., Yang, A.J., Thorel, F., Herrera, P.L., and Sander, M. (2011). Transgenic overexpression of the transcription factor Nkx6.1 in beta-cells of mice does not increase beta-cell proliferation, beta-cell mass, or improve glucose clearance. Molecular endocrinology *25*(11), 1904-1914.

Schisler, J.C., Fueger, P.T., Babu, D.A., Hohmeier, H.E., Tessem, J.S., Lu, D., Becker, T.C., Naziruddin, B., Levy, M., Mirmira, R.G.*, et al.* (2008). Stimulation of human and rat islet beta-cell proliferation with retention of function by the homeodomain transcription factor Nkx6.1. Molecular and cellular biology *28*(10), 3465-3476.

Schroeder, I.S., Rolletschek, A., Blyszczuk, P., Kania, G., and Wobus, A.M. (2006). Differentiation of mouse embryonic stem cells to insulin-producing cells. Nature protocols *1*(2), 495-507.

Seymour, P.A., Bennett, W.R., and Slack, J.M. (2004). Fission of pancreatic islets during postnatal growth of the mouse. Journal of anatomy *204*(2), 103-116.

Shapiro, A.M., Lakey, J.R., Ryan, E.A., Korbutt, G.S., Toth, E., Warnock, G.L., Kneteman, N.M., and Rajotte, R.V. (2000). Islet transplantation in seven patients with type 1 diabetes mellitus using a glucocorticoid-free immunosuppressive regimen. The New England journal of medicine *343*(4), 230-238.

Shapiro, A.M., Ricordi, C., Hering, B.J., Auchincloss, H., Lindblad, R., Robertson, R.P., Secchi, A., Brendel, M.D., Berney, T., Brennan, D.C.*, et al.* (2006). International trial of the Edmonton protocol for islet transplantation. The New England journal of medicine *355*(13), 1318-1330.

Shi, Y. (2010). Generation of functional insulin-producing cells from human embryonic stem cells in vitro. Methods in molecular biology *636*, 79-85.

Shi, Y., Hou, L., Tang, F., Jiang, W., Wang, P., Ding, M., and Deng, H. (2005). Inducing embryonic stem cells to differentiate into pancreatic beta cells by a novel three-step approach with activin A and all-trans retinoic acid. Stem cells *23*(5), 656-662.

Shim, J.H., Kim, S.E., Woo, D.H., Kim, S.K., Oh, C.H., McKay, R., and Kim, J.H. (2007). Directed differentiation of human embryonic stem cells towards a pancreatic cell fate. Diabetologia *50*(6), 1228-1238.

Siegel, E.G., Wollheim, C.B., Kikuchi, M., Renold, A.E., and Sharp, G.W. (1980). Dependency of cyclic AMP-induced insulin release on intra- and extracellular calcium in rat islets of Langerhans. J Clin Invest *65*(2), 233-241.

Slack, J.M. (1995). Developmental biology of the pancreas. Development *121*(6), 1569-1580.

Sorenby, A.K., Kumagai-Braesch, M., Sharma, A., Hultenby, K.R., Wernerson, A.M., and Tibell, A.B. (2008). Preimplantation of an immunoprotective device can lower the curative dose of islets to that of free islet transplantation: studies in a rodent model. Transplantation *86*(2), 364-366.

Stafford, D., and Prince, V.E. (2002). Retinoic acid signaling is required for a critical early step in zebrafish pancreatic development. Current biology : CB *12*(14), 1215-1220.

Stafford, D., White, R.J., Kinkel, M.D., Linville, A., Schilling, T.F., and Prince, V.E. (2006). Retinoids signal directly to zebrafish endoderm to specify insulin-expressing beta-cells. Development *133*(5), 949-956.

Steiner, D.F., Chan, S.J., and Rubenstein, A.H. (2010). Biosynthesis of Insulin. In Comprehensive Physiology (John Wiley & Sons, Inc.).

Su, D., Zhang, N., He, J., Qu, S., Slusher, S., Bottino, R., Bertera, S., Bromberg, J., and Dong, H.H. (2007). Angiopoietin-1 production in islets improves islet engraftment and protects islets from cytokine-induced apoptosis. Diabetes *56*(9), 2274-2283.

Sui, L., Mfopou, J.K., Chen, B., Sermon, K., and Bouwens, L. (2012). Transplantation of human embryonic stem cell-derived pancreatic endoderm reveals a site-specific survival, growth and differentiation. Cell transplantation [Epub ahead of print].

Tam, P.P., and Loebel, D.A. (2007). Gene function in mouse embryogenesis: get set for gastrulation. Nature reviews Genetics *8*(5), 368-381.

Teitelman, G., Alpert, S., Polak, J.M., Martinez, A., and Hanahan, D. (1993). Precursor cells of mouse endocrine pancreas coexpress insulin, glucagon and the neuronal proteins tyrosine hydroxylase and neuropeptide Y, but not pancreatic polypeptide. Development *118*(4), 1031-1039.

Teo, A.K.K., Ali, Y., Wong, K.Y., Chipperfield, H., Sadasivam, A., Poobalan, Y., Tan, E.K., Wang, S.T., Abraham, S., Tsuneyoshi, N.*, et al.* (2012). Activin and BMP4 Synergistically Promote Formation of Definitive Endoderm in Human Embryonic Stem Cells. Stem Cells *30*, 631-642.

Thomson, J.A., Itskovitz-Eldor, J., Shapiro, S.S., Waknitz, M.A., Swiergiel, J.J., Marshall, V.S., and Jones, J.M. (1998). Embryonic stem cell lines derived from human blastocysts. Science *282*(5391), 1145-1147.

Tuch, B.E., Keogh, G.W., Williams, L.J., Wu, W., Foster, J.L., Vaithilingam, V., and Philips, R. (2009). Safety and viability of microencapsulated human islets transplanted into diabetic humans. Diabetes care *32*(10), 1887-1889.

Vallier, L., Touboul, T., Chng, Z., Brimpari, M., Hannan, N., Millan, E., Smithers, L.E., Trotter, M., Rugg-Gunn, P., Weber, A.*, et al.* (2009). Early cell fate decisions of human embryonic stem cells and mouse epiblast stem cells are controlled by the same signalling pathways. PloS one *4*(6), e6082.

Van Hoof, D., D'Amour, K.A., and German, M.S. (2009). Derivation of insulin-producing cells from human embryonic stem cells. Stem cell research *3*(2-3), 73-87.

Van Hoof, D., Mendelsohn, A.D., Seerke, R., Desai, T.A., and German, M.S. (2011). Differentiation of human embryonic stem cells into pancreatic endoderm in patterned size-controlled clusters. Stem cell research *6*(3), 276-285.

Villasenor, A., Chong, D.C., and Cleaver, O. (2008). Biphasic Ngn3 expression in the developing pancreas. Developmental dynamics *237*(11), 3270-3279.

Villasenor, A., Marty-Santos, L., Dravis, C., Fletcher, P., Henkemeyer, M., and Cleaver, O. (2012). EphB3 marks delaminating endocrine progenitor cells in the developing pancreas. Developmental dynamics *241*(5), 1008-1019.

Wang, H., Brun, T., Kataoka, K., Sharma, A.J., and Wollheim, C.B. (2007). MAFA controls genes implicated in insulin biosynthesis and secretion. Diabetologia *50*(2), 348-358.

Watanabe, K., Ueno, M., Kamiya, D., Nishiyama, A., Matsumura, M., Wataya, T., Takahashi, J.B., Nishikawa, S., Muguruma, K., and Sasai, Y. (2007). A ROCK inhibitor permits survival of dissociated human embryonic stem cells. Nature biotechnology *25*(6), 681-686.

Wilkinson, D.G., Bhatt, S., and Herrmann, B.G. (1990). Expression pattern of the mouse T gene and its role in mesoderm formation. Nature *343*(6259), 657-659.

Winnier, G., Blessing, M., Labosky, P.A., and Hogan, B.L. (1995). Bone morphogenetic protein-4 is required for mesoderm formation and patterning in the mouse. Genes & development *9*(17), 2105-2116.

Wu, J.C., Sundaresan, G., Iyer, M., and Gambhir, S.S. (2001). Noninvasive optical imaging of firefly luciferase reporter gene expression in skeletal muscles of living mice. Molecular therapy *4*(4), 297-306.

Xu, X., Browning, V.L., and Odorico, J.S. (2011). Activin, BMP and FGF pathways cooperate to promote endoderm and pancreatic lineage cell differentiation from human embryonic stem cells. Mechanisms of development *128*(7-10), 412-427.

Yasunaga, M., Tada, S., Torikai-Nishikawa, S., Nakano, Y., Okada, M., Jakt, L.M., Nishikawa, S., Chiba, T., and Era, T. (2005). Induction and monitoring of definitive and visceral endoderm differentiation of mouse ES cells. Nature biotechnology *23*(12), 1542-1550.

Ye, D.Z., Tai, M.H., Linning, K.D., Szabo, C., and Olson, L.K. (2006). MafA expression and insulin promoter activity are induced by nicotinamide and related compounds in INS-1 pancreatic beta-cells. Diabetes *55*(3), 742-750.

Zhang, C., Moriguchi, T., Kajihara, M., Esaki, R., Harada, A., Shimohata, H., Oishi, H., Hamada, M., Morito, N., Hasegawa, K.*, et al.* (2005). MafA is a key regulator of glucose-stimulated insulin secretion. Molecular and cellular biology *25*(12), 4969-4976.

Zhang, D., Jiang, W., Liu, M., Sui, X., Yin, X., Chen, S., Shi, Y., and Deng, H. (2009). Highly efficient differentiation of human ES cells and iPS cells into mature pancreatic insulin-producing cells. Cell research *19*(4), 429-438.

Zhang, N., Richter, A., Suriawinata, J., Harbaran, S., Altomonte, J., Cong, L., Zhang, H., Song, K., Meseck, M., Bromberg, J.*, et al.* (2004). Elevated vascular endothelial growth factor production in islets improves islet graft vascularization. Diabetes *53*(4), 963-970.

Zielinski, B.A., and Aebischer, P. (1994). Chitosan as a matrix for mammalian cell encapsulation. Biomaterials *15*(13), 1049-1056.

Zimmermann, H., Shirley, S.G., and Zimmermann, U. (2007). Alginate-based encapsulation of cells: past, present, and future. Current diabetes reports *7*(4), 314-320.

# APPENDICES

**Figure Legends – Supplementary Material from Micallef et.al., 2012**

**ESM Fig. 1:**
Characterization of *INS* $^{GFP/w}$ hESC lines. Hematoxylin and eosin stained histological sections of teratomas generated by *INS* $^{GFP/w}$ MEL1 hESCs (**a**) and *INS* $^{GFP/w}$ HES3 hESCs (**b**) showing derivatives of the three primary germ layers. (**c**) Flow cytometric analysis of *INS* $^{GFP/w}$ MEL1 hESCs showing expression of stem cell surface markers (GCTM2, ECADHERIN, TRA-1-60) and intracellular OCT4. (**d**) Metaphase chromosome spread of *INS* $^{GFP/w}$ MEL1 hESCs showing a normal male karyotype. (**e**) Flow cytometric analysis of *INS* $^{GFP/w}$ HES3 hESCs showing expression of stem cell surface markers (GCTM2, ECADHERIN, TRA-1-60) and intracellular OCT4. (**f**) Metaphase chromosome spread of *INS* $^{GFP/w}$ HES3 hESCs showing a normal female karyotype

**ESM Fig. 2:**
Schematic diagram representing the flat culture differentiation protocol. Differentiation involved the following conditions: in stage 1, cells were grown in RPMI medium (Invitrogen), supplemented with 150 ng/ml of activin A and 25 ng/ml of Wnt3a for 1 day and supplemented 0.2% FCS for 2 days; in stage 2, RPMI was supplemented with 2% FCS and 30 ng/ml KGF; in stages 3–5 DMEM or IMDM (Invitrogen) containing 1× B27 supplement (Invitrogen) was used. These stages also included 2 μM RA, 0.25 μM cyclopamine and 50 ng/ml noggin (stage 3) and 10 mM nicotinamide and 100 nM glucagon-like peptide-1 (GLP1) (stage 4). As recently documented [12], addition of 50–150 ng/ml noggin and 6 μM SB431542 in stages 4 and 5 increased the frequency of INS$^+$ cells. As described by D'Amour and colleagues, stage 5 cultures were also supplemented with IGF-1

**ESM Fig. 3:**
Pairwise comparison of INS-GFP$^+$ and GFP$^-$ cell populations. Experiments 1 and 2 represent data derived from *INS* $^{GFP/w}$ MEL1 hESCs differentiated using a flat culture protocol based on D'Amour et al., whilst experiments 3 and 4 represent data generated from *INS* $^{GFP/w}$ HES3 hESCs differentiated as described by Nostro et al., 2011. (**a**) Scatter plots comparing the expression of 48,803 probe sets on Illumina HumanHT-12 v4 Expression BeadChips hybridized against labelled total RNA extracted from INS-GFP$^+$ and GFP$^-$ fractions derived from four separate sorting experiments. Parallel lines mark 2-fold differences in the relative signal intensity and probe sets falling outside these lines in all four experiments are highlighted in blue. Smaller black dots outside the parallel lines represent probe sets for which the relative signal intensity had changed more that twofold in 1, 2 or 3 of the pair wise comparisons. The number of probe sets for which signal intensity changed by more that twofold is indicated in each scatter plot. (**b**) List of genes whose expression was up regulated by more than 5 fold in the INS-GFP$^+$ fraction of any given experiment (Experiment number is shown across the top of each column)

**ESM Fig. 4:**
Gene expression analysis of differentiated *INS* $^{GFP/w}$ hESCs. Q-PCR analysis examining the expression the pancreatic genes INSULIN, PDX1, NKX6.1, NKX2.2, ISL1 and PAX6 in d20 flow cytometrically sorted INS-GFP$^+$ and GFP$^-$ cell populations derived using either the flat culture protocol (protocol 1) or the Nostro protocol (protocol 2). FP; fetal pancreas. ISLT; adult human islets

**ESM Fig. 5:**
PDX1 expression in *INS* $^{GFP/w}$ hESCs differentiated using the flat culture differentiation protocol. Immunofluorescence analysis of day 20 cultures demonstrated expression of PDX1 in INS-GFP$^+$ and INS-GFP$^-$ cells. Scale bar = 20 μm

**ESM Fig. 6:**
Transcription factor expression by cells within INS-GFP$^+$ spin EBs. Wholemount immunofluorescence of INS-GFP$^+$ EBs generated with the spin EB platform showing expression of PAX6, NKX2.2, ISL1, PDX1 and NKX6.1. Both overlays and single colour images are shown. Note that all transcription factors are also expressed by GFP$^-$ cells present within these cultures. Scale bar = 20 μm

**ESM Fig. 7:**
Two-colour heat map representation of beta and alpha cell enriched genes in INS-GFP$^+$ cell populations derived using different protocols. Two-colour heat map representation of the beta cell enriched genes and alpha cell enriched genes identified by Dorrell et al. 2011 [34], derived from INS-GFP$^+$ cell fractions generated using the 4 protocols indicated. Probes for 41 of the 51 beta cell enriched genes and 21 of the 29 alpha cell enriched genes were identified on the Illumina HT12 v3 and v4 BeadChips. In cases where multiple probes existed for a gene, the probe that had the highest signal level in the islets, adult pancreas and fetal pancreas was selected. Expression levels were background adjusted, quantile normalised and log2 transformed. The expression level for the four indicated protocols is the average of two independent sorted INS-GFP$^+$ cell fractions

**Supplementary Figure 1**

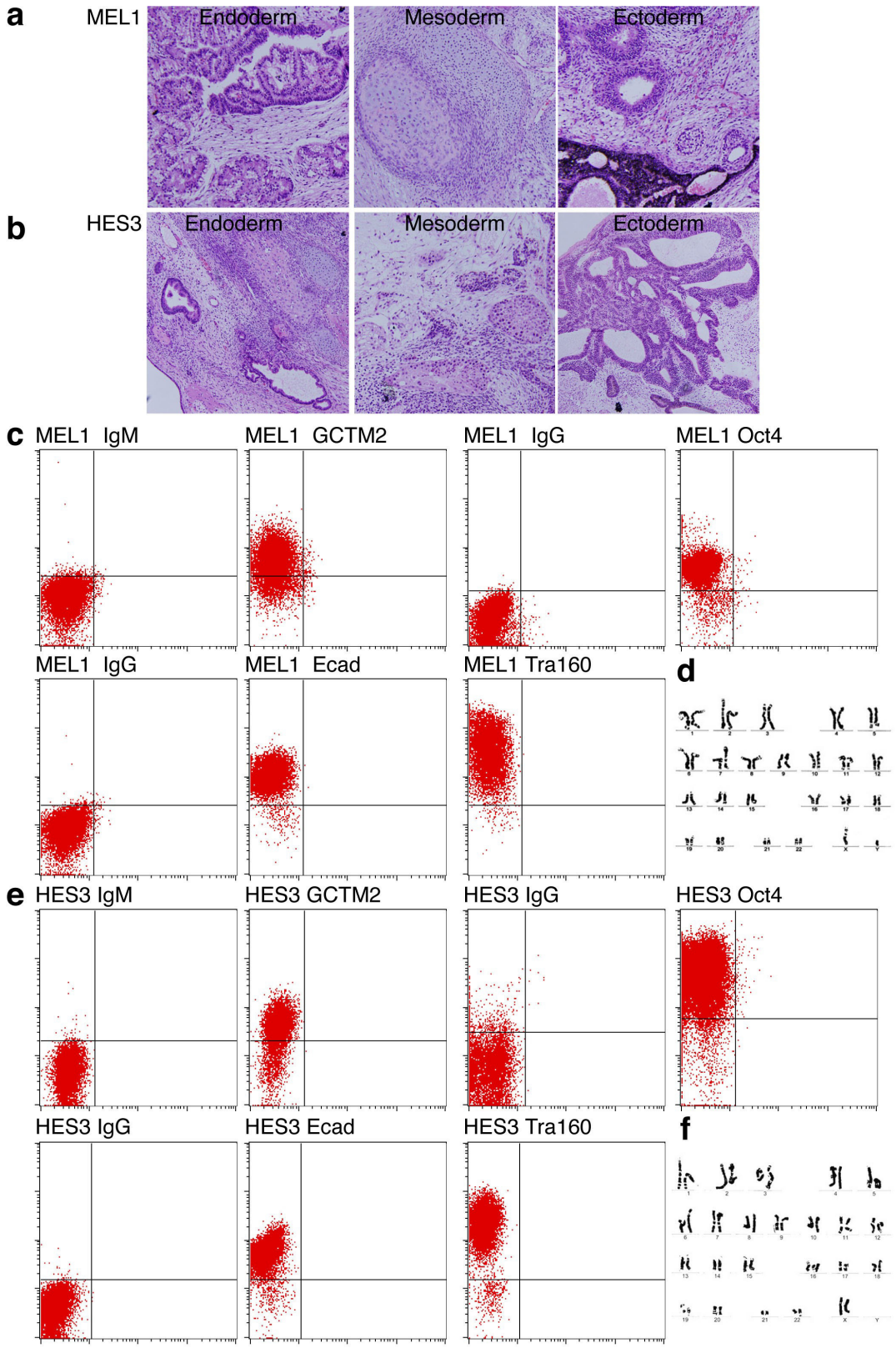

**Supplementary Figure 2**

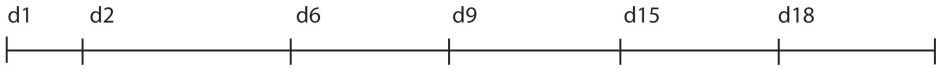


| Stage1 | | Stage2 | Stage3 | Stage4 | Stage5 |
|---|---|---|---|---|---|
| ActA+ Wnt3a | ActA+Wnt3a | KGF | RA+Cyc+Nog | Nic+GLP1±Nog±SB | Nic+GLP1+ IGF-1±Nog±SB |
| RPMI | RPMI+0.2%FCS | RPMI+2%FCS | DMEM+1xB27 | DMEM+1xB27 | IMDM+1xB27 |

**Supplementary Figure 3**

**a**

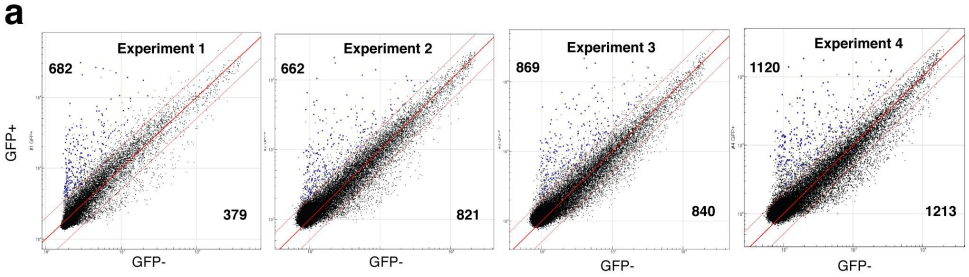


**b**

| SYMBOL | 1 | 2 | 3 | 4 |
|---|---|---|---|---|
| ABCC8 | | | | |
| AMPH | | | | |
| APLP1 | | | | |
| BTBD17 | | | | |
| C19orf30 | | | | |
| CRYBA2 | | | | |
| FSTL5 | | | | |
| GAD2 | | | | |
| GCG | | | | |
| INA | | | | |
| INS | | | | |
| INSM1 | | | | |
| KCNK16 | | | | |
| KCNK17 | | | | |
| KIAA1324 | | | | |
| LY6H | | | | |
| LY6H | | | | |
| MAFB | | | | |
| MFAP4 | | | | |
| MLXIPL | | | | |
| NKX2-2 | | | | |
| PAX6 | | | | |
| PTPRN | | | | |
| SCG2 | | | | |
| SCG3 | | | | |
| SCG3 | | | | |
| SCG5 | | | | |
| SST | | | | |
| SSTR2 | | | | |
| STX1A | | | | |
| SYP | | | | |
| SYT4 | | | | |
| TNRC4 | | | | |
| ARX | | | | |
| ASCL1 | | | | |
| BTBD11 | | | | |
| C1QL1 | | | | |
| C8orf13 | | | | |
| CACNA2D2 | | | | |
| CHGB | | | | |
| CNIH2 | | | | |
| CRIP2 | | | | |
| CRYBA2 | | | | |
| DDC | | | | |
| DRD1IP | | | | |
| ERO1LB | | | | |
| FEV | | | | |
| HEPACAM2 | | | | |
| IMAGE:6189945 | | | | |
| IRX2 | | | | |
| ISL1 | | | | |
| KCNJ6 | | | | |
| LMO2 | | | | |
| LOC649970 | | | | |
| LOC730994 | | | | |
| LOC90113 | | | | |
| MLXIPL | | | | |
| NEUROD1 | | | | |
| NLF2 | | | | |
| PAP2D | | | | |
| PNMA2 | | | | |
| PPP2R2B | | | | |
| PTPRN2 | | | | |
| RAB26 | | | | |
| RGS4 | | | | |
| RIMBP2 | | | | |
| RTN1 | | | | |
| RUNDC3A | | | | |
| RYR1 | | | | |
| SERPINE2 | | | | |
| SERPINI1 | | | | |
| SLC35F4 | | | | |
| SLC7A14 | | | | |
| SLC7A2 | | | | |
| ST6GALNAC5 | | | | |
| STMN2 | | | | |
| STMN2 | | | | |
| TMEFF2 | | | | |
| STMN2 | | | | |
| STMN2 | | | | |
| TUBA4A | | | | |
| VGF | | | | |

| SYMBOL | 1 | 2 | 3 | 4 |
|---|---|---|---|---|
| AGT | | | | |
| AIF1 | | | | |
| ALDH1A1 | | | | |
| ALDH1A1 | | | | |
| APLP1 | | | | |
| APOC3 | | | | |
| BEX2 | | | | |
| BSN | | | | |
| C1orf173 | | | | |
| CD36 | | | | |
| CDK5R2 | | | | |
| CELSR3 | | | | |
| CHGA | | | | |
| CKMT1A | | | | |
| CLDN14 | | | | |
| CNIH2 | | | | |
| CPE | | | | |
| CRMP1 | | | | |
| DLL3 | | | | |
| DNAJC12 | | | | |
| DNAJC12 | | | | |
| DNAJC12 | | | | |
| DPP4 | | | | |
| ELOVL4 | | | | |
| EPB41L3 | | | | |
| FLJ37366 | | | | |
| GARNL4 | | | | |
| GFRA3 | | | | |
| GNG4 | | | | |
| GPX3 | | | | |
| GRIN3A | | | | |
| GUCA2B | | | | |
| HAMP | | | | |
| HEPACAM2 | | | | |
| HTRA1 | | | | |
| IL13RA2 | | | | |
| KCNT2 | | | | |
| KIAA1244 | | | | |
| KIF12 | | | | |
| KIF5C | | | | |
| LDB2 | | | | |
| LHFPL4 | | | | |
| LOC150297 | | | | |
| LOC400120 | | | | |
| LOC644844 | | | | |
| LOC652377 | | | | |
| LOC731835 | | | | |
| LOC732150 | | | | |
| LOXL4 | | | | |
| LYSMD2 | | | | |
| MAOA | | | | |
| MARCH4 | | | | |
| NRCAM | | | | |
| PAPSS2 | | | | |
| PCSK1N | | | | |
| PDK4 | | | | |
| PGA3 | | | | |
| PYY | | | | |
| QPCT | | | | |
| RAB3C | | | | |
| RAP1GAP | | | | |
| RASD1 | | | | |
| SEC11C | | | | |
| SEPT5 | | | | |
| SERPINI1 | | | | |
| SLC32A1 | | | | |
| SLC6A4 | | | | |
| SLC8A2 | | | | |
| SMARCA2 | | | | |
| STXBP1 | | | | |
| SVOP | | | | |
| TAGLN3 | | | | |
| TMEM145 | | | | |
| TMEM22 | | | | |
| TSPAN7 | | | | |
| UNC5A | | | | |
| VSTM2L | | | | |

| SYMBOL | 1 | 2 | 3 | 4 |
|---|---|---|---|---|
| A1CF | | | | |
| A1CF | | | | |
| ABCB1 | | | | |
| ACAT1 | | | | |
| ADAMTSL2 | | | | |
| ANXA10 | | | | |
| AP3B2 | | | | |
| AQP10 | | | | |
| ARRDC4 | | | | |
| ARRDC4 | | | | |
| ASCL2 | | | | |
| ATP2A3 | | | | |
| BGN | | | | |
| BP397135 | | | | |
| BX117204 | | | | |
| C11orf70 | | | | |
| C14orf132 | | | | |
| C21orf58 | | | | |
| C3orf14 | | | | |
| C8B | | | | |
| CACNA1H | | | | |
| CAMK2B | | | | |
| CDH10 | | | | |
| CHST9 | | | | |
| CLDN11 | | | | |
| CPB1 | | | | |
| CPLX1 | | | | |
| CRH | | | | |
| CXorf57 | | | | |
| DCX | | | | |
| DNAJC12 | | | | |
| DPP6 | | | | |
| DUSP26 | | | | |
| ESRRG | | | | |
| F10 | | | | |
| FAM174B | | | | |
| FAM46A | | | | |
| FAM46C | | | | |
| FAM62A | | | | |
| FBXL16 | | | | |
| FFAR2 | | | | |
| FLJ25404 | | | | |
| FLJ34367 | | | | |
| FTCD | | | | |
| FTCD | | | | |
| GABRB3 | | | | |
| GABRB3 | | | | |
| GADD45G | | | | |
| GAL | | | | |
| GALR2 | | | | |
| GC | | | | |
| GCGR | | | | |
| GCH1 | | | | |
| GCLC | | | | |
| GHRL | | | | |
| GIP | | | | |
| GNG2 | | | | |
| GPR37 | | | | |
| GRIA3 | | | | |
| HIST1H2BK | | | | |
| HIST1H2BK | | | | |
| HIST2H2AA3 | | | | |
| HIST2H2AA3 | | | | |
| HIST2H2AC | | | | |
| HLA-A | | | | |
| HSPA5 | | | | |
| IMAGE:5262734 | | | | |
| IMAGE:5263177 | | | | |
| ITPR1 | | | | |
| JAM3 | | | | |
| KCNJ11 | | | | |
| KIF1A | | | | |
| KL | | | | |
| LIMCH1 | | | | |
| LOC647322 | | | | |
| MAP6 | | | | |
| MMRN1 | | | | |

| SYMBOL | 1 | 2 | 3 | 4 |
|---|---|---|---|---|
| NAT5 | | | | |
| NCALD | | | | |
| NCALD | | | | |
| NEFM | | | | |
| NPY | | | | |
| NRCAM | | | | |
| OLFM1 | | | | |
| PARP6 | | | | |
| PAX4 | | | | |
| PCSK1 | | | | |
| PCSK1 | | | | |
| PGA3 | | | | |
| PGM5 | | | | |
| PGM5 | | | | |
| PHLDA2 | | | | |
| PIM2 | | | | |
| PNMA3 | | | | |
| PNPLA7 | | | | |
| PPP1R1A | | | | |
| PPY | | | | |
| PRG-3 | | | | |
| RGS2 | | | | |
| RHBDD2 | | | | |
| RHBDD2 | | | | |
| RNF150 | | | | |
| SCGN | | | | |
| SERPINA1 | | | | |
| SERPINA1 | | | | |
| SERPINA10 | | | | |
| SERPIND1 | | | | |
| SERPINF2 | | | | |
| SEZ6L2 | | | | |
| SEZ6L2 | | | | |
| SH3GL2 | | | | |
| SLC30A8 | | | | |
| SLC35D3 | | | | |
| SLC7A8 | | | | |
| SPANXN2 | | | | |
| SPINK1 | | | | |
| SPIRE2 | | | | |
| SPON1 | | | | |
| ST8SIA3 | | | | |
| SYN1 | | | | |
| SYT11 | | | | |
| TCEAL2 | | | | |
| TF | | | | |
| TFF3 | | | | |
| TMEM151A | | | | |
| TMEM151A | | | | |
| TMEM176A | | | | |
| TMOD1 | | | | |
| TPR | | | | |
| TSPAN7 | | | | |
| VTN | | | | |

Genes up regulated in the INS-GFP⁺ fraction in:

- 4 of 4 experiments
- 3 of 4 experiments
- 2 of 4 experiments
- 1 of 4 experiments

**Supplementary Figure 4**

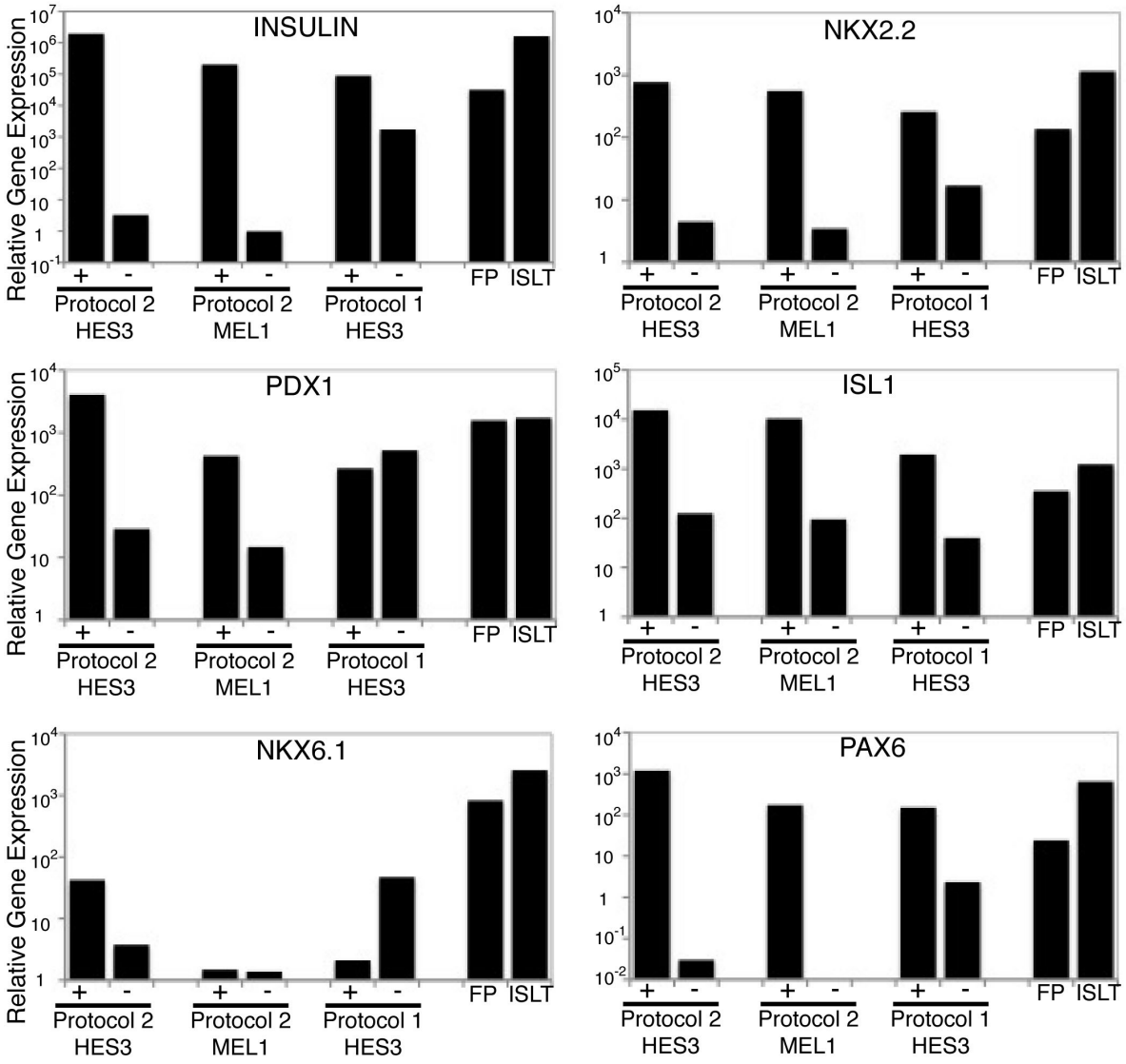

**Supplementary Figure 5**

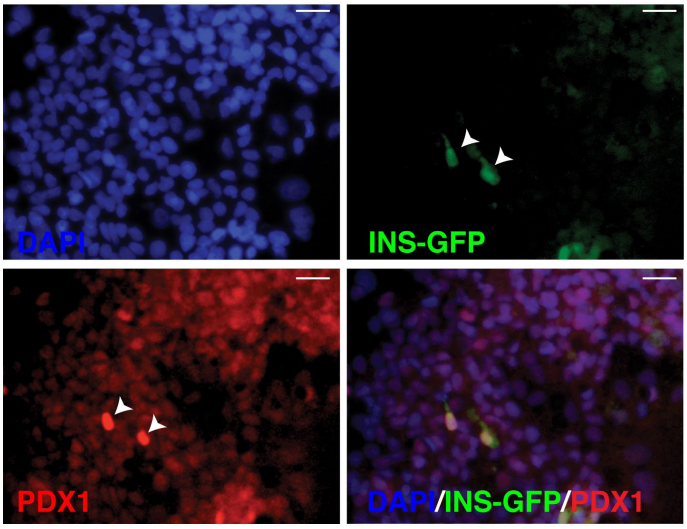

**Supplementary Figure 6**

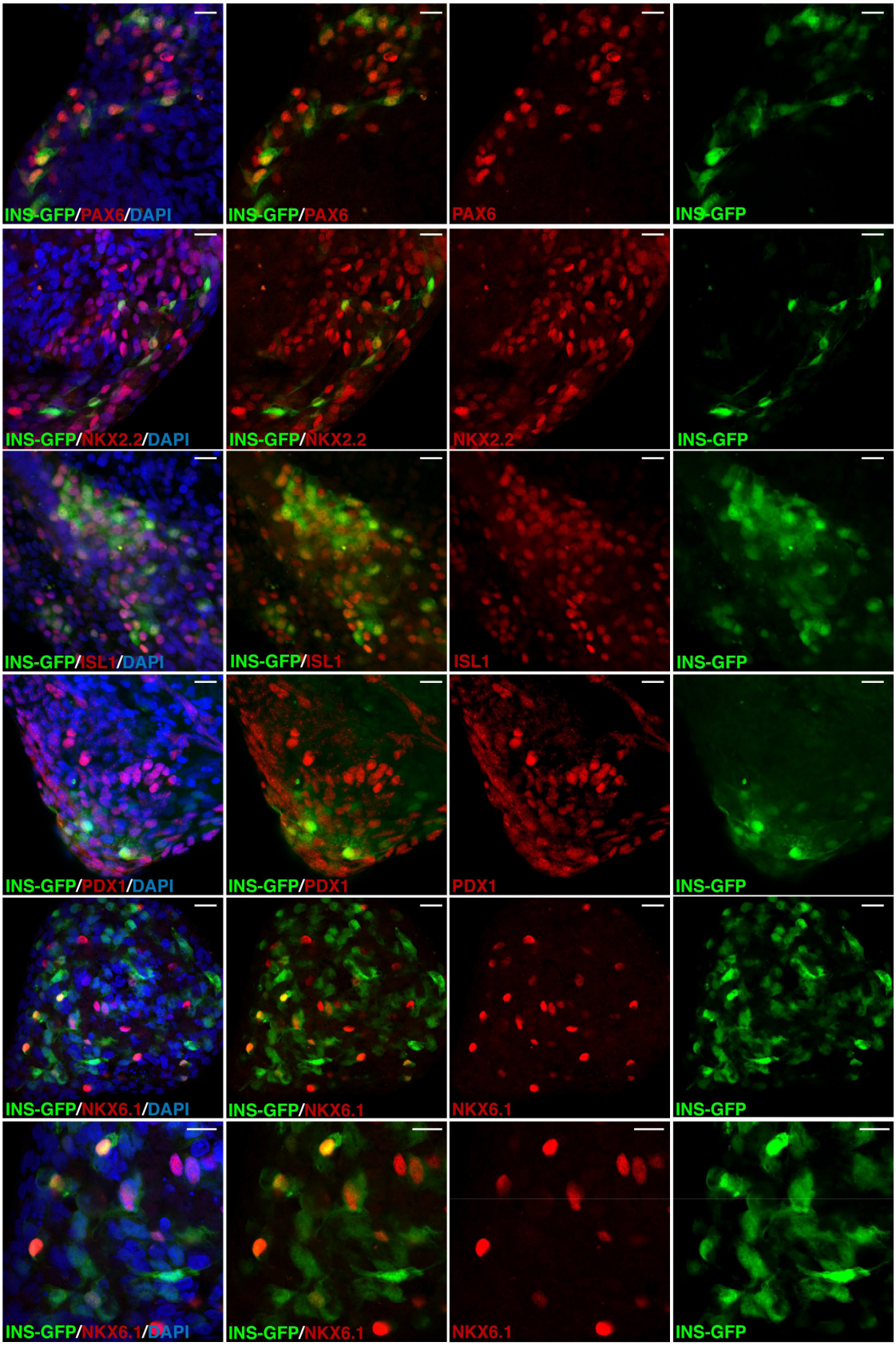

**Supplementary Figure 7**

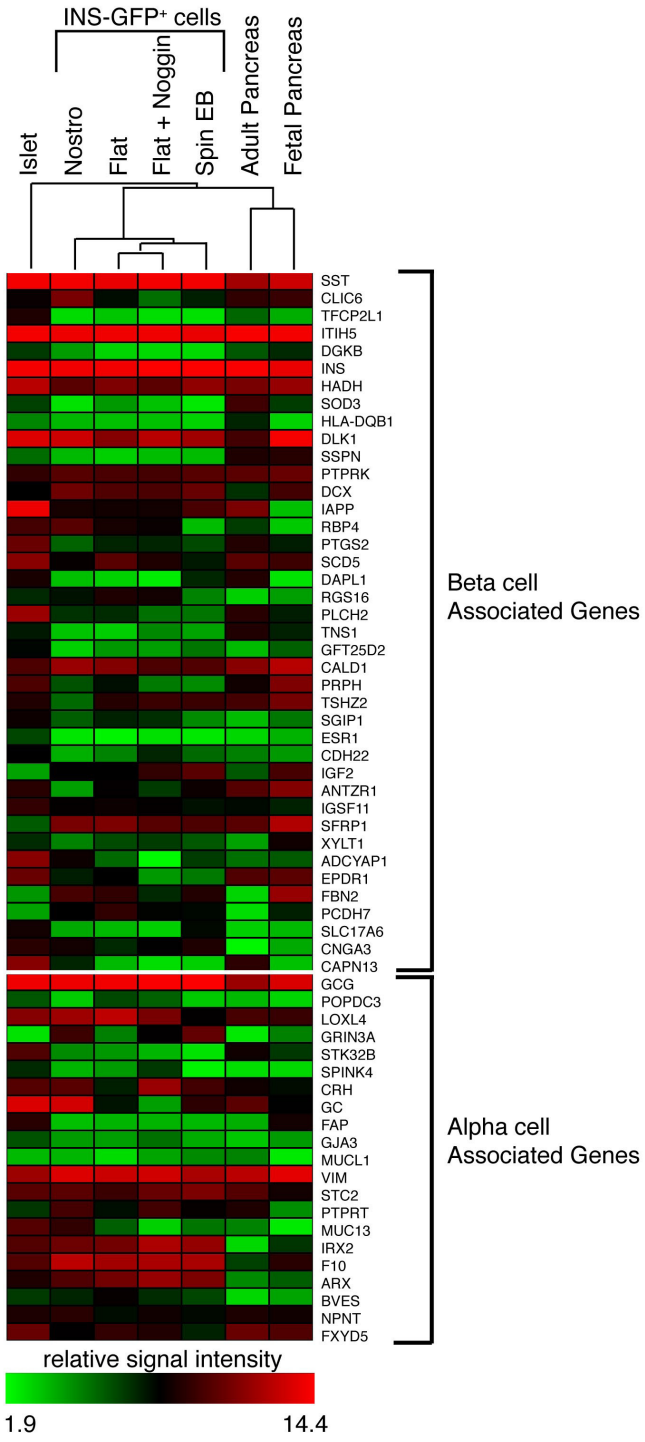

OPEN ACCESS Freely available online

PLoS one

# Differentiating Embryonic Stem Cells Pass through 'Temporal Windows' That Mark Responsiveness to Exogenous and Paracrine Mesendoderm Inducing Signals

**Steven A. Jackson[¤a¤b], Jacqueline Schiesser, Edouard G. Stanley[◔], Andrew G. Elefanty*[◔]**

Monash Immunology and Stem Cell Laboratories, Monash University, Clayton, Victoria, Australia

## Abstract

***Background:*** Mesendoderm induction during embryonic stem cell (ESC) differentiation *in vitro* is stimulated by the Transforming Growth Factor and Wingless (Wnt) families of growth factors.

***Principal Findings:*** We identified the periods during which Bone Morphogenetic Protein (BMP) 4, Wnt3a or Activin A were able to induce expression of the mesendoderm marker, *Mixl1*, in differentiating mouse ESCs. BMP4 and Wnt3a were required between differentiation day (d) 1.5 and 3 to most effectively induce *Mixl1*, whilst Activin A induced *Mixl1* expression in ESC when added between d2 and d4, indicating a subtle difference in the requirement for Activin receptor signalling in this process. Stimulation of ESCs with these factors at earlier or later times resulted in little *Mixl1* induction, suggesting that the differentiating ESCs passed through 'temporal windows' in which they sequentially gained and lost competence to respond to each growth factor. Inhibition of either Activin or Wnt signalling blocked *Mixl1* induction by any of the three mesendoderm-inducing factors. Mixing experiments in which chimeric EBs were formed between growth factor-treated and untreated ESCs revealed that BMP, Activin and Wnt signalling all contributed to the propagation of paracrine mesendoderm inducing signals between adjacent cells. Finally, we demonstrated that the differentiating cells passed through 'exit gates' after which point they were no longer dependent on signalling from inducing molecules for *Mixl1* expression.

***Conclusions:*** These studies suggest that differentiating ESCs are directed by an interconnected network of growth factors similar to those present in early embryos and that the timing of growth factor activity is critical for mesendoderm induction.

**Citation:** Jackson SA, Schiesser J, Stanley EG, Elefanty AG (2010) Differentiating Embryonic Stem Cells Pass through 'Temporal Windows' That Mark Responsiveness to Exogenous and Paracrine Mesendoderm Inducing Signals. PLoS ONE 5(5): e10706. doi:10.1371/journal.pone.0010706

**Editor:** Sui Huang, University of Calgary, Canada

**Received** January 25, 2010; **Accepted** April 26, 2010; **Published** May 19, 2010



**Funding:** This work was supported by the National Health and Medical Research Council (NHMRC) of Australia, the Juvenile Diabetes Research Foundation (JDRF) and the Australian Stem Cell Centre (ASCC). AGE and EGS are Senior Research Fellows of the NHMRC. The funders had no role in study design, data collection and analysis, decision to publish, or preparation of the manuscript.

**Competing Interests:** The authors have declared that no competing interests exist.

* E-mail: andrew.elefanty@med.monash.edu.au

◔ These authors contributed equally to this work.

¤a Current address: Biotechnology Center, University of Wisconsin, Madison, Wisconsin, United States of America
¤b Current address: Regenerative Biology, Morgridge Institute for Research, Madison, Wisconsin, United States of America

## Introduction

The in vitro differentiation of embryonic stem cells (ESCs) represents an accessible system for analyzing parameters influencing the early stages of lineage specification and commitment. During differentiation, ESCs pass through a series of developmental milestones that mirror those traversed by cells within the embryo [1 3]. For example, gene-profiling experiments indicate that differentiating mouse ESCs sequentially express genes marking successive stages of embryonic development, including *Oct4* and *Sox2* (inner cell mass), *Fgf5* (epiblast) and *Brachyury, Mixl1* and *Gsc* (primitive streak) [2]. Following the expression of these genes, induction of markers representing differentiated cell types can be observed, such as *Pdx1* (foregut endoderm), *Nkx2-5* (cardiac mesoderm) and βH1 *globin* (yolk sac erythroid cells) [2]. Thus, parallels exist between the differentiation pathways used by ESCs in vitro and the developmental roadmap followed by cells during the early stages of embryogenesis [4].

Not only is there a correspondence between the developmental pathways followed by cells in vitro and in vivo, but there is a similar concordance between the factors that induce and pattern ESCs and the embryo during differentiation. For example, induction of the primitive streak, the structural harbinger of mesendoderm formation in the embryo, requires the activity of a number of secreted growth factors (reviewed in [5]). Specifically, embryos lacking BMP4, Wnt3, nodal or their receptors, display gastrulation and mesendoderm patterning defects [6 14]. Similarly, in vitro studies on ESCs indicate that stimulation by these ligands initiates mesendoderm formation, as evidenced by the expression of primitive streak markers *Brachyury*, *Mixl1* and

*Goosecoid* [15 18]. Indeed, inhibitor studies have demonstrated that Wnt and Activin (nodal) signalling is absolutely required for this process, indicating that fundamental parallels exist between the differentiation of early embryonic cell types in vitro and in vivo [16,18 20].

In this study we determined the periods within which BMP4, Wnt3a and Activin A induced mesendoderm in differentiating mouse ESCs. These factors acted during discrete 'temporal windows' to induce expression of a GFP reporter gene targeted to the locus of the primitive streak gene, *Mixl1*. We demonstrated that endogenously produced factors propagated paracrine mesendodermal inducing signals through embryoid bodies (EBs). Finally, we observed that the differentiating cells passed through 'exit gates' after which point they were no longer dependent on signalling from inducing molecules for *Mixl1* expression. Overall, our study suggests that growth factor regulatory loops similar to those present in early embryos also exist within EBs. The timing of growth factor activity is critical for the initiation of mesendoderm formation from ESCs and paracrine signalling contributes to mesendoderm development.

## Results

### Maximal mesendoderm inducing activity of BMP4, Activin A and Wnt3a occurs within discrete temporal windows

We utilised a genetically modified mESC line, *Mixl1*$^{GFP/w}$ [17], in which sequences encoding GFP were inserted into one allele of *Mixl1*, a gene whose expression is restricted to the mesendodermal precursors of the primitive streak [21,22]. GFP acts as a surrogate marker for expression of Mixl1, and indicates the emergence of nascent mesoderm and endoderm from differentiating ESCs.

In order to identify the period during differentiation when cells were responsive to mesendoderm inducing growth factors. *Mixl1*$^{GFP/w}$ ESCs were differentiated in a chemically defined medium (CDM) [23] supplemented with BMP4 for 24 h, with the time of initial addition to the culture staggered at daily intervals from d0 to d4 (Figure 1A). At the end of each 24 h period, the BMP4-supplemented medium was removed and the EBs left to differentiate further in fresh medium without growth factor. The cells were analysed for GFP expression by flow cytometry at d5, since the highest percentage of GFP$^+$ cells were observed on this day, and expression rapidly waned thereafter. This was consistent with observations that GFP maturation and fluorescence lagged behind the peak of *Mixl1* mRNA expression that was maximal at d4 of differentiation [17,24]. These experiments revealed that BMP4 most effectively induced expression of GFP from the *Mixl1* locus (denoted Mixl1GFP) when present in the cultures from d1 2 (63.2±2.6%; mean±sd of GFP$^+$ cells from 3 independent experiments) and d2 3 (44.2±9.6%) (Figure 1B). Experiments in which the timing of BMP4 addition was offset by 12 h (Figure 1A) indicated that peak induction of Mixl1GFP$^+$ cells was observed when BMP4 was added from d1.5 2.5 (55.8±4.6%). A lower frequency of GFP$^+$ cells was seen in d5 cultures stimulated between d2.5 and d3.5 (21.2±7.4%) (Figure 1B). Finally, very few Mixl1GFP$^+$ cells were induced by stimulating the cells from d0.5 1.5 or from d3 4. Combining these data sets suggested that cells would be maximally responsive to BMP4 between d1.5 and d3 of differentiation. This prediction was confirmed in the experiment shown in Figure 2A, in which over 85% of the cumulative total of GFP$^+$ cells was observed in cultures stimulated with BMP4 between d1.5 and d3.

A similar series of 24 h pulse experiments conducted with Wnt3a and Activin A as the differentiation stimuli defined the

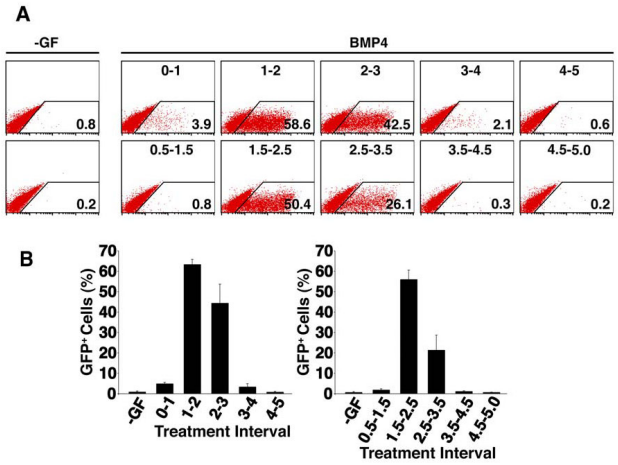


**Figure 1. Mesendoderm inducing activity of BMP4 is restricted to a specific temporal window during ESC differentiation.** (A) Flow cytometric analysis of d5 *Mixl1*$^{GFP/w}$ ESCs differentiated in cultures supplemented with 10 ng/ml BMP4 for 24 h with the time of initial growth factor addition to the culture staggered at daily intervals starting at d0 (upper panels) or day 0.5 (lower panels). The proportion of GFP$^+$ cells in this experiment is shown in the lower right of each plot. Flow cytometry profiles from no growth factor (-GF) control cultures are shown to the left of each series. (B) Histograms summarising flow cytometry data from three independent experiments, showing the average percentage of GFP$^+$ cells at d5 observed for each period of BMP4 addition. (mean±sd, $n=3$).
doi:10.1371/journal.pone.0010706.g001

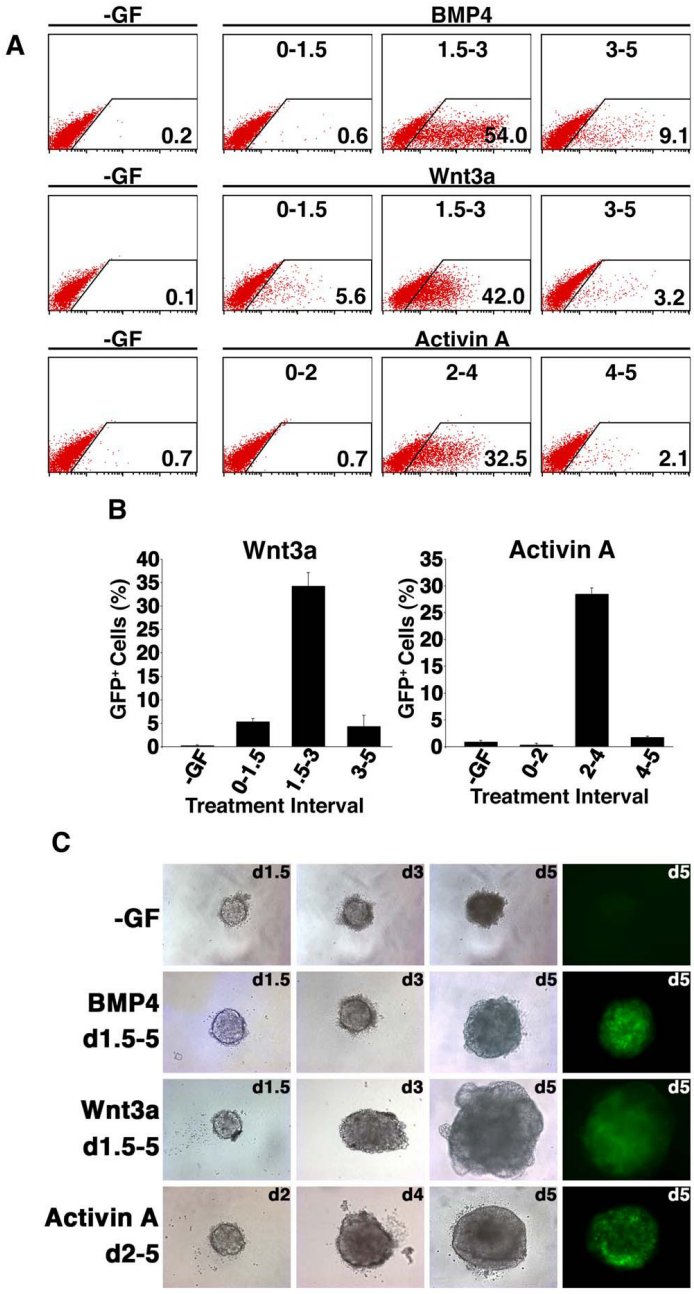
A
-GF
BMP4
0-1.5
1.5-3
3-5
0.2
0.6
54.0
9.1
-GF
Wnt3a
0-1.5
1.5-3
3-5
0.1
5.6
42.0
3.2
-GF
Activin A
0-2
2-4
4-5
0.7
0.7
32.5
2.1
B
Wnt3a
Activin A
GFP+ Cells (%)
Treatment Interval
-GF
0-1.5
1.5-3
3-5
0-2
2-4
4-5
C
-GF
BMP4
d1.5-5
Wnt3a
d1.5-5
Activin A
d2-5
d1.5
d3
d5
d2
d4

**Figure 2. Mesendoderm inducing activities of BMP4, Wnt3a and Activin A are restricted to specific temporal windows during ESC differentiation.** (A) Flow cytometry analysis at d5 of a representative experiment of *Mixl1*$^{GFP/w}$ ESCs differentiated in cultures supplemented with 10 ng/ml BMP4, 100 ng/ml Wnt3a or 100 ng/ml Activin A for the indicated time intervals (measured in days after initiation of differentiation). The proportion of GFP$^+$ cells is shown in the lower right of each plot. The flow cytometry profiles from no growth factor (-GF) control cultures are shown to the left of each series. (B) Histogram summarising flow cytometry data measuring the proportion of GFP$^+$ cells at d5 in EBs treated with Wnt3a or Activin A during the time intervals indicated (days) (mean±sd, *n* = *3*). (C) Brightfield and epifluorescence images of differentiating EBs. The growth factors and period of addition are indicated to the left of each row and day of differentiation when the image was taken in the top right hand corner of each panel. (Original magnification×100).
doi:10.1371/journal.pone.0010706.g002

optimal window for Wnt3a addition to be between d1.5 and d3 and that for Activin A to be between d2 and d4 (data not shown). On the basis of these preliminary studies, further differentiation experiments were performed in which the growth factors were included prior to, during and after the hypothesized optimal *Mixl1* induction window for each growth factor. These experiments confirmed that BMP4 and Wnt3a were most effective at inducing GFP$^+$ mesendoderm precursors when present in the cultures between d1.5 and d3 (Figure 2A, B). In contrast, Activin A most efficiently induced GFP expression when present between d2 and d4 of differentiation (Figure 2A, B). The inclusion of each growth factor during its optimal window of action also increased the size and viability of the EBs compared to EBs cultured in CDM without growth factors (Figure 2C and data not shown). The larger EB size suggests that the growth factors probably influenced cell survival and proliferation as well as differentiation. Indeed, we have previously shown that supplementation of serum free medium with BMP4 augmented the total cell number and viability of differentiating mouse ESCs, and that this effect was observed prior to the induction of GFP in *Mixl1*$^{GFP/w}$ ES cells [17]. We have argued that this may correspond to the growth-promoting effect of BMP4 on epiblast cells prior to gastrulation [6,11,12].

Similar outcomes in experiments performed with an independently targeted *Mixl1*$^{GFP/w}$ reporter ESC line, (clone Mix 114) [17], indicated that the temporal windows delineated in this study for each growth factor were not specific for a single ESC line (Figure S1). Nevertheless, because the two *Mixl1*$^{GFP/w}$ clones were derived from the same parental ESC line, we cannot rule out the possibility that different strains of ESCs might vary in their propensity to differentiate. However, in our experience, ESC lines generally respond to growth factors in a similar manner, with the main differences being in the concentration of factors required for the development of specific cell types (Elizabeth Ng, EGS and AGE, unpublished results).

Even in our relatively well defined, short-term differentiation experiments, we observed that, at best, 60 70% of cells expressed GFP from the *Mixl1* locus, and that the variable fluorescence intensity observed indicated that not all Mixl1GFP expressing cells were identical. Interestingly, we have previously observed that this heterogeneity for Mixl1GFP expression is more evident within individual EBs than between EBs [17]. In other words, most EBs express Mixl1GFP but not all cells in each EB express GFP.

## Interdependence of signalling pathways in mesendoderm induction

We sought to determine whether all three growth factor signalling pathways were required for GFP induction in differentiating *Mixl1*$^{GFP/w}$ cells. In the first instance, we examined the effects of adding inhibitors for Wnt and TGF-beta pathways on the ability of each ligand to induce MixlGFP expressing cells. ESCs were treated with BMP4 or Wnt3a from d1 or with Activin A from d2, because preliminary experiments showed that addition of this factor prior to d2 inhibited ESC mesendoderm differentiation (data not shown). Inhibitors of BMP4- (noggin), Activin receptor- (SB 431542) or canonical Wnt- (Dkk-1) signalling were added to the cultures at the same time as the growth factors. Cultures were analysed at differentiation d5 for expression of GFP by flow cytometry.

As anticipated, addition of a compound that inhibited the signalling pathway of the inducing agent completely ablated subsequent GFP-expression (Figure 3A). However, the Activin signalling inhibitor SB 431542 blocked GFP induction by all of the growth factors, underlining the pivotal role nodal signalling plays in mesendoderm formation [16,18]. Somewhat unexpectedly, addition of noggin to Wnt3a treated cultures consistently suppressed induction of GFP-expressing cells by about 50% (Figure 3A, B), suggesting that endogenously produced BMP activity synergised with the exogenously added Wnt3a. In contrast, noggin had no impact on the frequency of GFP$^+$ cells observed in d5 cultures which had been treated with Activin A (Figure 3A, B). The addition of Dkk-1 substantially reduced but did not eliminate subsequent induction of GFP$^+$ cells in BMP4 treated cultures, and, in agreement with the results of others, *Mixl1* induction was obviated by Dkk-1 treatment of Activin A induced cultures (Figure 3A, B) [16].

In order to investigate the ligands endogenously produced by differentiating ESCs, PCR analysis was performed on cDNA synthesized from d3 EBs differentiated in the presence of either BMP4, Wnt3a or Activin A. This survey focused on genes encoding factors that previous gene profiling experiments had shown were expressed during ES differentiation [2]. BMP4 induced expression of *Wnt3*, *Wnt8a* and *nodal*, factors that may have contributed to endogenously produced signals inhibited by Dkk-1 or SB 431542 (Figure 3C). Likewise, d3 cells that had been treated with Wnt3a produced transcripts representing *BMP4*, *Wnt3*, *Wnt8a* and *nodal* (Figure 3C). The presence of *BMP4* transcripts in these samples may explain the suppressive effect of noggin on the frequency of Mixl1GFP$^+$ cells induced by Wnt3a (Figure 3A, B). A similar analysis performed on d3 samples of Activin A treated cells revealed low levels of transcripts representing *Wnt3*, *Wnt8a* and *nodal*.

Real time PCR analysis confirmed the observation that both BMP4 and Wnt3a were able to induce substantial expression of *BMP4*, *Wnt3* and *nodal*. Activin A, only present for 24 hours at this time point, predominantly promoted the up regulation of *Wnt3* and *nodal*, with *BMP4* expression retained at similar levels to those observed in unstimulated cells (Figure 3D).

## Endogenously produced growth factors provide paracrine mesendoderm inducing signals in differentiating embryoid bodies

These results implied that endogenously produced BMP, Wnt and Activin-like molecules might play an important role during mesendoderm induction during ESC differentiation in vitro by complementing the actions of exogenously applied growth factors. To directly assay the paracrine mesendoderm inducing ability of these endogenous factors, we performed mixing experiments in which wild type *Mixl1*$^{w/w}$ ESCs differentiated for 3d in the

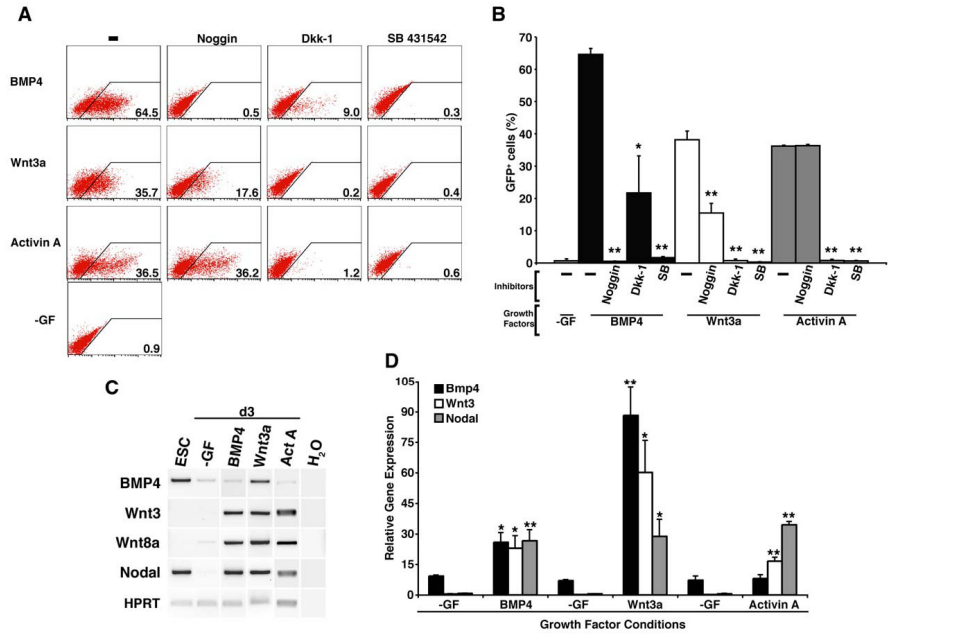


**Figure 3. Induction of maximal proportions of GFP$^+$ *Mixl1*$^{GFP/w}$ cells requires signalling via BMP, Wnt and Activin receptor pathways.** (A) Flow cytometry analysis at d5 of a representative experiment of *Mixl1*$^{GFP/w}$ ESCs differentiated in cultures supplemented with BMP4 (d1–d5), Wnt3a (d1–d5) or Activin A (d2–d5) alone or in the presence of the signalling pathway inhibitors noggin, Dkk-1 or SB 431542. Growth factors are shown to the left of each row and inhibitors are shown at the top of each column. Flow cytometry profiles obtained from control cells with no growth factor added (-GF) are shown in the bottom left panel. The percentage of GFP$^+$ positive cells is recorded in the bottom right corner of each plot. (B) Histogram summarising flow cytometry data measuring the proportion of GFP$^+$ cells at d5 in EBs treated with BMP4, Wnt3a or Activin A with and without inhibitors. (mean±sd, $n=3$) (* $p<0.05$, ** $p<0.01$ compared to cells not receiving inhibitor). SB; SB 431542. (C) Semi-quantitative RT-PCR analysis of growth factor gene expression in cells from d3 cultures stimulated with BMP4 (d1–d3), Wnt3a (d1–d3) or Activin A (d2–d3). The samples are indicated at the top of each column and the growth factor genes analysed on the left of each row. ESC; undifferentiated ESCs, -GF; no growth factor, Act A; Activin A, $H_2O$; no template control. (D) Real time PCR analysis of *BMP4*, *Wnt3* and *nodal* gene expression at d3 in ESCs differentiated in the presence of BMP4 (d1.5–d3), Wnt3a (d1.5–d3) and Activin A (d2–d3). (mean±sem, $n=3$). (* $p<0.05$, ** $p<0.01$ compared to samples collected from cells differentiated in the absence of growth factor.)
doi:10.1371/journal.pone.0010706.g003

presence of mesendoderm inducing factors were aggregated with *Mixl1*$^{GFP/w}$ cells that were derived from EBs differentiated for 3d in the absence of exogenous factors, to form chimeric EBs (Figure 4A). These chimeric spin EBs were left to differentiate for a further 2d in the absence of exogenous growth factors. We hypothesized that the wild type 'stimulator' EBs would differentiate towards mesendoderm in response to the growth factors during the first 3d but that the *Mixl1*$^{GFP/w}$ 'responder' EBs, cultured in the absence of stimulation, would not. Following the final 2d of differentiation as chimeric EBs, any mesendoderm inducing signal produced by the 'stimulator' cells transferred to the 'responder' *Mixl1*$^{GFP/w}$ cells would be read out as an induction of GFP$^+$ cells by flow cytometry at d5. We chose the period of growth factor stimulation to include at least part of the optimal windows of response to BMP4, Wnt3a and Activin A. Furthermore, based on our earlier results, we argued that the period of chimeric EB differentiation (d3 d5) fell outside the window of optimal responsiveness of the EBs to direct BMP4 or Wnt3a induction of Mixl1GFP$^+$ cells.

Analysis of Mixl1GFP expression in the chimeric EBs showed that, in the absence of exogenously added growth factors to the 'stimulator' cultures, no GFP$^+$ cells were observed in the chimeric EBs at d5 (Figure 4B, C). Conversely, wild type *Mixl1*$^{w/w}$ ESCs differentiated for 3d in the presence of BMP4 or Wnt3a produced a mesendoderm-inducing signal that stimulated the 'responder' *Mixl1*$^{GFP/w}$ cells to induce GFP (Figure 4B, C). On average, 10.2±4.6% and 10.2±7.2% Mixl1GFP$^+$ cells were observed in d5 chimeric EBs that included wild type cells stimulated from d0 d3 by BMP4 and Wnt3a respectively. Given that only ~50% of the cells in each chimeric EB were 'responder' *Mixl1*$^{GFP/w}$ cells, these data argue that ~20% of these cells upregulated *Mixl1* and expressed GFP in response to the co-cultivation with growth factor stimulated wild type ESCs. However, Activin A treated 'stimulator' wild type ESCs were not able to induce GFP expression in 'responder' *Mixl1*$^{GFP/w}$ cells (Figure 4B, C), perhaps reflecting the relatively low levels of growth factor gene expression observed in d3 EBs that had been stimulated with Activin A for only 24 hours (Figure 3C, D).

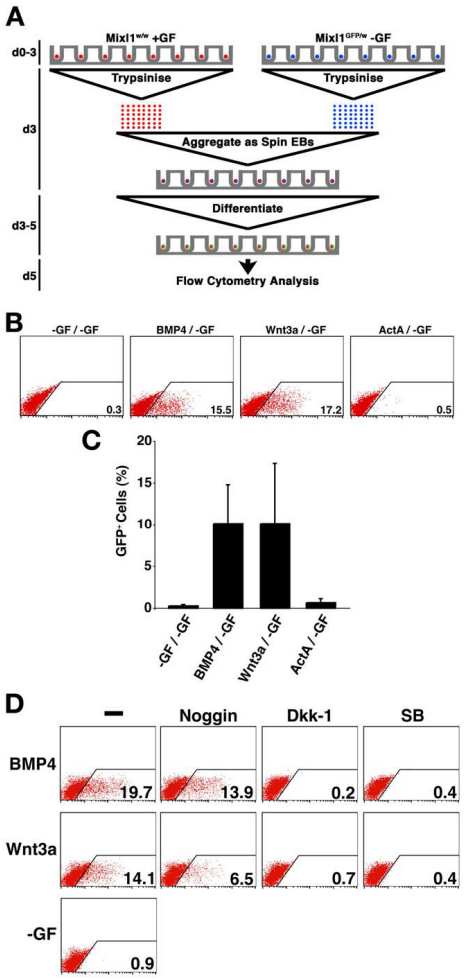


**Figure 4. ES Cells differentiated in response to BMP4 or Wnt3a generate paracrine signals that induce GFP in *Mixl1*$^{GFP/w}$ EBs.** (A) Method used to assess the ability of 'stimulator' wild type *Mixl1*$^{w/w}$ ESCs differentiated in the presence of growth factors to induce expression of GFP in 'responder' *Mixl1*$^{GFP/w}$ ESCs differentiated in absence of exogenous growth factors. After 3d of differentiation, both 'stimulator' and 'responder' EBs were disaggregated and chimeric spin EBs formed by re-aggregating 'stimulator' and 'responder' cells in a 1:1 ratio. After allowing differentiation to proceed for a further 2d in the absence of growth factors the chimeric EBs were harvested for analysis. (B) Flow cytometry analysis of d5 chimeric EBs. The growth factors used for the 'stimulator' and 'responder' cultures for the initial 3d of differentiation are shown above each panel of a representative experiment (stimulator/responder). All 'responder' differentiations were performed in the absence of added growth factors (/-GF). The flow cytometry profiles obtained using 'stimulator' cells not exposed to growth factor (-GF/-GF) are shown as a negative control. The percentage of GFP$^+$ cells is shown. (C) Histogram summarising the flow cytometry data at d5 (mean ±sd, $n = 3$). (D) Flow cytometry analysis of d5 chimeric EBs formed by aggregating growth factor stimulated wild type *Mixl1*$^{w/w}$ with unstimulated *Mixl1*$^{GFP/w}$ differentiating ESCs at d3. At the time of aggregation, inhibitors of BMP (noggin), canonical Wnt (Dkk-1) and Activin receptor (SB 431542) signalling were added to the cultures. Growth factors used to stimulate the wild type ESCs from d0–d3 are shown to the left of each row. Inhibitors are shown at the top of each column. Flow cytometry profiles obtained with cells from the no growth factor (-GF) control cultures are shown. The percentage of GFP$^+$ positive cells is recorded in the bottom right corner of each plot. SB; SB 431542.
doi:10.1371/journal.pone.0010706.g004

In order to dissect the requirements for BMP4, Wnt and Activin signaling pathways in the transfer of mesendoderm inducing signals, the effects of adding inhibitors of these pathways at the time of chimeric EB re-aggregation (at d3) was assessed. In the absence of inhibitors, wild type 'stimulator' ESCs treated with BMP4 or Wnt3a between d1 d3 effectively induced GFP expression in 'responder' *Mixl1*$^{GFP/w}$ cells (Figure 4D). Inclusion of Dkk-1 or SB 431542 completely abrogated transfer of the mesendoderm-inducing signal from the growth factor treated 'stimulator' cells to the *Mixl1*$^{GFP/w}$ 'responder' ESCs, indicating that signaling via these pathways was absolutely required (Figure 4D). In addition, noggin treatment of the chimeric EBs also diminished the frequency of GFP$^+$ cells seen in the 'responder' *Mixl1*$^{GFP/w}$ ESCs (Figure 4D). This argued that BMP signalling still played a role in paracrine stimulation of mesendoderm formation, even though, by itself, BMP4 was a poor inducer of mesendoderm after d3. The failure of noggin to completely abrogate the induction of GFP expression confirmed that factors in addition to BMP4 mediated the paracrine signal transfer (compare Figure 4D with Figure 3A).

## BMP, Wnt and Activin signaling are required after d3 to maintain mesendoderm gene expression

Results of studies presented thus far suggested that the window during which BMP4 and Wnt3a efficiently induced GFP expression in *Mixl1*$^{GFP/w}$ cells closed soon after d3, consistent with the observation that addition of these growth factors after this time did not recruit many new cells into the mesendoderm differentiation program. However, this scenario did not exclude an ongoing requirement for active signaling past d3 for maximal GFP induction and/or maintenance in cells that had already committed to mesendoderm formation, a possibility raised by the effects of signaling pathway inhibitors on paracrine mesendoderm signals shown in Figure 4.

Therefore, experiments were performed to examine the requirement for BMP, Wnt and Activin signaling after an initial period of mesendoderm induction by each growth factor. *Mixl1*$^{GFP/w}$ cells were differentiated until d3 in the presence of BMP4 or Wnt3a (both added at d1) or Activin A (added d2). At d3, the factors were removed and cells differentiated for a further two days in the presence or absence of inhibitors affecting each pathway (Figure 5A). Gene expression analysis indicated that by d3, cells treated with BMP4 and Wnt3a had up-regulated expression of the pan-mesendodermal markers, *Brachyury* and *Mixl1*, the anterior mesendodermal genes *Goosecoid* and *FoxA2* and the visceral and definitive endodermal marker *Sox17* (Figure 5C and real time PCR data shown in Figure S2). In the case of *Mixl1*, this expression at d3 translated into a substantial fraction of GFP$^+$ cells by d5 (Figure 5A, B). However, much lower levels of *Mixl1* and *Brachyury* were expressed by d3 in response to Activin A, which was only present in these experiments for 24 h (Figure 5C and

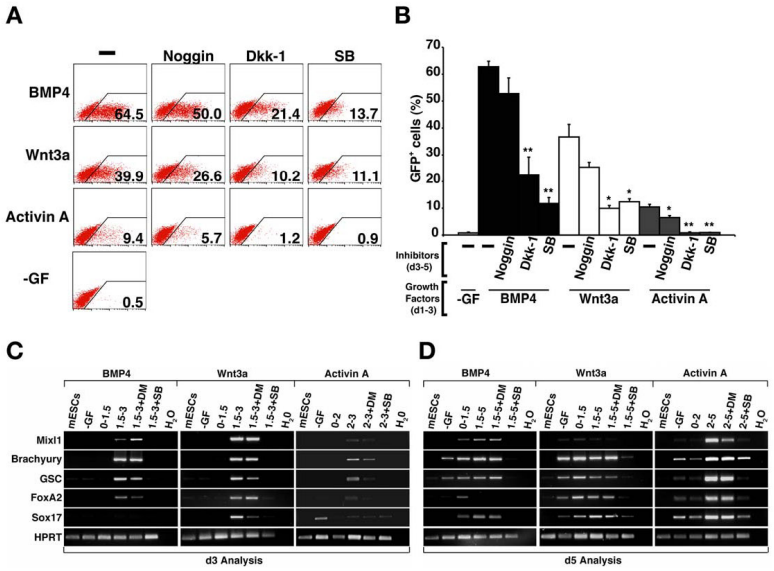


**Figure 5. BMP4, Wnt and Activin signalling are required after d3 for maximal GFP induction from *Mixl1*$^{GFP/w}$ EBs.** (A) Flow cytometry analysis of GFP expression in d5 *Mixl1*$^{GFP/w}$ EBs stimulated with BMP4 (d1–3), Wnt3a (d1–3) or Activin A (d2–3) and subsequently treated from d3–5 with the inhibitors noggin, Dkk-1 or SB 431542. SB; SB 431542. (B) Histogram summarising d5 flow cytometry data (mean±sd, $n=3$) (* $p<0.05$, ** $p<0.01$ compared to cells not receiving inhibitor). SB; SB 431542. (C, D) Gene expression analysis of (C) d3 and (D) d5 differentiating mESCs treated with exogenous BMP4, Wnt3a and Activin A. The growth factor and treatment days are indicated across the top of each sample. Samples to which the Activin signalling inhibitor SB 431542 was added are indicated (SB), as are control samples that were treated with DMSO carrier (DM). The genes analysed are shown on the left hand side of each row.
doi:10.1371/journal.pone.0010706.g005

Figure S2). This correlated with the induction of GFP expression in only ~10% of cells by d5, a proportion that represents only ~30% of the d5 expression observed when Activin was included from d2 d4.

In all cases, inclusion of either noggin, Dkk-1 or SB 431542 at d3 reduced the proportion of GFP$^+$ cells at d5 to varying degrees, suggesting that ongoing signaling through all of the pathways was required for maximal mesendoderm formation in response to each inducing growth factor. However, differences were observed in the patterns of GFP expression that largely depended upon the inhibitor that was used. In cells stimulated for 3d by BMP4, inclusion of noggin at d3 reduced the frequency of GFP$^+$ cells by ~20% (from 67.8±2.0% to 52.7±5.9%) whilst Dkk-1 and SB 431542 reduced the proportion of GFP expressing cells by ~70% (from 67.8±2.0% to 22.3±6.9%) and ~80% (from 67.8±2.0% to 11.7±2.3%) respectively (Fig. 5B). Similarly, in the case of cells stimulated by Wnt 3a or Activin A, the greatest reduction in the fraction of GFP$^+$ cells was seen following addition of Dkk-1 and SB 431542 (~75% and ~90% respectively), whilst a lesser reduction in the proportion of GFP$^+$ cells was observed in response to treatment of cells at d3 with noggin (~35%) (Figure 5B). Interestingly, for cells stimulated by either BMP4 or Wnt3a, inclusion of the SB 431542 inhibitor at d3 only partially inhibited the appearance of GFP$^+$ cells at d5 compared with results obtained when the inhibitor was included from the onset of the differentiation, which completely suppressed induction of Mixl1GFP$^+$ cells (see Figure 3B). This indicated that a proportion of d5 Mixl1GFP$^+$ cells were committed to mesendoderm formation by d3 and no longer dependent upon nodal signaling during the last 2 days of differentiation.

Examination of gene expression at d5 demonstrated that *Mixl1* RNA had begun to wane in cells stimulated by BMP4 or Wnt3a (Figure 5D). Conversely, d5 *Mixl1* expression was increased over d3 levels in Activin A stimulated cultures, illustrating differences in the kinetics of *Mixl1* induction. *Brachyury*, *Goosecoid*, *FoxA2* and *Sox17* were also expressed at higher levels in d5 Activin A stimulated samples. In all these cases, including the inhibitor SB 431542 significantly reduced gene expression, confirming that induction was dependent upon Activin A/nodal signaling. These trends in gene expression induced in response to BMP4, Wnt3a and Activin A stimulation were confirmed in an independent series of experiments (Figure S2).

The observation that Dkk-1 addition at d3 prevented the emergence of GFP$^+$ cells in EBs stimulated with Activin A, suggested that endogenously produced Wnt ligands were necessary for Activin A to recruit cells to mesendoderm formation, even after the window for optimal Wnt3a induction of *Mixl1* expression appeared to have passed. A corollary of this hypothesis would be that Wnt3a might synergise with Activin A in the induction of mesendoderm after d3. To test this hypothesis, we analysed the induction of *Mixl1* in response to combinations of growth factors added to cells at d3. Consistent with our earlier results, these

experiments confirmed that Wnt3a and BMP4 were poor inducers of GFP expression at d3, but that treatment of d3 cells with Activin A resulted in ~30% GFP expressing cells at d5 (Figure 6A, B). Furthermore, there was no evidence for synergy between BMP4 and Wnt3a or BMP4 and Activin A added at d3 since the frequency of $GFP^+$ cells was no higher than that observed by treating the cells with the single factors. However, addition of Wnt3a together with Activin A consistently resulted in a higher proportion of $GFP^+$ cells (42.6±4.7%) than that seen with either ligand alone (2.0±0.7% for Wnt3a and 29.6±6.3% for Activin A) and higher than that predicted by addition of contributions representing the individual factors (Figure 6A, B). The inclusion of all three factors did not further increase the percentage of GFP expressing cells. These results suggest a second function for Wnt signaling as a necessary but not sufficient component in the late induction or maintenance of $GFP^+$ mesendoderm distinct from its role as a direct inducer of early mesendoderm formation.

## Discussion

Before discussing the specific findings of this study in detail, it is valuable to place our results into a historical context, by relating our work to earlier studies that identified the nexus between ESCs and germ cell tumours. Benign germ cell tumours (teratomas) comprise mixtures of many different adult tissue types, whilst their malignant counterparts (teratocarcinomas) also include persistent undifferentiated stem cell components, termed embryonal carcinoma cells (ECCs) [25]. A number of excellent reviews over the years have covered this topic and the reader is referred to these for more complete descriptions of the research [25 28]. The concept that the multiple differentiated cell lineages found in teratomas might be derived from a single cell type was proposed over 100 years ago [29]. However, it was not until the 1950s, when Stevens and Little observed that inbred strain 129 mice developed spontaneous testicular teratomas, that there was an opportunity to systematically study these interesting tumours [30]. Stevens noted that teratocarcinomas maintained as an ascites tumour formed "thousands of free floating embryoid bodies similar to mouse embryos 5 and 6 days of age in the peritoneal fluid." [31]. In a technical tour de force, Kleinsmith and Pierce dissociated small embryoid bodies (which contained a high proportion of undifferentiated ECCs) from an ascites tumour and transplanted single cells intraperitoneally, successfully generating clonal tumorigenic ECC lines [32]. The ability of these clonal tumours to differentiate into many different tissue types formally demonstrated the multipotentiality of the ECCs. This data was complemented by the demonstration that teratocarcinoma cells cultured on irradiated feeder cells could also be cloned in vitro and that these clones were also mulipotential [33]. Martin and Evans characterised in detail the in vitro culture and differentiation of ECCs [25,26,34]. They demonstrated that undifferentiated ECCs maintained on a mitotically inactivated feeder cell layer (later recognized as a source of the differentiation inhibiting factor, LIF[35]) would form embryoid bodies when cultured for a few days in suspension in serum containing medium, and that allowing the cystic embryoid bodies to reattach to the tissue culture dish triggered further differentiation to many different tissue types, an observation confirmed by others [25,34,36]. These scientists recorded two key observations that have been borne out over subsequent decades. Firstly, they observed that tissues formed from ECCs differentiated in vitro retained a degree of structural organisation reminiscent of normal embryonic development, and secondly they noted "that the processes of cell determination and differentiation occur in defined stages which are accessible to experimental analysis and manipulation." [25,34]. Indeed, Strickland and Mahdavi later showed that retinoic acid induced parietal endoderm differentiation from F9 ECCs [37].

The link between normal embryos and teratocarcinomas had been made when Solter [38] and Stevens [39] showed that transplantation of early mouse embryos to an extrauterine site led to the development of transplantable teratocarcinomas. The eventual derivation of ESCs, which phenotypically resembled ECCs, from preimplantation mouse blastocysts in 1981 independently by Evans and Martin [40,41] shifted interest away from teratocarcinomas and ECCs and marked the beginning of the next era in pluripotent cell research, which has gained further momentum following the derivation of human embryonic stem cell lines in 1998 [42,43] and the reprogramming of somatic cells to a pluripotent state reported in 2006 [44].

We have built on these earlier observations though our investigations of the induction of mesendoderm precursors by exogenously acting growth factors in differentiating mouse ESCs. Whilst early studies proved that ECCs (and later ESCs) could differentiate to form derivatives of the germ layers, the signals initiating differentiation were provided by serum and a specific dissection of the control mechanisms was not possible. We have used a suspension, embryoid body differentiation system, in which a serum free defined medium enabled us to objectively assess the influence of specific growth factors. Our studies were also aided by the use of a genetically modified ES cell line in which the induction of *Mixl1*, a homeobox gene that marks the primitive streak of the mammalian embryo, was linked to a fluorescent reporter [17,21,45]. Whilst numerous recent studies prior to ours have identified factors that induce and pattern mesoderm and endoderm (reviewed in [46]), we have defined temporal limits that constrain this process. We have shown that ESCs pass through a series of 'windows' in which they gain and lose competence to respond to three inducers of primitive streak transcription factors, BMP4, Wnt3a and Activin A. Through a series of mixing experiments, we demonstrated that endogenously

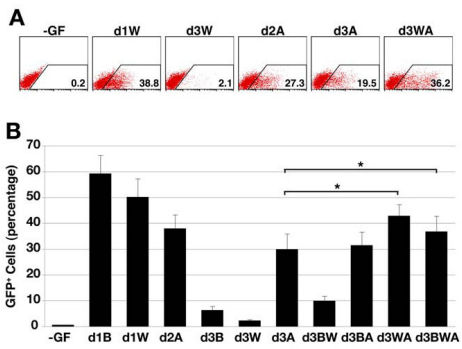


**Figure 6. Wnt3a and Activin A synergise to induce GFP in *Mixl1*$^{GFP/w}$ EBs.** (A) Flow cytometry analysis at d5 of a representative experiment of *Mixl1*$^{GFP/w}$ ESCs differentiated in cultures supplemented with 100 ng/ml Wnt3a (W) and/or 100 ng/ml Activin A (A) from the time indicated. The no growth factor (-GF) control is shown to the left. (B) Histogram summarising the d5 flow cytometry data from *Mixl1*$^{GFP/w}$ ESCs differentiated in cultures supplemented with the indicated growth factors from the time indicated. (mean±sd, $n=3$) (* $p<0.05$ compared to d3A). B; BMP4, W; Wnt3a, A; Activin A.
doi:10.1371/journal.pone.0010706.g006

generated TGF-beta - and Wnt-family growth factors induced by BMP4 and Wnt3a could propagate mesendoderm signals in differentiating EBs in a paracrine manner. Finally, we showed that a portion of the differentiating cells were committed to mesendoderm formation by d3 and did not require further signalling from inducing molecules during the last 2 days of differentiation for *Mixl1* expression.

Following the removal of the anti-differentiative signal, LIF, cells gained responsiveness to BMP4 and Wnt3a as mesendoderm inducing signals between d1.5 and d3, at a time corresponding to their upregulation of epiblast associated genes, such as *FGF5* [2]. This epiblast stage in ES cells, recently characterised by the (reversible) transition of cells from a $Rex1^{+}Oct4^{+}$ ESC phenotype to a $Rex1^{-}Oct4^{+}$ epiblast-like state [47], may be analogous to embryo derived pluripotent epiblast stem cells that are dependent on Activin and FGF signalling [48]. In this regard, our observations that Activin A treatment from day 0 to d2 maintained high levels of E-Cadherin and did not induce substantial GFP expression from $Mixl1^{GFP/w}$ cells (data not shown), were consistent with the hypothesized anti-differentiative role for nodal (which signals via the Activin receptor) during the earliest stages of differentiation [48 50]. Consistent with the hypothesis that the epiblast state correlates with BMP4 responsiveness, recent data demonstrates that differentiation of primordial germ cells from epiblast stem cells is a BMP4-dependent process [51].

From d3 of mESC differentiation, the window of competence began to close with cells no longer responding to BMP4 and Wnt signals alone, although cells remained Activin A responsive for a further day. This extended temporal window for mesendoderm induction by Activin A may reflect the prolonged role of nodal in maintaining the anterior streak at the latter stages of gastrulation [52,53]. In fact, gene expression analysis indicated that whilst both BMP4 and Wnt3a robustly induced the pan-mesendoderm markers *Brachyury* and *Mixl1* at d3, they only weakly up-regulated the anterior mesendoderm/early endoderm markers *Goosecoid*, *Foxa2*, and *Sox17*. Conversely, Activin A induced higher levels of these genes at d5 of differentiation (Figure 5 and Figure S2). These data are in accordance with the results reported by others that BMP4 and Wnt3a signals induced predominantly a posterior primitive streak mesoderm in differentiating ESCs whilst Activin A biased differentiation towards anterior primitive streak derivatives including definitive endoderm [16,18 20,54].

Our experiments illustrate the integration of signalling pathways required for induction of *Mixl1* (summarised in Figure 7A). In BMP4 stimulated cultures, transcription of *BMP4*, *Wnt3*, *Wnt8a* and *nodal* were induced and inhibition of either BMP or nodal signalling pathways eliminated Mixl1GFP expression. The consistent persistence of a residual percentage of $Mixl1GFP^{+}$ cells in the presence of Dkk-1 argued that some BMP4 mediated mesendoderm differentiation might be Wnt independent. Induction of $Mixl1GFP^{+}$ cells in Wnt3a or Activin A stimulated cultures was completely abrogated by inhibitors of either pathway. Treatment of Wnt3a-stimulated cultures with noggin consistently reduced the percentage of Mixl1GFP-expressing cells, perhaps suggesting a functional consequence of the significant level of *BMP4* transcription induced by Wnt3a. Conversely, treatment with noggin had little effect on Mixl1GFP induction by Activin A. These in vitro results contrast with findings in the embryo, in which a block in

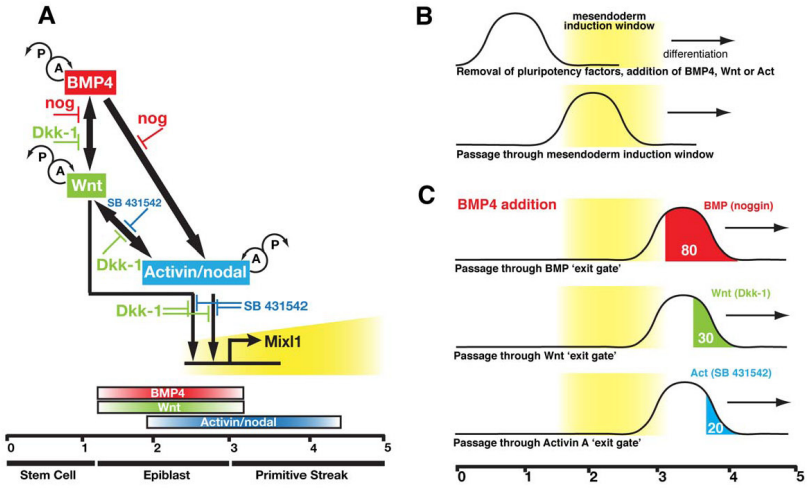


**Figure 7. Induction of *Mixl1* expression is regulated through the integration of signals from BMP, Wnt and Activin/nodal pathways.** (A) Interactions between signalling pathways and inhibitors impacting upon *Mixl1* induction. BMP4 stimulates expression of Wnt and Activin/nodal, which in turn induce *Mixl1*, perhaps acting through as yet unidentified intermediate molecules. The time periods (in days) and differentiation stages during which the differentiating ES cells are responsive to each stimulus are indicated. Probable autocrine (A) and paracrine (P) roles of the factors are indicated. (B) Removal of factors maintaining pluripotency enables ES cells to differentiate and to respond to BMP4, Wnt3a or Activin A signals delivered during a defined 'temporal window' for mesendoderm induction. (C) After cells pass through the mesendoderm window at d3, they then pass through 'exit gates' for each signalling pathway, after which time they are no longer dependent on that pathway for mesendoderm induction. In response to BMP4 addition between d1.5 and d3, the approximate percentage of cells that have passed the BMP4, Wnt3a or Activin A 'exit gates' at d3 is shown. See text for more details (Data taken from Figure 5B).
doi:10.1371/journal.pone.0010706.g007

BMP4 signalling abrogates mesoderm induction because the embryo is then unable to produce downstream Wnt and nodal, a block that can be bypassed through the addition of exogenous factors in vitro. Our results are also in general agreement with knockout studies in the mouse [7 11,14] and inhibitor experiments in ESCs [16,18 20] that indicated that Wnt and Activin signalling were essential for mesendoderm induction.

Our data demonstrating that BMP4 propagates mesendoderm-inducing signals in differentiating EBs via the induction of endogenous TGF and Wnt growth factors are also consistent with the autoregulatory induction loops proposed to initiate and maintain gastrulation in mouse embryos [55]. In this model, uncleaved nodal protein first up-regulates expression of *BMP4* in the extraembryonic ectoderm. In turn, extraembryonic BMP4 then signals to the embryo proper to initiate *Wnt3* expression in the posterior visceral endoderm and epiblast. Wnt3 specifies mesoderm and acts to maintain *nodal* expression within the epiblast [55]. We explored this integration of signalling pathways through mixing experiments which showed that ESCs differentiated in response to BMP4 or Wnt3a propagated a paracrine GFP-inducing signal to d3 unstimulated *Mixl1*$^{GFP/w}$ EBs. Intriguingly, the transferred inductive signals were blocked not only by nodal inhibition, but also by Dkk-1 and partly by noggin, indicating a requirement for Wnt and BMP4 signalling even after closure of the window for response to these factors at d3. Studies in which these factors were added alone and in combination at d3 of differentiation confirmed our findings that direct BMP4 and Wnt3a responsiveness were greatly reduced after d3 but demonstrated that a significant population of cells were still responsive to Activin A. This observation suggests that *nodal* is a strong candidate for the predominant paracrine signalling molecule. The synergy that we observed between Activin and Wnt3a has previously been reported in normal mouse development [56] and in the context of human cancers [57,58]. Mechanistically, in our experiments the results might reflect induction of *nodal* and its co receptor *cripto* (data not shown), by Wnt3a and Activin A. This synergy is also consistent with results reported by Hansson and colleagues who noted the late requirement for Wnt signalling in Activin A induction of Sox17$^+$ definitive endoderm [20].

The higher frequency of d5 GFP$^+$ cells observed in cultures where growth factors were removed at d3 compared with cultures that were also treated with inhibitors, suggested that mesendoderm formation remained dependent upon a growth factor for a short period even after it was removed from the culture. Experiments in which we evaluated the effects of adding inhibitors to growth factor induced cultures after d3 confirmed that the requirement for BMP4 was lost earlier than dependence upon Wnt or nodal signalling. This was evidenced by the higher percentages of d5 Mixl1 GFP$^+$ cells in noggin treated cultures compared to cultures in which Wnt or Activin signalling was inhibited (Figure 5B). In response to BMP4 stimulation, the frequency of GFP$^+$ cells in d3 noggin treated cultures was ~80% of the frequency without inhibitors whilst treatment with Dkk-1 or SB 431542 reduced the frequency of GFP$^+$ cells to ~30% and ~20% of this value respectively. Similarly, in cultures stimulated by Wnt3a or Activin A, the frequency of GFP$^+$ cells in d3 noggin treated cultures was ~65% of the frequency without inhibitors whilst the inclusion of either Dkk-1 or SB 431542 reduced the frequency of GFP$^+$ cells to ~25% of the untreated value for Wnt stimulated cultures and ~10% of this value for Activin A stimulated cultures. These data suggested that the wave of prospective mesendoderm passed through a series of 'gates' which marked its 'exit' from dependence on BMP4, Wnt and Activin/nodal signalling (Figure 7B). These 'exit gates' corresponded to the point at which addition of inhibitors no longer diminished the subsequent appearance of Mixl1GFP$^+$ cells. As such, the lesser reduction in the percentage of GFP$^+$ cells observed at d5 in cultures receiving noggin at d3 compared with cultures receiving Dkk-1 or SB 431542, indicated that dependence on BMP signalling was lost earlier than the requirement for Wnt or Activin/nodal signalling.

Overall, this study showed that differentiating mouse ESCs passed through specific 'temporal windows' in which cells gained and lost responsiveness to particular factors. It also demonstrated the requirement for an integrated network of signalling molecules to maintain the process of mesendoderm induction. Further studies investigating the detailed molecular mechanisms underpinning these observations will provide additional insights into the regulation of the germ layers during mammalian development.

## Materials and Methods

### ESC growth and differentiation

The *Mixl1*$^{w/w}$ (W9.5) [59] and *Mixl1*$^{GFP/w}$ (clone Mix147 and Mix114) [17,22] ESC lines were maintained as described [60]. Differentiation was initiated by allowing EBs to form in cultures of disaggregated ESCs seeded at $1\times10^4$ cells/ml in non-adherent 6 cm bacteriological dishes (Phoenix Biomedical) or by spin EB formation with $5\times10^2$ cells seeded per well in non-adherent round bottomed 96 well plates (Nunc) in a chemically defined medium (CDM) [17,23] as described [61]. The growth factors BMP4 (10 ng/ml), Activin A (100 ng/ml) (both from R&D Systems) and Wnt3a (100 ng/ml) (Millipore) were added at the indicated times in each experiment. The effective concentrations of the nodal signalling inhibitor, SB 431542 (Sigma Aldrich), the BMP signalling inhibitor, noggin (R&D Systems) and the Wnt inhibitor, Dkk-1 (R & D Systems) were determined by titrating each factor into mESC cultures differentiated in the presence of 100 ng/ml Activin A, 10 ng/ml BMP4 and 100 ng/ml Wnt3a, respectively. These experiments showed that 4 μM SB 431542, 100 ng/ml noggin or 200 ng/ml Dkk-1 was sufficient to block ligand-induced GFP expression in *Mixl1*$^{GFP/w}$ cells. Growth factors were removed from the cultures by pelleting EBs by centrifugation (480×*g*), aspirating the media, washing once with PBS, and resuspending the EBs in fresh CDM. The EBs were then transferred to a non-adherent bacteriological dish and returned to a humidified 37°C incubator (8% $CO_2$ in air). GFP expression was analysed by flow cytometry at day 5 of differentiation unless otherwise stated.

### Differentiation of chimeric embryoid bodies

*Mixl1*$^{w/w}$ and *Mixl1*$^{GFP/w}$ cells were differentiated as EBs in parallel cultures for 3d. *Mixl1*$^{w/w}$ EBs were differentiated in the absence of growth factors (control cells) or in the presence of BMP4 (10 ng/ml), Wnt3a (100 ng/ml) or Activin A (100 ng/ml) (stimulator cells). BMP4 and Wnt3a were included from the onset of differentiation whilst Activin A was added at d2. For the first 3d, *Mixl1*$^{GFP/w}$ cells (responder cells) were differentiated in the absence of added growth factors. After 3d, EBs from both lines were harvested, washed in PBS, and trypsinised to form a single cell suspension. The disaggregated *Mixl1*$^{w/w}$ and *Mixl1*$^{GFP/w}$ cells were combined at a ratio of 1:1 in CDM. Two thousand cells were placed into each well of low adherent round bottomed 96 well trays (Nunc) and chimeric spin EBs were formed by aggregation of the cells following centrifugation [61]. Inhibitors of signalling were added as indicated. The differentiation was allowed to proceed until d5 when the chimeric EBs were disaggregated with trypsin and the cells were analysed by flow cytometry for GFP expression.

### Gene expression analysis

RNA was extracted using an RNeasy Mini Kit (Qiagen) and cDNA synthesized using SuperScript III (Invitrogen Corporation) according to the manufacturer's instructions. PCR gene expression analysis was performed as described previously [62]. Samples from separate experiments involving BMP4, Wnt3a and Activin A treatments were all standardised against the HPRT expression from a single RNA sample derived from undifferentiated mESCs. PCRs were carried out using Platinum Taq DNA Polymerase High Fidelity (Invitrogen) with the primer pairs and PCR conditions listed in Table S1. Quantitative real time Taqman gene expression analysis was performed according to the manufacturer's instructions using the probe sets listed in Table S2 and processed as described [63].

## Supporting Information

**Figure S1** BMP4, Wnt3a and Activin A display a similar pattern of mesendoderm inducing activity in differentiating Mixl1GFP/w clone Mix 114. (A) Flow cytometry analysis of d5 Mixl1GFP/w clone 114 ESCs differentiated in cultures supplemented with 10ng/ml BMP4, 100ng/ml Wnt3a or 100ng/ml Activin A for the given time intervals, indicating the proportion of GFP+ cells. The growth factor treatment for each experiment is indicated and the corresponding no growth factor (-GF) control flow cytometry profiles are shown to the left of each series. (B) Representative brightfield and epifluorescence images of differentiating EBs. The growth factors and period of addition are indicated to the left of each row and day of differentiation when the image was taken in the top right hand corner of each panel. (Original magnification x 100).

Found at: doi:10.1371/journal.pone.0010706.s001 (12.87 MB TIF)

**Figure S2** Kinetics of mesendoderm gene expression in EBs differentiated in BMP4, Wnt3a and Activin A. Real time PCR analysis for the indicated genes at (A) d3 and (B) d5 in ESCs differentiated in the absence of growth factors (-GF) or presence of BMP4, Wnt3a or Activin A for the indicated periods (mean ± sem, n = 3).

Found at: doi:10.1371/journal.pone.0010706.s002 (2.19 MB TIF)

**Table S1** Sequences of primers used for PCR analysis shown in Figure 2 and 5.

Found at: doi:10.1371/journal.pone.0010706.s003 (0.04 MB DOC)

**Table S2** Probe sets for real-time PCR analysis shown in Figure 3 and Figure S2.

Found at: doi:10.1371/journal.pone.0010706.s004 (0.03 MB DOC)

## Acknowledgments

We wish to thank Anna Mossman and Claire Hirst for provision of reagents and Suzanne Micallef for assistance with the serum free culture system.

## Author Contributions

Conceived and designed the experiments: SAJ JS ES AGE. Performed the experiments: SAJ JS. Analyzed the data: SAJ JS ES AGE. Contributed reagents/materials/analysis tools: SAJ JS ES AGE. Wrote the paper: SAJ ES AGE.

## References

1. Keller GM (1995) In vitro differentiation of embryonic stem cells. Curr Opin Cell Biol 7: 862 869.
2. Hirst CE, Ng ES, Azzola L, Voss AK, Thomas T, et al. (2006) Transcriptional profiling of mouse and human ES cells identifies SLAIN1, a novel stem cell gene. Dev Biol 293: 90 103.
3. Gadue P, Huber TL, Nostro MC, Kattman S, Keller GM (2005) Germ layer induction from embryonic stem cells. Exp Hematol 33: 955 964.
4. Smith J, Wardle F, Loose M, Stanley E, Patient R (2007) Germ Layer Induction in ESC - Following the Vertebrate Roadmap. Current Protocols in Stem Cell Biology 1.
5. Tam PP, Loebel DA, Tanaka SS (2006) Building the mouse gastrula: signals, asymmetry and lineages. Curr Opin Genet Dev 16: 419 425.
6. Beppu H, Kawabata M, Hamamoto T, Chytil A, Minowa O, et al. (2000) BMP type II receptor is required for gastrulation and early development of mouse embryos. Dev Biol 221: 249 258.
7. Conlon FL, Lyons KM, Takaesu N, Barth KS, Kispert A, et al. (1994) A primary requirement for nodal in the formation and maintenance of the primitive streak in the mouse. Development 120: 1919 1928.
8. Gu Z, Nomura M, Simpson BB, Lei H, Feijen A, et al. (1998) The type I activin receptor ActRIB is required for egg cylinder organization and gastrulation in the mouse. Genes Dev 12: 844 857.
9. Gu Z, Reynolds EM, Song J, Lei H, Feijen A, et al. (1999) The type I serine/threonine kinase receptor ActRIA (ALK2) is required for gastrulation of the mouse embryo. Development 126: 2551 2561.
10. Kelly OG, Pinson KI, Skarnes WC (2004) The Wnt co-receptors Lrp5 and Lrp6 are essential for gastrulation in mice. Development 131: 2803 2815.
11. Liu P, Wakamiya M, Shea MJ, Albrecht U, Behringer RR, et al. (1999) Requirement for Wnt3 in vertebrate axis formation. Nat Genet 22: 361 365.
12. Mishina Y, Suzuki A, Ueno N, Behringer RR (1995) Bmpr encodes a type I bone morphogenetic protein receptor that is essential for gastrulation during mouse embryogenesis. Genes Dev 9: 3027 3037.
13. Winnier G, Blessing M, Labosky PA, Hogan BL (1995) Bone morphogenetic protein-4 is required for mesoderm formation and patterning in the mouse. Genes Dev 9: 2105 2116.
14. Zhou X, Sasaki H, Lowe L, Hogan BL, Kuehn MR (1993) Nodal is a novel TGF-beta-like gene expressed in the mouse node during gastrulation. Nature 361: 543 547.
15. Tada S, Era T, Furusawa C, Sakurai H, Nishikawa S, et al. (2005) Characterization of mesendoderm: a diverging point of the definitive endoderm and mesoderm in embryonic stem cell differentiation culture. Development 132: 4363 4374.
16. Gadue P, Huber TL, Paddison PJ, Keller GM (2006) Wnt and TGF-beta signaling are required for the induction of an in vitro model of primitive streak formation using embryonic stem cells. Proc Natl Acad Sci U S A 103: 16806 16811.
17. Ng ES, Azzola L, Sourris K, Robb L, Stanley EG, et al. (2005) The primitive streak gene Mixl1 is required for efficient haematopoiesis and BMP4-induced ventral mesoderm patterning in differentiating ES cells. Development 132: 873 884.
18. Nostro MC, Cheng X, Keller GM, Gadue P (2008) Wnt, Activin, and BMP Signaling Regulate Distinct Stages in the Developmental Pathway from Embryonic Stem Cells to Blood. Cell Stem Cell 2: 60 71.
19. Sumi T, Tsuneyoshi N, Nakatsuji N, Suemori H (2008) Defining early lineage specification of human embryonic stem cells by the orchestrated balance of canonical Wnt/beta-catenin, Activin/Nodal and BMP signaling. Development 135: 2969 2979.
20. Hansson M, Olesen DR, Peterslund JM, Engberg N, Kahn M, et al. (2009) A late requirement for Wnt and FGF signaling during activin-induced formation of foregut endoderm from mouse embryonic stem cells. Dev Biol 330: 286 304.
21. Robb L, Hartley L, Begley CG, Brodnicki TC, Copeland NG, et al. (2000) Cloning, expression analysis, and chromosomal localization of murine and human homologues of a Xenopus mix gene. Dev Dyn 219: 497 504.
22. Hart AH, Hartley L, Sourris K, Stadler ES, Li R, et al. (2002) Mixl1 is required for axial mesendoderm morphogenesis and patterning in the murine embryo. Development 129: 3597 3608.
23. Johansson BM, Wiles MV (1995) Evidence for involvement of activin A and bone morphogenetic protein 4 in mammalian mesoderm and hematopoietic development. Mol Cell Biol 15: 141 151.
24. Lim SM, Pereira L, Wong MS, Hirst CE, Van Vranken BE, et al. (2009) Enforced expression of Mixl1 during mouse ES cell differentiation suppresses hematopoietic mesoderm and promotes endoderm formation. Stem Cells 27: 363 374.
25. Martin GR (1975) Teratocarcinomas as a model system for the study of embryogenesis and neoplasia. Cell 5: 229 243.
26. Martin GR (1980) Teratocarcinomas and mammalian embryogenesis. Science 209: 768 776.
27. Andrews PW (2002) From teratocarcinomas to embryonic stem cells. Philos Trans R Soc Lond B Biol Sci 357: 405 417.

28. Solter D (2006) From teratocarcinomas to embryonic stem cells and beyond: a history of embryonic stem cell research. Nat Rev Genet 7: 319 327.
29. Askanazy M (1907) Die teratome nach ihrem bau, ihrem verlauf, ihren genese und im vergleich zum experimentellen teratoid. Verhandl Deutsch Pathol 11: 39 82.
30. Stevens LC, Little CC (1954) Spontaneous Testicular Teratomas in an Inbred Strain of Mice. Proc Natl Acad Sci U S A 40: 1080 1087.
31. Stevens LC (1960) Embryonic potency of embryoid bodies derived from a transplantable testicular teratoma of the mouse. Dev Biol 2: 285 297.
32. Kleinsmith LJ, Pierce GB, Jr. (1964) Multipotentiality of Single Embryonal Carcinoma Cells. Cancer Res 24: 1544 1551.
33. Kahan BW, Ephrussi B (1970) Developmental potentialities of clonal in vitro cultures of mouse testicular teratoma. J Natl Cancer Inst 44: 1015 1036.
34. Martin GR, Evans MJ (1975) Multiple differentiation of clonal teratocarcinoma stem cells following embryoid body formation in vitro. Cell 6: 467 474.
35. Williams RL, Hilton DJ, Pease S, Willson TA, Stewart CL, et al. (1988) Myeloid leukaemia inhibitory factor maintains the developmental potential of embryonic stem cells. Nature 336: 684 687.
36. Teresky AK, Marsden M, Kuff EL, Levine AJ (1974) Morphological criteria for the in vitro differentiation of embryoid bodies produced by a transplantable teratoma of mice. J Cell Physiol 84: 319 332.
37. Strickland S, Mahdavi V (1978) The induction of differentiation in teratocarcinoma stem cells by retinoic acid. Cell 15: 393 403.
38. Solter D, Skreb N, Damjanov I (1970) Extrauterine growth of mouse egg-cylinders results in malignant teratoma. Nature 227: 503 504.
39. Stevens LC (1970) The development of transplantable teratocarcinomas from intratesticular grafts of pre- and postimplantation mouse embryos. Dev Biol 21: 364 382.
40. Evans MJ, Kaufman MH (1981) Establishment in culture of pluripotential cells from mouse embryos. Nature 292: 154 156.
41. Martin GR (1981) Isolation of a pluripotent cell line from early mouse embryos cultured in medium conditioned by teratocarcinoma stem cells. Proc Natl Acad Sci U S A 78: 7634 7638.
42. Reubinoff BE, Pera MF, Fong CY, Trounson A, Bongso A (2000) Embryonic stem cell lines from human blastocysts: somatic differentiation in vitro. Nat Biotechnol 18: 399 404.
43. Thomson JA, Itskovitz-Eldor J, Shapiro SS, Waknitz MA, Swiergiel JJ, et al. (1998) Embryonic stem cell lines derived from human blastocysts. Science 282: 1145 1147.
44. Takahashi K, Yamanaka S (2006) Induction of pluripotent stem cells from mouse embryonic and adult fibroblast cultures by defined factors. Cell 126: 663 676.
45. Pearce JJ, Evans MJ (1999) Mml, a mouse Mix-like gene expressed in the primitive streak. Mech Dev 87: 189 192.
46. Murry CE, Keller G (2008) Differentiation of embryonic stem cells to clinically relevant populations: lessons from embryonic development. Cell 132: 661 680.
47. Toyooka Y, Shimosato D, Murakami K, Takahashi K, Niwa H (2008) Identification and characterization of subpopulations in undifferentiated ES cell culture. Development 135: 909 918.
48. Brons IG, Smithers LE, Trotter MW, Rugg-Gunn P, Sun B, et al. (2007) Derivation of pluripotent epiblast stem cells from mammalian embryos. Nature 448: 191 195.
49. Camus A, Perea-Gomez A, Moreau A, Collignon J (2006) Absence of Nodal signaling promotes precocious neural differentiation in the mouse embryo. Dev Biol 295: 743 755.
50. Mesnard D, Guzman-Ayala M, Constam DB (2006) Nodal specifies embryonic visceral endoderm and sustains pluripotent cells in the epiblast before overt axial patterning. Development 133: 2497 2505.
51. Hayashi K, Surani MA (2009) Self-renewing epiblast stem cells exhibit continual delineation of germ cells with epigenetic reprogramming in vitro. Development 136: 3549 3556.
52. Schier AF (2003) Nodal signaling in vertebrate development. Annu Rev Cell Dev Biol 19: 589 621.
53. Shen MM (2007) Nodal signaling: developmental roles and regulation. Development 134: 1023 1034.
54. Willems E, Leyns L (2008) Patterning of mouse embryonic stem cell-derived pan-mesoderm by Activin A/Nodal and Bmp4 signaling requires Fibroblast Growth Factor activity. Differentiation 76: 745 759.
55. Ben-Haim N, Lu C, Guzman-Ayala M, Pescatore L, Mesnard D, et al. (2006) The nodal precursor acting via activin receptors induces mesoderm by maintaining a source of its convertases and BMP4. Dev Cell 11: 313 323.
56. Morkel M, Huelsken J, Wakamiya M, Ding J, van de Wetering M, et al. (2003) Beta-catenin regulates Cripto- and Wnt3-dependent gene expression programs in mouse axis and mesoderm formation. Development 130: 6283 6294.
57. Hamada S, Watanabe K, Hirota M, Bianco C, Strizzi L, et al. (2007) beta-Catenin/TCF/LEF regulate expression of the short form human Cripto-1. Biochem Biophys Res Commun 355: 240 244.
58. Hirota M, Watanabe K, Hamada S, Sun Y, Strizzi L, et al. (2008) Smad2 functions as a co-activator of canonical Wnt/beta-catenin signaling pathway independent of Smad4 through histone acetyltransferase activity of p300. Cell Signal 20: 1632 1641.
59. Szabo P, Mann JR (1994) Expression and methylation of imprinted genes during in vitro differentiation of mouse parthenogenetic and androgenetic embryonic stem cell lines. Development 120: 1651 1660.
60. Barnett LD, Kontgen F (2001) Gene targeting in a centralized facility. Methods Mol Biol 158: 65 82.
61. Ng ES, Davis RP, Azzola L, Stanley EG, Elefanty AG (2005) Forced aggregation of defined numbers of human embryonic stem cells into embryoid bodies fosters robust, reproducible hematopoietic differentiation. Blood 106: 1601 1603.
62. Elefanty AG, Begley CG, Hartley L, Papaevangeliou B, Robb L (1999) SCL expression in the mouse embryo detected with a targeted lacZ reporter gene demonstrates its localization to hematopoietic, vascular, and neural tissues. Blood 94: 3754 3763.
63. Pick M, Azzola L, Mossman A, Stanley EG, Elefanty AG (2007) Differentiation of Human Embryonic Stem Cells in Serum Free Medium Reveals Distinct Roles for BMP4, VEGF, SCF and FGF2 in Hematopoiesis. Stem Cells 25: 2206 2014.

STEM CELLS AND DEVELOPMENT
Volume 21, Number 10, 2012

DOI: 10.1089/scd.2011.0513

# Temporal Restriction of Pancreatic Branching Competence During Embryogenesis Is Mirrored In Differentiating Embryonic Stem Cells

Sue Mei Lim, Xueling Li, Jacqueline Schiesser, Andrew M. Holland, Andrew G. Elefanty, Edouard G. Stanley, and Suzanne J. Micallef

To develop methods for the generation of insulin-producing β-cells for the treatment of diabetes, we have used GFP-tagged embryonic stem cells (ESCs) to elucidate the process of pancreas development. Using the reporter *Pdx1*$^{GFP/w}$ ESC line, we have previously described a serum-free differentiation protocol in which Pdx1-GFP$^{+}$ cells formed GFP bright (GFP$^{br}$) epithelial buds that resembled those present in the developing mouse pancreas. In this study we extend these findings to demonstrate that these cells can undergo a process of branching morphogenesis, similar to that seen during pancreatic development of the mid-gestation embryo. These partially disaggregated embryoid bodies containing GFP$^{br}$ buds initially form epithelial ring-like structures when cultured in Matrigel. After several days in culture, these rings undergo a process of proliferation and form a ramified network of epithelial branches. Comparative analysis of explanted dissociated pancreatic buds from E13.5 *Pdx1*$^{GFP/w}$ embryos and ESC-derived GFP$^{br}$ buds reveal a similar process of proliferation and branching, with both embryonic *Pdx1*$^{GFP/w}$ branching pancreatic epithelium and ESC-derived GFP$^{br}$ branching organoids expressing markers representing epithelial (EpCAM and E-Cadherin), ductal (Mucin1), exocrine (Amylase and Carboxypeptidase 1A), and endocrine cell types (Glucagon and Somatostatin). ESC-derived branching structures also expressed a suite of genes indicative of ongoing pancreatic differentiation, paralleling gene expression within similar structures derived from the E13.5 fetal pancreas. In summary, differentiating mouse ESCs can generate pancreatic material that has significant similarity to the fetal pancreatic anlagen, providing an in vitro platform for investigating the cellular and molecular mechanisms underpinning pancreatic development.

## Introduction

Pancreatic organogenesis is a dynamic process in which interactions between extracellular growth factors and intracellular mediators determine lineage specification and differentiation. A key player in this process is the pancreatic and duodenal homeodomain 1 transcription factor (Pdx1) that is expressed throughout pancreas development, with expression persisting in mature β-cells [1,2]. Inactivation of *Pdx1* leads to arrested growth of the pancreatic primordia, resulting in pancreatic agenesis in mice [3] and humans [4,5].

In the developing mouse embryo, pancreatic commitment is foreshadowed by regionalized upregulation of *Pdx1* expression within a restricted domain on the dorsal and ventral surfaces of the gut tube at embryonic day (E) 9 to 9.5 [6]. These *Pdx1*$^{+}$ areas evaginate to form the dorsal and ventral pancreatic buds that subsequently expand in response to signals from adjacent pancreatic mesenchyme [7]. By E12.5, the developing anlagen is further elaborated to incorporate lobular outgrowths at the distal tips of the expanding pancreatic tree. This process of branching morphogenesis concomitantly continues with further cell specification and differentiation events that incorporate acinar and endocrine components into the developing organ. Over this period *Pdx1* expression remains high in both the dorsal and ventral anlagen and is also detected in the posterior region of the stomach, the bile duct, and the duodenal epithelium [8]. Lineage-tracing experiments have demonstrated that *Pdx1* expressing progenitors in the early embryo give rise to all 3 types of pancreatic cells from the exocrine, endocrine, and duct [9]. In the adult, *Pdx1* is expressed at high levels in β-cells, where it activates insulin gene expression [6], while lower levels of Pdx1 expression can also be detected in the acinar tissue.

Embryonic stem cells (ESCs) are immortal pluripotent cell lines characterized by their ability to differentiate into specialized cell types representing derivatives of the ectodermal, endodermal, and mesodermal lineages [10,11]. The in vitro differentiation of these cells recapitulates many aspects of

Monash Immunology and Stem Cell Laboratories (MISCL), Monash University, Clayton, Australia.

early embryonic development and is a valuable model for studying processes occurring during inaccessible periods of embryogenesis. As such, we and others have utilized this model to investigate the in vitro requirements for the formation of pancreatic endoderm from ESCs and their subsequent differentiation to endocrine and exocrine cell types [12–26].

We had previously devised a serum-free differentiation protocol that fostered the generation of pancreatic bud-like structures from differentiating mouse *Pdx1*$^{GFP/w}$ ESCs and showed that GFP bright (GFP$^{br}$) buds harbored precursors of both the endocrine and exocrine lineages and could give rise to insulin$^{+}$ cells [25]. In the present study, we further dissect the potential of these ESC-derived GFP$^{br}$ buds by examining their ability to undergo branching morphogenesis in a Matrigel-based culture system and perform comparative analysis with pancreatic rudiments from the developing mouse embryo. Our study demonstrates that both the differentiating ESCs and the fetal pancreas pass through a transient stage during which they are competent to undergo branching morphogenesis. Indeed, comparative analysis showed parallels between the dynamics of branching in structures derived from Pdx1-GFP$^{br}$ bud containing embryoid bodies (EBs) and embryonic pancreas explants. These results, coupled with gene expression analyses of branching cultures, suggest similarities in the cellular composition of pancreatic-committed progenitors present in the in vitro and in vivo derived cell populations. Overall, our studies highlight the utility of ESCs in the exploration of key events during pancreatic development.

## Materials and Methods

### *ESC culture and differentiation*

The mouse embryonic stem cell line *Pdx1*$^{GFP/w}$ was maintained on irradiated primary mouse embryonic fibroblasts as previously described [18,25,27]. ESC differentiation was performed using a modification of the method previously described [27] and employed a "spin EB" platform originally developed for differentiation of human ESCs [28]. Briefly, individual spin EBs were formed by the forced aggregation of 350 cells/well in low attachment 96-well round-bottomed plates (Costar®) containing chemically defined medium (see Supplementary Table S1; Supplementary Data are available online at www.liebertonline.com/scd) supplemented with 5 ng/mL BMP4 (R & D Systems), 1 U/mL Leukemia Inhibitory Factor (LIF; Chemicon® International), and 0.001% polyvinyl alcohol (PVA; Sigma Aldrich) (added at day (d) 0). At d4, EBs were treated with a 24-h pulse of $10^{-5}$ M RA before being transferred to gelatin-treated adherent 96-well plates (Becton Dickinson Labware) containing CDM supplemented with 10 ng/mL basic FGF (bFGF; R & D Systems). EBs were allowed to adhere and were differentiated for a further 7 days. At d12, EBs were assessed for markers of pancreatic differentiation through visualization for GFP via the Zeiss Axiovert 200 inverted fluorescence microscope.

### *Generation of* Pdx1$^{GFP/w}$ *targeted heterozygous embryos*

*Pdx1*$^{GFP/w}$ embryos were generated by timed-matings of *Pdx1*$^{GFP/w}$ males [29] with C57/B6J females. The presence of the vaginal plug was designated as embryonic day 0.5 (E0.5) of gestation. Embryos of the desired age were dissected from the decidua and the pancreatic anlage, including both the dorsal and ventral pancreatic buds (including some surrounding mesenchyme), caudal stomach, and proximal duodenum was isolated (herein denoted as pancreatic/Pdx1$^{+}$ rudiments). Images of embryos expressing GFP were captured with a Leica fluorescence microscope. All animal experimentation was performed under the auspices and approval of the Monash University School of Biomedical Sciences animal ethics committee (approval number SOBSA/MIS/2010/21).

### *Explant cultures*

Pancreatic explants were cultured using a Matrigel based culture system. Briefly, 100 μL of a solution comprised of 50 μL CDM (see Supplementary Table S1) and 50 μL Growth Factor Reduced (GFR) BD Matrigel™ Matrix (Becton Dickinson) was added to each well of a 4-well Chamber Slide™ System (Nunc Lab-Tek®). The GFR-Matrigel was allowed to gel at 37°C for ~30 min. For the partial disaggregation of pancreatic rudiments or EBs, samples were collected and washed once in PBS. Samples were resuspended in 1 mL Trypsin/Versine containing 2% chicken serum and were incubated at 37°C for 4–7 min. Trypsin digestion was arrested with the addition of equivalent volume of fetal calf serum and the samples were gently pipetted to facilitate partial disaggregation. Following 2 rounds of washing with PBS, cells were resuspended in 500 μL of CDM per 5 fetal rudiments or per 12 disaggregated EBs. This cell suspension was then placed on top of the gelled Matrigel/CDM in each well of the chamber slide. Cultures were incubated at 37°C (5% $CO_2$). The emergence of branching structures over an 8-day period was monitored by fluorescence microscopy.

### *Histology-fixation*

Branching EBs and fetal pancreas rudiments derived from Matrigel explant cultures were fixed in 4% (w/v) paraformaldehyde (PFA) in PBS (pH 7.2) for 20 and 40 min at room temperature, respectively. Following fixation, samples were rinsed twice in PBS. Samples were then pelleted and embedded in 0.7% (w/v) low melt agarose. Agarose embedded samples were then dehydrated and embedded in paraffin wax. Blocks were sectioned at 5 μm, de-waxed, and processed for double indirect immunofluorescence labeling as previously described [30].

### *Immunohistochemistry*

Following de-waxing of paraffin sections, heat mediated-antigen retrieval was performed by microwaving sections for 20 min in 10 mM Sodium Citrate, pH 6.0. Sections were allowed to cool for 20 min, followed by a brief wash in deionized water and rinsed twice in PBS. Sections were incubated for 30 min in 5% FCS in PBS containing 0.1% Tween and 0.5% BSA. The sections were incubated overnight at 4°C with primary antibodies as described in Supplementary Table S2. The chicken anti-GFP antibody (Abcam) was detected with an Alexa Fluor® 488 goat-anti-chicken IgG secondary antibody (Molecular Probes). The rabbit anti-Pdx1 (a generous gift from C.V.E. Wright, Vanderbilt University), rabbit

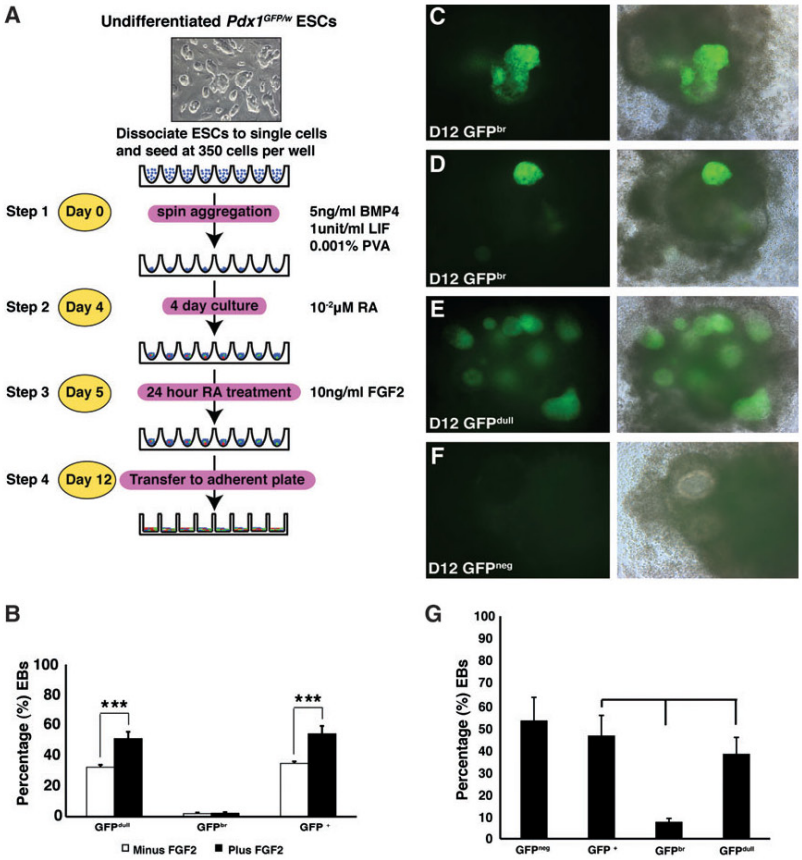


**FIG. 1.** Protocol for the differentiation of ESCs to pancreatic endoderm. **(A)** Schematic summary of the serum-free spin EB method employed to induce the formation of Pdx1$^+$ pancreatic endoderm. **(B)** Column graph showing the effect of FGF2 addition on the differentiation of GFP$^+$ EBs (mean ± SEM, $n = 25$). **(C–F)** Fluorescent and overlay images illustrating the 3 predominant morphologies observed on day 12 ESC differentiation cultures: **(C** and **D)** 2 examples of GFP$^{br}$ buds, **(E)** GFP$^{dull}$ structures, and **(F)** a GFP$^{negative}$ (GFP$^{neg}$) EB. **(G)** Column graph showing the frequency of GFP$^+$, GFP$^{br}$ buds, and GFP$^{dull}$ EBs at d12 of differentiation. Student's *t*-test values of $^{***}P < 0.005$ were considered as statistically significant. GFP$^{br}$, GFP bright; ESCs, embryonic stem cells; EBs, embryoid bodies; RA, retinoic acid. Color images available online at www.liebertonline.com/scd

anti-EpCAM (Abcam), rabbit anti-E-Cadherin (Santa Cruz Biotechnology), rabbit anti-Mucin1 (Abcam), rabbit anti-α-Amylase (Sigma-Aldrich), rabbit anti-Glucagon (Dako), and rabbit anti-Carboxypeptidase A (AbD Serotec) were detected with an Alexa Fluor® 568 goat anti-rabbit IgG secondary antibody (Molecular Probes). Nuclei were counterstained with 4′, 6-diamidino-2-phenylindole (DAPI; Sigma).

### *Microscopy*

Fluorescent and bright field images were captured on a Zeiss Axiovert 200 inverted fluorescence microscope (Carl Zeiss) and processed with Axiovision software. Confocal microscopy images were acquired using the Nikon C1 confocal laser-scanning microscope (40× and 63× oil immersion objectives). Data were processed using Image Processing and Analysis in Java (ImageJ) software.

### *Gene expression analysis*

Total RNA was extracted and prepared using the RNeasy™ Mini Kit (Qiagen) according to manufacturer's instructions. E16.5 and E19.5 GFP$^+$ sorted cells were dissected and isolated as previously described [29]. First-strand cDNA synthesis using random hexamer priming was performed with the SuperScript® III First-Strand Synthesis System for

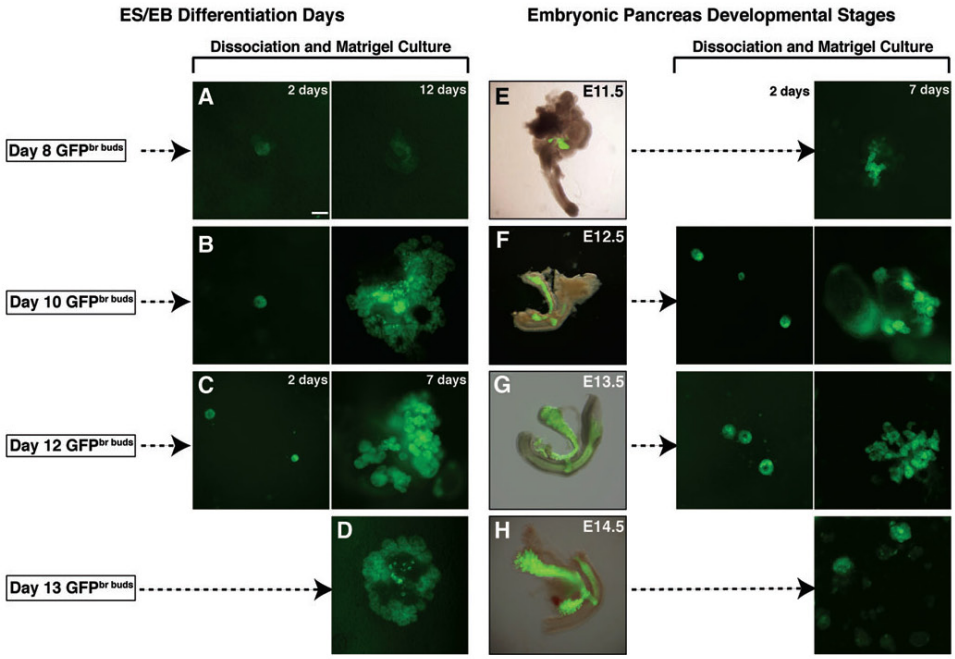


**FIG. 2.** Comparison of branching potential of *Pdx1*$^{GFP/w}$ EBs versus embryonic pancreata. Fluorescent images showing **(A)** Day 8 GFP$^{br}$ EBs cultured for 2 days and 12 days in Matrigel; **(B)** Day 10 GFP$^{br}$ EBs cultured for 2 and 12 days in Matrigel; **(C)** Day 12 GFP$^{br}$ EBs cultured for 2 and 7 days in Matrigel; **(D)** Day 13 GFP$^{br}$ EBs cultured for 7 days in Matrigel. **(E)** Overlay image showing viscera from E11.5 *Pdx1*$^{GFP/w}$ embryo and a fluorescent image of pancreatic explants cultured for 7 days. **(F)** Overlay image of viscera of E12.5 *Pdx1*$^{GFP/w}$ embryo and fluorescent images of cultured explants for 2 and 7 days in Matrigel culture. **(G)** Overlay image of viscera from E13.5 *Pdx1*$^{GFP/w}$ embryo Pdx1$^{+}$ pancreatic rudiments and fluorescent images of pancreatic explants cultured for 2 and 7 days. **(H)** Overlay image of viscera of an E14.5 *Pdx1*$^{GFP/w}$ embryo and a fluorescent image of an explant cultured for 7 days in Matrigel. Scale bar = 100 μm. Color images available online at www.liebertonline.com/scd

Real-Time-polymerase chain reaction (RT-PCR; Invitrogen). Quantitative gene expression assays were carried out according to the manufacturer's instructions using a 7500 RT-PCR System (Applied Biosystems by Life Technologies) with the following TaqMan® Gene Expression Assay probe sets as outlined in Supplementary Table S3. For each of the gene specific primer sets used, the signal was normalized against the expression of *Gapdh* as previously described [31], and the results referred to as relative gene expression. The results displayed are the mean ± SEM derived from 3 independent experiments.

### *Statistical analyses*

Data values obtained on the differentiation of EBs and pancreatic rudiments were subject to Student's *t*-test. Values of $P < 0.05$, $P < 0.01$, and $P < 0.005$ were considered as statistically significant. Analysis of gene expression data was conducted using 1-way analysis of variance , and significant group differences were established with Tukey's post hoc comparison. Values of $^{*}P < 0.05$, $^{**}P < 0.01$, and $^{***}P < 0.005$ were considered as statistically significant.

## Results

### *Directed differentiation of mouse ESCs to pancreatic endoderm*

We have previously described a multistep protocol for the differentiation of mouse ESCs to pancreatic endoderm cells in CDM [25,27]. This method entailed 4 days of treatment with low concentrations of BMP4 followed by a 24-h pulse of retinoic acid (RA) to induce the formation of *Pdx1*$^{+}$ EBs. EBs developed over the 7 days with Pdx1-GFP$^{+}$ cells being first visible at d8. In the current method, we replaced the BSA component within the CDM with recombinant human albumin (rHA), a modification that necessitated reassessment of the concentration and the timing of addition of growth factors required for reliable endoderm induction. In addition, we also included a low concentration of PVA, an additive we have previously shown to foster formation of EBs in 96-well low attachment plates (Fig. 1A). We observed that, unlike BSA containing CDM, rHA-CDM was unable to support efficient attachment of EBs transferred to adherent plates at differentiation d5. This difference could be obviated by

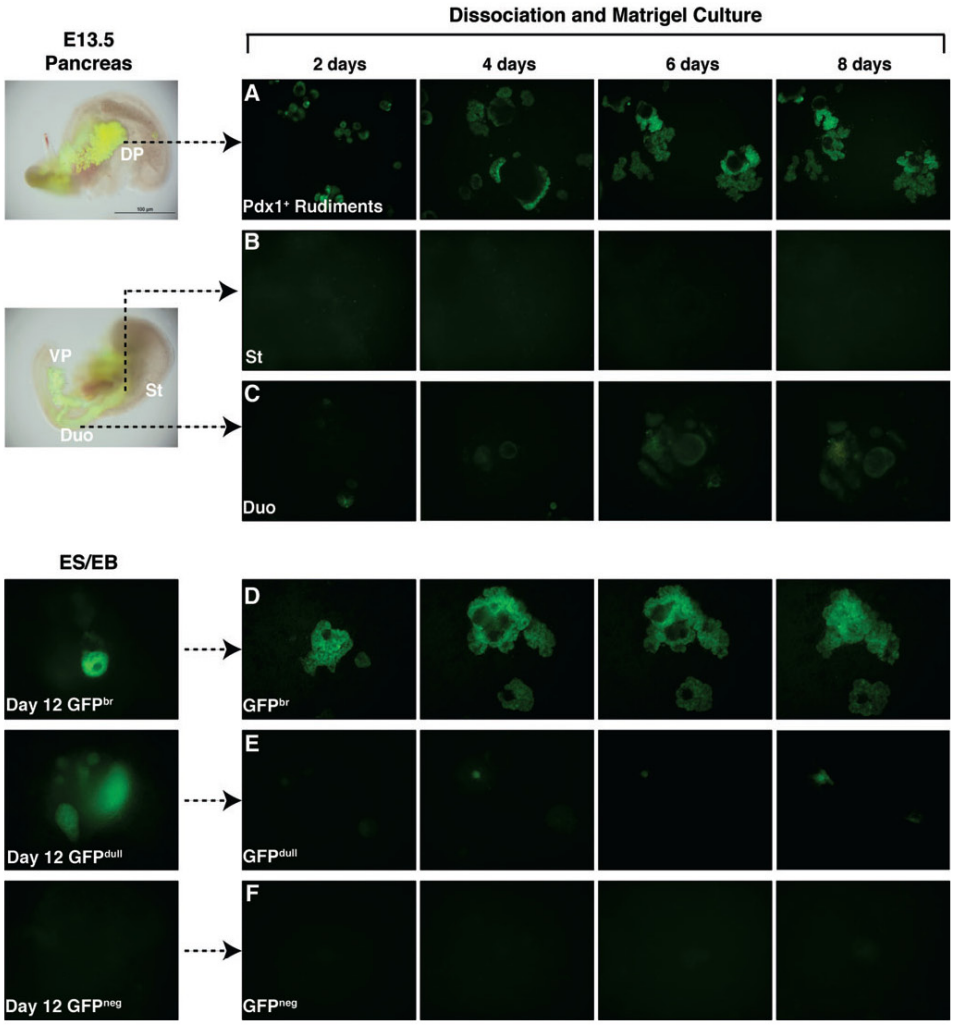


**FIG. 3.** Explant cultures derived from E13.5 Pdx1$^+$ pancreatic rudiments and d12 GFP$^{br}$ buds both undergo branching morphogenesis when cultured in Matrigel. Brightfield/GFP overlay image of an E13.5 *Pdx1*$^{GFP/w}$ embryo showing expression of GFP is restricted to the dorsal and ventral pancreatic buds, the proximal duodenum, and the distal stomach. **(A–C)** Fluorescent images showing the branching potential and morphogenesis of dissociated Pdx1$^+$ rudiments isolated from the pancreas **(A)**, stomach **(B)**, and duodenum **(C)** of E13.5 *Pdx1*$^{GFP/w}$ embryos following 2, 4, 6, and 8 days of Matrigel culture. **(D–F)** Fluorescent images showing the branching potential and morphogenesis of dissociated d12 GFP$^{br}$ **(D)**, GFP$^{dull}$ **(E)**, and GFP$^{neg}$ **(F)** EBs following 2, 4, 6, and 8 days of Matrigel culture. Scale bars = 100 μm. Color images available online at www.liebertonline.com/scd

addition of 10 ng/mL FGF2 at d5, a modification that promoted the outgrowth of an adherent stromal layer (data not shown). Although the role of this adherent layer was not specifically investigated, fluorescence microscopy demonstrated that, compared with controls, the overall percentage of Pdx1-GFP$^+$ foci was ~1.6-fold greater in FGF2 treated cultures (54.4% ± 3.7% vs. 33.9% ± 1.2%, mean ± SEM, $n = 4$ experiments) (Fig. 1B).

In d12 *Pdx1*$^{GFP/w}$ EBs, 3 predominant morphologies were observed and subsequently scored using fluorescence

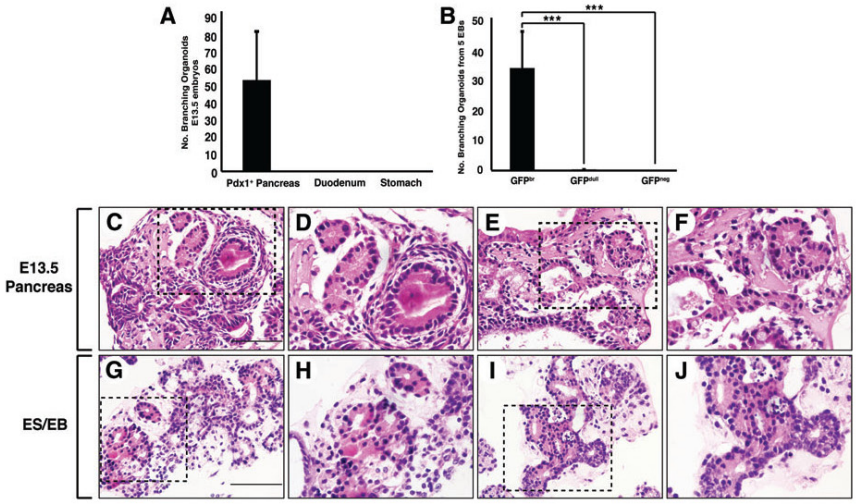


**FIG. 4.** Branching frequency and histology of branching Pdx1-GFP$^+$ foci derived from E13.5 pancreas and GFP$^{br}$ EBs. **(A)** A graph showing the frequency of branching organoids derived from E13.5 Pdx1$^+$ pancreatic rudiments of either the pancreas, proximal duodenum, or distal stomach following Matrigel culture (mean ± SEM, $n=4$ experiments). **(B)** A graph showing the frequency of branching organoids derived from the Matrigel culture of day 12 ESC-derived GFP$^{br}$, GFP$^{dull}$, or GFP$^{neg}$ EBs. Student's *t*-test values of $^{***}P<0.005$ were considered as statistically significant. **(C–F)** Micrographs of H&E stained sections of branching organoids derived from the Matrigel culture of E13.5 Pdx1$^+$ pancreas. **(G–J)** Micrographs of H&E stained sections of branching organoids derived from the Matrigel culture of ESC differentiated d12 GFP$^{br}$ buds. Scale bars = 50 μm. Color images available online at www.liebertonline.com/scd

microscopy (Fig. 1C–F); brightly fluorescing outgrowths designated as GFP bright buds (GFP$^{br}$, Fig 1C, D), diffuse GFP$^+$ (Pdx1$^+$) structures, referred to as GFP dull EBs (GFP$^{dull}$, Fig. 1E) [25], and EBs that did not appear to contain any Pdx1-GFP$^+$ endoderm (GFP$^{neg}$, Fig. 1F). Using our modified protocol, the frequency of GFP$^+$ EBs scored from d12 cultures was 46.6% ± 9% (mean ± SEM, $n=27$ experiments) (Fig. 1G), similar to the frequency previously observed when permissive batches of BSA were available (53%) [25]. GFP$^{br}$ buds and GFP$^{dull}$ structures were present in 8.0% ± 1.5% (mean ± SEM, $n=27$ experiments) and 38.4% ± 7.4% (mean ± SEM, $n=27$ experiments) of EBs respectively (Fig. 1G).

We have previously shown that GFP$^{br}$ buds contained precursors of the exocrine and endocrine lineages [25]. In this current series of experiments, we asked whether these bright buds possessed another property of pancreatic primordia, namely, the ability to undergo branching morphogenesis in a Matrigel-based culture system [32]. To this end, we compared the branching ability of EBs containing GFP$^{br}$ buds (d8, d10, and d12–d13) (Fig. 2A–D) and dissected embryonic pancreata from consecutive gestational ages (E11.5-E14.5) (Fig. 2E–H). Partially disaggregated EBs and fetal pancreata were cultured in GFR Matrigel diluted in rHA-CDM (Fig. 2). After 2 days in culture, cells from GFP$^{br}$ EBs and fetal pancreas formed tight epithelial rings, which underwent a process resembling branching morphogenesis over the following 7 days. The ability of EBs containing Pdx1-GFP$^+$ cells to undergo branching was optimal at specific stages of differentiation. For example, d8 GFP$^{br}$ EBs (Fig. 2A) failed to branch, whereas d10 (Fig. 2B) and d12 GFP$^{br}$ cells (Fig. 2C) formed convoluted GFP$^+$ epithelia that increased in size and complexity over a 12-day and 7-day culture period, respectively. Finally, cells from d13 or older GFP$^{br}$ EBs (Fig. 2D) possessed far more limited potential for branching (data not shown), and the structures that did develop displayed less intense GFP expression compared with that seen in those derived from d10 or d12 EBs. Correspondingly, in this culture system dissociated E11.5 derived Pdx1-GFP$^+$ pancreatic rudiments (Fig. 2E) gave rise to poorly defined structures whereas E12.5 explants (Fig. 2F) had a propensity to form both cystic and duct-like structures, and exhibited some degree of branching. Pancreata from E13.5 *Pdx1*$^{GFP/tu}$ embryos (Fig. 2G) underwent a process of growth and branching morphogenesis in which a highly elaborated tree developed over a 7-day period. Finally, E14.5 pancreatic explants had a reduced capacity to form branching structures and were more inclined to generate small clusters of brightly fluorescing GFP$^+$ cells with limited potential for further growth (Fig. 2H).

The evolution of branching structures derived from GFP$^{br}$ bud-containing EBs and pancreatic rudiments is further documented in Fig. 3. During the first 2 days following Matrigel culture, Pdx1-GFP$^+$ cells from partially disaggregated E13.5 pancreatic rudiments and d12 GFP$^{br}$ bud containing-EBs formed epithelial rings that were surrounded by GFP$^{negative}$ (GFP$^{neg}$) cells of mesenchymal appearance (Fig. 3A, D). On the fourth day of culture, small protrusions radiating from the epithelial clusters began to appear (Fig. 3A, D). In some instances, the tightly associated clusters of

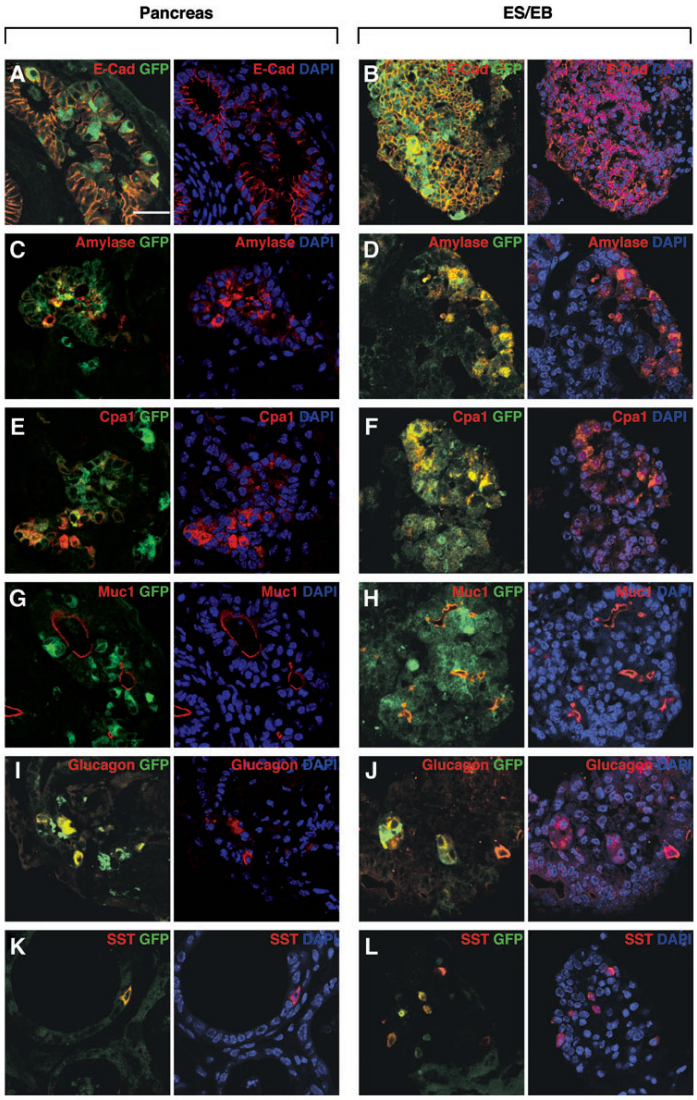


**FIG. 5.** Branching organoids derived from E13.5 Pancreas and d12 GFP$^{br}$ bud containing EBs express a suite of endocrine, exocrine, epithelial, and ductal markers. Confocal micrographs of branching organoids derived from either E13.5 pancreas or d12 GFP$^{br}$ bud containing EBs were generated by immunolabeling with antibodies directed against E-Cadherin **(A** and **B)**, Amylase **(C** and **D)**, Carboxypeptidase 1A **(E** and **F)**, Mucin1 **(G** and **H)**, Glucagon **(I** and **J)**, and Somatostatin **(K** and **L)**. Scale bar = 100 μm. E-Cad, E-Cadherin. Color images available online at www.liebertonline.com/scd

epithelial cells surrounded a small central lumen, which were indicative of the early signs of branching morphogenesis. From 6 to 8 days of culture, the epithelium expanded, with multiple branched structures forming a complex tree (Fig. 3A, D). Small independent lumina were always associated with these structures (Supplementary Fig. S1A–H). Beyond 8 days of culture, the fluorescence intensity of branching foci diminished and the epithelial clusters started to fragment, possibly reflecting exhaustion of nutrients within the culture medium. These same branching structures were not observed in cultures derived from GFP$^{dull}$ (Fig. 3E) and GFP$^{neg}$ EBs (Fig. 3F), nor did they arise from other Pdx1-GFP$^{+}$ areas within the embryos, such as the distal stomach (Fig. 3B) and duodenum (Fig. 3C). Instead, explants of stomach and duodenum gave rise to tubular-like structures that were also surrounded by mesenchyme-like cells (Supplementary

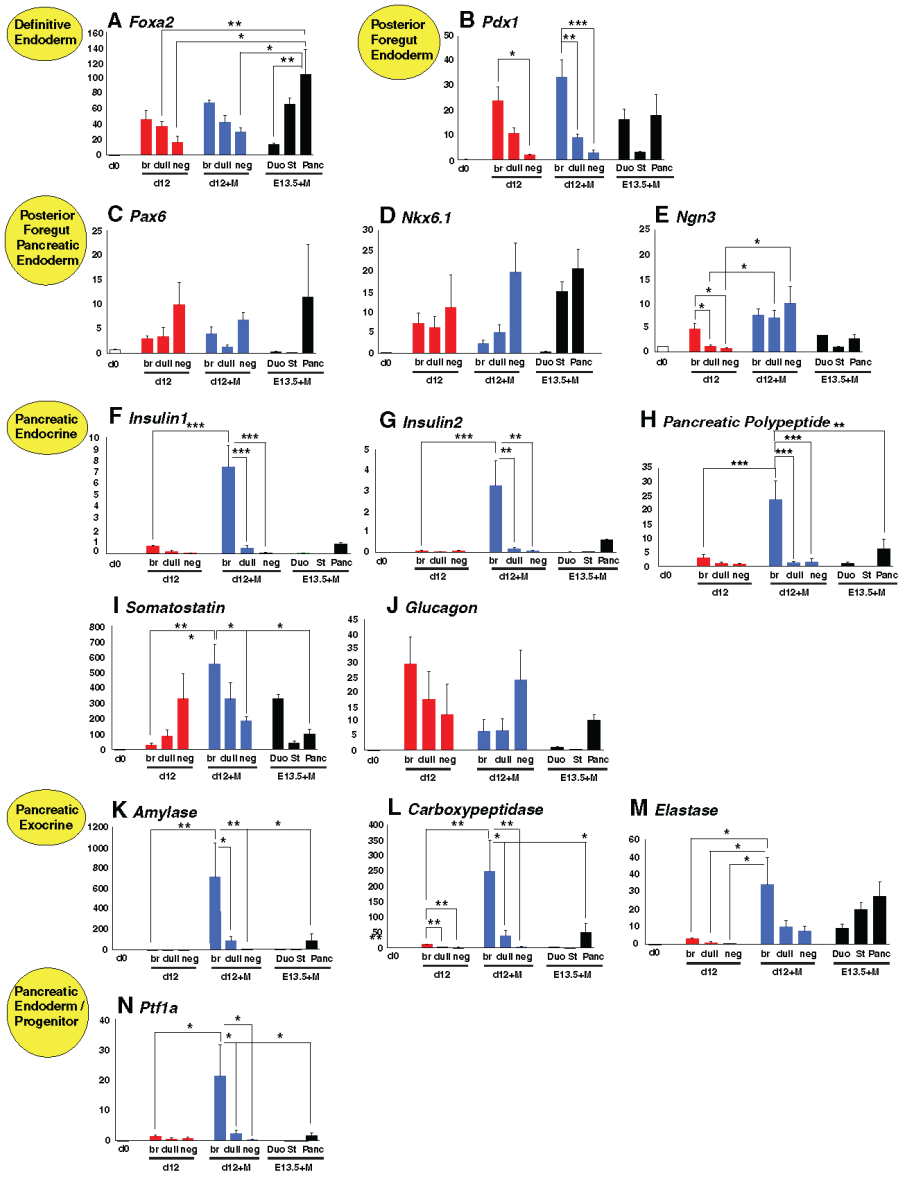


**FIG. 6.** Quantitative-PCR analysis of genes associated with pancreas development. Genes that were assayed included markers of **(A)** definitive endoderm *(Foxa2)*, **(B)** posterior foregut endoderm *(Pdx1)*, **(C–E)** posterior foregut pancreatic endoderm *(Pax6, Nkx6.1, Ngn3)*, **(F–J)** pancreatic endocrine *(Insulin1, Inulin2, Pancreatic Polypeptide, Somatostatin, Glucagon)*, and **(K–N)** pancreatic exocrine cells *(Amylase, Carboxypeptidase A1, Elastase, Ptf1a)*. Undifferentiated d0 ESCs are denoted as a *black* outline, d12 $GFP^{br}$, $GFP^{dull}$, and $GFP^{neg}$ EBs *(red)*; d12 + 8 days Matrigel explant culture of d12 $GFP^{br}$, $GFP^{dull}$, and $GFP^{neg}$ EBs, respectively *(blue)* and E13.5 + 8 days Matrigel culture of duodenum, stomach, and $Pdx1^{+}$ pancreatic rudiments *(black)*. Error bars are represented as the SEM from 3 independent experiments. Relative gene expression was calculated as the ratio of the value obtained for the test gene, relative to the value obtained for *Gapdh*. Student's *t*-test values of $^{*}P < 0.05$, $^{**}P < 0.01$, and $^{***}P < 0.005$ were considered as statistically significant. EBs, embryoid bodies. Color images available online at www.liebertonline.com/scd

Fig. S2A–P). Moreover, the intensity of GFP expression associated with the structures that did develop was discernibly lower than that present in the pancreatic derived counterparts. In addition, the dimensions of these tubular-like structures, which were already pronounced by d4, continued to expand in size, such that by day 6, pulsating waves of peristaltic contractions could be observed (data not shown). This phenomenon was also apparent in explant cultures derived from the duodenum.

The frequency of branching structures observed in cultures initiated with in vitro and in vivo cell populations is summarized in Fig. 4. These results indicate that Pdx1-GFP$^+$ pancreatic rudiments formed on average, 51.6±27.4 (mean± SEM, $n$=4 experiments) branching structures (Fig. 4A), while none were scored for the proximal duodenum and distal stomach explants (Fig. 4A). By comparison, GFP$^{br}$ bud containing EBs yielded ~31±12.6 (mean±SEM, $n$=6 experiments) branching organoids (Fig. 4B). As indicated, the number of similar structures derived from GFP$^{dull}$ or GFP$^{neg}$ EBs was negligible. Overall, these analyses vindicate the assignment of separate identities to EBs containing different levels of GFP expression and strengthen the conclusion that only those containing GFP$^{br}$ buds contain pancreatic progenitors.

Histological analysis of GFP$^+$ material collected from d12 Matrigel cultures indicated that branching structures contained cells of both epithelial and mesenchymal appearance. Branching organoids also characteristically contained multiple luminal epithelial ducts and adjacent to these, lobulated acinar-like structures (Fig. 4C–J). These small foci contained ductules with histological characteristics of acinar cells that were organized into discrete lobulated clusters containing abundant granular eosinophilic cytoplasm. These results, in combination with those described above, suggest that EBs containing GFP$^{br}$ buds harbored precursors capable of giving rise to structures in Matrigel that resembled branching organoids generated from fetal pancreatic explants.

The results above suggested that d12 GFP$^{br}$ EBs and E13.5 fetal pancreata contained pancreatic progenitors with a similar degree of developmental maturity. To explore this possibility further, we undertook a detailed analysis of branching structures derived from these 2 complementary experimental systems. In the first instance, we used immunofluorescence analysis to examine the expression of a cohort of pancreas-associated markers. Characterization of branching organoids derived from d12 GFP$^{br}$ EBs and E13.5 fetal pancreata showed that the explant cultures contained cells expressing the epithelial markers EpCAM (Supplementary Fig. S3C, D) and E-Cadherin (Fig. 5A, B). These markers were expressed on both GFP$^+$ and GFP$^{neg}$ cells, implying that Pdx1$^-$ epithelial cell types were present in the Matrigel cultures representing both in vitro and in vivo sources. Double staining of cells with antibodies recognizing GFP/Pdx1 (Supplementary Fig. S3A, B), Amylase (Fig. 5C, D), or Carboxypeptidase A1 (Cpa1) (Fig. 5E, F) revealed that cells expressing these exocrine markers formed localized foci that were integrated within the Pdx1-GFP$^+$ epithelium. Branching structures derived from both EBs and pancreata also expressed Mucin1 (Muc1), an apical cell surface epithelial and ductal marker (Fig. 5G, H). Indeed, we observed that branching epithelial foci were always associated with small developing Muc1$^+$ lumina (Fig. 5G, H). Similarly, scattered clusters of Glucagon$^+$ cells were also detected in the GFP$^+$ areas (Fig. 5I, J). Sparsely distributed single Somatostatin$^+$ (SST) cells were only occasionally observed and these were not always confined to GFP$^+$ epithelia (Fig. 5K, L). Significantly, no Insulin$^+$ cells were detected in the branching explant cultures, even in instances where the beta cell differentiation agent, Nicotinamide, was added to the cultures (data not shown).

The above immunofluorescence studies were complemented with quantitative (Q)-PCR gene expression assays, providing information regarding the overall gene expression profile of cells associated with selected GFP$^+$ and GFP$^{neg}$ epithelial structures within the Matrigel cultures (Fig. 6 and Supplementary). Gene expression analysis of GFP$^+$ and GFP$^{neg}$ cells isolated from E16.5 and E19.5 fetal pancreas demonstrates stage-specific expression profiles. Correlation of these profiles with in vitro generated cells enables elucidation of their representative developmental stage. Indeed, Q-PCR analysis of genes associated with pancreas development was enriched in E16.5 and E19.5 GFP$^+$ sorted cells (Supplementary Fig. S4A–N). In this respect, the elevated levels of *Foxa2* associated with structures derived from GFP$^{br}$ bud containing-EBs most likely reflected the overall enrichment for endoderm when GFP$^+$ areas were selected, rather than an increased frequency of endoderm within the cultures overall (Fig. 6A). Similar arguments can be made for the higher levels of *Pdx1* expression observed in GFP$^{br}$ bud and fetal pancreatic derived cultures (Fig. 6B). Collectively, these analyses demonstrate that criteria for selecting specific subpopulations within these mixed cultures enable the isolation of comparable material representing EB and fetal pancreatic derived cells.

Markers of pancreas differentiation, such as the transcription factors *Pax6*, *Nkx6.1*, and *Ngn3* were also expressed at relatively low levels in both EBs and Matrigel samples compared with the levels observed in the E16.5 and E19.5 sorted fractions (Fig. 6C–E and Supplementary Fig. S4C–E). Interestingly *Pax6* and *Nkx6.1* were upregulated in GFP$^{neg}$ samples, perhaps suggesting that EBs contained other cell types in which these genes are expressed (Fig. 6C, D). Despite the fact that the expression of Insulin was not observed by immunofluorescence, branching organoids derived from GFP$^{br}$ bud containing-EBs expressed detectable levels of *Insulin1* and *Insulin2*. This result, combined with the observation that these organoids also expressed *Pancreatic Polypeptide*, *Somatostatin*, and *Glucagon* reaffirms the conclusion that pancreatic cells are enriched within the branching structures (Fig. 6F–J). This conclusion was also supported by the observation that expression of the exocrine markers *Amylase*, *Carboxypeptidase*, *Elastase*, and *Ptf1a* was also highest in samples representing GFP$^{br}$ bud EBs (Fig. 6K–N). Statistical analysis of Q-PCR was also performed using analysis of variance (Supplementary Fig. S5). Interestingly, expression of exocrine markers in Matrigel cultures was substantially higher than that observed for the corresponding d12 EBs, suggesting that further culture in Matrigel resulted in enrichment or maturation of exocrine cells. Reassuringly, expression of these markers was also enriched in cultures derived from pancreatic rudiments relative to that observed in explants from the distal stomach and proximal duodenum.

## Discussion

We have further refined a protocol for the differentiation of mouse ESCs to Pdx1$^+$ pancreatic progenitors that arise in

the context of structures that bear morphological similarities to the developing pancreas. Our method employed a chemically defined medium containing rHA, a modification that eliminated the high degree of variability associated with different batches of BSA previously used. Anecdotally, we had noted that some BSA batches were permissive for pancreatic differentiation while others were not. It is not clear whether these differences reflected pro-differentiative activities in the permissive batches or inhibitory factors in the nonpermissive batches. Nevertheless, in this current study we observed that FGF2 was required when using rHA-CDM to restore pancreatic differentiation to levels seen with "good" permissive batches of BSA-containing CDM.

Several previous studies have demonstrated the inductive role of notochord derived FGF2 during dorsal pancreas formation in chicken, mice, and humans [33–35]. Consistent with these findings, addition of FGF2 in our protocol also increased the frequency of Pdx1-GFP$^+$ endodermal cells. Although the mechanism of this effect was not investigated, we observed that FGF2 promoted the rapid outgrowth of mesenchymal cells after EBs were transferred to adherent plates (data not shown). It is therefore possible that this mesenchymal population produced factors that further enhanced the generation of Pdx1$^+$ endoderm.

The ability of extracellular matrix to regulate the adhesion, migration, proliferation, differentiation, and maintenance of mature cell function has been well documented in the pancreas, most notably in β-cell development [36–39], adult ductal and fetal pancreatic cells [40,41], and in ESCs [42]. In agreement with previous studies, we found that the commercial basement membrane preparation, Matrigel, proved an effective substrate for growth and expansion of Pdx1$^+$ pancreatic progenitor cells via a process that resembled branching morphogenesis. The use of cultured pancreatic explants as a suitable model for studying branching epithelial morphogenesis has been meticulously documented [32,43–48]. In the present study, we did not examine the mechanisms underlying pancreatic branching, however our observations of the branching dynamics for both ESC and embryo derived Pdx1$^+$ progenitors were similar to those previously reported [32,43–48]. We observed that disaggregated cell clusters derived from E13.5 Pdx1$^+$ pancreatic rudiments and d12 GFP$^{br}$ containing-EBs generated 3-dimensional epithelial structures that could be readily visualized and enumerated. In Matrigel, GFP$^+$ cells formed clusters, which over time, progressively increased in size and differentiated into structures that appeared morphologically similar to acinar tissue.

Our EB explants contained a mixture of epithelial and mesenchymal cell types. Mesenchymal to epithelial signaling, mediated in part by soluble factors, plays a critical role in cell proliferation and differentiation of early pancreatic progenitor cells during pancreatic development [49,50]. Moreover, the correlation between mesenchymal signaling, epithelial morphogenesis, and cytodifferentiation were revealed in previous explant studies, in which there was a preferential allocation of cells to the endocrine versus the exocrine compartment depending on the presence/absence of mesenchymal signals [32,51]. These studies confirmed that mesenchyme surrounding the epithelium adopted an instructive role during pancreatic development. Our observations from branching experiments were similar to those previously reported by others, where depletion of mesenchyme resulted in the abrogation of branching [32,50,51] (data not shown). We have

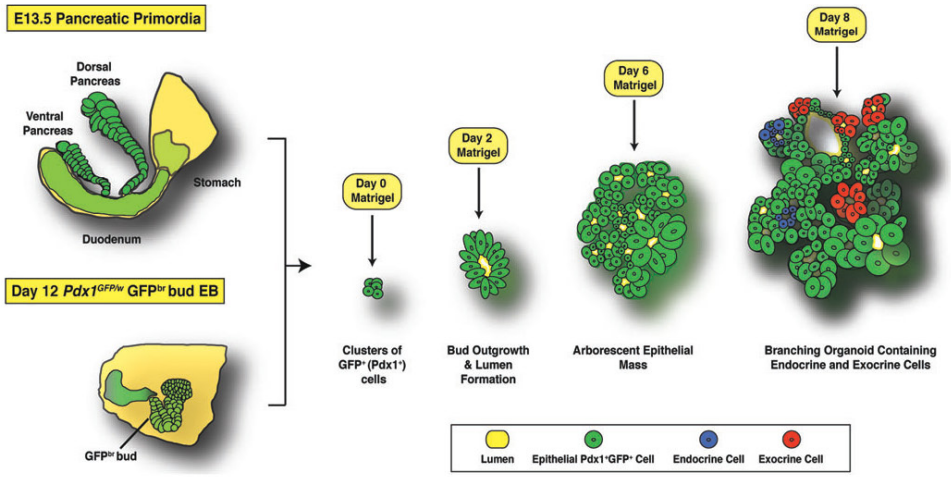


**FIG. 7.** Summary model of branching morphogenesis from ex vivo derived E13.5 Pdx1$^+$ pancreatic rudiments and in vitro cultured d12 GFP$^{br}$ bud cells. At d0 of explant culture, small clusters of GFP$^+$ cells coalesce, and these continue to generate bud outgrowths with the emergence of a central lumen. The continued proliferation of these bud outgrowths at d6, results in the formation of an arborescent epithelial mass with multiple lobules. By d8 the branching organoids contain precursor cells, which are representative of the endocrine, exocrine, and ductal cell lineages. Color images available online at www.liebertonline.com/scd

previously shown that day 12 GFP$^{br}$ EBs treated with nicotinamide for 7 days are able to differentiate to insulin-producing cells in vitro [25]. However, using the Matrigel culture system described here, insulin expression was unable to be induced even in the presence of nicotinamide, indicating that these culture conditions are not permissive for the differentiation of insulin-producing cells (data not shown). This interpretation is supported by studies demonstrating that Laminin-1, a major component of Matrigel, promotes the commitment of multipotent pancreatic progenitors to the acinar cell lineage [47]. In addition, a more recent study by Semb and colleagues demonstrated that disruption of epithelial tube formation in the developing pancreas resulted in an increase in acinar differentiation at the expense of endocrine differentiation, largely as a consequence of changes in epithelial cell polarity and epithelial-ECM interactions [47]. In this light, the study of Semb and colleagues is consistent with our observation that our Matrigel culture favored acinar versus endocrine differentiation. Therefore, reduced endocrine differentiation may have resulted either from the pro-acinar affects of laminin-1 within Matrigel or from the disruption of epithelial tube formation during the dissociation of pancreatic explants and GFP$^{br}$ EBs before Matrigel culture.

Although it was beyond the scope of the current study, future investigations will need to examine in greater detail the factors influencing the differentiation of these progenitors and whether the mesenchymal cells can be replaced by specific factors. In particular, Fgf10 [52] and laminin-1 [53, 54] have been shown to modulate the frequency and extent of branching morphogenesis in the absence and presence of an extracellular matrix.

Gene expression analysis of branching structures derived from both EBs and fetal pancreas indicated that our culture system favored the development of exocrine cell types. This was evident by the upregulation of markers such as Ptf1a/p48, Amylase, Carboxypeptidase, and Elastase, and the relatively low expression of genes associated with endocrine development. Although endocrine markers were present in branching structures, insulin$^+$ cells were never observed even in explants derived from the fetal pancreas (data not shown and Fig. 6F, G).

In summary, we have described a system in which mouse ESCs are able to mimic aspects of the pancreatic developmental program that results in the differentiation of cells from embryonic endoderm to the generation of pancreatic progenitors of the endocrine, exocrine, and ductal cell lineages (Fig. 7). Our data supports the notion that developmental pathways that regulate differentiation of the pancreatic cell lineages in the mouse embryo may also be partially recapitulated during the in vitro differentiation of mouse ESCs. Insight and knowledge from our findings may extend existing strategies for pancreatic lineage specific genetic selection and provide a novel foundation for research into pancreatic differentiation and disease.

## Acknowledgments

We would like to acknowledge Monash Micro Imaging Facility for the provision of instrumentation, training, and technical support from Mr. Stephen Firth, Mr. Chad Johnson, and Dr. Judy Callaghan and also Mr. Ian Boundy and Ms. Stefania Tombs at the Department of Anatomy and Histology, Monash University. We thank Professor Chris Wright for provision of the anti-mouse Pdx1 antibody. This work was supported by The National Health and Medical Research Council (NHMRC) of Australia and the Juvenile Diabetes Research Foundation (JDRF). AGE and EGS are both Senior Research Fellows of the NHMRC.

## Author Disclosure Statement

The authors have no conflict of interest.

## References

1. Jonsson J, L Carlsson, T Edlund and H Edlund. (1994). Insulin-promoter-factor 1 is required for pancreas development in mice. Nature 371:606–609.
2. Guz Y, MR Montminy, R Stein, J Leonard, LW Gamer, CV Wright and G Teitelman. (1995). Expression of murine STF-1, a putative insulin gene transcription factor, in beta cells of pancreas, duodenal epithelium and pancreatic exocrine and endocrine progenitors during ontogeny. Development 121:11–18.
3. Offield MF, TL Jetton, PA Labosky, M Ray, RW Stein, MA Magnuson, BLM Hogan and CVE Wright. (1996). PDX-1 is required for pancreatic outgrowth and differentiation of the rostral duodenum. Development 122:983–995.
4. Stoffers DA, NT Zinkin, V Stanojevic, WL Clarke and JF Habener. (1997). Pancreatic agenesis attributable to a single nucleotide deletion in the human IPF1 gene coding sequence. Nat Genet 15:106–110.
5. Schwitzgebel VM, A Mamin, T Brun, B Ritz-Laser, M Zaiko, A Maret, FR Jornayvaz, GE Theintz, O Michielin, D Melloul and J Philippe. (2003). Agenesis of human pancreas due to decreased half-life of insulin promoter factor 1. J Clin Endocrinol Metab 88:4398–406.
6. Ohlsson H, K Karlsson and T Edlund. (1993). IPF1, a homeodomain-containing transactivator of the insulin gene. EMBO J 12:4251–4259.
7. Kim SK and M Hebrok. (2001). Intercellular signals regulating pancreas development and function. Genes Dev 15: 111–27.
8. Li H, S Arber, TM Jessell and H Edlund. (1999). Selective agenesis of the dorsal pancreas in mice lacking homeobox gene Hlxb9. Nat Genet 23:67–70.
9. Gu G, J Dubauskaite and DA Melton. (2002). Direct evidence for the pancreatic lineage: NGN3+ cells are islet progenitors and are distinct from duct progenitors. Development 129: 2447–2457.
10. Evans MJ and MH Kaufman. (1981). Establishment in culture of pluripotential cells from mouse embryos. Nature 292:154–156.
11. Martin GR. (1981). Isolation of a pluripotent cell line from early mouse embryos cultured in medium conditioned by teratocarcinoma stem cells. Proc Natl Acad Sci U S A 78:7634–7638.
12. Soria B, E Roche, G Berna, T Leon-Quinto, JA Reig and F Martin. (2000). Insulin-secreting cells derived from embryonic stem cells normalize glycemia in streptozotocin-induced diabetic mice. Diabetes 49:157–162.
13. Hori Y, IC Rulifson, BC Tsai, JJ Heit, JD Cahoy and SK Kim. (2002). Growth inhibitors promote differentiation of insulin-producing tissue from embryonic stem cells. Proc Natl Acad Sci U S A 99:16105–16110.
14. Kubo A, K Shinozaki, JM Shannon, V Kouskoff, M Kennedy, S Woo, HJ Fehling and G Keller. (2004). Development of

definitive endoderm from embryonic stem cells in culture. Development 131:1651–1662.
15. Leon-Quinto T, J Jones, A Skoudy, M Burcin and B Soria. (2004). In vitro directed differentiation of mouse embryonic stem cells into insulin-producing cells. Diabetologia 47:1442–1451.
16. D'Amour KA, AD Agulnick, S Eliazer, OG Kelly, E Kroon and EE Baetge. (2005). Efficient differentiation of human embryonic stem cells to definitive endoderm. Nat Biotechnol 23:1534–1541.
17. Mfopou JK, E Willems, L Leyns and L Bouwens. (2005). Expression of regulatory genes for pancreas development during murine embryonic stem cell differentiation. Int J Dev Biol 49:915–922.
18. Micallef SJ, ME Janes, K Knezevic, RP Davis, AG Elefanty and EG Stanley. (2005). Retinoic acid induces Pdx1-positive endoderm in differentiating mouse embryonic stem cells. Diabetes 54:301–305.
19. Tada S, T Era, C Furusawa, H Sakurai, S Nishikawa, M Kinoshita, K Nakao and T Chiba. (2005). Characterization of mesendoderm: a diverging point of the definitive endoderm and mesoderm in embryonic stem cell differentiation culture. Development 132:4363–4374.
20. Yasunaga M, S Tada, S Torikai-Nishikawa, Y Nakano, M Okada, LM Jakt, S Nishikawa, T Chiba and T Era. (2005). Induction and monitoring of definitive and visceral endoderm differentiation of mouse ES cells. Nat Biotechnol 23:1542–1550.
21. D'Amour KA, AG Bang, S Eliazer, OG Kelly, AD Agulnick, NG Smart, MA Moorman, E Kroon, MK Carpenter and EE Baetge. (2006). Production of pancreatic hormone-expressing endocrine cells from human embryonic stem cells. Nat Biotechnol 24:1392–1401.
22. Gadue P, TL Huber, PJ Paddison and GM Keller. (2006). Wnt and TGF-beta signaling are required for the induction of an in vitro model of primitive streak formation using embryonic stem cells. Proc Natl Acad Sci U S A 103:16806–16811.
23. Miralles F, L Lamotte, D Couton and RL Joshi. (2006). Interplay between FGF10 and Notch signalling is required for the self-renewal of pancreatic progenitors. Int J Dev Biol 50:17–26.
24. Vaca P, F Martin, JM Vegara-Meseguer, JM Rovira, G Berna and B Soria. (2006). Induction of differentiation of embryonic stem cells into insulin-secreting cells by fetal soluble factors. Stem Cells 24:258–265.
25. Micallef SJ, X Li, ME Janes, SA Jackson, RM Sutherland, AM Lew, LC Harrison, AG Elefanty and EG Stanley. (2007). Endocrine cells develop within pancreatic bud-like structures derived from mouse ES cells differentiated in response to BMP4 and retinoic acid. Stem Cell Res 1:25–36.
26. Kroon E, LA Martinson, K Kadoya, AG Bang, OG Kelly, S Eliazer, H Young, M Richardson, NG Smart, et al. (2008). Pancreatic endoderm derived from human embryonic stem cells generates glucose-responsive insulin-secreting cells in vivo. Nat Biotechnol 26:443–452.
27. Micallef SJ, X Li, AG Elefanty and EG Stanley. (2007). Pancreas differentiation of mouse ES cells. Curr Protoc Stem Cell Biol Chapter 1:Unit 1G 2.
28. Ng ES, RP Davis, L Azzola, EG Stanley and AG Elefanty. (2005). Forced aggregation of defined numbers of human embryonic stem cells into embryoid bodies fosters robust, reproducible hematopoietic differentiation. Blood 106:1601–1603.
29. Holland AM, SJ Micallef, X Li, AG Elefanty and EG Stanley. (2006). A mouse carrying the green fluorescent protein gene targeted to the Pdx1 locus facilitates the study of pancreas development and function. Genesis 44:304–307.
30. Lim SM, L Pereira, MS Wong, CE Hirst, BE Van Vranken, M Pick, A Trounson, AG Elefanty and EG Stanley. (2009). Enforced expression of Mixl1 during mouse ES cell differentiation suppresses hematopoietic mesoderm and promotes endoderm formation. Stem Cells 27:363–374.
31. Pick M, L Azzola, A Mossman, EG Stanley and AG Elefanty. (2007). Differentiation of human embryonic stem cells in serum-free medium reveals distinct roles for bone morphogenetic protein 4, vascular endothelial growth factor, stem cell factor, and fibroblast growth factor 2 in Hematopoiesis. Stem Cells 25:2206–2214.
32. Gittes GK, PE Galante, D Hanahan, WJ Rutter and HT Debase. (1996). Lineage-specific morphogenesis in the developing pancreas: role of mesenchymal factors. Development 122:439–447.
33. Hebrok M, SK Kim and DA Melton. (1998). Notochord repression of endodermal Sonic hedgehog permits pancreas development. Genes Dev 12:1705–1713.
34. Kim SK and RJ MacDonald. (2002). Signaling and transcriptional control of pancreatic organogenesis. Curr Opin Genet Dev 12:540–547.
35. Ameri J, A Stahlberg, J Pedersen, JK Johansson, MM Johannesson, I Artner and H Semb. (2010). FGF2 specifies hESC-derived definitive endoderm into foregut/midgut cell lineages in a concentration-dependent manner. Stem Cells 28:45–56.
36. Lammert E, O Cleaver and D Melton. (2001). Induction of pancreatic differentiation by signals from blood vessels. Science 294:564–567.
37. Yoshitomi H and KS Zaret. (2004). Endothelial cell interactions initiate dorsal pancreas development by selectively inducing the transcription factor Ptf1a. Development 131:807–817.
38. Nikolova G, N Jabs, I Konstantinova, A Domogatskaya, K Tryggvason, L Sorokin, R Fassler, G Gu, HP Gerber, et al. (2006). The vascular basement membrane: a niche for insulin gene expression and Beta cell proliferation. Dev Cell 10:397–405.
39. Hamamoto K, S Yamada, A Hara, T Kodera, M Seno and I Kojima. (2011). Extracellular matrix modulates insulin production during differentiation of AR42J cells: functional role of Pax6 transcription factor. J Cell Biochem 112:318–329.
40. Jiang FX, DS Cram, HJ DeAizpurua and LC Harrison. (1999). Laminin-1 promotes differentiation of fetal mouse pancreatic beta-cells. Diabetes 48:722–730.
41. Bonner-Weir S, M Taneja, GC Weir, K Tatarkiewicz, KH Song, A Sharma and JJ O'Neil. (2000). In vitro cultivation of human islets from expanded ductal tissue. Proc Natl Acad Sci U S A 97:7999–8004.
42. Schroeder IS, A Rolletschek, P Blyszczuk, G Kania and AM Wobus. (2006). Differentiation of mouse embryonic stem cells to insulin-producing cells. Nat Protoc 1:495–507.
43. Percival AC and JM Slack. (1999). Analysis of pancreatic development using a cell lineage label. Exp Cell Res 247:123–132.
44. Horb LD and JMW Slack. (2000). Role of cell division in branching morphogenesis and differentiation of the embryonic pancreas. Int J Dev Biol 44:791–796.
45. Puri S and M Hebrok. (2007). Dynamics of embryonic pancreas development using real-time imaging. Dev Biol 306:82–93.

46. Hick AC, JM van Eyll, S Cordi, C Forez, L Passante, H Kohara, T Nagasawa, P Vanderhaeghen, PJ Courtoy, et al. (2009). Mechanism of primitive duct formation in the pancreas and submandibular glands: a role for SDF-1. BMC Dev Biol 9:66.
47. Kesavan G, FW Sand, TU Greiner, JK Johansson, S Kobberup, XW Wu, C Brakebusch and H Semb. (2009). Cdc42-Mediated Tubulogenesis Controls Cell Specification. Cell 139:791–801.
48. Villasenor A, DC Chong, M Henkemeyer and O Cleaver. (2010). Epithelial dynamics of pancreatic branching morphogenesis. Development 137:4295–4305.
49. Pictet R. (1972). Development of the embryonic pancreas. In: *Handbook of Physiology. Section 7: Endocrinology*. D Steiner, ed. Williams and Wilkins, Baltimore, pp 25–66.
50. Attali M, V Stetsyuk, A Basmaciogullari, V Aiello, MA Zanta-Boussif, B Duvillie and R Scharfmann. (2007). Control of beta-cell differentiation by the pancreatic mesenchyme. Diabetes 56:1248–1258.
51. Miralles F, P Czernichow and R Scharfmann. (1998). Follistatin regulates the relative proportions of endocrine versus exocrine tissue during pancreatic development. Development 125:1017–1024.
52. Bhushan A, N Itoh, S Kato, JP Thiery, P Czernichow, S Bellusci and R Scharfmann. (2001). Fgf10 is essential for maintaining the proliferative capacity of epithelial progenitor cells during early pancreatic organogenesis. Development 128:5109–5117.
53. Li L, M Seno, H Yamada and I Kojima. (2001). Promotion of beta-cell regeneration by betacellulin in ninety percent-pancreatectomized rats. Endocrinology 142:5379–5385.
54. Crisera CA, AS Kadison, GD Breslow, TS Maldonado, MT Longaker and GK Gittes. (2000). Expression and role of laminin-1 in mouse pancreatic organogenesis. Diabetes 49: 936–944.

Address correspondence to:
*Dr. Suzanne J. Micallef*
*Monash Immunology and Stem Cell Laboratories (MISCL)*
*Monash University*
*Level 3, Building 75*
*STRIP1, West Ring Road*
*Clayton*
*Victoria, 3800*
*Australia*

*E-mail:* suzanne.micallef@monash.edu

Received for publication September 11, 2011
Accepted after revision October 27, 2011
Prepublished on Liebert Instant Online October 28, 2011

# APELIN promotes hematopoiesis from human embryonic stem cells

*Qing C. Yu,[1] *Claire E. Hirst,[1] Magdaline Costa,[1] Elizabeth S. Ng,[1] Jacqueline V. Schiesser,[1] Karin Gertow,[2] Edouard G. Stanley,[1,3] and Andrew G. Elefanty[1,3]

[1]Monash Immunology and Stem Cell Laboratories, Monash University, Clayton, Australia; [2]School of Biotechnology, AlbaNova University Center, The Royal Institute of Technology, Stockholm, Sweden; and [3]Murdoch Childrens Research Institute, The Royal Children's Hospital, Parkville, Victoria, Australia

**Transcriptional profiling of differentiating human embryonic stem cells (hESCs) revealed that *MIXL1*-positive mesodermal precursors were enriched for transcripts encoding the G-protein–coupled *APELIN* receptor (*APLNR*). APLNR-positive cells, identified by binding of the fluoresceinated peptide ligand, APELIN (APLN), or an anti-APLNR mAb, were found in both posterior mesoderm and anterior mesendoderm populations and were enriched in hemangioblast colony-forming cells (Bl-CFC). The addition of APLN peptide to the media enhanced the growth of embryoid bodies (EBs), increased the expression of hematoendothelial genes in differentiating hESCs, and increased the frequency of Bl-CFCs by up to 10-fold. Furthermore, APLN peptide also synergized with VEGF to promote the growth of hESC-derived endothelial cells. These studies identified APLN as a novel growth factor for hESC-derived hematopoietic and endothelial cells. (*Blood*. 2012;119(26): 6243-6254)**

## Introduction

During embryogenesis, hematopoietic and vascular lineages arise from extraembryonic and lateral plate mesoderm, derivatives of the posterior and mid regions of the primitive streak (PS), respectively.[1] In mouse embryos, the PS appears at embryonic day 6.25 and early stages of mesoderm induction can be tracked by monitoring the expression of key transcription factors such as *Brachyury*[2] and *Mixl1*,[3,4] or cell-surface molecules like Flk-1 and PDGFRα.[5,6]

Given that the in vitro differentiation of human embryonic stem cells (hESCs) recapitulates aspects of vertebrate development,[7] it is not surprising that, analogous to the mouse, genes such as *BRACHYURY*, *MIXL1*, *KDR* (the human *Flk-1* homologue), and *PDGFRα* are expressed during the in vitro mesoderm differentiation of hESCs.[8,9] Hemangioblasts, common hematovascular progenitors that emerge from the posterior PS in the mouse embryo,[10] also appear in cultures of differentiating mouse[11] and human[8,9] ESCs after 2-4 days and are followed by the later emergence of primitive erythroid cells, macrophage, and other myeloid and lymphoid lineages.[12-15]

We have established an in vitro hESC differentiation system to study the development of early hematopoietic mesoderm in a defined, serum-free medium, showing that exogenously added TGFβ-family molecules induce primitive streak-like cells that subsequently differentiate into blood.[16-18] To assist in these studies, we modified a hESC line by inserting GFP into the locus of the *MIXL1* homeobox gene (*MIXL1*$^{GFP/w}$), thus enabling identification and isolation of viable, PS-like cells.[8]

To discover cell-surface markers and growth factors that would facilitate the identification and generation of hematopoietic lineages, we performed transcriptional profiling during mesoderm induction from *MIXL1*$^{GFP/w}$ hESCs in cell populations isolated based on their expression of E-CADHERIN (E-CAD), PDGFRα, and GFP. Analysis of these populations demonstrated that GFP$^+$PDGFRα$^+$ and E-CAD$^-$GFP$^+$ cells were highly enriched for the expression of the G-protein–coupled APELIN receptor,[19] consistent with the expression of the peptide ligand, APELIN (APLN),[20] and its cognate receptor (APLNR) in the PS of the mouse embryo.[21] Isolated APLNR$^+$ cell populations were enriched in hemangioblast colony-forming cells (Bl-CFCs), as also shown in a recent report.[13] We extended these prior observations by showing that APLNR expression was also observed in MIXL1$^+$ cells representing the anterior primitive streak, a region harboring cells fated to become dorsal mesoderm and endoderm.[8,22-24] Furthermore, we showed that APLN enhanced the growth of embryoid bodies (EBs), increased the frequency of hemangioblast colonies, and synergized with VEGF to increase growth of endothelial cells. Collectively, our study demonstrates that APLN is a growth factor that can promote hematopoietic differentiation of hESCs and suggests a hitherto unrecognized role for the APLN/APLNR axis in the regulation of early human hematopoiesis.

## Methods

### Cell culture and differentiation

The HES3,[25] MEL1 (Millipore), H9 (WiCell Research Institute), and *MIXL1*$^{GFP/w}$ HES3[8] hESC lines were passaged and differentiated as spin EBs in APEL medium[16,17] supplemented with the following growth factor combinations: 100 ng/mL fibroblast growth factor 2 (FGF2); BVS (30 ng/mL bone morphogenetic protein [BMP4], 30 ng/mL VEGF, 40 ng/mL SCF); B$^{lo}$VSA$^{hi}$ (5 ng/mL BMP4, 30 ng/mL VEGF, 40 ng/mL SCF, 100 ng/mL ACTIVIN A); BV$^{hi}$S (40 ng/mL BMP4, 50 ng/mL VEGF, 25 ng/mL SCF); BVSA (20 ng/mL BMP4, 30 ng/mL VEGF, 40 ng/mL SCF, 20 ng/mL ACTIVIN A); and BVSW (30 ng/mL BMP4, 30 ng/mL VEGF, 40 ng/mL SCF, 100 ng/mL Wnt3a). BMP4, FGF2, VEGF, and SCF were purchased

Submitted December 1, 2011; accepted May 12, 2012. Prepublished online as *Blood* First Edition paper, May 18, 2012; DOI 10.1182/blood-2011-12-396093.

*Q.C.Y. and C.E.H. contributed equally to this study.

The online version of this article contains a data supplement.

The publication costs of this article were defrayed in part by page charge payment. Therefore, and solely to indicate this fact, this article is hereby marked "advertisement" in accordance with 18 USC section 1734.

from PeproTech, and ACTIVIN A from R&D Systems. In some cultures, 50 ng/mL APELIN-13 pyroglutamate (APLN; Sigma-Aldrich) was added. Work on hESCs was approved by the Monash University Human Research Ethics Committee.

To identify Bl-CFCs, dissociated day 3 EBs were cultured at 5 to $10 \times 10^3$ cells/well in serum-free MethoCult (StemCell Technologies) or in a formulation denoted MC-APEL (1% methylcellulose in APEL medium). MethoCult cultures were supplemented with 30 ng/mL VEGF, 50 ng/mL SCF, and 3 U/mL erythropoietin (EPO) with or without 50 ng/mL APLN, while 10 ng/mL FGF2 was also added to MC-APEL cultures to facilitate the efficient generation of Bl-CFCs.

To bias differentiation toward hematopoiesis, after 4 days in BVS, EBs were cultured in fresh medium with 20 ng/mL BMP4, 50 ng/mL VEGF, 50 ng/mL SCF, 10 ng/mL FGF2, and 30 ng/mL insulin-like growth factor 2 (IGF2).

Endothelial differentiation of hESCs was induced in $BV^{hi}S$. After sorting day 6 EBs for $CD34^{bright\ (br)}KDR^{br}$ progenitors, cells were matured in medium with 50 ng/mL VEGF, with or without APLN addition.

Endodermal differentiation of hESCs was induced in $B^{lo}VSA^{hi}$ for 3 days. Cells were sorted based on EPCAM and APLNR expression, reaggregated and cultured further in APEL containing 400 ng/mL noggin (R&D Systems). At day 6, medium was replaced with APEL containing $10^{-5}$M retinoic acid (RA). At day 9, the medium was changed to APEL without polyvinyl alcohol (AEL) containing $10^{-5}$M RA, 100μM glucagon-like peptide-1, B27, and 10mM nicotinamide. At day 15 of differentiation, EBs were transferred to gelatinized 96-well plates and further maturation was induced in AEL containing 10mM nicotinamide and 50 ng/mL IGF-1.[26]

### Immunofluorescence of adherent cells cultured from hemangioblast colonies

Hemangioblast colonies generated from day 3 EBs were grown for 4 days in methylcellulose, and individual colonies were replated onto gelatinized plates in medium with 30 ng/mL VEGF, 50 ng/mL SCF, and 3 U/mL erythropoietin with or without 50 ng/mL APLN. To assess low-density lipoprotein (LDL) uptake, adherent cells were incubated overnight with 10 μg/mL DiI-labeled acetylated LDL (Molecular Probes), washed in PBS, and imaged. For immunofluorescence, cells were fixed with 4% paraformaldehyde, permeabilized in 0.1% Triton X-100, washed in PBS then blocked in PBS/2% FCS/1% goat serum/1% rabbit serum before sequential incubation with mouse anti–human smooth muscle actin (SMA; DAKO), anti–mouse AlexaFluor 488 (Molecular Probes), and 4′,6-diamino-2-phenylindole (DAPI; Sigma-Aldrich). Alternatively, unfixed adherent cells were stained with mouse anti–human CD34 (BD Pharmingen) followed by anti–mouse AlexaFluor 594 and DAPI. Images were captured on a Zeiss Axiovert 200 microscope and processed with Axiovision software (Carl Zeiss).

### Flow cytometric analysis

Embryoid bodies were dissociated, and single-cell suspensions were labeled with the following Abs: mouse anti–human E-CADHERIN (Zymed), allophycocyanin-conjugated goat anti–mouse Ig, mouse anti–human PDGFRα, PE-conjugated anti–human IgG, PE-conjugated anti–human EPCAM, PE-conjugated anti–human CD34, allophycocyanin-conjugated anti–human CD33, allophycocyanin-conjugated anti–human CD41a, allophycocyanin-conjugated anti–human GLYCOPHORIN A (CD235a), PE-conjugated anti–human CD45 (all from BD Biosciences), allophycocyanin-conjugated anti–human CD43 (BioLegend), and allophycocyanin-conjugated anti–human APLNR (R&D Systems). Binding and internalization of fluoresceinated APELIN-13 pyroglutamate (APLN-13-Fl; Sigma-Aldrich) was also used to identify APLNR-expressing cells. EBs were cultured with APLN-13-Fl at 400 ng/mL for 4 hours at 37°C before dissociation, followed by labeling with Abs directed to either PDGFRα or EPCAM. Flow cytometric analysis was performed using FACSCalibur, and cell sorting was done using an Influx cell sorter (BD Biosciences).

### Microarray analysis

Total RNA was prepared using the High Pure RNA Isolation Kit (Roche Applied Science) according to the manufacturer's instructions. RNA samples were amplified, labeled, and hybridized to Human WG-6 Version 2.0 and HT-12 Version 3 BeadChips (Illumina) by the Australian Genome Research Facility (http://www.agrf.org.au/). Data were analyzed with GenomeStudio Gene Expression Module Version 1.7 (Illumina) using average normalization across all samples. Subsequent data analysis was performed using MultiExperiment Viewer.[27] Hierarchical clustering of genes was performed using Pearson correlation with average linkage clustering. Data are available at ArrayExpress (http://www.ebi.ac.uk/microarray_as/ae/) via accession number E-MEXP-3380.

### Gene expression analysis

Selected microarray data were validated by quantitative real-time PCR using RNA extracted from the same samples used for microarray analysis. Samples harvested at indicated time points during endoderm differentiation were also analyzed by real-time PCR. TaqMan gene expression probes (Applied Biosystems) are shown in supplemental Table 1 (available on the *Blood* Web site; see the Supplemental Materials link at the top of the online article). Relative gene expression levels were calculated as described.[18]

### Morphologic analysis of day 4 differentiating EBs

Day 4 EBs were collected, washed with PBS buffer, and fixed for 20 minutes in 4% paraformaldehyde. Fixed EBs were rinsed in PBS and embedded in 0.7% low-melt agarose and subsequently in paraffin. Histologic sections of day 4 EBs were stained with H&E and images were captured on an Olympus BX51 upright microscope.

## Results

### The APLNR is highly expressed during mesendodermal differentiation

Previous studies in both mouse and human ESCs demonstrated that induction of *MIXL1* expression during the early stages of mesoderm differentiation was followed by the reciprocal down-regulation of E-CAHERIN (E-CAD) and up-regulation of PDGFRα expression.[8,24] Therefore, to identify additional cell-surface markers of mesodermal precursors, we flow-sorted differentiated GFP-positive, MIXL1-expressing progenitor cells from $MIXL1^{GFP/W}$ hESCs,[8] further separating them on the basis of either E-CAD or PDGFRα expression (Figure 1). RNA was extracted from the sorted cell subpopulations, and transcriptional profiles were analyzed using Illumina whole-genome arrays. We identified 162/48 701 probes (148 genes) that were up-regulated at least 5-fold in the $E\text{-}CAD^{-}GFP^{+}$ ($E^{-}G^{+}$) mesoderm population compared with the least differentiated $E\text{-}CAD^{+}GFP^{-}$ ($E^{+}G^{-}$) cell fraction (Figure 1C). A similar number of probes (162 probes, 144 genes) were differentially expressed in samples derived from an independent experiment in which a $GFP^{br}PDGFR\alpha^{+}$ ($G^{br}P^{+}$) nascent mesoderm fraction was compared with a less differentiated $GFP^{-}PDGFR\alpha^{-}$ ($G^{-}P^{-}$) fraction (Figure 1D). Consistent with the reciprocal expression of E-CADHERIN and PDGFRα during mesendodermal induction, 126 (76%) of 166 of the genes up-regulated in the mesoderm fraction were common to both experiments (Figure 1E). In addition to *MIXL1* and *PDGFRα*, the list of genes also included other primitive streak markers such as *DKK1*, *FOXF1*, *TBX3*, *EOMES*, *LHX1*, *NCAM1*, *MESP1*, *MSX1*, and members of the *HOXB* cluster (supplemental Table 2), validating our conclusion that both the $G^{br}P^{+}$ and $E^{-}G^{+}$ fractions marked similar populations.

In addition to previously characterized mesendodermal genes, we found that the *APLNR* (also known as *AGTRL1/hAPJ*),[19] a G-protein–coupled receptor for the peptide ligand APELIN (APLN),[20,28] was highly enriched in both $E^{-}G^{+}$ and $G^{br}P^{+}$

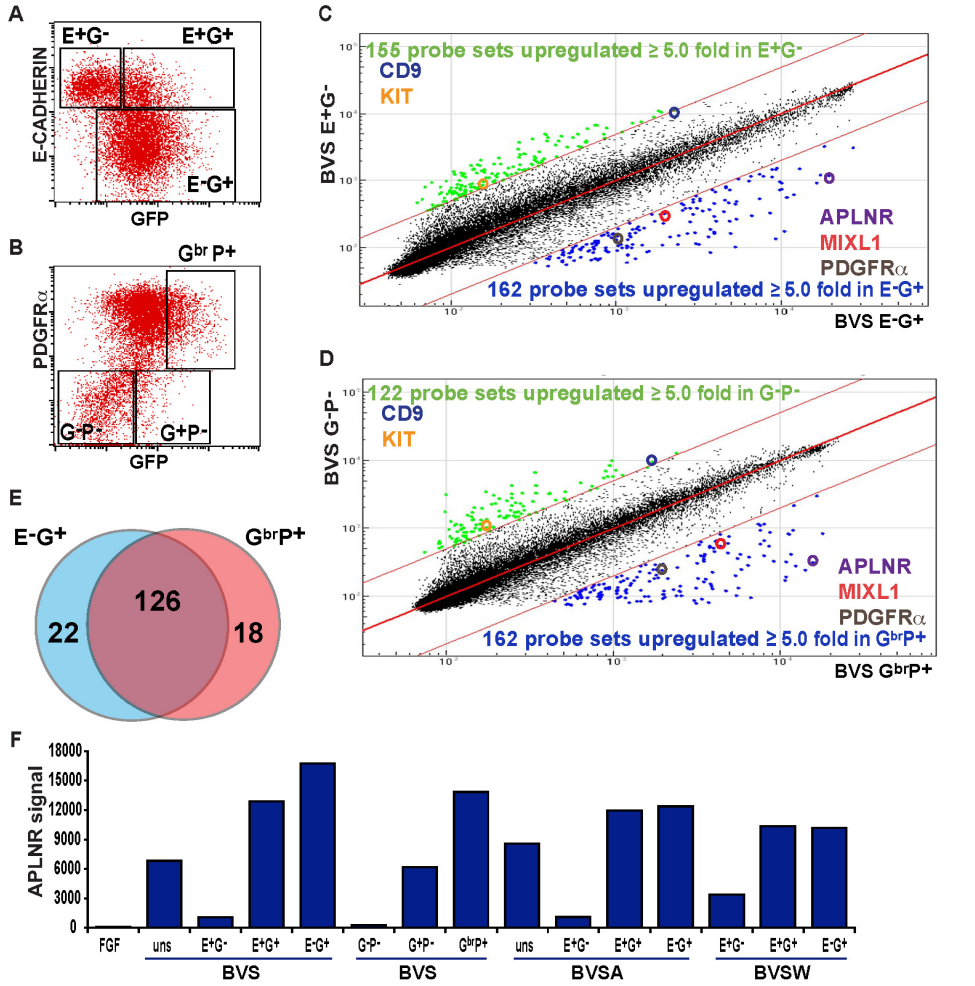


**Figure 1. APLNR expression during mesoderm induction.** Flow cytometric analysis of (A) E-CADHERIN and GFP and (B) PDGFRα and GFP expression in *MIXL1*$^{GFP/w}$ EBs differentiated in medium supplemented with mesodermal-inducing growth factors (BVS). Regions used to sort cells into fractions for further analysis are shown. Comparison of transcriptional profiles of sorted (C) E-CAD$^+$GFP$^-$ (E$^+$G$^-$) versus E-CAD$^-$GFP$^+$ (E$^-$G$^+$) cells and (D) GFP$^-$PDGFRα$^-$ (G$^-$P$^-$) versus GFP$^{br}$PDGFRα$^+$ (G$^{br}$P$^+$) cell fractions. Colored dots indicate probes with expression differing by ≥ 5.0-fold from the mean. Several key genes present in each cell population are highlighted. (E) Venn diagram displaying the overlap of genes up-regulated in E$^-$G$^+$ and G$^{br}$P$^+$ sorted populations. (F) Relative signal intensities from 4 independent microarray analyses indicating the enrichment of APLNR expression in E$^-$G$^+$, E$^+$G$^+$, G$^+$P$^+$, and G$^{hi}$P$^+$ nascent mesodermal populations from BVS-, BVSA-, and BVSW-treated EBs (growth factor concentrations provided in "Cell culture and differentiation" and supplemental Figure 1). Samples differentiated under neurectodermal conditions in FGF2 (FGF) served as a negative control for mesoderm differentiation. uns indicates unsorted.

fractions. A similar selective enrichment for *APLNR* was observed in 4 independent experiments in which BMP4-based growth factor combinations (supplemental Figure 1) were used to induce GFP$^+$ mesoderm, but *APLNR* was not expressed in cells differentiated in the presence of FGF2 (a protocol that would bias differentiation toward neuroectoderm[29]; Figure 1F). The increased expression of *APLNR* in selected cell fractions was confirmed by quantitative (real-time) RT-PCR (supplemental Figure 1).

### APLN binds mesodermal and endodermal progenitors in differentiating hESCs

We used 2 independent and complementary methods to evaluate the expression of *APLNR* on differentiating cells. In the first instance, we identified APLNR-expressing cells by using a fluorescein-ated version of its endogenous ligand, APLN. PREPRO-APELIN is a 77-aa protein that is sequentially cleaved to smaller

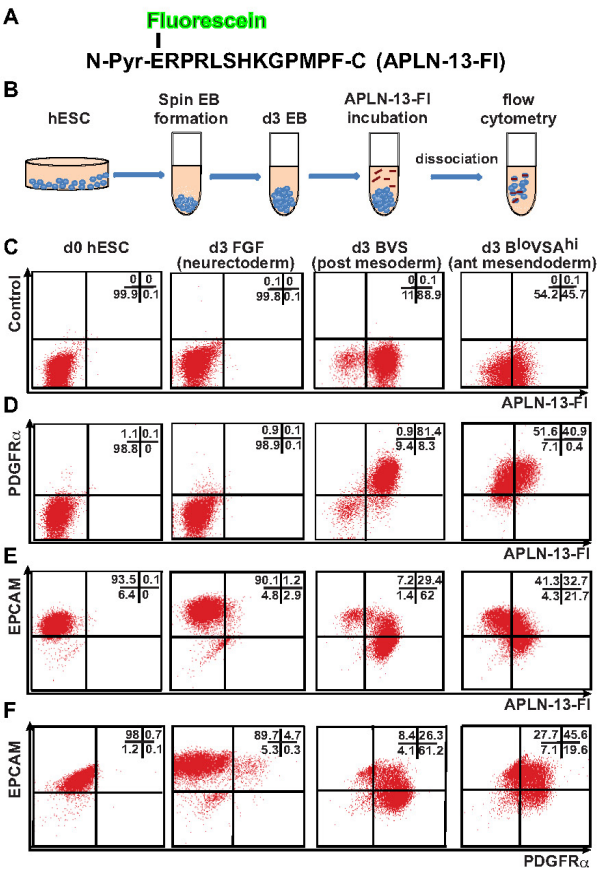


**Figure 2. APLN binds posterior mesodermal and anterior mesendodermal progenitors in differentiating hESCs.** (A) Amino acid sequence of synthesized APLN-13 N-terminal pyroglutamate (N-Pyr) peptide conjugated to fluorescein (FI). (B) Staining protocol used to label cells with APLN-13–FI. (C-F) Flow cytometric analysis of undifferentiated (d0) hESCs and day 3 EBs differentiated under neurectodermal (FGF), posterior mesodermal (BVS), and anterior mesendodermal ($B^{lo}VSA^{hi}$) conditions labeled with APLN-13–FI and Abs to PDGFRα or EPCAM. The growth factor concentrations are provided in "Cell culture and differentiation" and supplemental Figure 1. The percentage of cells falling into each quadrant is indicated in top right of each plot.

peptides, finally giving rise to an N-terminal pyroglutamated 13-mer, denoted Pyr–APLN-13.[20,28] This peptide displays a greater binding efficiency and biologic activity than a longer intermediate, APLN-36.[28] Therefore, we synthesized a fluorescein-conjugated APLN-13 N-terminal pyroglutamate peptide (APLN-13–Fl; Figure 2A), based on the previously reported ability of radio-iodinated APLN-13 to bind $APLNR^+$ human endothelial and cardiac cells.[30] We empirically determined the optimal duration of APLN-13–Fl incubation before disaggregation of the embryoid bodies to be 4 hours, suggesting that the APLN-13–Fl/APLNR complex was internalized and retained intracellularly over this time. Under these conditions, binding of this peptide proved to be robust method with which to identify APLNR-expressing cell populations during mesodermal induction (Figure 2B). No APLNR expression was detected on undifferentiated hESCs or in cells differentiated in FGF2 for 3 days (Figure 2C).

Flow cytometry demonstrated that day 3 EBs generated using growth factor combinations that biased differentiation toward posterior mesoderm (BVS) generated a greater percentage of $APLNR^+$ cells than growth factor combinations that included a high concentration of ACTIVIN A, which promoted a more anterior mesendodermal fate[8,22-24] ($B^{lo}VSA^{hi}$; Figure 2C). Nevertheless, under both conditions, APLNR was coexpressed with PDGFRα, although there was a higher proportion of double-positive cells (> 80%) in BVS-treated EBs (Figure 2D). Conversely, a higher proportion of $APLNR^+$ cells in $B^{lo}VSA^{hi}$ treated EBs coexpressed EPCAM, a marker for endodermal precursors as well as for undifferentiated hESCs[31] (Figure 2E), suggesting APLNR expression was more strongly up-regulated in posterior mesodermal compared with anterior mesendodermal precursors.

We compared the binding efficiency of the synthesized APLN-13–Fl peptide to a commercially available anti-APLNR Ab by flow cytometry. We found that both detection methods marked similar populations of cells in EBs cultured for 3 days in FGF, BVS, or $B^{lo}VSA^{hi}$ (supplemental Figure 2). A greater proportion of the cells were labeled by the APLN-13–Fl than the anti-APLNR Ab (supplemental Figure 2), suggesting this method may be a more sensitive measure of APLNR expression.

Using the anti-APLNR Ab, we compared the expression profiles of MIXL1 and APLNR from days 2 to 6 of differentiation

under both posterior mesoderm (BVS) and anterior mesendoderm ($B^{lo}VSA^{hi}$) differentiation conditions. APLNR-expressing cells represented a minority of $MIXL1^+$ cells at day 2, but by day 3 the majority of $MIXL1^+$ cells were also $APLNR^+$ (supplemental Figure 3). This double-positive population was retained until day 6 in BVS-treated cultures but APLNR was rapidly down-regulated after day 4 in high ACTIVIN A–containing cultures. These data relating to the APLNR expression pattern are in accordance with mouse in situ hybridization studies, where APLNR probes labeled the whole primitive streak and adjacent mesoderm but not the endoderm.[21] Consistent with our earlier results,[8] anterior mesendoderm cells expressed MIXL1 at a higher intensity and for a more prolonged duration (supplemental Figure 3).

#### Hemangioblast colony-forming cells express APLNR

The earliest hematopoietic precursors, Bl-CFC, generate both hematopoietic cells and endothelium.[11] They are detected after 2 to 4 days of hESC differentiation,[9] and we have previously shown that most Bl-CFCs are contained in a $MIXL1^+PDGFR\alpha^+$ fraction of the population.[8] Considering the high levels of APLNR expression in day 3 EBs, we examined the frequency of Bl-CFCs in flow-sorted populations from BVS and $B^{lo}VSA^{hi}$-treated cultures (Figure 3A-B; the differentiation potential of these colonies is shown in Figure 6 and supplemental Figure 11). Most colony-forming potential resided in the day 3 BVS-treated $EPCAM^-APLNR^+$ ($Ep^-AR^+$) cell fraction, with fewer colonies arising from the more immature $EPCAM^+APLNR^+$ ($Ep^+AR^+$) fraction. In the subpopulations isolated from $B^{lo}VSA^{hi}$ cultures, suppression of posterior mesoderm by ACTIVIN A greatly reduced colony frequency (Figure 3C).

Illumina microarray analysis was performed on RNA generated from the sorted posterior mesoderm and anterior mesendoderm fractions (Figure 3). Comparison of the BVS-derived $Ep^-AR^+$ fraction with the least differentiated $Ep^+AR^-$ fraction identified 165 probes (134 genes) that were at least 3-fold up-regulated (Figure 3D). This group included mesodermal markers such as *PDGFRα* and several *HOXB* cluster genes (Figure 3D, supplemental Table 3), consistent with the $Ep^-AR^+$ fraction marking cells undergoing a transition from primitive streak to nascent mesoderm. A similar comparison between $Ep^-AR^+$ and $Ep^+AR^-$ fractions from $B^{lo}VSA^{hi}$ EBs identified 83 probes (66 genes) up-regulated in the $Ep^-AR^+$ fraction that contained genes associated with the anterior mesendoderm such as *HAND1*, *FST*, *FOXN4* (Figure 3E, supplemental Table 4). Comparison of the up-regulated gene lists from both differentiation conditions indicated that 47 of the genes were shared between the two. These shared genes included several primitive streak markers (*BMP4*, *HAND1*, *IRX3*, *MSX1* as well as *APLNR*), consistent with our observation that APLNR marks bipotential mesendoderm. Indeed, the heatmap generated from the 475 probes differentially expressed between $Ep^-AR^+$ and $Ep^+AR^-$ fractions from both posterior mesodermally and anterior mesendodermally differentiated EBs highlighted the overall similarity of gene expression patterns observed under both sets of differentiations as cells progressed from least to most differentiated (Figure 3F, supplemental Table 5).

Therefore, to highlight the differences in outcomes between BVS and $B^{lo}VSA^{hi}$ differentiations, we compared the transcriptional profiles of the most differentiated $Ep^-AR^+$ samples (Figure 3G). We identified 61 probes (53 genes) that were up-regulated in BVS posterior mesodermally biased APLNR-expressing cells and 83 probes (76 genes) with increased signals in $B^{lo}VSA^{hi}$ anterior mesendodermally biased cultures (supplemental Tables 6-7). The genes up-regulated in BVS $Ep^-AR^+$ cells included a subset expressed in mesoderm (such as *LEF1*, *MSX1*, cardiac *ACTIN* and *HOXB* genes) while the $B^{lo}VSA^{hi}$ $Ep^-AR^+$ cells expressed genes associated with anterior mesendoderm or endoderm lineages (such as *SOX17*, *CER1*, *FOXA2*, *GSC*). To confirm the ability of APLNR-expressing cells induced in $B^{lo}VSA^{hi}$-differentiated EBs to generate definitive endoderm, we differentiated whole EBs and populations sorted on the basis of EPCAM and APLNR expression toward pancreatic endoderm.[26] Endodermally differentiated EBs up-regulated expression of E-CADHERIN and FOXA2, followed by expression of PDX1, AFP, and ALB (supplemental Figure 4). These data suggested that this protocol supported the emergence of both pancreatic and hepatic lineages. Although differentiation of the sorted fractions was less efficient than whole EBs, endodermally differentiated $Ep^-AR^+$ cells also expressed both pancreatic and hepatic genes (supplemental Figure 4). These results supported our microarray findings that the expression of APLNR marks both posterior and anterior streak populations.

#### APLN influences EB size and morphology

To explore the role of APLNR signaling during differentiation, we investigated the effect of APLN addition on hESC differentiation to mesoderm. Spin EBs were differentiated in medium supplemented with BVS, with APLN added on day 2, to coincide with the earliest expression of APLNR (supplemental Figure 3). In the presence of APLN, EBs were consistently larger and developed prominent thin-walled "cysts" that were seldom observed in EBs formed in BVS alone (Figure 4A-C). We confirmed the growth-promoting effect of APLN during mesoderm differentiation with 2 independent hESC lines (Figure 4D, supplemental Figure 5). The increased cell numbers might have resulted from increased cell proliferation and/or a decrease in programmed cell death, given that APLN influences both processes.[32,33]

#### APLN increases hematopoietic gene expression

To determine the changes in gene expression accompanying the addition of APLN to the culture medium, we compared the transcriptional profiles of hESCs differentiated in BVS with those of cells that also received a single pulse of APLN at day 2 of differentiation. Differentially transcribed genes (179) were observed from day 3 to day 8 of differentiation and many of the genes up-regulated have been associated with mesoderm development (Figure 4E-I, supplemental Figure 6, supplemental Table 8).

The earliest up-regulated genes included *NKD1* (naked cuticle homolog 1), an antagonist of WNT signaling, and the pan-cardiac transcription factor *NKX2-5* (Figure 4F). We observed peak expression of transcription factors expressed in hematoendothelial development from day 4 to day 5, including *EGR1*, *GFI1*, *GATA2*, *MYC, LYL1*, *MYB,* and *SOX18* (Figure 4G-H). Genes involved in angiogenesis that were also up-regulated in response to APLN included *CDH5*, *NOSTRIN*, *ICAM2*, *PECAM1*, *CD34*, *CD44*, and *VASH1* (Figure 4, supplemental Figure 6, supplemental Table 8). Up-regulation of the smooth muscle markers *TAGLN* and *TAGLN2* suggested a role for APLN in the generation of other mesodermal components of the vascular wall (Figure 4, supplemental Table 8). At day 5 and day 6, there was a peak in the expression of genes associated with hematopoiesis that included the heme synthesis gene *ALAS2*, embryonic and fetal globins (*HBZ*, *HBA2*, *HBE1*,

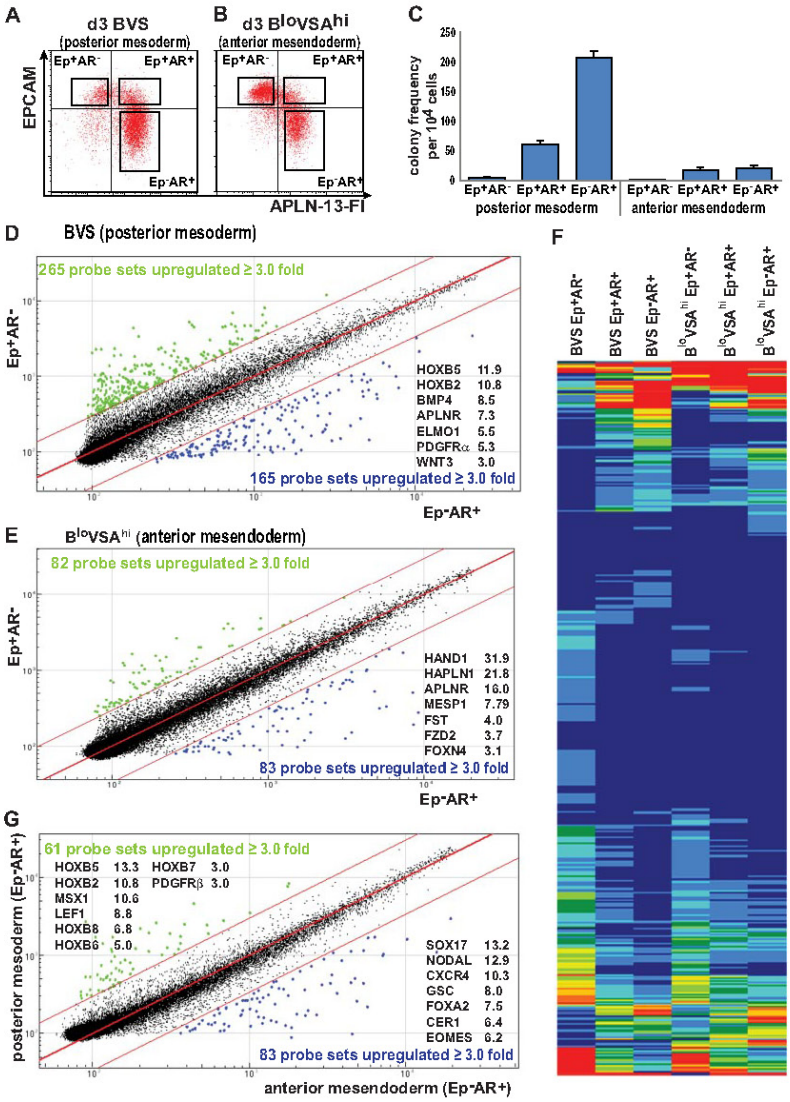


**Figure 3. Analysis of APLNR- and EPCAM-sorted cells from differentiated EBs.** Paired samples of (A) posterior mesodermally (BVS) and (B) anterior mesendodermally ($B^{lo}VSA^{hi}$) differentiated day 3 EBs were flow sorted based on the expression of APLNR and EPCAM expression (boxed areas in the panel). The same gates were used to sort cells differentiated under both protocols to ensure that phenotypically similar populations were compared. (C) Hematopoietic colony-forming potential of sorted cell populations indicating enrichment of hemangioblast colony-forming cells in the APLNR+ fractions ($Ep^+AR^+$ and $Ep^-AR^+$). Colony frequency was markedly diminished in the anterior mesendoderm differentiations. Error bars represent SEM for n = 3 independent sorting experiments. (D-E) Comparison of microarray-derived gene expression profiles of $EPCAM^+APLNR^-$ ($Ep^+AR^-$) and $EPCAM^-APLNR^+$ ($Ep^-AR^+$) cells sorted from EBs generated under conditions that favor the formation of (D) posterior mesoderm (BVS) or (E) anterior mesendoderm ($B^{lo}VSA^{hi}$). (F) Heatmap comparing the expression profiles of differentially expressed genes in sorted cell fractions generated under posterior mesodermal (BVS) and anterior mesendodermal ($B^{lo}VSA^{hi}$) conditions, showing similar patterns of expression in both sets of differentiations. (G) Microarray comparison of $EPCAM^-APLNR^+$ ($Ep^-AR^+$) cell fractions from BVS and $B^{lo}VSA^{hi}$ cell fractions representing the most posterior mesoderm and anterior mesendoderm committed fractions. Blue and green dots indicate probes differing by ≥ 3.0-fold from the mean. The fold change of several key genes is indicated for each plot.

*HBG1*), and *TESC*, a calcium-binding protein required for megakaryocytic development from human hematopoietic cells.[34] These results suggested that major effects of APLN involved the regulation of both blood and endothelial differentiation genes.

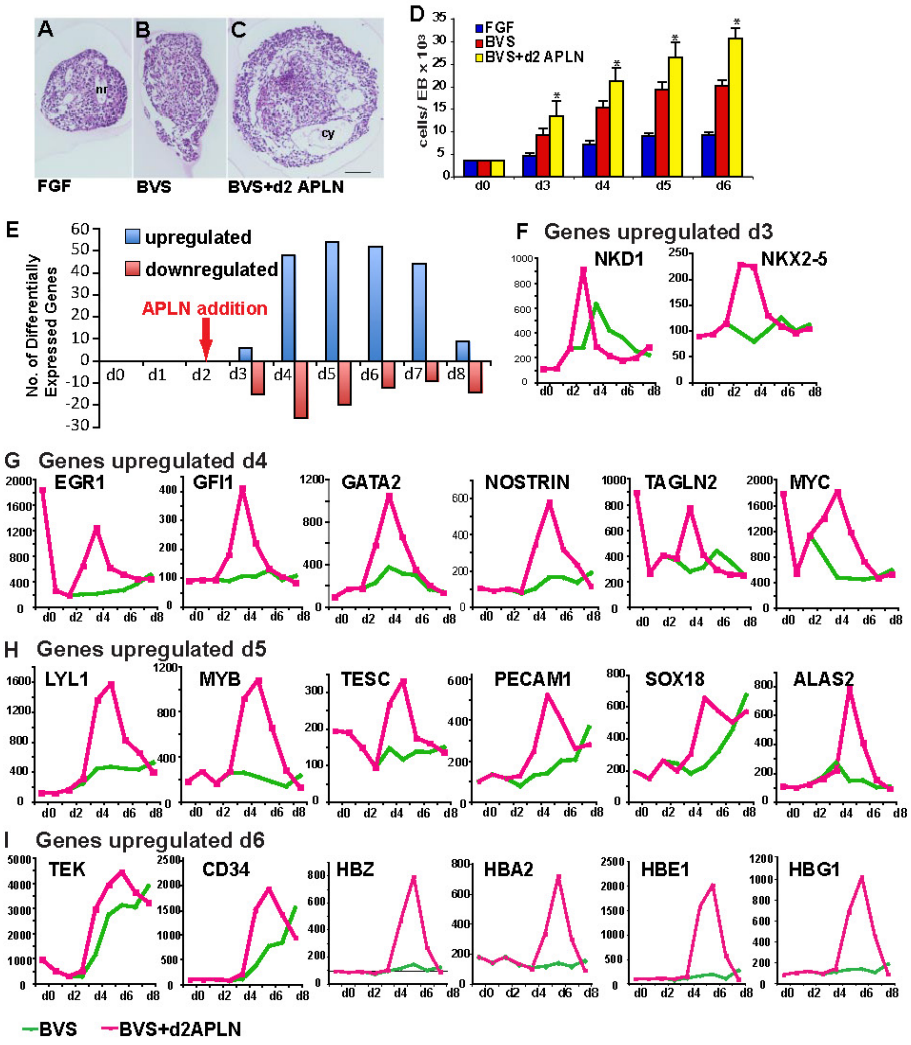


**Figure 4. APLN alters EB morphology and increases expression of hematopoietic and endothelial genes during mesodermal differentiation.** (A-C) Images of H&E-stained paraffin sections showing morphologic appearances of day 4 EBs differentiated in FGF2 alone or in BVS with and without APLN addition at day 2. Several neural rosettes (nr) are evident in the FGF2 EB. EBs that received BVS and APLN were larger with more prominent thin-walled cysts (cy). Scale bar: 100 μM. (C) Histogram depicting the mean cell number per EB from day 3 to day 6 under each of these culture conditions. Error bars represent SEM for n = 6 independent experiments. *$P < .01$ comparing BVS+d2 APLN with BVS at each time point (see also supplemental Figure 5). (E) Histogram indicating the number of genes whose expression was up-regulated or down-regulated (≥ 2.5 fold change) at each time point in EBs cultured with BVS plus a single pulse of APLN at day 2 compared with those receiving BVS alone. (F-I) Histograms comparing the kinetics of gene expression in cells differentiated with or without APLN for selected genes. Panels are grouped to show the profiles of genes whose expression was maximal from day 3 to day 6 as indicated (see also supplemental Figure 6). Abbreviations for gene names are expanded in supplemental Table 8.

### APLN augments hematopoiesis

We complemented these gene expression studies by comparing mesodermal and hematopoietic lineage markers on hESC differentiated in BVS with or without APLN from day 2 of differentiation. To bias differentiation toward hematopoiesis, day 4 EBs were cultured in fresh medium with BMP4, VEGF, SCF, FGF2, and IGF2, with or without readdition of APLN. Inclusion of APLN did not affect the expression of mesodermal markers such as MIXL1, PDGFRα, or APLNR for the first 4 days of differentiation (supplemental Figure 7). However, EBs cultured in APLN more rapidly down-regulated PDGFRα expression from day 6 of differentiation. A greater percentage of cells in APLN-supplemented cultures

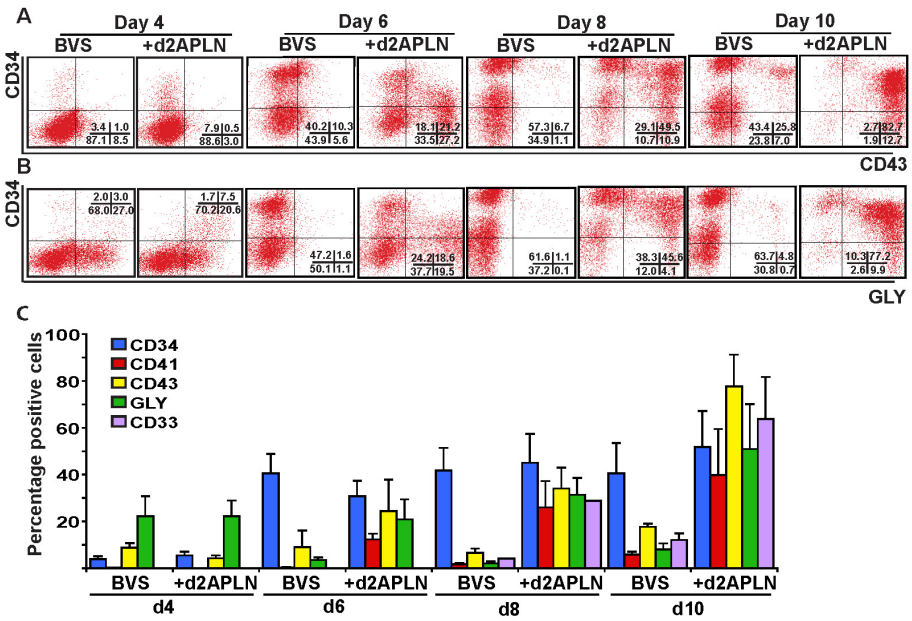


**Figure 5. APLN increases expression of hematopoietic markers during hESC differentiation.** (A-B) Flow cytometry time-course analysis of CD34, CD43, and GLYCOPHORIN A (GLY) expression on hESCs differentiated in APEL medium supplemented with BVS or BVS with APLN added from day 2. The percentage of cells in each quadrant is shown in the bottom right of each panel. (C) Histogram showing the mean percentage of cells expressing the indicated markers. Error bars represent SEM of 3 independent experiments. Inclusion of APLN resulted in an increased percentage of CD41 ($P < .05$), CD43 ($P < .001$), GLYCOPHORIN A ($P < .002$), and CD33 ($P < .05$) expressing cells from day 6 of differentiation. Statistical analysis used a 2-way ANOVA with Bonferroni posttest. Detailed FACS plots for all the markers are provided in supplemental Figure 8.

expressed the hematopoietic markers CD41, CD43, CD33, and GLYCOPHORIN A, complementing the rapid reduction in PDGFRα-expressing cells (Figure 5, supplemental Figure 8). Interestingly, the percentage of $CD34^+$ cells did not differ significantly between the treatment groups, indicating that APLN promoted the accumulation of more differentiated hematopoietic cells.

We examined the influence of exogenously added APLN peptide on the frequency of BI-CFCs. EBs formed from HES3 hESCs differentiated for 3 days in BVS medium were dissociated and seeded into methylcellulose containing VEGF, SCF, and EPO. The addition of APLN to the methylcellulose augmented colony formation at least 3-fold (Figure 6A). Although addition of APLN solely to the initial EB differentiation had little effect on BI-CFC frequency, the inclusion of APLN from day 2 in both the EB differentiation and the subsequent methylcellulose cultures synergistically augmented the frequency of hemangioblast colony formation, resulting in an ~ 10-fold increase in colony numbers over non-APLN–supplemented cultures (Figure 6A-B). A similar pattern and magnitude of enhanced colony frequency in response to APLN supplementation was observed with 2 additional independent hESC lines (MEL1 and H9; supplemental Figure 9). Flow cytometric analysis of differentiating hemangioblast colonies harvested from methylcellulose revealed transient expression of CD34 and CD41 and persistent expression of CD43 and GLYCOPHORIN A, consistent with EPO-induced erythroid differentiation. The addition of APLN did not significantly alter the differentiation outcome, suggesting that the major effect of APLN was to increase the frequency of hemangioblast colonies (supplemental Figure 10).

To demonstrate their endothelial differentiation potential, individual hemangioblast colonies from MC-APEL cultures at day 4 of differentiation were transferred to tissue culture–treated plates and cultured for 5-11 days in medium with VEGF, SCF, and EPO, with or without APLN. The majority of colonies (75 of 77; 97%) generated both adherent and floating cells, regardless of the inclusion of APLN (Figure 6C-D, supplemental Figure 11). Immunostaining of these adherent cells indicated the presence of $CD34^+$ endothelial cells, but also a population of $CD34^-$ adherent cells (Figure 6E-F, supplemental Figure 11). We examined the ability of the adherent cells to take up LDL, an attribute of endothelial cells, costaining the cultures for expression of the vascular mural marker, SMA. We observed that cells avidly taking up LDL (arrows in Figure 6G and supplemental Figure 11) did not stain strongly for SMA and vice versa, indicating the presence of 2 phenotypically distinct adherent cell populations. Flow cytometric analysis of the differentiated colonies indicated that the nonadherent population was composed of GLYCOPHORIN $A^+CD45^-$ erythroid cells with very few GLYCOPHORIN $A^-CD45^+$ myeloid cells (Figure 6H, supplemental Figure 11), similar to the differentiated cells harvested from methylcellulose (supplemental Figure 10). Conversely, over 50% of the adherent cells were $CD34^+CD45^-$ cells, consistent with endothelium. However, ~ 40% of the adherent cells were $CD34^-CD45^-$ cells, consistent with the proportion of $SMA^+$

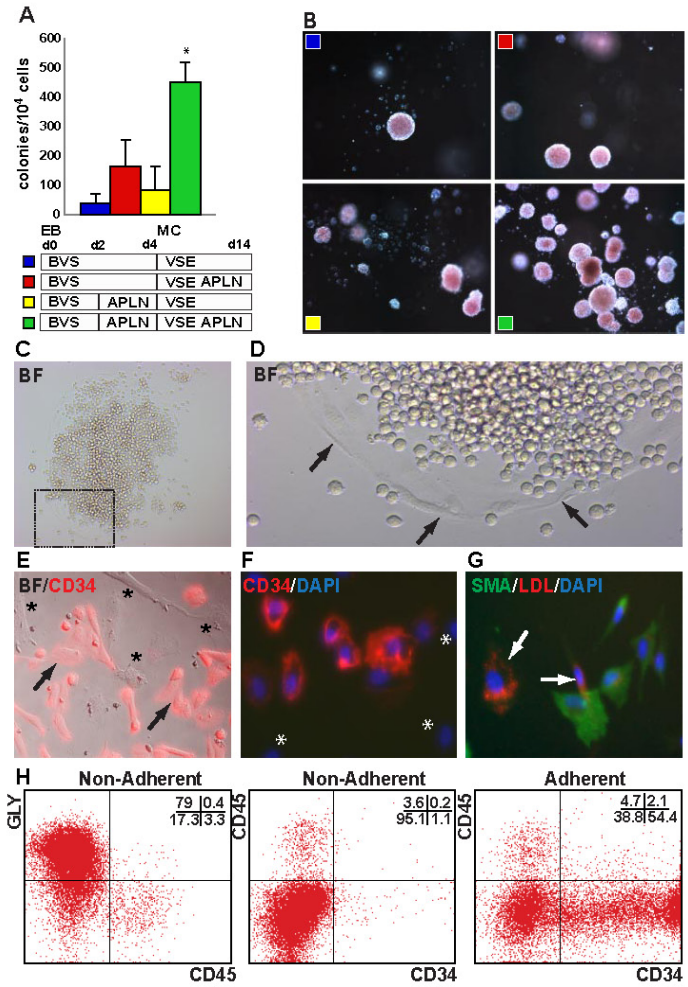


**Figure 6. APLN augments hemangioblast colony formation.** (A) Augmentation of day 3 hemangioblast colony formation in methylcellulose cultures supplemented with APLN. HES3 hESCs were differentiated as EBs for 3 days in BVS alone or in BVS with APLN added at day 2 (BVS/APLN). Dissociated cells were cultured further in methylcellulose (MC) supplemented with VEGF, SCF, and EPO (VSE) alone or in combination with APLN (VSE/APLN) as indicated. Error bars represent SEM for n = 4 independent experiments; *$P < .01$ for pairwise comparisons between BVS/APLN VSE/APLN and all other conditions. (B) Dark field images of hematopoietic colonies demonstrating the effect of APLN addition to both the initial mesoderm induction phase (EB) and the methylcellulose (MC) cultures. Original magnification, ×50. (C-D) Bright field images of replated hemangioblast colony demonstrating the presence of both hematopoietic cells and adherent cells (arrows). (E-F) Bright field and immunofluorescence overlay images demonstrating the presence of CD34+ (arrows) as well as CD34− adherent cells (asterisks). (G) Immunofluorescence overlay demonstrating that adherent cells either expressed SMA or took up DiI-Ac LDL (arrows). (H) Flow cytometric analysis of nonadherent and adherent cell fractions from pooled hemangioblast colonies differentiated for 11 days. Samples were stained with Abs to GLYCOPHORIN A (GLY), CD45, and CD34. The percentage of cells falling into each quadrant is indicated in the top right of each plot. Nonadherent cells predominantly comprised GLYCOPHORIN A+ CD45− erythroid cells with a small percentage of CD34−CD45+ myeloid cells whereas over 50% of the adherent cells were CD34+CD45− cells, many of which are likely to be endothelial cells. (G) Approximately 40% of the adherent cells were CD34−CD45− cells, consistent with the proportion of SMA+ smooth muscle cells observed by immunofluorescence (see also supplemental Figure 11). Original magnification: (C) ×50; (D) ×100; (E-G) ×200.

smooth muscle cells observed by immunofluorescence (Figure 6H, supplemental Figure 11). The demonstration that most hemangioblast colonies generated hematopoietic cells, endothelium, and smooth muscle is reminiscent of a similar tripotential Bl-CFC isolated from the early mouse embryo.[10] As far as we are aware, tripotential differentiation has not previously been documented for human Bl-CFCs.

When colony-forming assays were performed using human CD34+ cord blood cells, the addition of APLN did not alter colony frequency or morphology, consistent with our finding that APLNR

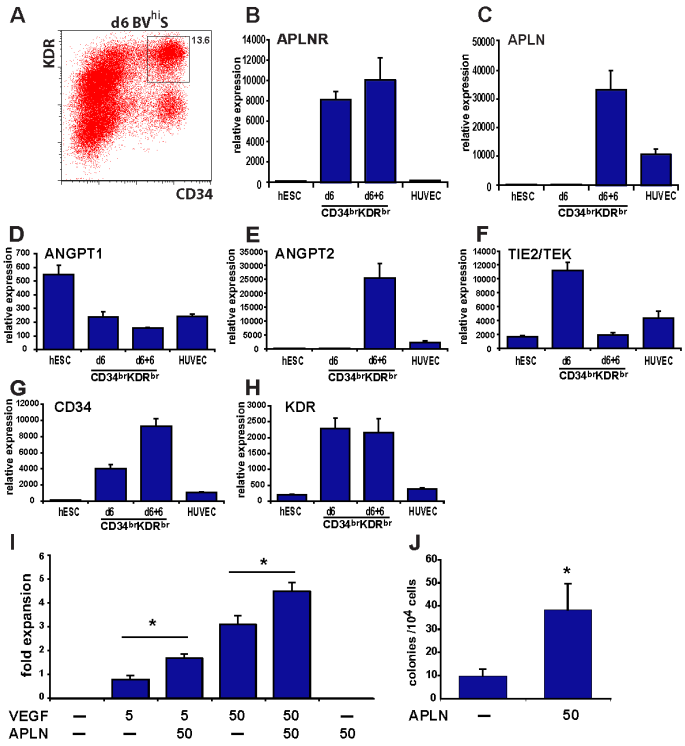


**Figure 7. APLN enhances the growth of endothelial and hematopoietic cells from CD34$^{br}$KDR$^{br}$ progenitors.** (A) Flow cytometric analysis of KDR and CD34 expression in day 6 EBs differentiated under endothelium-inducing growth conditions (BV$^{hi}$S). The CD34$^{br}$KDR$^{br}$ sorted cell population is indicated by the boxed area. (B-H) Microarray expression data for the indicated genes in undifferentiated hESC cells (hESC), day 6 CD34$^{br}$KDR$^{br}$ sorted progenitor cells (d6), CD34$^{br}$KDR$^{br}$ cells cultured in vitro for an additional 6 days (d6 + 6), and HUVEC cells. (I) Histogram showing the fold expansion after culturing $1.5 \times 10^4$ sorted day 6 CD34$^{br}$KDR$^{br}$ cells for 8 days in medium supplemented with the indicated concentrations (ng/mL) of VEGF and APLN. Error bars represent SEM for n = 5 independent experiments. *$P < .0005$ for VEGF/APLN vs VEGF. (J) Histogram showing the mean frequency of hematopoietic colony-forming cells in methylcellulose cultures seeded with day 6 sorted CD34$^{br}$KDR$^{br}$ progenitor cells, cultured with VEGF, SCF, and EPO in the presence or absence of 50 ng/mL APLN. Error bars represent SEM for n = 6 independent experiments. *$P < .03$ for APLN addition.

was not expressed on CD34$^+$ cord blood cells (supplemental Figure 12).

### APLN enhances the endothelial growth and hematopoietic colony-forming potential of day 6 CD34brKDRbr cells

Both APLNR and APLN are highly expressed in endothelial precursors of the nascent vasculature and play a role during angiogenesis in regulating blood vessel diameter.[35-38] Therefore, we investigated the expression of APLNR and APLN during the differentiation of endothelial progenitors from hESCs.

Cells coexpressing high levels of CD34 and KDR are enriched for endothelial progenitors in adults[39] and endothelial progenitors from differentiating hESCs also express high levels of CD34[40] and KDR (M.C., E.G.S., and A.G.E., unpublished results, March 2010). The *APLNR* was expressed in CD34$^{br}$KDR$^{br}$ cells sorted from day 6 EBs differentiated in medium with BV$^{hi}$S (Figure 7A). *APLNR* expression was maintained when these cells were cultured for a further 6 days in VEGF, but was absent from a more mature source of endothelium, HUVECs, consistent with previous reports[37] (Figure 7B). Although day 6 CD34$^{br}$KDR$^{br}$ cells expressed high levels of the *TIE2/TEK* receptor and its ligand, *ANGPT1*, which has been shown to induce *APLN* expression in HUVECS,[37] transcripts for *APLN* were initially absent in CD34$^{br}$KDR$^{br}$ cells (Figure 7C-D). However, during the 6-day period in culture, *APLN* transcription was markedly up-regulated, associated with high levels of expression of *ANGPT2* and a down-regulation of the *TIE2/TEK* receptor (Figure 7E-F). Transcripts for *CD34* and *KDR* were retained by the hESC-derived endothelial cells in contrast to HUVECs, which only expressed low levels of these genes (Figure 7G-H).

We evaluated the ability of APLN to augment endothelial growth. While APLN alone did not promote expansion of sorted day 6 CD34$^{br}$KDR$^{br}$ cells, the inclusion of APLN significantly enhanced the endothelial growth-promoting effects of VEGF (Figure 7I), a result reminiscent of the observation that the combination of Apln and Vegf induced larger vessels in a mouse model of angiogenesis.[36] Finally, we also demonstrated that the same day 6 CD34$^{br}$KDR$^{br}$ population included committed hematopoietic CFCs that were responsive to APLN (Figure 7J).

## Discussion

We have defined a novel role for APLN, the peptide ligand for the APLNR, during the in vitro hematopoietic differentiation of hESCs. The combination of increased EB size and enhanced frequency of Bl-CFC in response to APLN resulted in an ~ 10-fold increase in the yield of colony-forming cells, documented in 3 independent hESC lines. The inclusion of APLN from day 2 of differentiation enhanced the generation of hematopoietic cells from differentiating hESC and hematopoietic CFCs present in sorted day 6 CD34$^{br}$KDR$^{br}$ cells retained APLN responsiveness. We also showed that treatment of the APLNR-expressing CD34$^{br}$KDR$^{br}$

progenitors with APLN and VEGF synergistically promoted endothelial cell growth. This role for APLN in human hematopoiesis complements its cardiovascular actions in adult tissues, in which APLN antagonizes the pressor functions of vasopressin, stimulates water intake, induces arterial vasodilation in a nitric oxide–dependent fashion, and has positive inotropic effects on the heart.[41-43]

The earliest observable effects of APLN coincided with a period of differentiation during which its sole receptor, APLNR, was up-regulated on MIXL1$^+$ mesendoderm, consistent with reports documenting APLNR expression during gastrulation in the frog, zebrafish, and mouse.[21,44-47] Vodyanik and colleagues also recently identified *APLNR* expression on hESCs differentiated by coculture with mouse OP9 cells.[13] In their study, the absence of *FOXA2* expression in APLNR$^+$ cells coupled with the ability of this population to generate mesenchymal and hemangioblast colonies suggested APLNR might be restricted to progenitors of lateral plate and extraembryonic mesoderm.[13] While we also identified *APLNR* expression on mesodermal populations, our data showed that hESCs differentiated toward more anterior primitive streak derivatives, including endoderm, also transiently expressed the APLNR. This conclusion was supported by the observation that endoderm-associated genes such as *SOX17*, *NODAL*, *GSC*, and *FOXA2* were up-regulated in APLNR$^+$ cells generated in medium containing high levels of ACTIVIN A. Under such conditions, we observed a concomitant decrease in the Bl-CFC frequency of the APLNR$^+$ population, consistent with ACTIVIN A–mediated suppression of posterior mesoderm. Finally, we showed that sorted APLNR$^+$ populations could be further differentiated to cells expressing pancreatic and hepatic endoderm genes. Taken together, our results suggest that early APLNR expression marks a broad spectrum of primitive streak-like cells during hESC differentiation, consistent with its expression throughout the entire length of the primitive streak of the gastrulating mouse embryo.[21]

In all species examined thus far, the *APLNR* homologue is expressed in mesendodermal precursors from which cardiovascular and hematopoietic lineages subsequently develop.[21,44-47] Later in embryogenesis, mouse *Aplnr* is highly expressed on endothelial cells undergoing angiogenesis, especially at the tips of intersomitic vessels, and on endothelial cells in the AGM region, on vascular smooth muscle, and on the myocardium.[37,38,42] Similar patterns of cardiovascular expression are seen in the zebrafish and frog.[35,47,48] Analysis of transcriptional profiles of mesodermally biased differentiating hESC cultures pulsed with APLN at day 2 of differentiation revealed a subsequent up-regulation in transcription of genes associated with hematoendothelial differentiation. Given the documented expression of APLNR in the midgestation myocardium,[42] it was noteworthy that APLN-treated cultures also transiently up-regulated the WNT antagonist *NKD1* and the pan-cardiac transcription factor *NKX2.5*.

In the context of these findings, it is relevant that morpholino knockdown of *Xapelin* or *Xmsr* (the *Xenopus* APLNR homologue) in the frog embryo impaired blood, endothelial, and cardiac development.[44] Conversely, embryos injected with *Xpreproapelin* displayed expanded domains of endothelial and hematopoietic gene expression.[44] Cox et al similarly observed that a localized source of Apln stimulated endothelial outgrowth and that *Xapelin* and *Xmsr* morpholinos led to reduced and disordered endothelial development.[35]

In the zebrafish, embryos mutant for either of 2 redundantly acting APLNR-like genes (*Agtrla* and *Agtrlb*) displayed abnormal cardiac development as the dominant phenotype.[45,47] As in *Xenopus*, overexpression of Apln also perturbed myocardial development in zebrafish probably by affecting cell migration, but hematopoietic and vascular abnormalities were not described.[44,45,47] However, the *Apln* knockout mouse exhibited a mild phenotype characterized by a reduced diameter of intersomitic vessels during embryogenesis, narrow blood vessels in the trachea and skin postnatally, and impaired recovery from hind-limb ischemia, consistent with the role for Apln in angiogenesis.[36,37,49] In one study examining the phenotype of *Aplnr* deleted mice, null mutants were born at close to the expected Mendelian frequency (19%) but displayed an increased vasopressor response to angiotensin II.[50] Conversely, 2 other groups reported a more severe phenotype with reduced numbers of viable homozygous *Aplnr*$^{-/-}$ embryos.[43,49] Although details of the embryonic mutants have not been published, surviving *Apln*$^{-/-}$ and *Aplnr*$^{-/-}$ mice displayed decreased exercise capacity and impaired sarcomeric function in isolated cardiomyocytes.[49] In another study, *Aplnr*$^{-/-}$ mice displayed reduced water intake and were unable to concentrate urine in response to water deprivation.[43] To date, no hematopoietic phenotype has been reported in surviving *Apln*$^{-/-}$ or *Aplnr*$^{-/-}$ mice. As such, it is possible that other signaling systems operating during the critical period of hematopoietic progenitor specification are able to compensate for loss of both APLN and its receptor. In this context, given that APLN synergized with VEGF in promoting endothelial cell growth from hESCs, it would be of interest to examine the effect of APLNR signaling loss under conditions in which VEGF signaling was compromised.

In conclusion, our observations indicate a previously unrecognized role for APLNR signaling in regulating hematopoiesis in differentiating hESCs. Early hematopoietic progenitors express APLNR and the inclusion of APLN peptide in culture media enhances the efficiency of blood cell formation from differentiating hESCs. It is tempting to speculate that APLN might play a role in the generation of hematopoietic cells from endothelium, given the documented expression of APLNR in AGM vasculature on the mouse embryo.[38] The molecular cascades downstream of APLN/APLNR signaling that mediate these hematopoietic effects remain to be elucidated.

## Acknowledgments

The authors thank Robyn Mayberry and the staff of StemCore Vic for provision of hESCs, David Haylock and Susie Nilsson for provision of CD34$^+$ cells purified from human umbilical cord blood, and Andrew Fryga and the staff of FlowCore for cell sorting.

This work was supported by grants from the Australian Stem Cell Center, Stem Cells Australia, the Juvenile Diabetes Research Foundation, and the National Health and Medical Research Council of Australia (NHMRC).

A.G.E. and E.G.S. are Senior Research Fellows of the NHMRC.

## Authorship

Contribution: Q.C.Y., C.E.H., M.C., E.S.N., J.V.S., and K.G. performed the research and analyzed data; and Q.C.Y., C.E.H., E.G.S., and A.G.E. designed the research, analyzed data, and wrote the manuscript.

Conflict-of-interest disclosure: The authors declare no competing financial interests.

Correspondence: Andrew G. Elefanty, Monash Immunology and Stem Cell Laboratories, Building 75, STRIP 1, West Ring Road, Monash University, Clayton, Victoria 3800, Australia; e-mail: andrew.elefanty@monash.edu.

## References


1. Dzierzak E, Speck NA. Of lineage and legacy: the development of mammalian hematopoietic stem cells. *Nat Immunol.* 2008;9(2):129-136.
2. Wilkinson DG, Bhatt S, Herrmann BG. Expression pattern of the mouse T gene and its role in mesoderm formation. *Nature.* 1990;343(6259):657-659.
3. Pearce JJ, Evans MJ. Mml, a mouse Mix-like gene expressed in the primitive streak. *Mech Dev.* 1999;87(1-2):189-192.
4. Robb L, Hartley L, Begley CG, et al. Cloning, expression analysis, and chromosomal localization of murine and human homologues of a Xenopus mix gene. *Dev Dyn.* 2000;219(4):497-504.
5. Kataoka H, Takakura N, Nishikawa S, et al. Expressions of PDGF receptor alpha, c-Kit and Flk1 genes clustering in mouse chromosome 5 define distinct subsets of nascent mesodermal cells. *Dev Growth Differ.* 1997;39(6):729-740.
6. Takakura N, Yoshida H, Ogura Y, Kataoka H, Nishikawa S. PDGFR alpha expression during mouse embryogenesis: immunolocalization analyzed by whole-mount immunohistostaining using the monoclonal anti-mouse PDGFR alpha antibody APA5. *J Histochem Cytochem.* 1997;45(6):883-893.
7. Murry CE, Keller G. Differentiation of embryonic stem cells to clinically relevant populations: lessons from embryonic development. *Cell.* 2008;132(4):661-680.
8. Davis RP, Ng ES, Costa M, et al. Targeting a GFP reporter gene to the MIXL1 locus of human embryonic stem cells identifies human primitive streak-like cells and enables isolation of primitive hematopoietic precursors. *Blood.* 2008;111(4):1876-1884.
9. Kennedy M, D'Souza SL, Lynch-Kattman M, Schwantz S, Keller G. Development of the hemangioblast defines the onset of hematopoiesis in human ES cell differentiation cultures. *Blood.* 2007;109(7):2679-2687.
10. Huber TL, Kouskoff V, Fehling HJ, Palis J, Keller G. Haemangioblast commitment is initiated in the primitive streak of the mouse embryo. *Nature.* 2004;432(7017):625-630.
11. Choi K, Kennedy M, Kazarov A, Papadimitriou JC, Keller G. A common precursor for hematopoietic and endothelial cells. *Development.* 1998;125(4):725-732.
12. Vodyanik MA, Thomson JA, Slukvin II. Leukosialin (CD43) defines hematopoietic progenitors in human embryonic stem cell differentiation cultures. *Blood.* 2006;108(6):2095-2105.
13. Vodyanik MA, Yu J, Zhang X, et al. A mesoderm-derived precursor for mesenchymal stem and endothelial cells. *Cell Stem Cell.* 2010;7(6):718-729.
14. Galic Z, Kitchen SG, Subramanian A, et al. Generation of T lineage cells from human embryonic stem cells in a feeder free system. *Stem Cells Dev.* 2009;27(1):100-107.
15. Tseng SY, Nishimoto KP, Silk KM, et al. Generation of immunogenic dendritic cells from human embryonic stem cells without serum and feeder cells. *Regen Med.* 2009;4(4):513-526.
16. Ng ES, Davis R, Stanley EG, Elefanty AG. A protocol describing the use of a recombinant protein-based, animal product-free medium (APEL) for human embryonic stem cell differentiation as spin embryoid bodies. *Nat Protoc.* 2008;3(5):768-776.
17. Ng ES, Davis RP, Azzola L, Stanley EG, Elefanty AG. Forced aggregation of defined numbers of human embryonic stem cells into embryoid bodies fosters robust, reproducible hematopoietic differentiation. *Blood.* 2005;106(5):1601-1603.
18. Pick M, Azzola L, Mossman A, Stanley EG, Elefanty AG. Differentiation of human embryonic stem cells in serum-free medium reveals distinct roles for bone morphogenetic protein 4, vascular endothelial growth factor, stem cell factor, and fibroblast growth factor 2 in hematopoiesis. *Stem Cells.* 2007;25(9):2206-2214.
19. O'Dowd BF, Heiber M, Chan A, et al. A human gene that shows identity with the gene encoding the angiotensin receptor is located on chromosome 11. *Gene.* 1993;136(1-2):355-360.
20. Tatemoto K, Hosoya M, Habata Y, et al. Isolation and characterization of a novel endogenous peptide ligand for the human APJ receptor. *Biochem Biophys Res Commun.* 1998;251(2):471-476.
21. D'Aniello C, Lonardo E, Iaconis S, et al. G protein-coupled receptor APJ and its ligand apelin act downstream of Cripto to specify embryonic stem cells toward the cardiac lineage through extracellular signal-regulated kinase/p70S6 kinase signaling pathway. *Circ Res.* 2009;105(3):231-238.
22. Green MD, Chen A, Nostro MC, et al. Generation of anterior foregut endoderm from human embryonic and induced pluripotent stem cells. *Nat Biotechnol.* 2011;29(3):267-272.
23. Kubo A, Shinozaki K, Shannon JM, et al. Development of definitive endoderm from embryonic stem cells in culture. *Development.* 2004;131(7):1651-1662.
24. Tada S, Era T, Furusawa C, et al. Characterization of mesendoderm: a diverging point of the definitive endoderm and mesoderm in embryonic stem cell differentiation culture. *Development.* 2005;132(19):4363-4374.
25. Richards M, Fong CY, Chan WK, Wong PC, Bongso A. Human feeders support prolonged undifferentiated growth of human inner cell masses and embryonic stem cells. *Nat Biotechnol.* 2002;20(9):933-936.
26. Micallef SJ, Li X, Schiesser JV, et al. INS(GFP/w) human embryonic stem cells facilitate isolation of in vitro derived insulin-producing cells. *Diabetologia.* 2012;55(3):694-706.
27. Saeed AI, Bhagabati NK, Braisted JC, et al. TM4 microarray software suite. *Methods Enzymol.* 2006;411:134-193.
28. Japp AG, Cruden NL, Amer DA, et al. Vascular effects of apelin in vivo in man. *J Am Coll Cardiol.* 2008;52(11):908-913.
29. Goulburn AL, Alden D, Davis RP, et al. A targeted NKX2.1 human embryonic stem cell reporter line enables identification of human basal forebrain derivatives. *Stem Cells.* 2011;29(3):462-473.
30. Katugampola SD, Maguire JJ, Matthewson SR, Davenport AP. [(125)I]-(Pyr(1))Apelin-13 is a novel radioligand for localizing the APJ orphan receptor in human and rat tissues with evidence for a vasoconstrictor role in man. *Br J Pharmacol.* 2001;132(6):1255-1260.
31. Chen HF, Chuang CY, Lee WC, et al. Surface marker epithelial cell adhesion molecule and E-cadherin facilitate the identification and selection of induced pluripotent stem cells. *Stem Cell Rev.* 2011;7(3):722-735.
32. Cui RR, Mao DA, Yi L, et al. Apelin suppresses apoptosis of human vascular smooth muscle cells via APJ/PI3-K/Akt signaling pathways. *Amino Acids.* 2010;39(5):1193-1200.
33. Eyries M, Siegfried G, Ciumas M, et al. Hypoxia-induced apelin expression regulates endothelial cell proliferation and regenerative angiogenesis. *Circ Res.* 2008;103(4):432-440.
34. Levay K, Slepak VZ. Tescalcin is an essential factor in megakaryocytic differentiation associated with Ets family gene expression. *J Clin Invest.* 2007;117(9):2672-2683.
35. Cox CM, D'Agostino SL, Miller MK, Heimark RL, Krieg PA. Apelin, the ligand for the endothelial G-protein-coupled receptor, APJ, is a potent angiogenic factor required for normal vascular development of the frog embryo. *Dev Biol.* 2006;296(1):177-189.
36. Kidoya H, Naito H, Takakura N. Apelin induces enlarged and nonleaky blood vessels for functional recovery from ischemia. *Blood.* 2010;115(15):3166-3174.
37. Kidoya H, Ueno M, Yamada Y, et al. Spatial and temporal role of the apelin/APJ system in the caliber size regulation of blood vessels during angiogenesis. *EMBO J.* 2008;27(3):522-534.
38. Takakura N, Kidoya H. Maturation of blood vessels by haematopoietic stem cells and progenitor cells: involvement of apelin/APJ and angiopoietin/Tie2 interactions in vessel caliber size regulation. *Thromb Haemost.* 2009;101(6):999-1005.
39. Peichev M, Naiyer AJ, Pereira D, et al. Expression of VEGFR-2 and AC133 by circulating human CD34(+) cells identifies a population of functional endothelial precursors. *Blood.* 2000;95(3):952-958.
40. Chen T, Bai H, Shao Y, et al. Stromal cell-derived factor-1/CXCR4 signaling modifies the capillary-like organization of human embryonic stem cell-derived endothelium in vitro. *Stem Cells.* 2007;25(2):392-401.
41. Barnes G, Japp AG, Newby DE. Translational promise of the apelin–APJ system. *Heart.* 2010;96(13):1011-1016.
42. Ashley EA, Powers J, Chen M, et al. The endogenous peptide apelin potently improves cardiac contractility and reduces cardiac loading in vivo. *Cardiovasc Res.* 2005;65(1):73-82.
43. Roberts EM, Newson MJ, Pope GR, Landgraf R, Lolait SJ, O'Carroll AM. Abnormal fluid homeostasis in apelin receptor knockout mice. *J Endocrinol.* 2009;202(3):453-462.
44. Inui M, Fukui A, Ito Y, Asashima M. Xapelin and Xmsr are required for cardiovascular development in Xenopus laevis. *Dev Biol.* 2006;298(1):188-200.
45. Scott IC, Masri B, D'Amico LA, et al. The g protein-coupled receptor agtrl1b regulates early development of myocardial progenitors. *Dev Cell.* 2007;12(3):403-413.
46. Tucker B, Hepperle C, Kortschak D, et al. Zebrafish angiotensin II receptor-like 1a (agtrl1a) is expressed in migrating hypoblast, vasculature, and in multiple embryonic epithelia. *Gene Expr Patterns.* 2007;7(3):258-265.
47. Zeng XX, Wilm TP, Sepich DS, Solnica-Krezel L. Apelin and its receptor control heart field formation during zebrafish gastrulation. *Dev Cell.* 2007;12(3):391-402.
48. Devic E, Paquereau L, Vernier P, Knibiehler B, Audigier Y. Expression of a new G protein-coupled receptor X-msr is associated with an endothelial lineage in Xenopus laevis. *Mech Dev.* 1996;59(2):129-140.
49. Charo DN, Ho M, Fajardo G, et al. Endogenous regulation of cardiovascular function by apelin-APJ. *Am J Physiol Heart Circ Physiol.* 2009;297(5):H1904-H1913.
50. Ishida J, Hashimoto T, Hashimoto Y, et al. Regulatory roles for APJ, a seven-transmembrane receptor related to angiotensin-type 1 receptor in blood pressure in vivo. *J Biol Chem.* 2004;279(25):26274-26279.

# Primer and plasmid sequences used to construct a luciferase expression vector

## A. Primer sequences

| Primer name | Primer Sequence |
|---|---|
| SalMluIT2ALuc | GTCGACACGCGTGGCGGCGGGTCCGGAGGAGAGGGCAGAGGAAGTCTTCTAACATGCGGTGACGTGGAGGAGAATCCTGGCCCAATGGAAGACGCCAAAAAC |
| LucRev1 | GCCCATATCGTTTCATAGCTTCTG |

## B. pEFBOSLuciferaseIRESPuro plasmid information

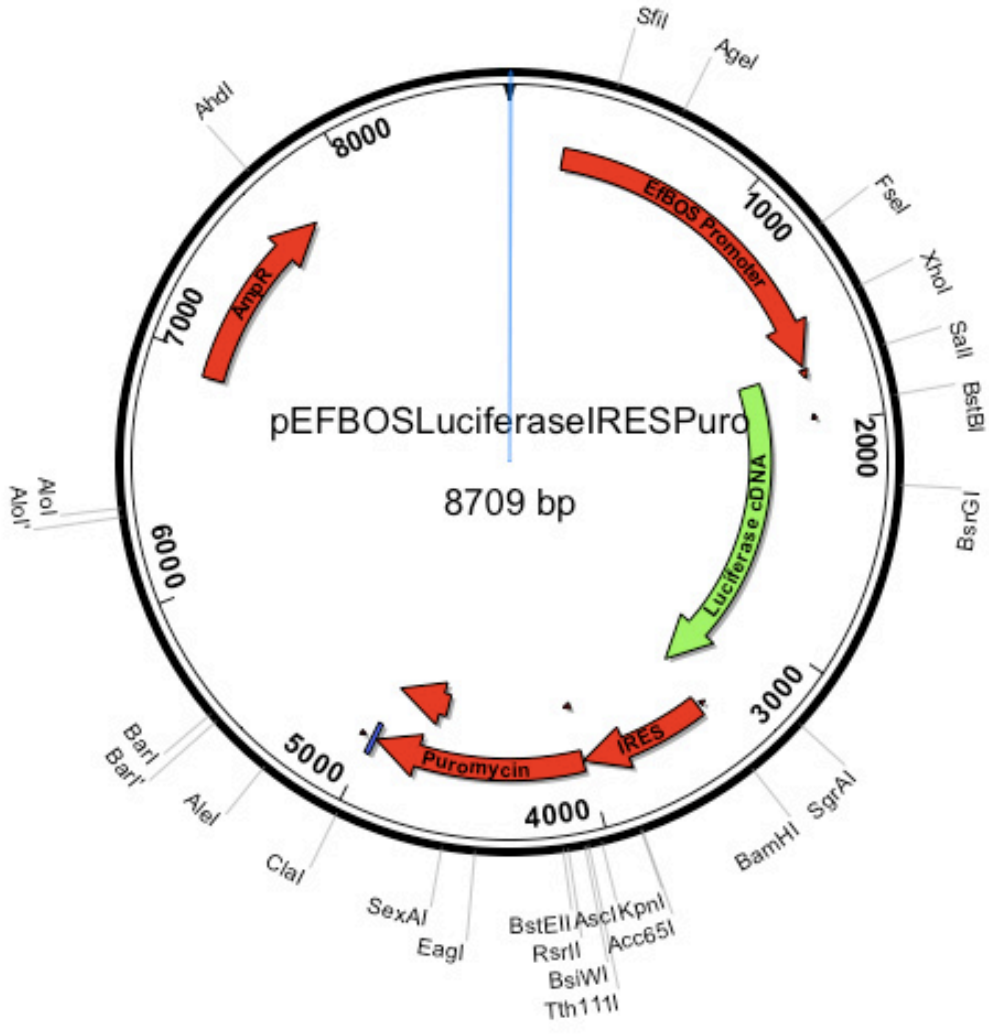

**pEFBOSLuciferaseIRESPuro sequence**

AGCGCCCAATACGCAAACCGCCTCTCCCCGCGCGTTGGCCGATTCATTAATGCAGCTGGCACGAC
AGGTTTCCCGACTGGAAAGCGGGCAGTGAGCGCAACGCAATTAATGTGAGTTAGCTCACTCATT
AGGCACCCCAGGCTTTACACTTTATGCTTCCGGCTCGTATGTTGTGTGGAATTGTGAGCGGATAA
CAATTTCACACAGGAAACAGCTATGACCATGATTACGCCAAGCTTCCAGGCACTCCTTTCAAGAC
CTAGAAGGTCCATTAGCTGCAAAGATTCCTCTCTGTTTAAAACTTTATCCATCTTTGCAAAGCTT
TTTGCAAAAGCCTAGGCCTCCAAAAAAGCCTCCTCACTACTTCTGGAATAGCTCAGAGGCCGAGG
CGGCCTCGGCCTCTGCATAAATAAAAAAAATTAGTCAGCCATGGGGCGGAGAATGGGCGGAACT
GGGCGGAGTTAGGGGCGGGATGGGCGGAGTTAGGGGCGGGACTATGGTTGCTGACTAATTGAGA
TGCATGCTTTGCATACTTCTGCCTGCTGGGGAGCCTGGCGTGAGGCTCCGGTGCCCGTCAGTGGG
CAGAGCGCACATCGCCCACAGTCCCCGAGAAGTTGGGGGGAGGGGTCGGCAATTGAACCGGTGCC
TAGAGAAGGTGGCGCGGGGTAAACTGGGAAAGTGATGTCGTGTACTGGCTCCGCCTTTTTCCCGA
GGGTGGGGGAGAACCGTATATAAGTGCAGTAGTCGCCGTGAACGTTCTTTTTCGCAACGGGTTT
GCCGCCAGAACACAGGTAAGTGCCGTGTGTGGTTCCCGCGGGCCTGGCCTCTTTACGGGTTATGG
CCCTTGCGTGCCTTGAATTACTTCCACGCCCCTGGCTGCAGTACGTGATTCTTGATCCCGAGCTT
CGGGTTGGAAGTGGGTGGGAGAGTTCGAGGCCTTGCGCTTAAGGAGCCCCTTCGCCTCGTGCTTG
AGTTGAGGCCTGGCCTGGGCGCTGGGGCCGCCGCGTGCGAATCTGGTGGCACCTTCGCGCCTGTC
TCGCTGCTTTCGATAAGTCTCTAGCCATTTAAAATTTTTGATGACCTGCTGCGACGCTTTTTTTC
TGGCAAGATAGTCTTGTAAATGCGGGCCAAGATCTGCACACTGGTATTTCGGTTTTTGGGGCCGC
GGGCGGCGACGGGGCCCGTGCGTCCCAGCGCACATGTTCGGCGAGGCGGGGCCTGCGAGCGCGGC
CACCGAGAATCGGACGGGGGTAGTCTCAAGCTGGCCGGCCTGCTCTGGTGCCTGGCCTCGCGCCG
CCGTGTATCGCCCCGCCCTGGGCGGCAAGGCTGGCCCGGTCGGCACCAGTTGCGTGAGCGGAAAG
ATGGCCGCTTCCCGGCCCTGCTGCAGGGAGCTCAAAATGGAGGACGCGGCGCTCGGGAGAGCGGG
CGGGTGAGTCACCCACACAAAGGAAAAGGGCCTTTCCGTCCTCAGCCGTCGCTTCATGTGACTCC
ACGGAGTACCGGGCGCCGTCCAGGCACCTCGATTAGTTCTCGAGCTTTTGGAGTACGTCGTCTTT
AGGTTGGGGGGAGGGGTTTTATGCGATGGAGTTTCCCCACACTGAGTGGGTGGAGACTGAAGTT
AGGCCAGCTTGGCACTTGATGTAATTCTCCTTGGAATTTGCCCTTTTTGAGTTTGGATCTTGGTT
CATTCTCAAGCCTCAGACAGTGGTTCAAAGTTTTTTTCTTCCATTTCAGGTGTCGTGAGGAATTC
TCTAGGTCGACAGATCTATGGAAGACGCCAAAAACATAAAGAAAGGCCCGGCGCCATTCTATCC
GCTGGAAGATGGAACCGCTGGAGAGCAACTGCATAAGGCTATGAAGAGATACGCCCTGGTTCCT
GGAACAATTGCTTTTACAGATGCACATATCGAGGTGGACATCACTTACGCTGAGTACTTCGAAA
TGTCCGTTCGGTTGGCAGAAGCTATGAAACGATATGGGCTGAATACAAATCACAGAATCGTCGT
ATGCAGTGAAAACTCTCTTCAATTCTTTATGCCGGTGTTGGGCGCGTTATTTATCGGAGTTGCAG
TTGCGCCCGCGAACGACATTTATAATGAACGTGAATTGCTCAACAGTATGGGCATTTCGCAGCCT
ACCGTGGTGTTCGTTTCCAAAAAGGGGTTGCAAAAAATTTTGAACGTGCAAAAAAAGCTCCCAA
TCATCCAAAAAATTATTATCATGGATTCTAAAACGGATTACCAGGGATTTCAGTCGATGTACAC
GTTCGTCACATCTCATCTACCTCCCGGTTTTAATGAATACGATTTTGTGCCAGAGTCCTTCGATA
GGGACAAGACAATTGCACTGATCATGAACTCCTCTGGATCTACTGGTCTGCCTAAAGGTGTCGCT
CTGCCTCATAGAACTGCCTGCGTGAGATTCTCGCATGCCAGAGATCCTATTTTTGGCAATCAAAT
CATTCCGGATACTGCGATTTTAAGTGTTGTTCCATTCCATCACGGTTTTGGAATGTTTACTACAC
TCGGATATTTGATATGTGGATTTCGAGTCGTCTTAATGTATAGATTTGAAGAAGAGCTGTTTCT
GAGGAGCCTTCAGGATTACAAGATTCAAAGTGCGCTGCTGGTGCCAACCCTATTCTCCTTCTTCG
CCAAAAGCACTCTGATTGACAAATACGATTTATCTAATTTACACGAAATTGCTTCTGGTGGCGCT
CCCCTCTCTAAGGAAGTCGGGGAAGCGGTTGCCAAGAGGTTCCATCTGCCAGGTATCAGGCAAGG
ATATGGGCTCACTGAGACTACATCAGCTATTCTGATTACACCCGAGGGGGATGATAAACCGGGC
GCGGTCGGTAAAGTTGTTCCATTTTTTGAAGCGAAGGTTGTGGATCTGGATACCGGGAAAACGC
TGGGCGTTAATCAAAGAGGCGAACTGTGTGTGAGAGGTCCTATGATTATGTCCGGTTATGTAAA
CAATCCGGAAGCGACCAACGCCTTGATTGACAAGGATGGATGGCTACATTCTGGAGACATAGCT
TACTGGGACGAAGACGAACACTTCTTCATCGTTGACCGCCTGAAGTCTCTGATTAAGTACAAAGG
CTATCAGGTGGCTCCCGCTGAATTGGAATCCATCTTGCTCCAACACCCCAACATCTTCGACGCAG

GTGTCGCAGGTCTTCCCGACGATGACGCCGGTGAACTTCCCGCCGCCGTTGTTGTTTTGGAGCAC
GGAAAGACGATGACGGAAAAAGAGATCGTGGATTACGTCGCCAGTCAAGTAACAACCGCGAAAA
AGTTGCGCGGAGGAGTTGTGTTTGTGGACGAAGTACCGAAAGGTCTTACCGGAAAACTCGACGC
AAGAAAAATCAGAGAGATCCTCATAAAGGCCAAGAAGGGCGGAAAGATCGCCGTGTAATTCTAG
GGATCCGCCCCTCTCCCTCCCCCCCCCCTAACGTTACTGGCCGAAGCCGCTTGGAATAAGGCCGGT
GTGCGTTTGTCTATATGTTATTTTCCACCATATTGCCGTCTTTTGGCAATGTGAGGGCCCGGAAA
CCTGGCCCTGTCTTCTTGACGAGCATTCCTAGGGGTCTTTCCCCTCTCGCCAAAGGAATGCAAGG
TCTGTTGAATGTCGTGAAGGAAGCAGTTCCTCTGGAAGCTTCTTGAAGACAAACAACGTCTGTA
GCGACCCTTTGCAGGCAGCGGAACCCCCCACCTGGCGACAGGTGCCTCTGCGGCCAAAAGCCACG
TGTATAAGATACACCTGCAAAGGCGGCACAACCCCAGTGCCACGTTGTGAGTTGGATAGTTGTG
GAAAGAGTCAAATGGCTCTCCTCAAGCGTATTCAACAAGGGGCTGAAGGATGCCCAGAAGGTAC
CCCATTGTATGGGATCTGATCTGGGGCCTCGGTACACATGCTTTACATGTGTTTAGTCGAGGTTA
AAAAAACGTCTAGGCCCCCCGAACCACGGGGACGTGGTTTTCCTTTGAAAAACACGATGATAAT
ATGGCCACAACCATGGCGCGCCTTACCGAGTACAAGCCCACGGTGCGCCTCGCCACCCGCGACGA
CGTCCCCAGGGCCGTACGCACCCTCGCCGCCGCGTTCGCCGACTACCCCGCCACGCGCCACACCGT
CGATCCGGACCGCCACATCGAGCGGGTCACCGAGCTGCAAGAACTCTTCCTCACGCGCGTCGGGC
TCGACATCGGCAAGGTGTGGGTCGCGGACGACGGCGCCGCGGTGGCGGTCTGGACCACGCCGGAG
AGCGTCGAAGCGGGGGCGGTGTTCGCCGAGATCGGCCCGCGCATGGCCGAGTTGAGCGGTTCCCG
GCTGGCCGCGCAGCAACAGATGGAAGGCCTCCTGGCGCCGCACCGGCCCAAGGAGCCCGCGTGGT
TCCTGGCCACCGTCGGCGTCTCGCCCGACCACCAGGGCAAGGGTCTGGGCAGCGCCGTCGTGCTCC
CCGGAGTGGAGGCGGCCGAGCGCGCCGGGGTGCCCGCCTTCCTGGAGACCTCCGCGCCCCGCAACC
TCCCCTTCTACGAGCGGCTCGGCTTCACCGTCACCGCCGACGTCGAGGTGCCCGAAGGACCGCGC
ACCTGGTGCATGACCCGCAAGCCCGGTGCCTGACGCCCGCCCCACGACCCGCAGCGCCCGACCGAA
AGGAGCGCACGACCCCATGCATCGTAGAGCTCGCTGATCAGCCTCGACTGTGCCTTCTAGTTGCC
AGCCATCTGTTGTTTGCCCCTCCCCCGTGCCTTCCTTGACCCTGGAAGGTGCCACTCCCACTGTCC
TTTCCTAATAAAATGAGGAAATTGCATCGCATTGTCTGAGTAGGTGTCATTCTATTCTGGGGGG
TGGGGTGGGGCAGGACAGCAAGGGGGAGGATTGGGAAGACAATAGCAGGCATGCTGGGGATGCG
GTGGGCTCTATGGCTTCTGAGGCGGAAAGAACCAGCTGGGGCTCGATGGCGCGTTCTAGACGCGT
ATCGATACGCGTCTAGAGTGAGGGTCCCCACCTGGGACCCTTGAGAGTATCAGGTCTCCCACGTG
GGAGACAAGAAATCCCTGTTTAATATTTAAACAGCAGTGTTCCCCATCTGGGTCCTTGCACCCCT
CACTCTGGCCTCAGCCGACTGCACAGCGGCCCCTGCATCCCCTTGGCTGTGAGGCCCCTGGACAAG
CAGAGGTGGCCAGAGCTGGGAGGCATGGCCCTGGGGTCCCACGAATTTGCTGGGGAATCTCGTTT
TTCTTCTTAAGACTTTTGGGACATGGTTTGACTCCCGAACATCACCGACGTGTCTCCTGTTTTTC
TGGGTGGCCTCGGGACACCTGCCCTGCCCCCACGAGGGTCAGGACTGTGACTCTTTTTAGGGCCA
GGCAGGTGCCTGGACATTTGCCTTGCTGGATGGGGACTGGGGATGTGGGAGGGAGCAGACAGGA
GGAATCATGTCAGGCCTGTGTGTGAAAGGAAGCTCCACTGTCACCCTCCACCTCTTCACCCCCCA
CTCACCAGTGTCCCCTCCACTGTCACATTGTAACTGAACTTCAGGATAATAAAGTGTTTGCCTCC
AGTCACGTCCTTCCTCCTTCTTGAGTCCAGCTGGTGCCTGGCCAGGGGCTGGGGAGGTGGCTGAA
GGGTGGGAGAGGCCAGAGGGAGGTCGGGGAGGAGGTCTGGGGAGGAGGTCCAGGGAGGAGGAGG
AAAGTTCTCAAGTTCGTCTGACATTCATTCCGTTAGCACATATTTATCTGAGCACCTACTCTGTG
CAGACGCTGGGCTAAGTGCTGGGGACACAGCAGGGAACAAGGCAGACATGGAATCTGCACTCGA
NNGAATTCACTGGCCGTCGTTTTACAACGTCGTGACTGGGAAAACCCTGGCGTTACCCAACTTAA
TCGCCTTGCAGCACATCCCCCTTTCGCCAGCTGGCGTAATAGCGAAGAGGCCCGCACCGATCGCC
CTTCCCAACAGTTGCGCAGCCTGAATGGCGAATGGCGCCTGATGCGGTATTTTCTCCTTACGCAT
CTGTGCGGTATTTCACACCGCATACGTCAAAGCAACCATAGTACGCGCCCTGTAGCGGCGCATTA
AGCGCGGCGGGTGTGGTGGTTACGCGCAGCGTGACCGCTACACTTGCCAGCGCCCTAGCGCCCGC
TCCTTTCGCTTTCTTCCCTTCCTTTCTCGCCACGTTCGCCGGCTTTCCCCGTCAAGCTCTAAATCG
GGGGCTCCCTTTAGGGTTCCGATTTAGTGCTTTACGGCACCTCGACCCCAAAAAACTTGATTTGG
GTGATGGTTCACGTAGTGGGCCATCGCCCTGATAGACGGTTTTTCGCCCTTTGACGTTGGAGTCC
ACGTTCTTTAATAGTGGACTCTTGTTCCAAACTGGAACAACACTCAACCCTATCTCGGGCTATTC
TTTTGATTTATAAGGGATTTTGCCGATTTCGGCCTATTGGTTAAAAAATGAGCTGATTTAACAA

AAATTTAACGCGAATTTTAACAAAATATTAACGTTTACAATTTTATGGTGCACTCTCAGTACAA
TCTGCTCTGATGCCGCATAGTTAAGCCAGCCCCGACACCCGCCAACACCCGCTGACGCGCCCTGAC
GGGCTTGTCTGCTCCCGGCATCCGCTTACAGACAAGCTGTGACCGTCTCCGGGAGCTGCATGTGT
CAGAGGTTTTCACCGTCATCACCGAAACGCGCGAGACGAAAGGGCCTCGTGATACGCCTATTTTT
ATAGGTTAATGTCATGATAATAATGGTTTCTTAGACGTCAGGTGGCACTTTTCGGGGAAATGTG
CGCGGAACCCCTATTTGTTTATTTTTCTAAATACATTCAAATATGTATCCGCTCATGAGACAATA
ACCCTGATAAATGCTTCAATAATATTGAAAAAGGAAGAGTATGAGTATTCAACATTTCCGTGTC
GCCCTTATTCCCTTTTTTGCGGCATTTTGCCTTCCTGTTTTTGCTCACCCAGAAACGCTGGTGAA
AGTAAAAGATGCTGAAGATCAGTTGGGTGCACGAGTGGGTTACATCGAACTGGATCTCAACAGC
GGTAAGATCCTTGAGAGTTTTCGCCCCGAAGAACGTTTTCCAATGATGAGCACTTTTAAAGTTCT
GCTATGTGGCGCGGTATTATCCCGTATTGACGCCGGGCAAGAGCAACTCGGTCGCCGCATACACT
ATTCTCAGAATGACTTGGTTGAGTACTCACCAGTCACAGAAAAGCATCTTACGGATGGCATGAC
AGTAAGAGAATTATGCAGTGCTGCCATAACCATGAGTGATAACACTGCGGCCAACTTACTTCTG
ACAACGATCGGAGGACCGAAGGAGCTAACCGCTTTTTTGCACAACATGGGGGATCATGTAACTC
GCCTTGATCGTTGGGAACCGGAGCTGAATGAAGCCATACCAAACGACGAGCGTGACACCACGATG
CCTGTAGCAATGGCAACAACGTTGCGCAAACTATTAACTGGCGAACTACTTACTCTAGCTTCCCG
GCAACAATTAATAGACTGGATGGAGGCGGATAAAGTTGCAGGACCACTTCTGCGCTCGGCCCTTC
CGGCTGGCTGGTTTATTGCTGATAAATCTGGAGCCGGTGAGCGTGGGTCTCGCGGTATCATTGCA
GCACTGGGGCCAGATGGTAAGCCCTCCCGTATCGTAGTTATCTACACGACGGGGAGTCAGGCAAC
TATGGATGAACGAAATAGACAGATCGCTGAGATAGGTGCCTCACTGATTAAGCATTGGTAACTG
TCAGACCAAGTTTACTCATATATACTTTAGATTGATTTAAAACTTCATTTTTAATTTAAAAGGA
TCTAGGTGAAGATCCTTTTTGATAATCTCATGACCAAAATCCCTTAACGTGAGTTTTCGTTCCAC
TGAGCGTCAGACCCCGTAGAAAAGATCAAAGGATCTTCTTGAGATCCTTTTTTTCTGCGCGTAAT
CTGCTGCTTGCAAACAAAAAAACCACCGCTACCAGCGGTGGTTTGTTTGCCGGATCAAGAGCTAC
CAACTCTTTTTCCGAAGGTAACTGGCTTCAGCAGAGCGCAGATACCAAATACTGTCCTTCTAGTG
TAGCCGTAGTTAGGCCACCACTTCAAGAACTCTGTAGCACCGCCTACATACCTCGCTCTGCTAAT
CCTGTTACCAGTGGCTGCTGCCAGTGGCGATAAGTCGTGTCTTACCGGGTTGGACTCAAGACGAT
AGTTACCGGATAAGGCGCAGCGGTCGGGCTGAACGGGGGGTTCGTGCACACAGCCCAGCTTGGAG
CGAACGACCTACACCGAACTGAGATACCTACAGCGTGAGCTATGAGAAAGCGCCACGCTTCCCGA
AGGGAGAAAGGCGGACAGGTATCCGGTAAGCGGCAGGGTCGGAACAGGAGAGCGCACGAGGGAG
CTTCCAGGGGGAAACGCCTGGTATCTTTATAGTCCTGTCGGGTTTCGCCACCTCTGACTTGAGCG
TCGATTTTTGTGATGCTCGTCAGGGGGGCGGAGCCTATGGAAAAACGCCAGCAACGCGGCCTTTT
TACGGTTCCTGGCCTTTTGCTGGCCTTTTGCTCACATGTTCTTTCCTGCGTTATCCCCTGATTCTG
TGGATAACCGTATTACCGCCTTTGAGTGAGCTGATACCGCTCGCCGCAGCCGAACGACCGAGCGC
AGCGAGTCAGTGAGCGAGGAAGCGGAAG

Plasmid size
8709bp

Features
EFBOS: 293 – 1743
Luciferase cDNA: 1757 – 3427
IRES: 3445 – 4020
Puromycin resistance: 4021 – 4976

## C. TOPOXL-T2ALuciferase plasmid information

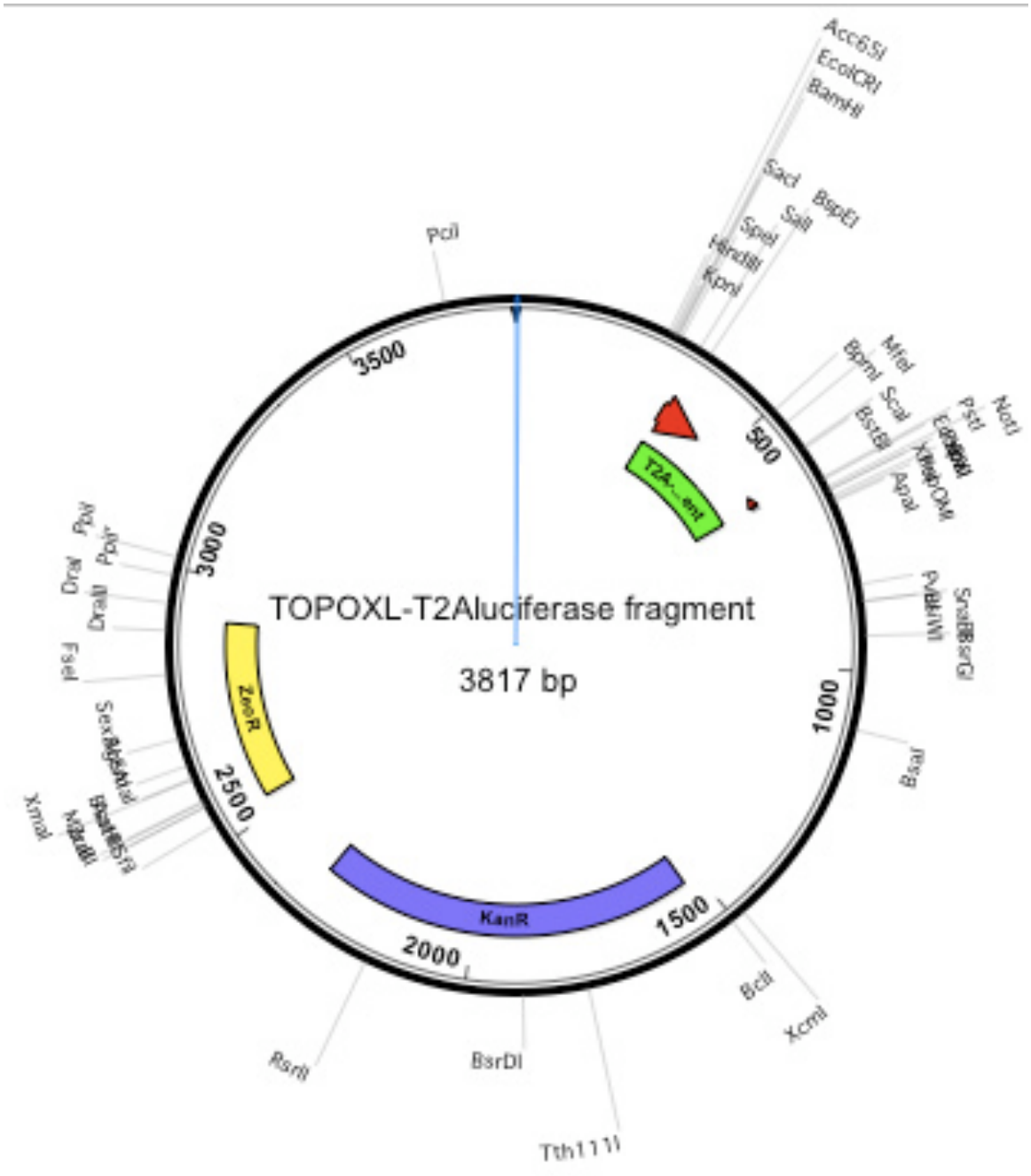

**TOPOXL-T2ALuciferase fragment sequence**

AGCGCCCAATACGCAAACCGCCTCTCCCCGCGCGTTGGCCGATTCATTAATGCAGCTGGCACGAC
AGGTTTCCCGACTGGAAAGCGGGCAGTGAGCGCAACGCAATTAATGTGAGTTAGCTCACTCATT
AGGCACCCCAGGCTTTACACTTTATGCTTCCGGCTCGTATGTTGTGTGGAATTGTGAGCGGATAA
CAATTTCACACAGGAAACAGCTATGACCATGATTACGCCAAGCTATTTAGGTGACGCGTTAGAA
TACTCAAGCTATGCATCAAGCTTGGTACCGAGCTCGGATCCACTAGTAACGGCCGCCAGTGTGCT
GGAATTCGCCCTTGTCGACACGCGTGGCGGCGGGTCCGGAGGAGAGGGCAGAGGAAGTCTTCTAA
CATGCGGTGACGTGGAGGAGAATCCTGGCCCAATGGAAGACGCCAAAAACATAAAGAAAGGCCC
GGCGCCATTCTATCCGCTGGAAGATGGAACCGCTGGAGAGCAACTGCATAAGGCTATGAAGAGA
TACGCCCTGGTTCCTGGAACAATTGCTTTTACAGATGCACATATCGAGGTGGACATCACTTACGC
TGAGTACTTCGAAATGTCCGTTCGGTTGGCAGAAGCTATGAAACGATATGGGCAAGGGCGAATT
CTGCAGATATCCATCACACTGGCGGCCGCTCGAGCATGCATCTAGAGGGCCCAATTCGCCCTATA
GTGAGTCGTATTACAATTCACTGGCCGTCGTTTTACAACGTCGTGACTGGGAAAACCCTGGCGTT
ACCCAACTTAATCGCCTTGCAGCACATCCCCCTTTCGCCAGCTGGCGTAATAGCGAAGAGGCCCG
CACCGATCGCCCTTCCCAACAGTTGCGCAGCCTATACGTACGGCAGTTTAAGGTTTACACCTATA
AAAGAGAGAGCCGTTATCGTCTGTTTGTGGATGTACAGAGTGATATTATTGACACGCCGGGGCG
ACGGATGGTGATCCCCCTGGCCAGTGCACGTCTGCTGTCAGATAAAGTCTCCCGTGAACTTTACC
CGGTGGTGCATATCGGGGATGAAAGCTGGCGCATGATGACCACCGATATGGCCAGTGTGCCGGTC
TCCGTTATCGGGGAAGAAGTGGCTGATCTCAGCCACCGCGAAAATGACATCAAAAACGCCATTA
ACCTGATGTTCTGGGGAATATAAATGTCAGGCATGAGATTATCAAAAAGGATCTTCACCTAGAT
CCTTTTCACGTAGAAAGCCAGTCCGCAGAAACGGTGCTGACCCCGGATGAATGTCAGCTACTGGG
CTATCTGGACAAGGGAAAACGCAAGCGCAAAGAGAAAGCAGGTAGCTTGCAGTGGGCTTACATG
GCGATAGCTAGACTGGGCGGTTTTATGGACAGCAAGCGAACCGGAATTGCCAGCTGGGGCGCCCT
CTGGTAAGGTTGGGAAGCCCTGCAAAGTAAACTGGATGGCTTTCTCGCCGCCAAGGATCTGATGG
CGCAGGGGATCAAGCTCTGATCAAGAGACAGGATGAGGATCGTTTCGCATGATTGAACAAGATG
GATTGCACGCAGGTTCTCCGGCCGCTTGGGTGGAGAGGCTATTCGGCTATGACTGGGCACAACAG
ACAATCGGCTGCTCTGATGCCGCCGTGTTCCGGCTGTCAGCGCAGGGGCGCCCGGTTCTTTTTGT
CAAGACCGACCTGTCCGGTGCCCTGAATGAACTGCAAGACGAGGCAGCGCGGCTATCGTGGCTGG
CCACGACGGGCGTTCCTTGCGCAGCTGTGCTCGACGTTGTCACTGAAGCGGGAAGGGACTGGCTG
CTATTGGGCGAAGTGCCGGGGCAGGATCTCCTGTCATCTCACCTTGCTCCTGCCGAGAAAGTATC
CATCATGGCTGATGCAATGCGGCGGCTGCATACGCTTGATCCGGCTACCTGCCCATTCGACCACC
AAGCGAAACATCGCATCGAGCGAGCACGTACTCGGATGGAAGCCGGTCTTGTCGATCAGGATGA
TCTGGACGAAGAGCATCAGGGGCTCGCGCCAGCCGAACTGTTCGCCAGGCTCAAGGCGAGCATGC
CCGACGGCGAGGATCTCGTCGTGACCCATGGCGATGCCTGCTTGCCGAATATCATGGTGGAAAAT
GGCCGCTTTTCTGGATTCATCGACTGTGGCCGGCTGGGTGTGGCGGACCGCTATCAGGACATAGC
GTTGGCTACCCGTGATATTGCTGAAGAGCTTGGCGGCGAATGGGCTGACCGCTTCCTCGTGCTTT
ACGGTATCGCCGCTCCCGATTCGCAGCGCATCGCCTTCTATCGCCTTCTTGACGAGTTCTTCTGA
ATTATTAACGCTTACAATTTCCTGATGCGGTATTTTCTCCTTACGCATCTGTGCGGTATTTCACA
CCGCATACAGGTGGCACTTTTCGGGGAAATGTGCGCGGAACCCCTATTTGTTTATTTTTCTAAAT
ACATTCAAATATGTATCCGCTCATGAGACAATAACCCTGATAAATGCTTCAATAATAGCACGTG
AGGAGGGCCACCATGGCCAAGTTGACCAGTGCCGTTCCGGTGCTCACCGCGCGCGACGTCGCCGG
AGCGGTCGAGTTCTGGACCGACCGGCTCGGGTTCTCCCGGGACTTCGTGGAGGACGACTTCGCCG
GTGTGGTCCGGGACGACGTGACCCTGTTCATCAGCGCGGTCCAGGACCAGGTGGTGCCGGACAAC
ACCCTGGCCTGGGTGTGGGTGCGCGGCCTGGACGAGCTGTACGCCGAGTGGTCGGAGGTCGTGTC
CACGAACTTCCGGGACGCCTCCGGGCCGGCCATGACCGAGATCGGCGAGCAGCCGTGGGGGCGGG
AGTTCGCCCTGCGCGACCCGGCCGGCAACTGCGTGCACTTCGTGGCCGAGGAGCAGGACTGACAC
GTGCTAAAACTTCATTTTTAATTTAAAAGGATCTAGGTGAAGATCCTTTTTGATAATCTCATGA
CCAAAATCCCTTAACGTGAGTTTTCGTTCCACTGAGCGTCAGACCCCGTAGAAAAGATCAAAGGA
TCTTCTTGAGATCCTTTTTTTCTGCGCGTAATCTGCTGCTTGCAAACAAAAAAACCACCGCTACC
AGCGGTGGTTTGTTTGCCGGATCAAGAGCTACCAACTCTTTTTCCGAAGGTAACTGGCTTCAGCA

GAGCGCAGATACCAAATACTGTCCTTCTAGTGTAGCCGTAGTTAGGCCACCACTTCAAGAACTCT
GTAGCACCGCCTACATACCTCGCTCTGCTAATCCTGTTACCAGTGGCTGCTGCCAGTGGCGATAA
GTCGTGTCTTACCGGGTTGGACTCAAGACGATAGTTACCGGATAAGGCGCAGCGGTCGGGCTGAA
CGGGGGGTTCGTGCACACAGCCCAGCTTGGAGCGAACGACCTACACCGAACTGAGATACCTACAG
CGTGAGCTATGAGAAAGCGCCACGCTTCCCGAAGGGAGAAAGGCGGACAGGTATCCGGTAAGCG
GCAGGGTCGGAACAGGAGAGCGCACGAGGGAGCTTCCAGGGGGAAACGCCTGGTATCTTTATAG
TCCTGTCGGGTTTCGCCACCTCTGACTTGAGCGTCGATTTTTGTGATGCTCGTCAGGGGGGCGGA
GCCTATGGAAAAACGCCAGCAACGCGGCCTTTTTACGGTTCCTGGGCTTTTGCTGGCCTTTTGCT
CACATGTTCTTTCCTGCGTTATCCCCTGATTCTGTGGATAACCGTATTACCGCCTTTGAGTGAGC
TGATACCGCTCGCCGCAGCCGAACGACCGAGCGCAGCGAGTCAGTGAGCGAGGAAGCGGAAG

Plasmid size
3817bp

Features
T2A-Luciferase PCR fragment: 337 – 634
Kanamycin resistance: 1535 – 2329
Zeocin resistance: 2536 - 2910

## D. pEFBOS-T2ALuciferaseIRESPuro plasmid information

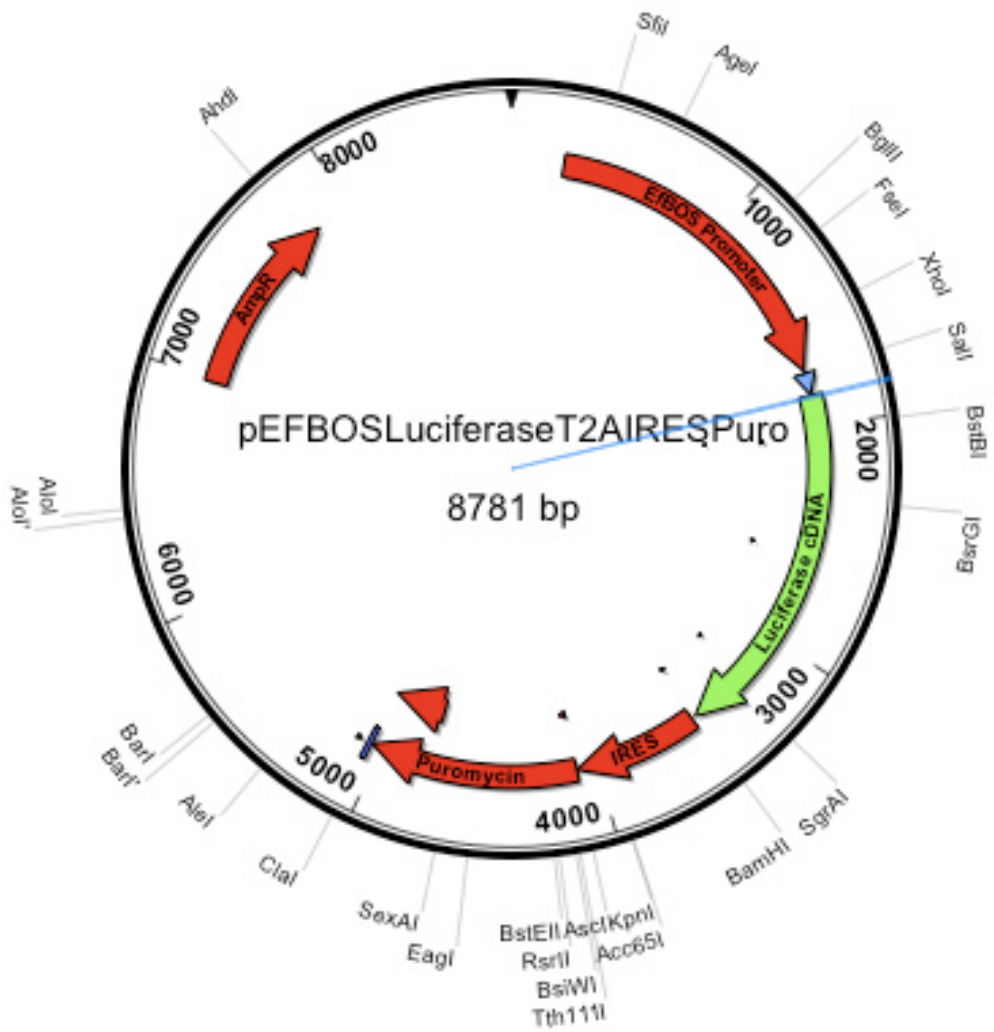

**pEFBOS-T2ALuciferaseIRESPuro sequence**

AGCGCCCAATACGCAAACCGCCTCTCCCCGCGCGTTGGCCGATTCATTAATGCAGCTGGCACGAC
AGGTTTCCCGACTGGAAAGCGGGCAGTGAGCGCAACGCAATTAATGTGAGTTAGCTCACTCATT
AGGCACCCCAGGCTTTACACTTTATGCTTCCGGCTCGTATGTTGTGTGGAATTGTGAGCGGATAA
CAATTTCACACAGGAAACAGCTATGACCATGATTACGCCAAGCTTCCAGGCACTCCTTTCAAGAC
CTAGAAGGTCCATTAGCTGCAAAGATTCCTCTCTGTTTAAAACTTTATCCATCTTTGCAAAGCTT
TTTGCAAAAGCCTAGGCCTCCAAAAAAGCCTCCTCACTACTTCTGGAATAGCTCAGAGGCCGAGG
CGGCCTCGGCCTCTGCATAAATAAAAAAAATTAGTCAGCCATGGGGCGGAGAATGGGCGGAACT
GGGCGGAGTTAGGGGCGGGATGGGCGGAGTTAGGGGCGGGACTATGGTTGCTGACTAATTGAGA
TGCATGCTTTGCATACTTCTGCCTGCTGGGGAGCCTGGCGTGAGGCTCCGGTGCCCGTCAGTGGG
CAGAGCGCACATCGCCCACAGTCCCCGAGAAGTTGGGGGGAGGGGTCGGCAATTGAACCGGTGCC
TAGAGAAGGTGGCGCGGGGTAAACTGGGAAAGTGATGTCGTGTACTGGCTCCGCCTTTTTCCCGA
GGGTGGGGGAGAACCGTATATAAGTGCAGTAGTCGCCGTGAACGTTCTTTTTCGCAACGGGTTT
GCCGCCAGAACACAGGTAAGTGCCGTGTGTGGTTCCCGCGGGCCTGGCCTCTTTACGGGTTATGG
CCCTTGCGTGCCTTGAATTACTTCCACGCCCCTGGCTGCAGTACGTGATTCTTGATCCCGAGCTT
CGGGTTGGAAGTGGGTGGGAGAGTTCGAGGCCTTGCGCTTAAGGAGCCCCTTCGCCTCGTGCTTG
AGTTGAGGCCTGGCCTGGGCGCTGGGGCCGCCGCGTGCGAATCTGGTGGCACCTTCGCGCCTGTC
TCGCTGCTTTCGATAAGTCTCTAGCCATTTAAAATTTTTGATGACCTGCTGCGACGCTTTTTTTC
TGGCAAGATAGTCTTGTAAATGCGGGCCAAGATCTGCACACTGGTATTTCGGTTTTTGGGGCCGC
GGGCGGCGACGGGGCCCGTGCGTCCCAGCGCACATGTTCGGCGAGGCGGGGCCTGCGAGCGCGGC
CACCGAGAATCGGACGGGGGTAGTCTCAAGCTGGCCGGCCTGCTCTGGTGCCTGGCCTCGCGCCG
CCGTGTATCGCCCCGCCCTGGGCGGCAAGGCTGGCCCGGTCGGCACCAGTTGCGTGAGCGGAAAG
ATGGCCGCTTCCCGGCCCTGCTGCAGGGAGCTCAAAATGGAGGACGCGGCGCTCGGGAGAGCGGG
CGGGTGAGTCACCCACACAAAGGAAAAGGGCCTTTCCGTCCTCAGCCGTCGCTTCATGTGACTCC
ACGGAGTACCGGGCGCCGTCCAGGCACCTCGATTAGTTCTCGAGCTTTTGGAGTACGTCGTCTTT
AGGTTGGGGGGAGGGGTTTTATGCGATGGAGTTTCCCCACACTGAGTGGGTGGAGACTGAAGTT
AGGCCAGCTTGGCACTTGATGTAATTCTCCTTGGAATTTGCCCTTTTTGAGTTTGGATCTTGGTT
CATTCTCAAGCCTCAGACAGTGGTTCAAAGTTTTTTTCTTCCATTTCAGGTGTCGTGAGGAATTC
TCTAGGTCGACACGCGTGGCGGCGGGTCCGGAGGAGAGGGCAGAGGAAGTCTTCTAACATGCGG
TGACGTGGAGGAGAATCCTGGCCCAATGGAAGACGCCAAAAACATAAAGAAAGGCCCGGCGCCA
TTCTATCCGCTGGAAGATGGAACCGCTGGAGAGCAACTGCATAAGGCTATGAAGAGATACGCCC
TGGTTCCTGGAACAATTGCTTTTACAGATGCACATATCGAGGTGGACATCACTTACGCTGAGTAC
TTCGAAATGTCCGTTCGGTTGGCAGAAGCTATGAAACGATATGGGCTGAATACAAATCACAGAA
TCGTCGTATGCAGTGAAAACTCTCTTCAATTCTTTATGCCGGTGTTGGGCGCGTTATTTATCGGA
GTTGCAGTTGCGCCCGCGAACGACATTTATAATGAACGTGAATTGCTCAACAGTATGGGCATTTC
GCAGCCTACCGTGGTGTTCGTTTCCAAAAAGGGGTTGCAAAAAATTTTGAACGTGCAAAAAAAG
CTCCCAATCATCCAAAAAATTATTATCATGGATTCTAAAACGGATTACCAGGGATTTCAGTCGA
TGTACACGTTCGTCACATCTCATCTACCTCCCGGTTTTAATGAATACGATTTTGTGCCAGAGTCC
TTCGATAGGGACAAGACAATTGCACTGATCATGAACTCCTCTGGATCTACTGGTCTGCCTAAAGG
TGTCGCTCTGCCTCATAGAACTGCCTGCGTGAGATTCTCGCATGCCAGAGATCCTATTTTTGGCA
ATCAAATCATTCCGGATACTGCGATTTTAAGTGTTGTTCCATTCCATCACGGTTTTGGAATGTTT
ACTACACTCGGATATTTGATATGTGGATTTCGAGTCGTCTTAATGTATAGATTTGAAGAAGAGC
TGTTTCTGAGGAGCCTTCAGGATTACAAGATTCAAAGTGCGCTGCTGGTGCCAACCCTATTCTCC
TTCTTCGCCAAAAGCACTCTGATTGACAAATACGATTTATCTAATTTACACGAAATTGCTTCTGG
TGGCGCTCCCCTCTCTAAGGAAGTCGGGGAAGCGGTTGCCAAGAGGTTCCATCTGCCAGGTATCA
GGCAAGGATATGGGCTCACTGAGACTACATCAGCTATTCTGATTACACCCGAGGGGATGATAA
ACCGGGCGCGGTCGGTAAAGTTGTTCCATTTTTTGAAGCGAAGGTTGTGGATCTGGATACCGGG
AAAACGCTGGGCGTTAATCAAAGAGGCGAACTGTGTGTGAGAGGTCCTATGATTATGTCCGGTT
ATGTAAACAATCCGGAAGCGACCAACGCCTTGATTGACAAGGATGGATGGCTACATTCTGGAGA
CATAGCTTACTGGGACGAAGACGAACACTTCTTCATCGTTGACCGCCTGAAGTCTCTGATTAAGT

ACAAAGGCTATCAGGTGGCTCCCGCTGAATTGGAATCCATCTTGCTCCAACACCCCAACATCTTC
GACGCAGGTGTCGCAGGTCTTCCCGACGATGACGCCGGTGAACTTCCCGCCGCCGTTGTTGTTTT
GGAGCACGGAAAGACGATGACGGAAAAAGAGATCGTGGATTACGTCGCCAGTCAAGTAACAACC
GCGAAAAAGTTGCGCGGAGGAGTTGTGTTTGTGGACGAAGTACCGAAAGGTCTTACCGGAAAAC
TCGACGCAAGAAAAATCAGAGAGATCCTCATAAAGGCCAAGAAGGGCGGAAAGATCGCCGTGTA
ATTCTAGGGATCCGCCCCTCTCCCTCCCCCCCCCCTAACGTTACTGGCCGAAGCCGCTTGGAATAA
GGCCGGTGTGCGTTTGTCTATATGTTATTTTCCACCATATTGCCGTCTTTTGGCAATGTGAGGGC
CCGGAAACCTGGCCCTGTCTTCTTGACGAGCATTCCTAGGGGTCTTTCCCCTCTCGCCAAAGGAA
TGCAAGGTCTGTTGAATGTCGTGAAGGAAGCAGTTCCTCTGGAAGCTTCTTGAAGACAAACAAC
GTCTGTAGCGACCCTTTGCAGGCAGCGGAACCCCCCACCTGGCGACAGGTGCCTCTGCGGCCAAA
AGCCACGTGTATAAGATACACCTGCAAAGGCGGCACAACCCCAGTGCCACGTTGTGAGTTGGATA
GTTGTGGAAAGAGTCAAATGGCTCTCCTCAAGCGTATTCAACAAGGGGCTGAAGGATGCCCAGA
AGGTACCCCATTGTATGGGATCTGATCTGGGGCCTCGGTACACATGCTTTACATGTGTTTAGTCG
AGGTTAAAAAAACGTCTAGGCCCCCCGAACCACGGGGACGTGGTTTTCCTTTGAAAAACACGATG
ATAATATGGCCACAACCATGGCGCGCCTTACCGAGTACAAGCCCACGGTGCGCCTCGCCACCCGC
GACGACGTCCCCAGGGCCGTACGCACCCTCGCCGCCGCGTTCGCCGACTACCCCGCCACGCGCCAC
ACCGTCGATCCGGACCGCCACATCGAGCGGGTCACCGAGCTGCAAGAACTCTTCCTCACGCGCGT
CGGGCTCGACATCGGCAAGGTGTGGGTCGCGGACGACGGCGCCGCGGTGGCGGTCTGGACCACGC
CGGAGAGCGTCGAAGCGGGGGCGGTGTTCGCCGAGATCGGCCCGCGCATGGCCGAGTTGAGCGGT
TCCCGGCTGGCCGCGCAGCAACAGATGGAAGGCCTCCTGGCGCCGCACCGGCCCAAGGAGCCCGC
GTGGTTCCTGGCCACCGTCGGCGTCTCGCCCGACCACCAGGGCAAGGGTCTGGGCAGCGCCGTCG
TGCTCCCCGGAGTGGAGGCGGCCGAGCGCGCCGGGGTGCCCGCCTTCCTGGAGACCTCCGCGCCCC
GCAACCTCCCCTTCTACGAGCGGCTCGGCTTCACCGTCACCGCCGACGTCGAGGTGCCCGAAGGA
CCGCGCACCTGGTGCATGACCCGCAAGCCCGGTGCCTGACGCCCGCCCCACGACCCGCAGCGCCCG
ACCGAAAGGAGCGCACGACCCCATGCATCGTAGAGCTCGCTGATCAGCCTCGACTGTGCCTTCTA
GTTGCCAGCCATCTGTTGTTTGCCCCTCCCCCGTGCCTTCCTTGACCCTGGAAGGTGCCACTCCCA
CTGTCCTTTCCTAATAAAATGAGGAAATTGCATCGCATTGTCTGAGTAGGTGTCATTCTATTCTG
GGGGGTGGGGTGGGGCAGGACAGCAAGGGGGAGGATTGGGAAGACAATAGCAGGCATGCTGGGG
ATGCGGTGGGCTCTATGGCTTCTGAGGCGGAAAGAACCAGCTGGGGCTCGATGGCGCGTTCTAGA
CGCGTATCGATACGCGTCTAGAGTGAGGGTCCCCACCTGGGACCCTTGAGAGTATCAGGTCTCCC
ACGTGGGAGACAAGAAATCCCTGTTTAATATTTAAACAGCAGTGTTCCCCATCTGGGTCCTTGCA
CCCCTCACTCTGGCCTCAGCCGACTGCACAGCGGCCCCTGCATCCCCTTGGCTGTGAGGCCCCTGG
ACAAGCAGAGGTGGCCAGAGCTGGGAGGCATGGCCCTGGGGTCCCACGAATTTGCTGGGGAATC
TCGTTTTTCTTCTTAAGACTTTTGGGACATGGTTTGACTCCCGAACATCACCGACGTGTCTCCTG
TTTTTCTGGGTGGCCTCGGGACACCTGCCCTGCCCCCACGAGGGTCAGGACTGTGACTCTTTTTA
GGGCCAGGCAGGTGCCTGGACATTTGCCTTGCTGGATGGGGACTGGGGATGTGGGAGGGAGCAG
ACAGGAGGAATCATGTCAGGCCTGTGTGTGAAAGGAAGCTCCACTGTCACCCTCCACCTCTTCAC
CCCCCACTCACCAGTGTCCCCTCCACTGTCACATTGTAACTGAACTTCAGGATAATAAAGTGTTT
GCCTCCAGTCACGTCCTTCCTCCTTCTTGAGTCCAGCTGGTGCCTGGCCAGGGGCTGGGGAGGTG
GCTGAAGGGTGGGAGAGGCCAGAGGGAGGTCGGGGAGGAGGTCTGGGGAGGAGGTCCAGGGAGG
AGGAGGAAAGTTCTCAAGTTCGTCTGACATTCATTCCGTTAGCACATATTTATCTGAGCACCTAC
TCTGTGCAGACGCTGGGCTAAGTGCTGGGGACACAGCAGGGAACAAGGCAGACATGGAATCTGC
ACTCGANNGAATTCACTGGCCGTCGTTTTACAACGTCGTGACTGGGAAAACCCTGGCGTTACCCA
ACTTAATCGCCTTGCAGCACATCCCCCTTTCGCCAGCTGGCGTAATAGCGAAGAGGCCCGCACCG
ATCGCCCTTCCCAACAGTTGCGCAGCCTGAATGGCGAATGGCGCCTGATGCGGTATTTTCTCCTT
ACGCATCTGTGCGGTATTTCACACCGCATACGTCAAAGCAACCATAGTACGCGCCCTGTAGCGGC
GCATTAAGCGCGGCGGGTGTGGTGGTTACGCGCAGCGTGACCGCTACACTTGCCAGCGCCCTAGC
GCCCGCTCCTTTCGCTTTCTTCCCTTCCTTTCTCGCCACGTTCGCCGGCTTTCCCCGTCAAGCTCT
AAATCGGGGGCTCCCTTTAGGGTTCCGATTTAGTGCTTTACGGCACCTCGACCCCAAAAAACTTG
ATTTGGGTGATGGTTCACGTAGTGGGCCATCGCCCTGATAGACGGTTTTTCGCCCTTTGACGTTG
GAGTCCACGTTCTTTAATAGTGGACTCTTGTTCCAAACTGGAACAACACTCAACCCTATCTCGGG

CTATTCTTTTGATTTATAAGGGATTTTGCCGATTTCGGCCTATTGGTTAAAAAATGAGCTGATT
TAACAAAAATTTAACGCGAATTTTAACAAAATATTAACGTTTACAATTTTATGGTGCACTCTCA
GTACAATCTGCTCTGATGCCGCATAGTTAAGCCAGCCCCGACACCCGCCAACACCCGCTGACGCG
CCCTGACGGGCTTGTCTGCTCCCGGCATCCGCTTACAGACAAGCTGTGACCGTCTCCGGGAGCTG
CATGTGTCAGAGGTTTTCACCGTCATCACCGAAACGCGCGAGACGAAAGGGCCTCGTGATACGCC
TATTTTTATAGGTTAATGTCATGATAATAATGGTTTCTTAGACGTCAGGTGGCACTTTTCGGGG
AAATGTGCGCGGAACCCCTATTTGTTTATTTTTCTAAATACATTCAAATATGTATCCGCTCATGA
GACAATAACCCTGATAAATGCTTCAATAATATTGAAAAAGGAAGAGTATGAGTATTCAACATTT
CCGTGTCGCCCTTATTCCCTTTTTTGCGGCATTTTGCCTTCCTGTTTTTGCTCACCCAGAAACGCT
GGTGAAAGTAAAAGATGCTGAAGATCAGTTGGGTGCACGAGTGGGTTACATCGAACTGGATCTC
AACAGCGGTAAGATCCTTGAGAGTTTTCGCCCCGAAGAACGTTTTCCAATGATGAGCACTTTTAA
AGTTCTGCTATGTGGCGCGGTATTATCCCGTATTGACGCCGGGCAAGAGCAACTCGGTCGCCGCA
TACACTATTCTCAGAATGACTTGGTTGAGTACTCACCAGTCACAGAAAAGCATCTTACGGATGGC
ATGACAGTAAGAGAATTATGCAGTGCTGCCATAACCATGAGTGATAACACTGCGGCCAACTTAC
TTCTGACAACGATCGGAGGACCGAAGGAGCTAACCGCTTTTTTGCACAACATGGGGGATCATGT
AACTCGCCTTGATCGTTGGGAACCGGAGCTGAATGAAGCCATACCAAACGACGAGCGTGACACCA
CGATGCCTGTAGCAATGGCAACAACGTTGCGCAAACTATTAACTGGCGAACTACTTACTCTAGCT
TCCCGGCAACAATTAATAGACTGGATGGAGGCGGATAAAGTTGCAGGACCACTTCTGCGCTCGGC
CCTTCCGGCTGGCTGGTTTATTGCTGATAAATCTGGAGCCGGTGAGCGTGGGTCTCGCGGTATCA
TTGCAGCACTGGGGCCAGATGGTAAGCCCTCCCGTATCGTAGTTATCTACACGACGGGGAGTCAG
GCAACTATGGATGAACGAAATAGACAGATCGCTGAGATAGGTGCCTCACTGATTAAGCATTGGT
AACTGTCAGACCAAGTTTACTCATATATACTTTAGATTGATTTAAAACTTCATTTTTAATTTAA
AAGGATCTAGGTGAAGATCCTTTTTGATAATCTCATGACCAAAATCCCTTAACGTGAGTTTTCG
TTCCACTGAGCGTCAGACCCCGTAGAAAAGATCAAAGGATCTTCTTGAGATCCTTTTTTTCTGCG
CGTAATCTGCTGCTTGCAAACAAAAAAACCACCGCTACCAGCGGTGGTTTGTTTGCCGGATCAAG
AGCTACCAACTCTTTTTCCGAAGGTAACTGGCTTCAGCAGAGCGCAGATACCAAATACTGTCCTT
CTAGTGTAGCCGTAGTTAGGCCACCACTTCAAGAACTCTGTAGCACCGCCTACATACCTCGCTCT
GCTAATCCTGTTACCAGTGGCTGCTGCCAGTGGCGATAAGTCGTGTCTTACCGGGTTGGACTCAA
GACGATAGTTACCGGATAAGGCGCAGCGGTCGGGCTGAACGGGGGGTTCGTGCACACAGCCCAGC
TTGGAGCGAACGACCTACACCGAACTGAGATACCTACAGCGTGAGCTATGAGAAAGCGCCACGCT
TCCCGAAGGGAGAAAGGCGGACAGGTATCCGGTAAGCGGCAGGGTCGGAACAGGAGAGCGCACG
AGGGAGCTTCCAGGGGGAAACGCCTGGTATCTTTATAGTCCTGTCGGGTTTCGCCACCTCTGACT
TGAGCGTCGATTTTTGTGATGCTCGTCAGGGGGGCGGAGCCTATGGAAAAACGCCAGCAACGCG
GCCTTTTTACGGTTCCTGGCCTTTTGCTGGCCTTTTGCTCACATGTTCTTTCCTGCGTTATCCCCT
GATTCTGTGGATAACCGTATTACCGCCTTTGAGTGAGCTGATACCGCTCGCCGCAGCCGAACGAC
CGAGCGCAGCGAGTCAGTGAGCGAGGAAGCGGAAG

Plasmid size
8781bp

Features
EFBOS: 239 - 1743
T2A: 1756 - 1857
Luciferase cDNA: 1858 - 3499
IRES: 3517 - 4092
Puromycin resistance: 4093 - 5048

## E. pEFBOS-T2ALuciferaseIRESMeo (Luciferase expression vector) plasmid information

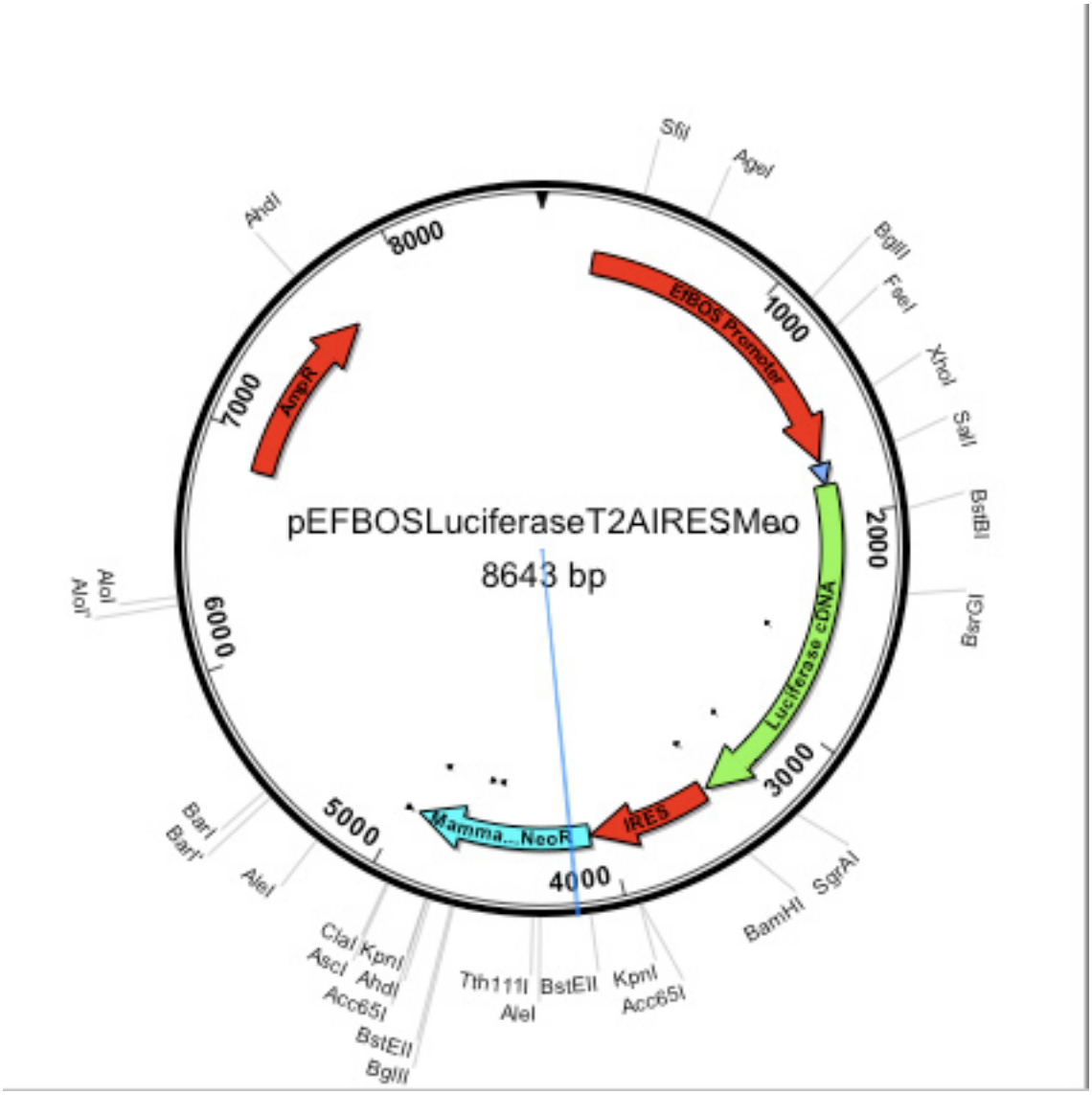

**pEFBOS-T2ALuciferaseIRESMeo (Luciferase expression vector) sequence**

AGCGCCCAATACGCAAACCGCCTCTCCCCGCGCGTTGGCCGATTCATTAATGCAGCTGGCACGAC
AGGTTTCCCGACTGGAAAGCGGGCAGTGAGCGCAACGCAATTAATGTGAGTTAGCTCACTCATT
AGGCACCCCAGGCTTTACACTTTATGCTTCCGGCTCGTATGTTGTGTGGAATTGTGAGCGGATAA
CAATTTCACACAGGAAACAGCTATGACCATGATTACGCCAAGCTTCCAGGCACTCCTTTCAAGAC
CTAGAAGGTCCATTAGCTGCAAAGATTCCTCTCTGTTTAAAACTTTATCCATCTTTGCAAAGCTT
TTTGCAAAAGCCTAGGCCTCCAAAAAAGCCTCCTCACTACTTCTGGAATAGCTCAGAGGCCGAGG
CGGCCTCGGCCTCTGCATAAATAAAAAAAATTAGTCAGCCATGGGGCGGAGAATGGGCGGAACT
GGGCGGAGTTAGGGGCGGGATGGGCGGAGTTAGGGGCGGGACTATGGTTGCTGACTAATTGAGA
TGCATGCTTTGCATACTTCTGCCTGCTGGGGAGCCTGGCGTGAGGCTCCGGTGCCCGTCAGTGGG
CAGAGCGCACATCGCCCACAGTCCCCGAGAAGTTGGGGGGAGGGGTCGGCAATTGAACCGGTGCC
TAGAGAAGGTGGCGCGGGGTAAACTGGGAAAGTGATGTCGTGTACTGGCTCCGCCTTTTTCCCGA
GGGTGGGGGAGAACCGTATATAAGTGCAGTAGTCGCCGTGAACGTTCTTTTTCGCAACGGGTTT
GCCGCCAGAACACAGGTAAGTGCCGTGTGTGGTTCCCGCGGGCCTGGCCTCTTTACGGGTTATGG
CCCTTGCGTGCCTTGAATTACTTCCACGCCCCTGGCTGCAGTACGTGATTCTTGATCCCGAGCTT
CGGGTTGGAAGTGGGTGGGAGAGTTCGAGGCCTTGCGCTTAAGGAGCCCCTTCGCCTCGTGCTTG
AGTTGAGGCCTGGCCTGGGCGCTGGGGCCGCCGCGTGCGAATCTGGTGGCACCTTCGCGCCTGTC
TCGCTGCTTTCGATAAGTCTCTAGCCATTTAAAATTTTTGATGACCTGCTGCGACGCTTTTTTTC
TGGCAAGATAGTCTTGTAAATGCGGGCCAAGATCTGCACACTGGTATTTCGGTTTTTGGGGCCGC
GGGCGGCGACGGGGCCCGTGCGTCCCAGCGCACATGTTCGGCGAGGCGGGGCCTGCGAGCGCGGC
CACCGAGAATCGGACGGGGGTAGTCTCAAGCTGGCCGGCCTGCTCTGGTGCCTGGCCTCGCGCCG
CCGTGTATCGCCCCGCCCTGGGCGGCAAGGCTGGCCCGGTCGGCACCAGTTGCGTGAGCGGAAAG
ATGGCCGCTTCCCGGCCCTGCTGCAGGGAGCTCAAAATGGAGGACGCGGCGCTCGGGAGAGCGGG
CGGGTGAGTCACCCACACAAAGGAAAAGGGCCTTTCCGTCCTCAGCCGTCGCTTCATGTGACTCC
ACGGAGTACCGGGCGCCGTCCAGGCACCTCGATTAGTTCTCGAGCTTTTGGAGTACGTCGTCTTT
AGGTTGGGGGGAGGGGTTTTATGCGATGGAGTTTCCCCACACTGAGTGGGTGGAGACTGAAGTT
AGGCCAGCTTGGCACTTGATGTAATTCTCCTTGGAATTTGCCCTTTTTGAGTTTGGATCTTGGTT
CATTCTCAAGCCTCAGACAGTGGTTCAAAGTTTTTTTCTTCCATTTCAGGTGTCGTGAGGAATTC
TCTAGGTCGACACGCGTGGCGGCGGGTCCGGAGGAGAGGGCAGAGGAAGTCTTCTAACATGCGG
TGACGTGGAGGAGAATCCTGGCCCAATGGAAGACGCCAAAAACATAAAGAAAGGCCCGGCGCCA
TTCTATCCGCTGGAAGATGGAACCGCTGGAGAGCAACTGCATAAGGCTATGAAGAGATACGCCC
TGGTTCCTGGAACAATTGCTTTTACAGATGCACATATCGAGGTGGACATCACTTACGCTGAGTAC
TTCGAAATGTCCGTTCGGTTGGCAGAAGCTATGAAACGATATGGGCTGAATACAAATCACAGAA
TCGTCGTATGCAGTGAAAACTCTCTTCAATTCTTTATGCCGGTGTTGGGCGCGTTATTTATCGGA
GTTGCAGTTGCGCCCGCGAACGACATTTATAATGAACGTGAATTGCTCAACAGTATGGGCATTTC
GCAGCCTACCGTGGTGTTCGTTTCCAAAAAGGGGTTGCAAAAAATTTTGAACGTGCAAAAAAAG
CTCCCAATCATCCAAAAAATTATTATCATGGATTCTAAAACGGATTACCAGGGATTTCAGTCGA
TGTACACGTTCGTCACATCTCATCTACCTCCCGGTTTTAATGAATACGATTTTGTGCCAGAGTCC
TTCGATAGGGACAAGACAATTGCACTGATCATGAACTCCTCTGGATCTACTGGTCTGCCTAAAGG
TGTCGCTCTGCCTCATAGAACTGCCTGCGTGAGATTCTCGCATGCCAGAGATCCTATTTTTGGCA
ATCAAATCATTCCGGATACTGCGATTTTAAGTGTTGTTCCATTCCATCACGGTTTTGGAATGTTT
ACTACACTCGGATATTTGATATGTGGATTTCGAGTCGTCTTAATGTATAGATTTGAAGAAGAGC
TGTTTCTGAGGAGCCTTCAGGATTACAAGATTCAAAGTGCGCTGCTGGTGCCAACCCTATTCTCC
TTCTTCGCCAAAAGCACTCTGATTGACAAATACGATTTATCTAATTTACACGAAATTGCTTCTGG
TGGCGCTCCCCTCTCTAAGGAAGTCGGGGAAGCGGTTGCCAAGAGGTTCCATCTGCCAGGTATCA
GGCAAGGATATGGGCTCACTGAGACTACATCAGCTATTCTGATTACACCCGAGGGGATGATAA
ACCGGGCGCGGTCGGTAAAGTTGTTCCATTTTTTGAAGCGAAGGTTGTGGATCTGGATACCGGG
AAAACGCTGGGCGTTAATCAAAGAGGCGAACTGTGTGTGAGAGGTCCTATGATTATGTCCGGTT
ATGTAAACAATCCGGAAGCGACCAACGCCTTGATTGACAAGGATGGATGGCTACATTCTGGAGA
CATAGCTTACTGGGACGAAGACGAACACTTCTTCATCGTTGACCGCCTGAAGTCTCTGATTAAGT

ACAAAGGCTATCAGGTGGCTCCCGCTGAATTGGAATCCATCTTGCTCCAACACCCCAACATCTTC
GACGCAGGTGTCGCAGGTCTTCCCGACGATGACGCCGGTGAACTTCCCGCCGCCGTTGTTGTTTT
GGAGCACGGAAAGACGATGACGGAAAAAGAGATCGTGGATTACGTCGCCAGTCAAGTAACAACC
GCGAAAAAGTTGCGCGGAGGAGTTGTGTTTGTGGACGAAGTACCGAAAGGTCTTACCGGAAAAC
TCGACGCAAGAAAAATCAGAGAGATCCTCATAAAGGCCAAGAAGGGCGGAAAGATCGCCGTGTA
ATTCTAGGGATCCGCCCCTCTCCCTCCCCCCCCCCTAACGTTACTGGCCGAAGCCGCTTGGAATAA
GGCCGGTGTGCGTTTGTCTATATGTTATTTTCCACCATATTGCCGTCTTTTGGCAATGTGAGGGC
CCGGAAACCTGGCCCTGTCTTCTTGACGAGCATTCCTAGGGGTCTTTCCCCTCTCGCCAAAGGAA
TGCAAGGTCTGTTGAATGTCGTGAAGGAAGCAGTTCCTCTGGAAGCTTCTTGAAGACAAACAAC
GTCTGTAGCGACCCTTTGCAGGCAGCGGAACCCCCCACCTGGCGACAGGTGCCTCTGCGGCCAAA
AGCCACGTGTATAAGATACACCTGCAAAGGCGGCACAACCCCAGTGCCACGTTGTGAGTTGGATA
GTTGTGGAAAGAGTCAAATGGCTCTCCTCAAGCGTATTCAACAAGGGGCTGAAGGATGCCCAGA
AGGTACCCCATTGTATGGGATCTGATCTGGGGCCTCGGTACACATGCTTTACATGTGTTTAGTCG
AGGTTAAAAAAACGTCTAGGCCCCCCGAACCACGGGGACGTGGTTTTCCTTTGAAAAACACGATG
ATAATATGGCCACAACCATGGCGCGTATGGCTCGGGGCATTGAACAGGATGGGCTGCACGCCGGG
TCACCTGCTGCTTGGGTCGAAAGACTGTTTGGGTATGATTGGGCTCAGCAGACAATCGGCTGCTC
TGACGCCGCCGTGTTCAGGCTGAGTGCTCAGGGACGCCCCGTGCTGTTTGTCAAGACTGACCTGT
CAGGGGCACTGAACGAGCTGCAGGATGAGGCAGCCCGCCTGAGCTGGCTGGCAACCACAGGAGTG
CCTTGTGCTGCAGTCCTGGACGTGGTCACTGAGGCCGGACGAGATTGGCTGCTGCTGGGAGAAGT
GCCAGGACAGGACCTGCTGAGCTCCCACCTGGCACCAGCTGAGAAGGTCTCCATCATGGCAGATG
CCATGAGGAGACTGCATACTCTGGACCCCGCCACCTGCCCTTTCGATCACCAGGCTAAACATCGC
ATTGAGCGGGCTCGCACACGAATGGAAGCAGGCCTGGTGGACCAGGACGATCTGGATGAGGAAC
ACCAGGGACTGGCTCCTGCAGAGCTGTTTGCAAGGCTGAAAGCCAGAATGCCAGACGGCGAAGA
TCTGGTGGTCACCCATGGAGACGCTTGCCTGCCCAACATCATGGTGGAGAATGGAAGATTCAGTG
GGTTTATTGATTGTGGCCGACTGGGAGTCGCCGACAGGTACCAGGATATCGCCCTGGCTACAAGA
GACATTGCAGAGGAACTGTGCGGGGAATGGGCCGATCGGTTCCTGGTGCTGTATGGCATTGCTGC
TCCCGACAGTCAGAGGATTGCTTTTTACAGGCTGCTGGACGAGTTCTTTTGAATCTAGAGGCGCG
CCATCGATACGCGTCTAGAGTGAGGGTCCCCACCTGGGACCCTTGAGAGTATCAGGTCTCCCACG
TGGGAGACAAGAAATCCCTGTTTAATATTTAAACAGCAGTGTTCCCCATCTGGGTCCTTGCACCC
CTCACTCTGGCCTCAGCCGACTGCACAGCGGCCCCTGCATCCCCTTGGCTGTGAGGCCCCTGGACA
AGCAGAGGTGGCCAGAGCTGGGAGGCATGGCCCTGGGGTCCCACGAATTTGCTGGGGAATCTCGT
TTTTCTTCTTAAGACTTTTGGGACATGGTTTGACTCCCGAACATCACCGACGTGTCTCCTGTTTT
TCTGGGTGGCCTCGGGACACCTGCCCTGCCCCCACGAGGGTCAGGACTGTGACTCTTTTTAGGGC
CAGGCAGGTGCCTGGACATTTGCCTTGCTGGATGGGGACTGGGGATGTGGGAGGGAGCAGACAG
GAGGAATCATGTCAGGCCTGTGTGTGAAAGGAAGCTCCACTGTCACCCTCCACCTCTTCACCCCC
CACTCACCAGTGTCCCCTCCACTGTCACATTGTAACTGAACTTCAGGATAATAAAGTGTTTGCCT
CCAGTCACGTCCTTCCTCCTTCTTGAGTCCAGCTGGTGCCTGGCCAGGGGCTGGGGAGGTGGCTG
AAGGGTGGGAGAGGCCAGAGGGAGGTCGGGGAGGAGGTCTGGGGAGGAGGTCCAGGGAGGAGGA
GGAAAGTTCTCAAGTTCGTCTGACATTCATTCCGTTAGCACATATTTATCTGAGCACCTACTCTG
TGCAGACGCTGGGCTAAGTGCTGGGGACACAGCAGGGAACAAGGCAGACATGGAATCTGCACTC
GANNGAATTCACTGGCCGTCGTTTTACAACGTCGTGACTGGGAAAACCCTGGCGTTACCCAACTT
AATCGCCTTGCAGCACATCCCCCTTTCGCCAGCTGGCGTAATAGCGAAGAGGCCCGCACCGATCG
CCCTTCCCAACAGTTGCGCAGCCTGAATGGCGAATGGCGCCTGATGCGGTATTTTCTCCTTACGC
ATCTGTGCGGTATTTCACACCGCATACGTCAAAGCAACCATAGTACGCGCCCTGTAGCGGCGCAT
TAAGCGCGGCGGGTGTGGTGGTTACGCGCAGCGTGACCGCTACACTTGCCAGCGCCCTAGCGCCC
GCTCCTTTCGCTTTCTTCCCTTCCTTTCTCGCCACGTTCGCCGGCTTTCCCCGTCAAGCTCTAAAT
CGGGGGCTCCCTTTAGGGTTCCGATTTAGTGCTTTACGGCACCTCGACCCCAAAAAACTTGATTT
GGGTGATGGTTCACGTAGTGGGCCATCGCCCTGATAGACGGTTTTTCGCCCTTTGACGTTGGAGT
CCACGTTCTTTAATAGTGGACTCTTGTTCCAAACTGGAACAACACTCAACCCTATCTCGGGCTAT
TCTTTTGATTTATAAGGGATTTTGCCGATTTCGGCCTATTGGTTAAAAAATGAGCTGATTTAAC
AAAAATTTAACGCGAATTTTAACAAAATATTAACGTTTACAATTTTATGGTGCACTCTCAGTAC

AATCTGCTCTGATGCCGCATAGTTAAGCCAGCCCCGACACCCGCCAACACCCGCTGACGCGCCCT
GACGGGCTTGTCTGCTCCCGGCATCCGCTTACAGACAAGCTGTGACCGTCTCCGGGAGCTGCATG
TGTCAGAGGTTTTCACCGTCATCACCGAAACGCGCGAGACGAAAGGGCCTCGTGATACGCCTATT
TTTATAGGTTAATGTCATGATAATAATGGTTTCTTAGACGTCAGGTGGCACTTTTCGGGGAAAT
GTGCGCGGAACCCCTATTTGTTTATTTTTCTAAATACATTCAAATATGTATCCGCTCATGAGACA
ATAACCCTGATAAATGCTTCAATAATATTGAAAAAGGAAGAGTATGAGTATTCAACATTTCCGT
GTCGCCCTTATTCCCTTTTTTGCGGCATTTTGCCTTCCTGTTTTTGCTCACCCAGAAACGCTGGT
GAAAGTAAAAGATGCTGAAGATCAGTTGGGTGCACGAGTGGGTTACATCGAACTGGATCTCAAC
AGCGGTAAGATCCTTGAGAGTTTTCGCCCCGAAGAACGTTTTCCAATGATGAGCACTTTTAAAG
TTCTGCTATGTGGCGCGGTATTATCCCGTATTGACGCCGGGCAAGAGCAACTCGGTCGCCGCATA
CACTATTCTCAGAATGACTTGGTTGAGTACTCACCAGTCACAGAAAAGCATCTTACGGATGGCAT
GACAGTAAGAGAATTATGCAGTGCTGCCATAACCATGAGTGATAACACTGCGGCCAACTTACTT
CTGACAACGATCGGAGGACCGAAGGAGCTAACCGCTTTTTTGCACAACATGGGGGATCATGTAA
CTCGCCTTGATCGTTGGGAACCGGAGCTGAATGAAGCCATACCAAACGACGAGCGTGACACCACG
ATGCCTGTAGCAATGGCAACAACGTTGCGCAAACTATTAACTGGCGAACTACTTACTCTAGCTTC
CCGGCAACAATTAATAGACTGGATGGAGGCGGATAAAGTTGCAGGACCACTTCTGCGCTCGGCCC
TTCCGGCTGGCTGGTTTATTGCTGATAAATCTGGAGCCGGTGAGCGTGGGTCTCGCGGTATCATT
GCAGCACTGGGGCCAGATGGTAAGCCCTCCCGTATCGTAGTTATCTACACGACGGGGAGTCAGGC
AACTATGGATGAACGAAATAGACAGATCGCTGAGATAGGTGCCTCACTGATTAAGCATTGGTAA
CTGTCAGACCAAGTTTACTCATATATACTTTAGATTGATTTAAAACTTCATTTTTAATTTAAAA
GGATCTAGGTGAAGATCCTTTTTGATAATCTCATGACCAAAATCCCTTAACGTGAGTTTTCGTTC
CACTGAGCGTCAGACCCCGTAGAAAAGATCAAAGGATCTTCTTGAGATCCTTTTTTTCTGCGCGT
AATCTGCTGCTTGCAAACAAAAAAACCACCGCTACCAGCGGTGGTTTGTTTGCCGGATCAAGAGC
TACCAACTCTTTTTCCGAAGGTAACTGGCTTCAGCAGAGCGCAGATACCAAATACTGTCCTTCTA
GTGTAGCCGTAGTTAGGCCACCACTTCAAGAACTCTGTAGCACCGCCTACATACCTCGCTCTGCT
AATCCTGTTACCAGTGGCTGCTGCCAGTGGCGATAAGTCGTGTCTTACCGGGTTGGACTCAAGAC
GATAGTTACCGGATAAGGCGCAGCGGTCGGGCTGAACGGGGGGTTCGTGCACACAGCCCAGCTTG
GAGCGAACGACCTACACCGAACTGAGATACCTACAGCGTGAGCTATGAGAAAGCGCCACGCTTCC
CGAAGGGAGAAAGGCGGACAGGTATCCGGTAAGCGGCAGGGTCGGAACAGGAGAGCGCACGAGG
GAGCTTCCAGGGGGAAACGCCTGGTATCTTTATAGTCCTGTCGGGTTTCGCCACCTCTGACTTGA
GCGTCGATTTTTGTGATGCTCGTCAGGGGGGCGGAGCCTATGGAAAAACGCCAGCAACGCGGCCT
TTTTACGGTTCCTGGCCTTTTGCTGGCCTTTTGCTCACATGTTCTTTCCTGCGTTATCCCCTGATT
CTGTGGATAACCGTATTACCGCCTTTGAGTGAGCTGATACCGCTCGCCGCAGCCGAACGACCGAG
CGCAGCGAGTCAGTGAGCGAGGAAGCGGAAG

Plasmid size
8643bp

Features
EFBOS: 239 - 1743
T2A: 1756 - 1857
Luciferase cDNA: 1858 - 3499
IRES: 3517 - 4092
Mammalian optimised neomycin resistance: 4097 - 5922

## Appendix 6. Raw data and statistical analysis of C-peptide and proinsulin secretion

Table 1. Absolute levels of C-peptide secretion (pM) from reaggregated hESC-derived INSULIN-GFP+ cells under a variety of stimulatory conditions.

| | Low Glucose | High Glucose | High Glucose + KCl | Low Glucose |
|---|---|---|---|---|
| Reaggregate #1 | 121.564 | 57.5359 | 163.9508 | 69.16908 |
| Reaggregate #2 | 258.1676 | 135.01762 | 434.345 | 98.96746 |
| Reaggregate #3 | 201.4292 | 190.44236 | 259.5282 | 103.50624 |
| Reaggregate #4 | 314.3932 | 288.4964 | 502.4206 | 130.5409 |
| Reaggregate #5 | 123.8112 | 141.71922 | 310.0828 | 80.6975 |

Table 2. Absolute levels of proinsulin secretion (pM) from reaggregated hESC-derived INSULIN-GFP+ cells under a variety of stimulatory conditions.

| | Low Glucose | High Glucose | High Glucose + KCl | Low Glucose |
|---|---|---|---|---|
| Reaggregate #1 | 2.120034 | 1.70782 | 1.897683 | 1.071543 |
| Reaggregate #2 | 4.439656 | 2.564723 | 4.852815 | 0.8807685 |
| Reaggregate #3 | 4.980028 | 3.454216 | 4.725614 | 1.707082 |
| Reaggregate #4 | 3.867309 | 4.248716 | 9.058824 | 2.310616 |
| Reaggregate #5 | 3.613087 | 3.041203 | 6.221076 | 1.135119 |

Table 3. Percentage proinsulin secretion (pM) from reaggregated hESC-derived INSULIN-GFP+ cells under a variety of stimulatory conditions

| | Low Glucose | High Glucose | High Glucose + KCl | Low Glucose |
|---|---|---|---|---|
| Reaggregate #1 | 1.74% | 2.97% | 1.16% | 1.55% |
| Reaggregate #2 | 1.72% proinsulin | 1.90% | 1.12% | 0.89% |
| Reaggregate #3 | 2.47% proinsulin | 1.81% | 1.82% | 1.65% |
| Reaggregate #4 | 1.23% proinsulin | 1.47% | 1.80% | 1.77% |
| Reaggregate #5 | 2.92% proinsulin | 2.15% | 2.01% | 1.41% |

Table 4. Statistical analysis of data presented in table 3, showing the percentage C-peptide secretion (pM) ) from reaggregated hESC-derived INSULIN-GFP+ cells under a variety of stimulatory conditions.

| | Low glucose | High Glucose | High Glucose + KCl | Low Glucose |
|---|---|---|---|---|
| Mean % proinsulin | 2.02 | 2.06 | 1.58 | 1.45 |
| SEM | 0.30 | 0.25 | 0.18 | 0.15 |

Table 5. Percentage proinsulin secretion (pM) from reaggregated hESC-derived INSULIN-GFP+ cells under a variety of stimulatory conditions

| | Low Glucose | High Glucose | High Glucose + KCl | Low Glucose |
|---|---|---|---|---|
| Reaggregate #1 | 98.26% | 97.03% | 98.84% | 98.45% |
| Reaggregate #2 | 98.28% | 98.10% | 98.88% | 99.11% |
| Reaggregate #3 | 97.53% | 98.19% | 98.18% | 98.35% |
| Reaggregate #4 | 98.77% | 98.53% | 98.20% | 98.23% |
| Reaggregate #5 | 97.08% | 97.85% | 97.99% | 98.59% |

Table 6. Statistical analysis of data presented in table 3, showing the percentage proinsulin secretion (pM) ) from reaggregated hESC-derived INSULIN-GFP+ cells under a variety of stimulatory conditions.

| | Low glucose | High Glucose | High Glucose + KCl | Low Glucose |
|---|---|---|---|---|
| Mean % C-peptide | 97.98 | 97.94 | 98.42 | 98.55 |
| SEM | 0.30 | 0.25 | 0.18 | 0.15 |